REGULATION OF FIBRONECTIN AND TRANSFORMING GROWTH FACTOR-ß EXPRESSION IN DUCTUS ARTERIOSUS

by

Bin Zhou

A thesis submitted in conformity with the requirements for the Degree of Doctor of Philosophy in the Graduate Department of Laboratory Medicine and Pathobiology,
University of Toronto

Regulation of Fibronectin and Transforming Growth Factor-β Expression in Ductus Arteriosus

Ph.D. Degree, 1998

Bin Zhou

Department of Laboratory Medicine and Pathobiology, University of Toronto

ABSTRACT

Intimal cushion formation in the fetal ductus arteriosus (DA) is characterized by subendothelial accumulation of extracellular matrix (ECM) and smooth muscle cell (SMC) migration. Elevated endothelial cell (EC) hyaluronan and SMC fibronectin (FN) synthesis in DA versus aortic (Ao) SMC modulate the elongated 'migratory' phenotype of DA SMC. Increased DA EC hyaluronan synthesis is transforming growth factor-β1 (TGF-β)-dependent, and increased DA SMC FN synthesis is attributed to enhanced mRNA translation. This thesis addressed whether TGF-β1 expression was increased in DA versus Ao EC and whether the level of regulation was transcriptional or post-transcriptional. It then focused on the molecular mechanism regulating enhanced FN mRNA translation in DA SMC. We demonstrated a one-fold greater synthesis of TGF-β protein in cultured DA compared to Ao EC accompanied by increased EC TGF-β expression in 100-day gestation (term =145 days) DA versus Ao tissues. By 138-day gestation, TGF-β protein synthesis and mRNA levels were reduced in DA EC to that observed in Ao EC. The increased TGF-β expression in 100-day DA EC was related to enhanced transcription and translation of a relatively unstable TGF-β1 mRNA. We then showed that an AU-rich element (ARE) in the 3'UTR, promotes mRNA translation in both DA and Ao SMC, with the effect augmented in DA SMC. Gel shift assay revealed ARE-binding activities in both DA and Ao SMC cytoplasmic extracts, with increased activities found in DA SMC. Ultraviolet-crosslinking assay indicated three binding complexes of M_r at ~15, 30, and 60 kD, respectively. The 15 kD ARE-

binding protein was purified from sheep Ao tissues and identified as light chain 3 (LC3) of microtubule (MT)-associated protein 1 (MAP1). Overexpression of LC3 in Ao SMC results in an enhanced FN mRNA translation. Polysome profile analysis showed more FN mRNA and LC3 protein, associated with heavy polysomes in DA versus Ao or colchicine-treated DA SMC. Similarly, expression of LC3 in HT1080 cells promotes FN mRNA translation associated with enhanced ribosome recruitment. These data suggest that LC3-ARE interaction facilitates FN mRNA translation.

Acknowledgments

In retrospect, I see clearly how lucky I was to have been awarded the opportunity to conduct my Ph.D. training at the University of Toronto. At the time I began my studies, it was the dream of many young graduates back in China to be so fortunate. It was even more fortuitous to have Dr. Marlene Rabinovitch, an renowned vascular biologist, as my mentor. I would like to thank her for her tireless support and excellent guidance throughout my Ph.D. training. Her determination to succeed in and her dedication to science has been an enormous influence and will stand as the model on which I hope to shape my future career.

I am thankful to the members of my Thesis Advisory Committee: Drs. P. Hamel, M. Ranadive, P. Ray, J. Squire, and P. Thorner, for their insights and critical reviews of my thesis. Thanks must also go to Drs. Fred Keeley and Alex Hinek for helpful discussions and suggestions, and to Dr. Clayton Buck who granted his time to read my thesis and to provide important comments.

I am indebted to members of Dr. Rabinovitch's laboratory. They include Ms. Claire Coulber, the 'master of all' lab managers, whose daily help in my 'lab exercises' was continuous and unconditional; Ms. Joan Jowlabar and Susy Taylor for always supporting my efforts, preparing countless slides and mounds of paperwork, and making my English more English! Other people in the lab have been of enormous support and have helped me to grow professionally. I am also grateful to Professors in the Department of Laboratory Medicine and Pathobiology and Cardiovascular Sciences Collaborative Program. They exposed me to various fields of scientific endeavor and expanded my education in different disciplines.

Lastly, I owe my deepest thanks to my wife and son who endured numerous nights alone, while I was surrounded by 'cells and molecules'. Their understanding, support, and love are invaluable. Without them, this thesis would not be a finished task. I dedicate this thesis to my beloved wife and son.

CONTENTS

Lists of Figures and Tables

LIST OF ABBREVIATIONS

A, adenosine,

Ao, aorta

ARE, AU-rich element

AUBF, adenosine-uridine binding factor

bFGF, basic fibroblast growth factor

C, cytosine

CAT, chloramphenicol acetyl transferase

DA, ductus arteriosus

DAPI, 4', 6-diamidino-2-phenylindole

DTT, dithiothreitol

EC, endothelial cells

ECL, enhanced chemiluminescence

EGF, epidermal growth factor

ELAV, embryonic lethal abnormal vision

ER, endoplasmic reticulum

FBS, fetal bovine serum

FISH, Fluorescence *In Situ* Hybridization

FITC, fluorescein isothiocyanate

FN, fibronectin

G, guanosine

GAPDH, Glyceraldehyde-3-phosphate dehydrogenase

GLUT1, glucose transporter 1

GM-CSF, granulocyte macrophage colony-stimulating factor

GST, glutathione *S*-transferase

Hel-N1, human embryonic lethal abnormal vision-like neuronal protein 1

hnRNP, heterogeneous nuclear ribonucleoprotein

HRP, Horseradish peroxidase

IL-1, interleukin

INF-α, interferon-α

INF-γ, interferon-γ

IRE, iron-response element

IRE-BP, iron-response element binding protein

IRES, internal ribosome entry site

LC3, light chain 3

LPS, lipopolysaccharide

MAP, microtubule-associated protein

ß-ME, ß-mercaptoethanol

MT, microtubule

mRNP, mRNA ribonucleoprotein

NEM, *N*-ethylmaleimide

NP-40, Nonidet P-40

PA, pulmonary artery

PAGE, polyacrylamide gel electrophoresis

PBS, phosphate-buffered saline

PCR, polymerase chain reaction

PDGF, platelet-derived growth factor

PVDF, polyvinyldifluoride transfer membrane

RHAMM, the receptor for hyaluronan-mediated motility

RNPs, ribonucleoproteins

RRM, RNA recognition motif

RT, reverse transcriptase

SDS, sodium dodecyl sulfate

SMC, smooth muscle cells

TBE, Tris-borate-EDTA

TGF-β1, transforming growth factor-β

TNF-α, tumor necrosis factor-α

TPA, 12-*O*-tetradecanoylphorbol-13-acetate

TRITC, tetramethylrhodamine isothiocyanate

3'UTR, 3' untranslated region

U, uridine

UV, Ultraviolet

VEGF, vascular epidermal growth factor

INTRODUCTION

General Introduction

This thesis investigates the regulation of endothelial cell (EC) transforming growth factor-β1 (TGF-β1) and smooth muscle cell (SMC) fibronectin (FN) expression in the ductus arteriosus (DA). Expression of TGF-β1 in DA EC is regulated at both transcriptional and translational levels. whereas an interaction of an RNA-binding protein with the 3' untranslated region (3'UTR) of FN mRNA is demonstrated as the mechanism contributing to the enhanced FN mRNA translational efficiency in DA SMC. The following introduction first briefly describes normal vascular biology and the pathology of neointimal formation, then addresses the DA as a working model to study expression and function of tissue-specific and developmentally-regulated genes related to vascular intimal thickening, emphasizing TGF-β1 and FN. Regulation of TGF-β1 and FN expression is then reviewed, highlighting post-transcriptional and translational control mechanisms. Next, the interaction of specific RNA-binding protein(s) with AU-rich elements (ARE) in 3'UTR are addressed and their role in controlling gene expression is outlined.

Normal Vascular Biology

The normal vascular wall consists of three layers from the lumen outward: intima, media, and adventitia. The intima consists of a single layer of EC. In large elastic arteries, such as the human aorta, there are also some subendothelial SMC proximal to an internal elastic laminae. The media contains multiple layers of SMC which, depending on the size of the vessel, are separated by distinct elastic laminae, and organized extracellular matrix (ECM) components, such as collagen types I and III, as well as a variety of glycosaminoglycans and glycoproteins. The adventitia is relatively less well organized and consists of fibroblasts, collagen, and poorly assembled elastin, in addition to other ECM components. Physiologically, because it resides at an interface between the blood and the vessel wall, the EC is a potential regulator of arterial wall homeostasis. It senses, transduces, and responds to stimuli generated from changes in the mechanical, chemical, and humoral environments (Ryan and Rubanyi, 1992; Davies and Tripathi, 1993). It synthesizes and secretes factors that modulate vascular tone, preserves the antithrombotic inner surface of vessel wall, maintains the anticoagulated state of the blood, and expresses cell surface molecules that recruit inflammatory cells (Busse *et al.*, 1993; Davies and Hagen, 1993; Springer, 1995). The EC also maintains the structural integrity of vessel wall by producing factors which both promote and inhibit cell growth and by regulating the production and turnover of ECM (Eisenberg, 1991; Vanhoutte, 1991; Ryan and Rubanyi, 1992; Davies and Hagen, 1993; Davies and Tripathi, 1993). During angiogenesis and vasculogenesis, the EC and its cell surface receptors determine formation of the vessel wall by recruiting SMC (Risau, 1995; Shalaby *et al.*, 1995; Folkman and D'Amore, 1996).

Smooth muscle cells, together with the ECM in the media, provide mechanical and structural support to the vessel and regulate vascular tone. Quiescent SMC are well differentiated cells characterized by an abundance of contractile proteins, predominantly smooth muscle-specific actin and myosin, but little rough endoplasmic reticulum (ER) (Chambley-Campbell *et al.*, 1981; Campbell and Campbell, 1986; Mosse *et al.*, 1986; Owens *et al.*, 1986; Campbell *et al.*, 1988).

and very slow turnover (Clowes *et al.*, 1983b). These SMC are also called 'contractile SMC'. Once activated, SMC de-differentiate into a so-called synthetic phenotype, characterized by a rich cellular endoplasmic reticulum (ER) and the ability to synthesize and secrete a large amount of ECM components and growth factors (Chambley-Campbell, *et al.*, 1981; Campbell and Campbell. 1986; Mosse, *et al.*, 1986; Campbell, *et al.*, 1988; Nilsson, 1993; Davies and Hagen, 1994). Extracellular matrix components produced by SMC contribute to the biologic activities of EC and these range from providing mechanical support, to allowing cell adhesion, as well as affecting migration and proliferation (Liu *et al.*, 1989; Wight, 1989; Hardingham and Fosang, 1992; Ross. 1993; Davies and Hagen, 1994; Farhadian *et al.*, 1996).

Vascular Neointima

Vascular neointima is a thickened intima that forms in vessels in response to various injuries. It was first described in 1906 by Carrel and Guthrie (1906) who observed within a few days of a vascular bypass operation, an endothelium-like glistening substance covering the sutures at the anastomotic sites. Vascular neointima is now found in vessels injured by electrical burning. radiation, suturation, angioplasty, venous and prosthetic bypass grafts, and endarterectomy (Chervu and Moore, 1990; Ip *et al.*, 1990; Schwartz *et al.*, 1995). The neointima also forms the primary lesion of atherosclerosis (Ross, 1986; Ross, 1993). The restenosis following coronary angioplasty is also characterized by the rapid production of a neointima (Liu, *et al.*, 1989; Clowes. 1993).

Morphologic Changes Related to Vascular Neointimal Formation. The neointima is characterized by abnormal migration and proliferation of SMC and accumulation of ECM components. The histology of the neointima that develops in association with restenosis after coronary angioplasty is that of fibrocellular proliferation, accumulation of loose collagen fibrils and proteoglycans or formation of dense collagen scar, with few inflammatory cells and little lipid (Dartsch *et al.*, 1989; Gravanis and Roubin, 1989; Farb *et al.*, 1990). Under light

microscopy, most of the cells have a mesenchymal appearance, similar to that of fibroblasts. Electron microscopy reveals a variety of phenotypes. Cells that are clearly of smooth muscle derivation are characterized by substantial myofilament bundles, a basement membrane and positive immunoreactivity for α1-smooth muscle actin, vimentin and desmin. Other cells lack these features and may represent a more de-differentiated phenotype (Dartsch, *et al.*, 1989) similar to the proliferating, migrating, and matrix-secreting neointimal SMC in the carotid balloon-injury animal model (Schwartz *et al.*, 1990).

Process of Vascular Neointimal Formation. Balloon catheter-induced injury of the rat carotid artery was used to establish the evolution of the neointima and this model indicated that SMC proliferation began 24 hours after arterial injury (Clowes *et al.*, 1983a; Clowes, *et al.*, 1983b; Schwartz, *et al.*, 1990). Migration of the SMC from the media to the intima occurred 4 days after injury, and proliferation continued in the intima to a maximum at 2 weeks after balloon injury. Further intimal thickening continues up to 3 months after injury and is largely due to the accumulation of ECM components produced by the SMC. A similar time course has also been demonstrated following balloon angioplasty of carotid artery stenosis induced by electrical stimulation in an atherosclerotic rabbit model (Hanke *et al.*, 1990; Kocher *et al.*, 1991).

Mechanisms related to Vascular Neointimal Formation. According to the response-to-injury hypothesis, neointimal formation is a repair process or a vascular form of fibrosis (Ross, 1986; Schwartz, *et al.*, 1995). Activation of EC and SMC by injury induces a cascade of intercellular and intracellular events leading to neointimal formation (Libby *et al.*, 1992). There is deposition of platelets, thrombus formation, migration of inflammatory cells and the release of various growth factors and cytokines, such as platelet-derived growth factor (PDGF), basic fibroblast growth factor (bFGF), interleukin 1 (IL-1), and TGF-β from platelets, circulating monocytes, EC and SMC themselves. The initial generation of cytokines and growth factors evokes a sustained process owing to autocrine and paracrine expression of cytokines and growth

factors. Expression of proto-oncogenes, such as *c*-fos and *c*-myc was observed in the rat carotid after balloon injury with the *c*-fos mRNA peaking at 30 minutes and *c*-myc mRNA at two hours after injury (Miano *et al.*, 1990; Miano *et al.*, 1993a) and proposed to play a role in the autocrine cascade model (Miano *et al.*, 1993b). *In situ* hybridization has been used to show expression of *c*-myc in SMC of human atherosclerotic plaque retrieved from the coronary vasculature (Nagamine *et al.*, 1989) and high *c*-myc mRNA levels have been found in SMC cultures from human proliferating plaque cells compared to proliferating SMC derived from healthy human Ao and saphenous vein (Parkes *et al.*, 1991). The upregulation of these proto-oncogenes, such as c-*myb* (Brown *et al.*, 1992; Simons and Rosenberg, 1992) and c-*myc* (Biro *et al.*, 1993; Shi *et al.*, 1993), is involved in mitogen-induced proliferation and migration of vascular SMC *in vitro* and *in vivo* (Simons *et al.*, 1992) and may therefore represent a common pathway to intimal thickening.

Ductus Arteriosus as a Model to Study Neointimal Thickening

While the rat carotid balloon injury model was important in elucidating on the mechanism of neointimal formation, there were several drawbacks. The lesion was mostly helpful in the study of the proliferative characteristics of SMC, but was less effective in mimicking features of migration or ECM production. As an 'experiment of nature', the fetal ductus arteriosus (DA) develops 'intimal cushions'. Although the initiating factors which regulate intimal cushion formation in the DA are still unknown, it is in many ways morphologically similar to the neointima observed in a variety of vascular diseases including atherosclerosis, pulmonary hypertension, and restenosis. In addition, the biochemical and cellular events associated with intimal cushion formation in the DA were relevant to pathological intimal thickening in that there was increased expression of growth factors, distinct alterations in ECM production, and a phenotypic switch of SMC from a 'contractile' to a 'synthetic and migratory' state. In this respect, study of the mechanisms involved in intimal cushion formation in the DA will not only potentially aid in the clinical management of patent DA but will also provide insight into the pathologic processes underlying development of the neointima in abnormal vessels.

Ductus Arteriosus

The DA is a fetal muscular artery which develops from the 6th aortic arch and connects the pulmonary artery (PA) and Ao (Figure 1). In the fetal circulation, the DA serves to shunt the majority of the right ventricle output away from the uninflated lungs and back into the systemic circulation. Closure of the DA shortly after birth is therefore of physiological importance in assuring the transition from fetal to post-natal circulation. Absence of closure, as in the persistent DA, causes significant hemodynamic disorders resulting in pulmonary hypertension, congestive heart failure, and cardiac hypertrophy (Cassels, 1973). Triggered by the onset of breathing at birth, the DA starts to close with a strong vascular constriction. This constriction is oxygen-dependent and is regulated by a cytochrome-P450-mediated mechanism (Coceani *et al.*, 1988) which induces endothelin production (Coceani, 1994). The initial muscular constriction is reversible and is followed by an anatomical closure which takes days and depends on the development of preexisting structural changes, known as 'intimal cushions' (Gittenberger-de Groot *et al.*, 1980; Gittenberger-de Groot *et al.*, 1985).

Intimal Cushion Formation

Intimal cushion formation begins at the pulmonary end of the vessel and continues towards the Ao end (Gittenberger-de Groot, *et al.*, 1985). The nature of intimal cushion formation has been studied in humans (Gittenberger-de Groot *et al.*, 1980; Gittenberger-de Groot, *et al.*, 1980; Silver *et al.*, 1981) and a number of animal species, including mouse (Tada and Kishimoto, 1990; Colbert *et al.*, 1996), dog (Gittenberger-de Groot, *et al.*, 1985; de Reeder *et al.*, 1988; de Reeder *et al.*, 1989), rabbit (Yoder *et al.*, 1978), and lamb (Rabinovitch *et al.*, 1988; Strengers, 1988; Rabinovitch *et al.*, 1989; Boudreau, 1990; Zhu *et al.*, 1990; Boudreau and Rabinovitch, 1991; Boudreau *et al.*, 1991; Hinek *et al.*, 1991; Boudreau *et al.*, 1992; Hinek and Rabinovitch, 1993). The process is initiated in the intima where it appears that accumulation of ECM components separates the EC from the internal elastic laminae. Smooth muscle cells from the muscular media

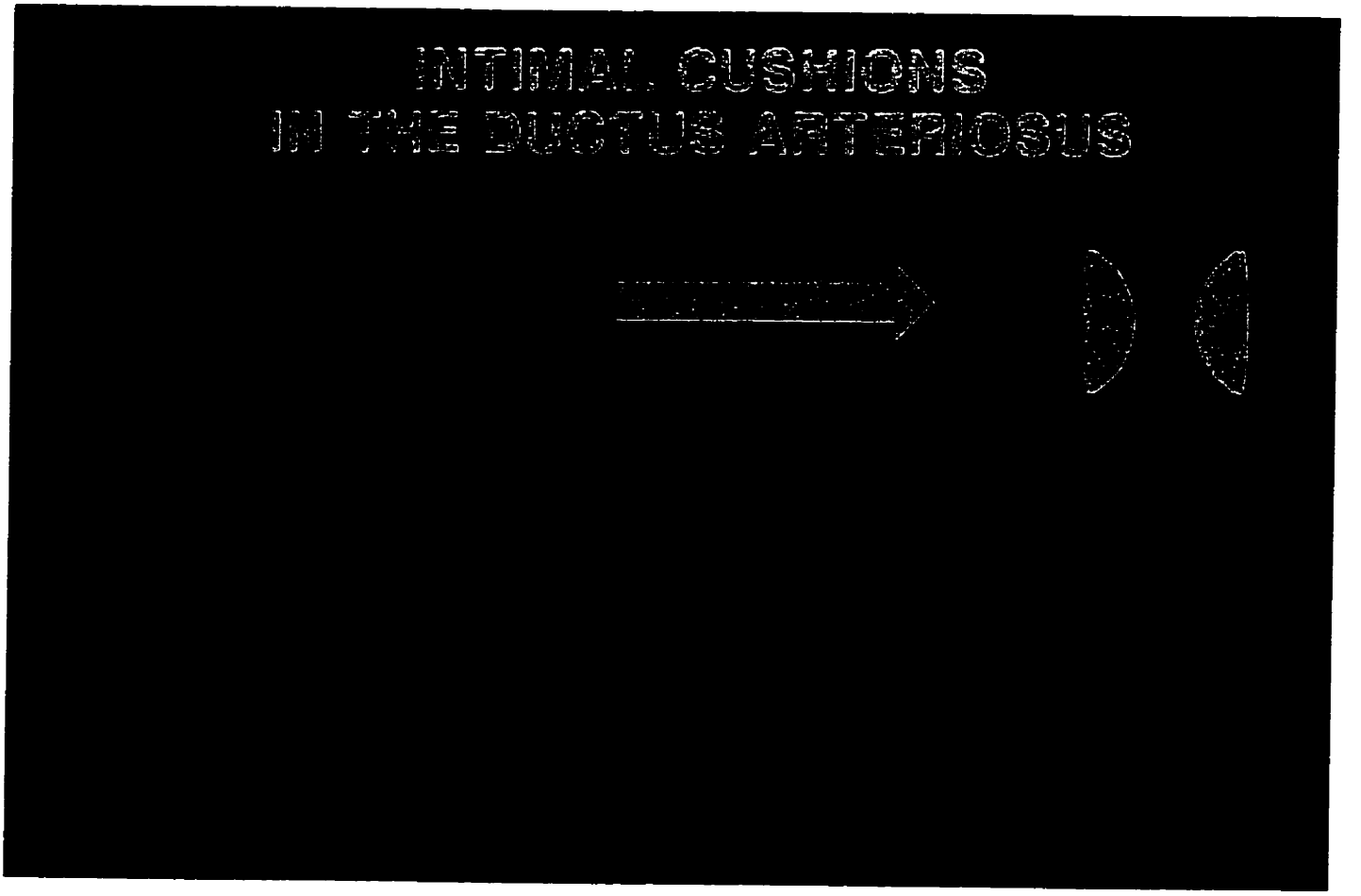

Figure 1

Figure 1. Anatomic Features of Ductus Arteriosus

Ductus arteriosus (within green circle), which connects between aortic arch and pulmonary artery. develops intimal cushion (indicated by arrow) during late gestation time.

of the vessel wall then migrate into this matrix-enriched subendothelial region which forms an intimal cushion.

Morphologic Changes Related to Intimal Cushion Formation

Sequential morphological studies addressing intimal cushion development in the human and dog DA revealed that glycosaminoglycans were the major contributors (de Reeder, *et al.*, 1988: Slomp *et al.*, 1992) to the increased deposition of ECM components in the subendothelial space (Gittenberger-de Groot, *et al.*, 1985). Other ECM components included FN and collagen III (de Reeder, *et al.*, 1989). In contrast, a loss of laminin and collagen I were noted (de Reeder, *et al.*, 1989). As well, splitting or loss of the internal elastin laminae and reduced elastin content was observed especially in the modified radially oriented SMC in the intimal cushions compared to circularly oriented medial SMC (de Reeder *et al.*, 1990). In a genetic strain of poodle dogs with a patent DA resulting from defective intimal cushion development, there is diminished subendothelial accumulation of hydrophilic glycosaminoglycans, as well as adhesive matrix proteins, FN and collagen III. These data suggested that these ECM components may be directly involved in the formation of intimal cushions by providing the water-bound and matrix-enriched environment which favored SMC migration.

Natural Process of Intimal Cushion Formation

Similar histological changes associated with the intimal cushion formation have been found in the fetal lamb (Boudreau, 1990). No evidence of the intimal cushion formation is found in the fetal lamb at the 100-day of gestation time-point (term is about 145 days). The structure of the DA (**A**) at this time is similar to that of the adjacent Ao (**B**) (Figure 2), although impaired assembly of the medial elastic laminae is evident when assessed by electron microscopy (Zhu, *et al.*, 1990). By 115-days of gestation however, accumulation of glycosaminoglycans in the subendothelial space, impaired assembly of all elastic laminae, and migration of SMC from the medial layer into subendothelial space are evident at the light microscopic level. These changes continue and by

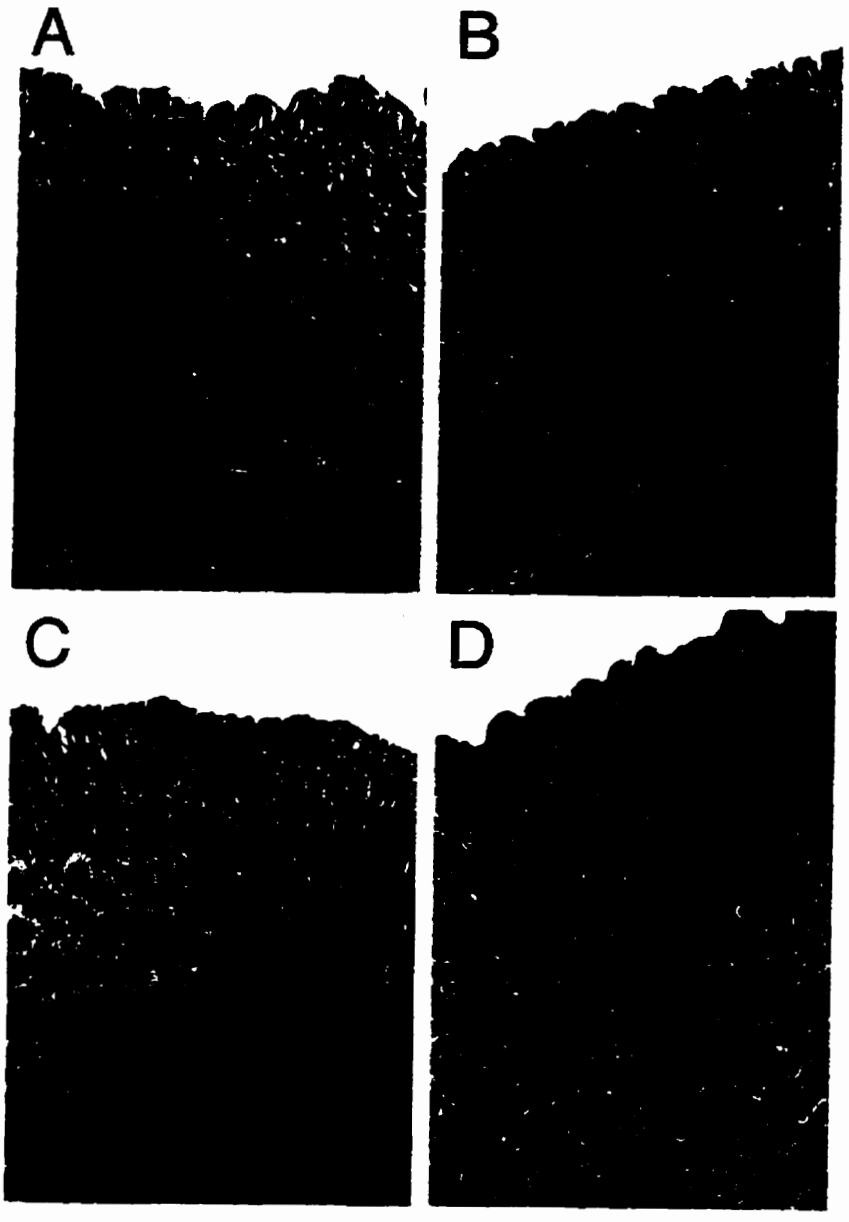

Figure 2

Figure 2. Histologic Features of the Intimal Cushion of Ductus Arteriosus

Light microscopic sections of a Movat staining of DA in (**A**), and Ao in (**B**) from 100-day gestation fetal lambs. Both vessels are similar in appearance. By 138 days of gestation, well-developed "intimal cushions" are visible in the DA tissue section in (**C**), which are characterized by an expanded subendothelial space (the blue stained region). As well, elastic laminae are fragmented, and SMC of inner media appear to migrate towards subendothelial space (indicated by arrows). This is in contrast to the 138-day Ao tissue section (**D**) (Modified from Boudreau N and Rabinovitch M, Lab Invest 64:187-199, 1991).

138 days of gestation, the intimal cushion of the DA (**C**) is well developed compared to Ao (**D**). In addition, medial SMC near the expanded subendothelial space are detached from each other and surrounded by increased amount of ECM materials. They are radially oriented and appear to be migrating toward the subendothelium.

Mechanisms Related to Intimal Cushion Formation

Characterization of specific features of the intimal cushion *in vivo* provided the morphological basis for studying the biochemical and cellular events related to their formation. Thus, primary cultures of DA EC and SMC were developed and characterized by cell-specific antigens and by other features which assured that they had maintained their phenotypic properties related to their vascular site of origin (Rabinovitch, *et al.*, 1988). DA EC and SMC showed quantitative and qualitative differences in protein synthesis compared to cells from the Ao and PA (Rabinovitch, *et al.*, 1988). A 43 kD protein present in increased concentration in the DA EC was later identified as SPARC (secreted protein rich in aspartic acid and cysteine) (Rabinovitch, unpublished data) and a 52 kD protein in DA SMC not found in the Ao or PA SMC was further purified and identified as a truncated form of tropoelastin (Hinek and Rabinovitch, 1993). As well, DA SMC show unique alterations in prostaglandin synthesis in response to altered oxygen tension (Rabinovitch, *et al.*, 1989) that mimics the response elicited *in vivo* (Clyman, 1987). That is, in response to hyperoxia, DA EC and SMC increase production of PGE_2 and 6-keto $PGF_{1\alpha}$, respectively.

Extracellular matrix production. A series of studies was subsequently undertaken using the primary EC and SMC cultures isolated from the fetal lamb DA (Boudreau, 1990; Boudreau and Rabinovitch, 1991; Boudreau, *et al.*, 1991; Hinek, *et al.*, 1991; Hinek and Rabinovitch, 1993; Hinek and Rabinovitch, 1994) to investigate biosynthesis of ECM components and their role in SMC migration. The DA-specific changes in ECM production were established by comparing DA cells with cells from adjacent vascular sites, the Ao and PA. As well, the

developmentally regulated changes in ECM production related to the *in vivo* intimal cushion formation were determined by comparing their production in DA cells from the 100-day gestation lamb with that from 138-day gestation lambs. The results of these studies are summarized in the Schema in Figure 3. Our laboratory demonstrated an increased synthesis of glycosaminoglycans, hyaluronan, and heparin sulfate, as well as their incorporation into ECM in cultured DA EC compared to Ao and PA EC. Synthesis of FN and chondroitin sulfate in DA SMC was also increased. Interestingly however, all these DA-specific increases in the ECM production were apparent in cells cultured from the 100-day gestation lambs before the appearance of intimal cushions observed *in vivo*. This suggests that DA cells have differentiated from other vascular cells within the first 100 days of gestation. The high synthetic activities of DA EC and SMC at this early gestation time-point appear to engineer the production of a matrix-enriched environment that facilitates subsequent SMC migration into the subendothelial space and ultimately leads to the formation of the intimal cushions observed *in vivo*.

In addition to quantitative differences in matrix production, DA cells also appear to generate matrix proteins that are also qualitatively different. For example, the tropoelastin produced by DA SMC is largely in the form of a truncated species with a molecular weight of 52 kD, as compared to its 68 kD counterpart found in the Ao SMC (Hinek and Rabinovitch, 1993). The truncated DA tropoelastin seems to result from reduced availability of the elastin binding protein in DA SMC, since this molecule serves as a companion protein protecting elastin from both intracellular and extracellular enzymatic degradation (Hinek, *et al.*, 1991; Hinek and Rabinovitch, 1994). As a result, a secreted truncated product of tropoelastin remains as a soluble and highly chemotactic peptide.

Smooth muscle cell migration. As mentioned above, the ability of hyaluronan to bind large amounts of water results in expansion of tissue space and allows for easy movement of cells (Toole *et al.*, 1984). Interaction of hyaluronan with its cell surface receptor, hyaluronan binding protein, promotes cell migration in a hyaluronan-rich environment (Turley and Torrance,

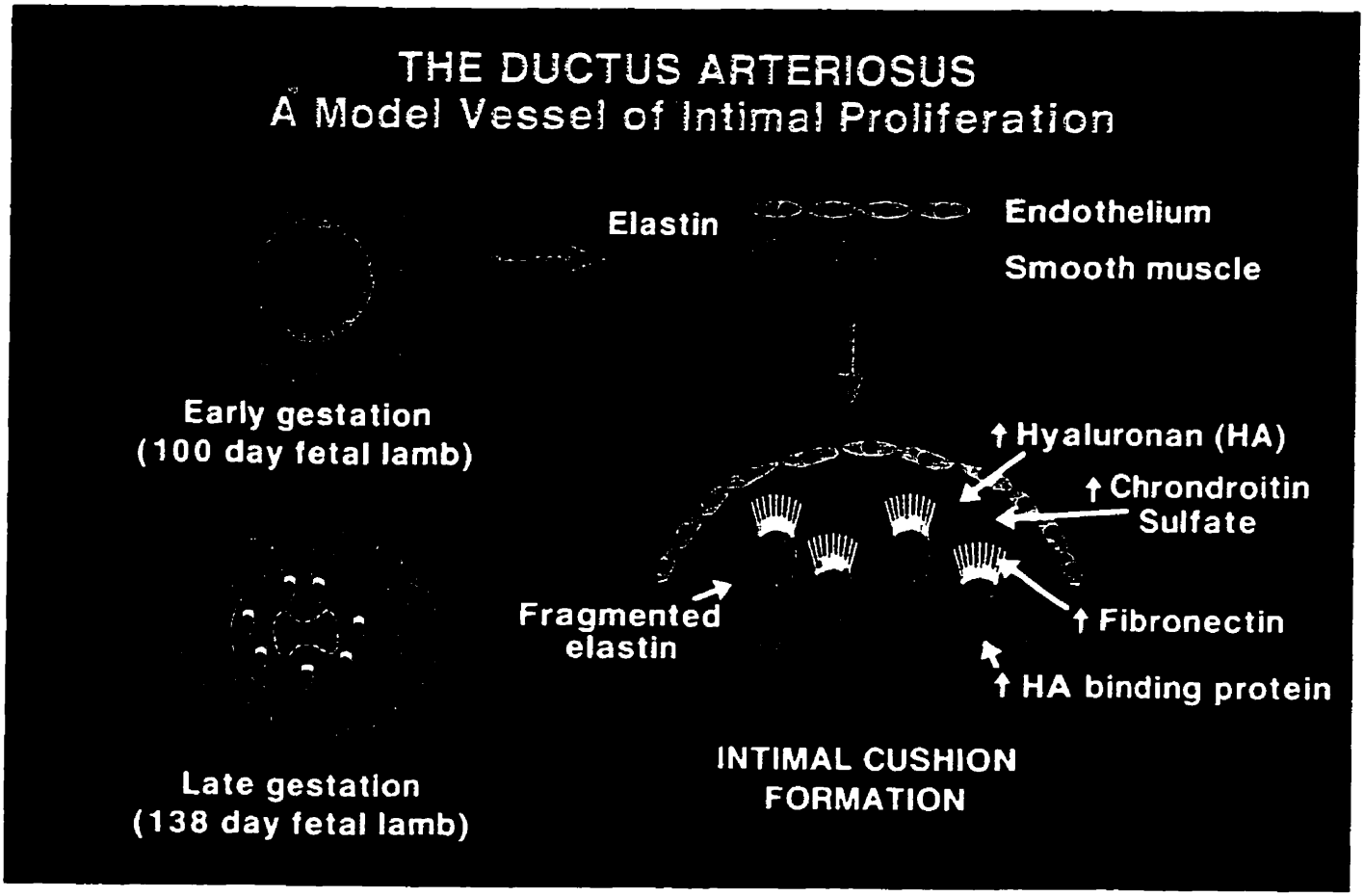
THE DUCTUS ARTERIOSUS
A Model Vessel of Intimal Proliferation
Elastin
Endothelium
Smooth muscle
Early gestation
(100 day fetal lamb)
Hyaluronan (HA)
Chrondroitin
Sulfate
Fragmented
elastin
Fibronectin
HA binding protein
Late gestation
(138 day fetal lamb)
INTIMAL CUSHION
FORMATION

Figure 3

Figure 3. Schematic summary of mechanisms related to DA neointimal formation as described in the text

1985). Similarly, FN production is increased in organogenesis and wound healing where activated cell migration is observed (Hynes, 1990). Indeed, in a subsequent *in vitro* cell migration assay. the increased synthesis of both DA-specific EC hyaluronan and SMC FN was correlated with the enhanced migration of DA SMC (Boudreau and Rabinovitch, 1991; Boudreau, *et al.*, 1991). For the first time, the phenotypic differences between DA and Ao SMC were appreciated *in vitro*. When DA SMC were cultured on a 3-dimensional collagen matrix, they exhibited an elongated fibroblast-like morphology with peripheral lamellae and lamellipodia extending from the leading edge (Figure 4**A**). A similar phenotype has been described in the other vascular SMC with locomotory behavior (Delovs *et al.*, 1982; Heath and Holifield, 1991; Bauriedel *et al.*, 1992). After a two-day culture, DA SMC that had migrated from the surface into the collagen gel could be detected (Figure 4**B**). In contrast, Ao SMC display a flattened stellate morphology and decreased ability to migrate into the collagen gel (Figure 4**C**). It appears that the migratory phenotype of DA SMC is dependent on their interaction with FN, since functional blockade of FN with polyclonal antibodies alters their shape (they become more like Ao SMC) (Figure 4**D**) and decreases their migration. Likewise, inhibition of interaction of cell surface integrin receptors with their ligands by addition of arginine-glycine-aspartate (RGD) peptide, a known cellular binding motif in FN and other ECM proteins, also changes the shape of DA SMC from elongated to stellate in appearance and reduces their migration.

The integrins involved in the FN-dependent migration of DA SMC are likely $\alpha 5\beta 1$ or $\alpha v\beta 3$, as their interaction with FN is susceptible to RGD inhibition (Hynes, 1990). This notion is supported by a later experiment in which integrin receptors involved in adhesion and migration of DA SMC on different ECM protein-coated surfaces were examined by blocking antibodies and immunofluorescent staining, and isolated by ligand affinity chromatography and immunoprecipitation (Clyman *et al.*, 1992). Adhesion and early migration of DA SMC on FN appears to rely on $\beta 1$ integrins, including $\alpha 5\beta 1$. Later migration however, depends on $\alpha v\beta 3$ integrin. Recently, transient expression of integrins, including $\alpha 5\beta 1$ and $\alpha v\beta 3$, has been documented during intimal cushion formation *in vivo* in the DA (Clyman *et al.*, 1996).

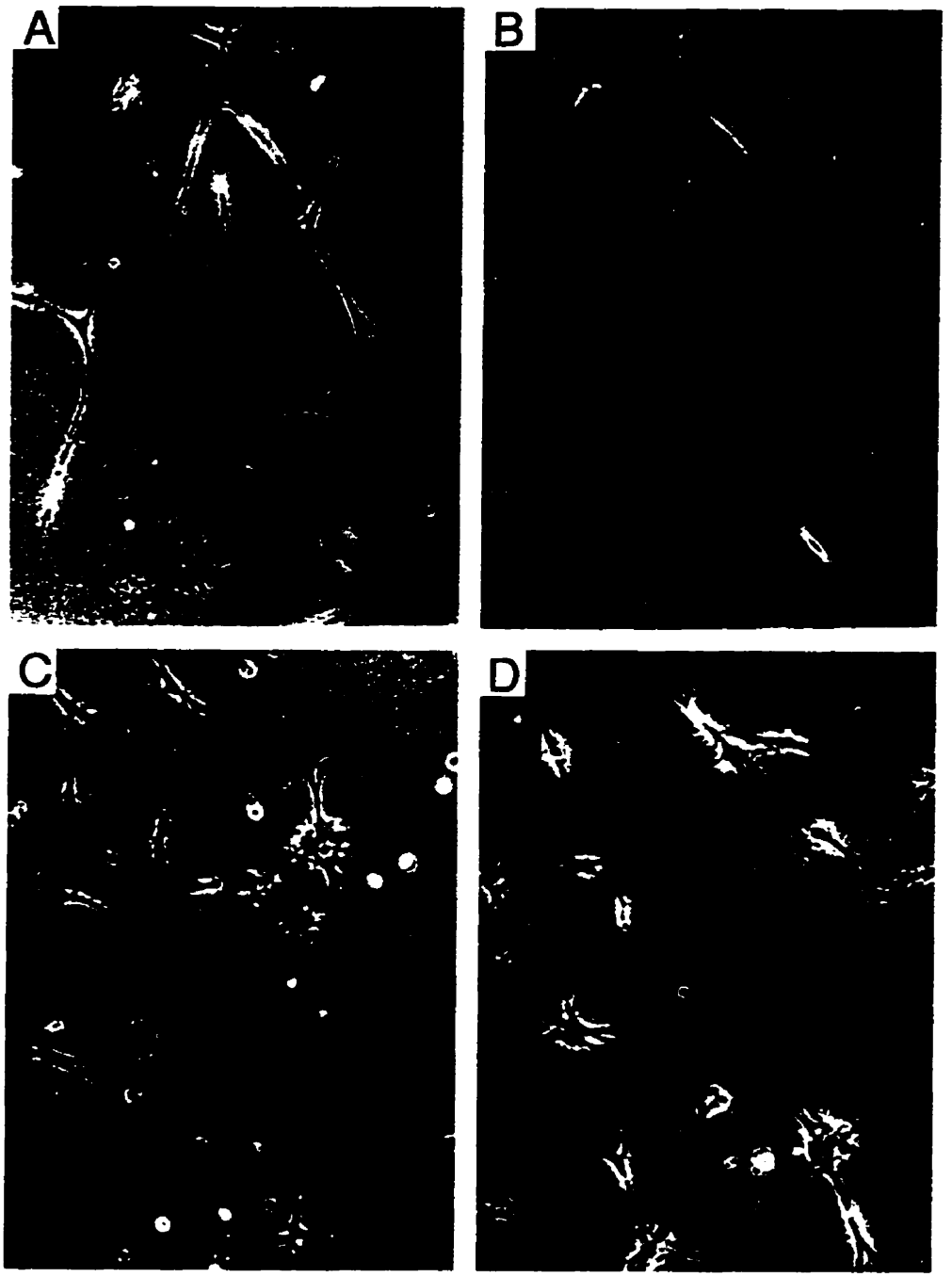

Figure 4

Figure 4. Migratory Phenotype of Ductus Arteriosus Smooth Muscle Cells

Phase-contrast microscopic photograph of DA and Ao SMC on collagen gel. DA SMC in (**A**) exhibit a spindle-like elongated morphology, and migrate into collagen two days after seeding (indicated by the arrow) (**B**). In contrast, Ao SMC in (**C**) have a more flattened and stellate-like phenotype, and fewer cells migrate into collagen (not shown in the picture). In addition, the presence of antibodies against FN alters phenotype of DA SMC in (**D**) into a more flattened and stellate appearance and inhibits migration of DA SMC (not shown in the picture) (Modified from Boudreau B., *et al.*, Dev Biol 143:235-247, 1991).

The increased synthesis of hyaluronan by DA EC may also contribute to migration of SMC *in vivo* through interaction of this matrix component with SMC receptors, i.e., the hyaluronan binding protein (renamed the receptor for hyluronan-mediated motility or RHAMM) (Hardwick *et al.*, 1992). Supplement of collagen gels with hyaluronan selectively enhanced migration of DA but not Ao SMC, and addition of antibodies against RHAMM selectively inhibited migration of DA SMC. In addition, DA SMC produce an increased amount of RHAMM which is concentrated in lamellipodia at the leading edges of the cells (Boudreau, *et al.*, 1991). Thus, the increased production of FN by DA SMC is essential in keeping their elongated mobile phenotype. In addition, FN and hyaluronan appear to interact cooperatively with their cell surface receptors to allow enhanced migration by DA SMC into a hyaluronan enriched subendothelial environment.

The increased synthesis of chondroitin sulfate by DA SMC may also promote their migration *in vivo*, since it can remove elastin binding proteins from the cell surface, leading to impaired assembly of elastin fibers, a feature characteristic of DA *in vivo* (Hinek, *et al.*, 1991). Removal of elastin binding proteins by chondroitin sulfate is associated with the induction of migration of DA SMC on elastin substrates (Hinek *et al.*, 1992). The truncated elastin peptide produced by DA SMC also lacks the C-terminal required for crosslinking and thereby fails to incorporate into a mature elastic fiber. This may contribute to the impaired assembly of elastin laminae observed *in vivo*. As well, the highly soluble and chemotactic properties of the truncated elastin peptide might also promote SMC migration independent of the features related to hyaluronan and fibronectin described above.

Transforming Growth Factor-β. Once the morphologic changes during DA intimal cushion formation were identified and the cellular events related to alterations in ECM production and migration of SMC were elucidated, further studies were undertaken to address the mechanisms involved in initiating these changes. The presence and potential influence of transforming growth factor-β (TGF-β), a known potent stimulator of ECM synthesis (Roberts and Sporn, 1989; Amento *et al.*, 1991), has been assessed during the development of the intimal cushions and

closure of the DA (Boudreau, *et al.*, 1992; Tannenbaum *et al.*, 1996). Abundant TGF-β1 was found in DA compared to Ao tissues from 100-day gestation fetal lambs by immunohistochemistry (Boudreau, *et al.*, 1992). Increased expression of all three isoforms of TGF-β is also noted associated with the closing DA shortly in the newborn lambs (Tannenbaum, *et al.*, 1996). The role of TGF-β on the synthesis of ECM proteins has been studied in the cultured EC and SMC from the fetal lamb DA and Ao. The increased hyaluronan synthesis in DA compared to Ao EC is TGF-β-dependent, since a TGF-β neutralizing antibody reduced synthesis of hyaluronan in the cultured DA EC to the levels observed in Ao EC, but has no effect on its synthesis in the Ao EC. However, unlike other studies showing that TGF-β increases FN expression by enhancing its transcription and mRNA stability (Dean *et al.*, 1988; Kahari *et al.*, 1991; Kahari *et al.*, 1992), the enhanced FN synthesis in DA SMC did not appear to be TGF-β-mediated. Instead, a post-transcriptional mechanism which increases FN mRNA translation appeared to be involved (Boudreau, *et al.*, 1992).

Transforming Growth Factor-β

TGF-β is a member of the polypeptide growth factor families that control embryonic development and tissue homeostasis. It was originally isolated from human platelets (Assoian *et al.*, 1983), human placenta (Frolik *et al.*, 1983), and bovine kidney (Roberts *et al.*, 1983). Three isoforms (TGF-β1, TGF-β2, TGF-β3) exist in mammals with 60% to 80% identities (Massague. 1990). They are disulfide-linked homodimeric peptides with a molecular weight of 25 kD.

Structure and Function

The human TGF-β1 gene is located at chromosome 19q13.1-q13.3 (Fujii *et al.*, 1986) and contains 7 exons (Derynck *et al.*, 1987). TGF-β1 mRNA is approximately 2.4 kb, encoding a TGF-β1 precursor with 390 amino acids that contains a signal peptide, the active peptide, and the latency associated peptide (Gentry *et al.*, 1987) (Figure 5). The disulfide-linked homodimers of

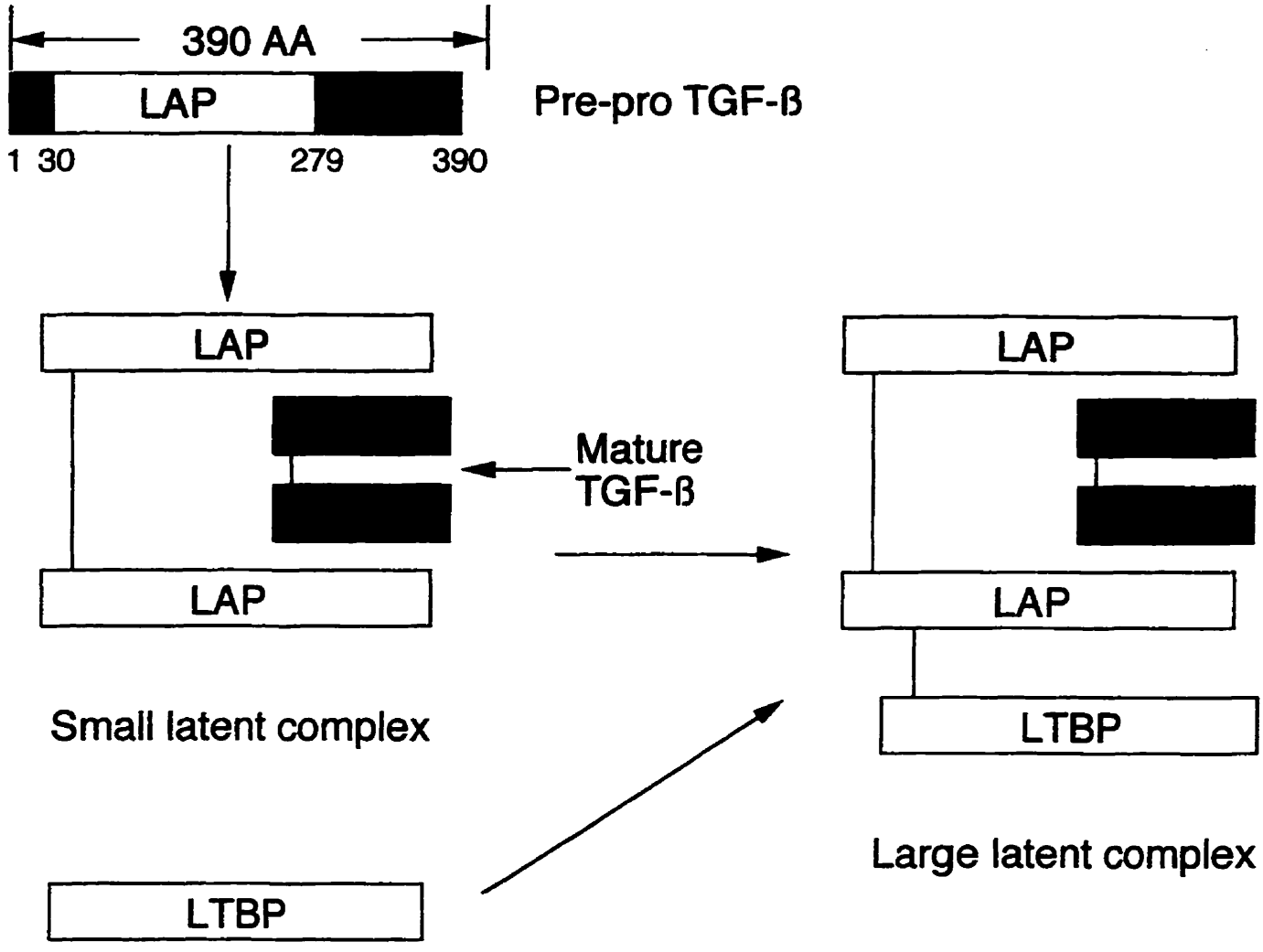
390 AA
LAP
Pre-pro TGF-ß
1 30
279
390
LAP
LAP
Mature
TGF-ß
LAP
LAP
LTBP
Small latent complex
Large latent complex
LTBP

Figure 5

Figure 5. Scheme of TGF-β1 and its latent complexes

TGF-β1 is synthesized as a 390-amino acid (AA) precursor peptide (top). The precursor peptide contains the signal peptide (AA residues 1-29), the latency associated peptide (LAP, AA residues 30-278), and mature TGF-β peptide (residues 279-390). The small latent complex consists of the TGF-β homodimer, noncovalently associated with the homodimeric form of LAP (middle). In some cells, the small latent complex associates with an additional 125- to 160-kD protein, the latent TGF-β binding protein (LTBP), to form the large latent complex (Modified from Rrande J.P., Proc Soc Exp Biol Med 214:27-40, 1997).

TGF-β1 noncovalently interact with homodimers of the latency associated peptide and form a small latent complex (Harpel *et al.*, 1992; Olofsson *et al.*, 1992). This small latent complex associates with an additional protein, named the latent TGF-β-binding protein (Pircher *et al.*, 1986; Kanzaki *et al.*, 1990)), and is secreted as an inactive high molecular weight precursor polypeptide (Wakefield *et al.*, 1988; Miyazono *et al.*, 1990). After removal of the signal peptide (1-29 amino acid residues), the complex undergoes proteolytic cleavage between two arginine residues at position 278 and 279 to generate the mature TGF-β1 monomer, a 112-amino acid peptide from the carboxyl-terminal of the precursor, and a proximal 249-amino acid peptide, the latent associated peptide (Olson *et al.*, 1986; Gentry, *et al.*, 1987; Gentry *et al.*, 1988). The mature TGF-β1 can be released from the latent complexes and activated by a number of different processes, including transient acidification or alkalization, exposure to 0.02% sodium dodecyl sulfate (SDS) or 8 M urea, and protease activation (Lyons *et al.*, 1988; Miyazono *et al.*, 1988; Lyons *et al.*, 1990; Miyazono, *et al.*, 1990). It has also been shown that co-cultures of vascular EC and SMC produce activated TGF-β1 (Antonelli-Olridge *et al.*, 1989). TGF-β1 has a variety of effects on development, differentiation, wound healing, and tissue remodeling. TGF-β1 has also been extensively studied in the cardiovascular system.

Expression and Role of TGF-β1 during Cardiovascular Development

The temporal and spatial expression of TGF-β1 has been characterized in association with cardiac development (Choy *et al.*, 1991; Millan *et al.*, 1991). The epithelial-mesenchymal cell transformation in the embryonic heart appears to be mediated in part by TGF-β1 (Potts and Runyan, 1989). "Knockout" experiments indicate that TGF-β1 is important in normal cardiogenesis, since severe cardiac abnormalities, including a poorly developed ventricular lumen with disorganized ventricular muscle and valves, have been observed in mice homozygous for the mutant TGF-β1 allele born to a homozygous TGF-β1 null female to prevent trans-placental transmission of TGF-β1 (Letterio *et al.*, 1994). TGF-β1 is also required for the normal development of the vascular system, since 50% of TGF-β1 null mice die from a severe defect in

yolk-sac vasculogenesis, probably resulting from abnormal interaction between epithelial and mesenchymal cells (Dickson *et al.*, 1995). In an organ culture that fuses myocardial cell aggregates with cardiac mesenchymal cell aggregates, TGF-β1-mediated induction of interstitial matrix production and deposition leads to the differentiation of these two tissues (Armstrong and Armstrong, 1990) and stimulates cellular proliferation (Choy *et al.*, 1990). In normal development, latent TGF-β1 produced by EC is activated when these cells interact with mesenchymal cells (Antonelli-Olridge, *et al.*, 1989). The activated TGF-β1 then stimulates matrix production and deposits (Roberts and Sporn, 1989; Nabel *et al.*, 1993; Kanzaki *et al.*, 1995; Saltis *et al.*, 1996; Grande, 1997), induces differentiation of the mesenchymal cells into SMC, and inhibits EC proliferation (Antonelli-Olridge, *et al.*, 1989).

The presence of TGF-β1 in Vascular Intimal Thickening

Upregulation of TGF-β1 expression is associated with vascular intimal thickening resulting from hypertension (Sarzani *et al.*, 1989; Sarzani *et al.*, 1991), atherosclerosis (Ross, 1993; Lopez-Candales *et al.*, 1995), vein graft (Hoch *et al.*, 1995), and angioplasty (Majesky *et al.*, 1991; Nikol *et al.*, 1992), as well as advanced pulmonary vascular disease in patients (Bahadori *et al.*, 1995) and in rats or sheep with experimental pulmonary hypertension (Perkett *et al.*, 1994; Tanaka *et al.*, 1996a; Tanaka *et al.*, 1996b). TGF-β1 expression is increased in the thickening intima in human coronary arteries (Merrilees and Beaumont, 1993). TGF-β1 mRNA levels in Ao are also elevated in chronic steroid hypertension, induced in rats by deoxycorticosterone and a high salt diet (Sarzani, *et al.*, 1989), and in spontaneously hypertensive rats (Sarzani, *et al.*, 1991). The upregulation of TGF-β1 expression in the spontaneously hypertensive rats is dependent on both age and the severity of hypertension. In a rabbit renal hypertensive model, however, the expression of TGF-β1 in Ao appears normal once the hypertension develops, but elevated matrix production is prolonged, presumably due to the activation of latent TGF-β1 complex (Pauletto *et al.*, 1994). In a balloon-injured rat carotid artery, induction of TGF-β1 gene transcription occurs within 6 hours after injury, reaches a maximum by 24 hours, and is sustained for the next 1-2 wk

(Majesky, *et al.*, 1991; Kim *et al.*, 1995). The neointimal SMC are the sources of TGF-β1 production, and its distribution correlates with increased production of matrix proteins, particularly FN and collagens. This observation suggests that TGF-β1 promotes the progression of neointimal thickening by augmenting matrix deposition.

Effects of TGF-β1 on Vascular Neointima Formation

The influence of TGF-β1 on vascular neointimal formation has been studied with respect to its ability to stimulate matrix synthesis (Amento, *et al.*, 1991; Rasmussen *et al.*, 1995), alter cell growth (Owens *et al.*, 1988; Halloran *et al.*, 1995), and induce de-differentiation (Owens, *et al.*, 1988). Cultured Ao SMC isolated from the neointima contain more TGF-β1 mRNA and are stimulated by TGF-β1 to produce more proteoglycans compared to SMC isolated from the normal vessel wall (Rasmussen, *et al.*, 1995). TGF-β1 also stimulates collagen I and III synthesis in human vascular SMC (Amento, *et al.*, 1991; Villarreal *et al.*, 1996). TGF-β1 inhibits proliferation of vascular SMC (Owens, *et al.*, 1988; Halloran, *et al.*, 1995) and induces cellular hypertrophy (Owens, *et al.*, 1988). The direct evidence for the participation of TGF-β1 in the development of the vascular neointima comes from *in vivo* experiments in which infusion of TGF-β1 (Kanzaki, *et al.*, 1995) or direct transfer of the TGF-β1 gene (Nabel, *et al.*, 1993) into the vessel wall induced intimal hyperplasia predominantly due to production of ECM components, including proteoglycans, collagens, and FN. Conversely, antibodies against TGF-β1 suppress intimal hyperplasia in an acutely injured vessel by reducing accumulation of ECM components, such as FN (Wolf *et al.*, 1994). Molecular mechanisms governing TGF-β1-induced matrix protein synthesis have been elucidated at transcriptional (Kahari, *et al.*, 1991; Marigo *et al.*, 1993), post-transcriptional (Kahari, *et al.*, 1991; Wrana *et al.*, 1991; Kahari, *et al.*, 1992; Marigo, *et al.*, 1993), and translational levels (Fine and Goldstein, 1993).

Regulation of TGF-β1 Expression

TGF-β1 can be regulated by mechanisms which influence its transcriptional activation.

mRNA stability, or mRNA translational efficiency. Post-translational activation of latent TGF-β1 and inactivation of mature TGF-β1 by binding to ECM macromolecules also contribute to the functional regulation of TGF-β1 (Massague, 1990). The proposed mechanisms for transcriptional, post-transcriptional, and translational regulation of TGF-β1 will be outlined, since they are directly related to the findings of this thesis.

Transcriptional Regulation. Upregulation of TGF-β1 is a common feature in a variety of wound healing and tissue remodeling responses in many organ systems, including vessels (Border and Nobel, 1994). Transcriptional activation of the TGF-β1 gene is an important and early cell response to injury. The human (Kim *et al.*, 1989a) and mouse (Geiser *et al.*, 1991) TGF-β1 promoter has been cloned and there is a high degree of similarity. The TGF–β1 promoter contains no TATA or CAAT box (Kim, *et al.*, 1989a; Geiser, *et al.*, 1991). Human TGF-β1 has an extremely high G-C content with multiple CCGCCC repeats (Kim, *et al.*, 1989a). At least two of these G-C repeats have been shown to bind the transcription factor Sp1 (Kim *et al.*, 1989b). Gel mobility shift assays have also demonstrated that formation of AP-1 complexes (jun and fos) are involved in TGF-β1 transcription in response to phorbol ester and TGF-β1 itself (Kim *et al.*, 1990). A downstream phorbol ester responsive element has been also identified in the 3'UTR (Scotto *et al.*, 1990). These observations suggest that the initiating signal for stimulation of synthesis of TGF-β1 may occur via the activation of protein kinase C. In addition, the TGF-β1 promoter contains several sequences with homology to the retinoblastoma gene product control element which is modulated by the retinoblastoma gene product (Kim *et al.*, 1991), as well as an element responsive to H-*ras* oncogene activation (Geiser, *et al.*, 1991). However, the influence of these regulatory controls on TGF-β1 expression in vascular cells during vascular injury has not been evaluated. Auto-regulation of TGF-β1 via the activity of AP-1 and Sp1 transcription factors (Kim, *et al.*, 1989b; Kim, *et al.*, 1990) is likely to be an important mechanism in sustaining TGF-β1 expression at sites of injury. As a consequence, elevated production of matrix proteins gives rise to matrix accumulation.

Post-transcriptional Regulation. There is also increasing evidence indicating that expression of TGF-β1 is modulated at post-transcriptional and translational levels (Assoian *et al.*, 1987; Wager and Assoian, 1990; Ahuja *et al.*, 1995; Cosgaya and Aranda, 1995). For example, in a rat pheochromocytoma PC12 cell line, nerve growth factor induces TGF-β1 expression partly by increasing its mRNA half life from 6 h to 30 h (Cosgaya and Aranda, 1995). In activated human T lymphocytes, the immunosuppressant cyclosporine prolongs the half life of TGF-β1 mRNA (Ahuja, *et al.*, 1995). In human osteosarcoma, exogenous administration of TGF-β1 raises the steady-state TGF-β mRNA level by enhancing its stability (Liu *et al.*, 1996). As well, treatment of hematopoietic cells with phorbol ester leads to 30-fold increase in TGF-β1 expression, resulting from a stabilized mRNA because phorbol ester blocks a ribonuclease system that degrades TGF-β1 mRNA (Wager and Assoian, 1990). Thus, control of TGF-β1 expression via phorbol ester-induced protein kinase C may operate at both transcriptional and post-transcriptional levels.

Regulation of TGF-β1 mRNA translation. TGF-β1 expression may also be regulated at the level of mRNA translation. Several studies indicated that the GC-rich sequence in the 5' untranslated region may play a role in controlling TGF-β1 mRNA translation (Kim *et al.*, 1992). This region in the 5'UTR contains a stable secondary stem-loop structure between sequences +49 to +76. This stem-loop region alone is sufficient to inhibit growth hormone gene expression, suggesting that it may contain a *cis* element which plays an important role in the translational regulation of TGF-β1 gene expression. Binding of a cytoplasmic factor in C2C12 myoblastic cells to the stem-loop containing region has been demonstrated by *in vitro* gel shift and UV-crosslinking assays (Romeo *et al.*, 1993). In addition, a GC-rich domain in the TGF-β1 3'UTR has been shown to have a bifunctional effect on overall protein expression (Scotto and Assoian, 1993); it may decrease the steady-state levels of TGF-β1 mRNA while increasing its protein production by improving translational efficiency. The relative contributions of these inhibitory and stimulatory bifunctional elements to TGF-β1 protein production may result from temporal or cell-specific expression of certain *trans*-acting factors (Scotto and Assoian, 1993).

Fibronectin

The first description of FN appeared in 1948 when Morrison and colleagues (Morrison *et al.*, 1948) studied the fractionation of plasma and separated a protein fraction from the bulk of the fibrinogen by its cold insolubility. They termed this protein fraction "cold-insoluble globulin" (CIg) and further work indicated that it was a mixture of several components, including fibrinogen (Edsall *et al.*, 1955). It was only in 1970, some 20 years after the first description of CIg, that the purified CIg was obtained and identified as a protein distinct from other plasma proteins (Mosesson and Umfleet, 1970). In the early 70's, immunologic studies indicated that a large glycoprotein lost from the cell surface of virus-transformed fibroblasts (Grahmberg and Hakomori. 1973; Hynes, 1973b) is related to CIg (Ruoslahti and Vaheri, 1974; Vaheri and Ruoslahti, 1974) and further biochemical studies confirmed their similarities (Mosesson *et al.*, 1975; Engvall and Ruoslahti, 1977; Hynes and Destree, 1977; Yamada *et al.*, 1977). In 1976, a unified term. fibronectin, was used to refer to this class of proteins (Keski-Oja *et al.*, 1976; Kuusela *et al.*. 1976).

Structure and Function

Fibronectin is a large dimeric glycoprotein composed of two homogeneous subunits of molecular weight 220-250 kDa linked by disulfide bonds. This characteristic applies to both plasma FN and cellular or ECM-bound FN. For practical purposes, three other criteria are also used to define a protein as FN: immunological recognition by specific antibodies, gelatin-binding activity and a molecular weight of 220-250 kD. The latter is based on a gelatin affinity chromatography method used for rapid purification of both plasma and cellular FN (Engvall and Ruoslahti, 1977; Hynes and Yamada, 1982; Ruoslahti *et al.*, 1982). A single gene encodes all known forms of FN (Kornblihtt *et al.*, 1983; Schwarbauer *et al.*, 1983; Kornblihtt *et al.*, 1984a; Kornblihtt *et al.*, 1984b). Analysis of the 5' and 3' ends of the rat FN gene indicates that the primary transcript has a single transcriptional initiation site and a single polyadenylation site 71 kb

downstream (Patel *et al.*, 1987). This primary transcript is spliced into a 7.5-8.0 kb mature transcript (mRNA), including 45 invariant exons and three alternatively spliced exons. The alternative splicing of these exons gives rise to variant forms of FN.

Fibronectin sequence is composed of a series of three different repeating domains (I, II, III) of similar sequence elements which are 40-90 amino acids long (Figure 6). Both fibrin-binding domains contain type I repeats, the gelatin-binding domain consists of both type I and type II repeats, and the central segment (the cell and heparin-binding domain) is composed of type III repeats (Hynes, 1990). The three alternatively spliced regions are located at the type III regions of the central segment. They are the EIIIA and EIIIB regions with identical sequence to type III repeat, and the variable insertion of fragments of sequence (V region), which are also called type III connecting segment (IIICS), near the carboxyl terminal. The EIIIA and EIIIB regions are alternatively spliced in many cell types and present only in the cellular forms of FN (Garcia-Pardo *et al.*, 1985; Kubomura *et al.*, 1987; Norton and Hynes, 1987).

The primary and usual function of FN is that of cell adhesion. Cell adhesion is an active process starting from initial attachment, spreading and cytoskeletal organization, to the formation of focal contacts with the substrate (Grinnell, 1978; Thom *et al.*, 1979; Couchman and Hook, 1983). Fibronectin is functionally involved in all these processes through a family of transmembrane extracellular matrix binding receptors, integrins. Integrins are comprised of heterodimeric α- and β-subunits that mediate cell adhesion (Albelda and Buck, 1990), as well as cell-matrix interactions (Buck and Horwitz, 1987). Fibronectin has multiple cell-binding sites that mediate cell adhesion. One is located in the 10th type III repeat of the cell-binding domain that contains a tripeptide sequence, RGD (Arg-Gly-Asp) (Pierschbacer and Ruoslahti, 1984). It is recognized by a variety of cells through the cell surface integrin receptors $\alpha 5\beta_1$, the 'classic' FN receptor (Ruoslahti and Pierschbacher, 1987; Ruoslahti, 1991). The 10th type III repeat is constitutively spliced in and present in all FN variants. Another cell-binding site is located in the IIICS which contains the LDV (Leu-Asp-Val) sequence (Komoriya *et al.*, 1991). The cell surface receptor for the LDV ligand is $\alpha 4\beta_1$, a member of the very late antigens (VLA) family.

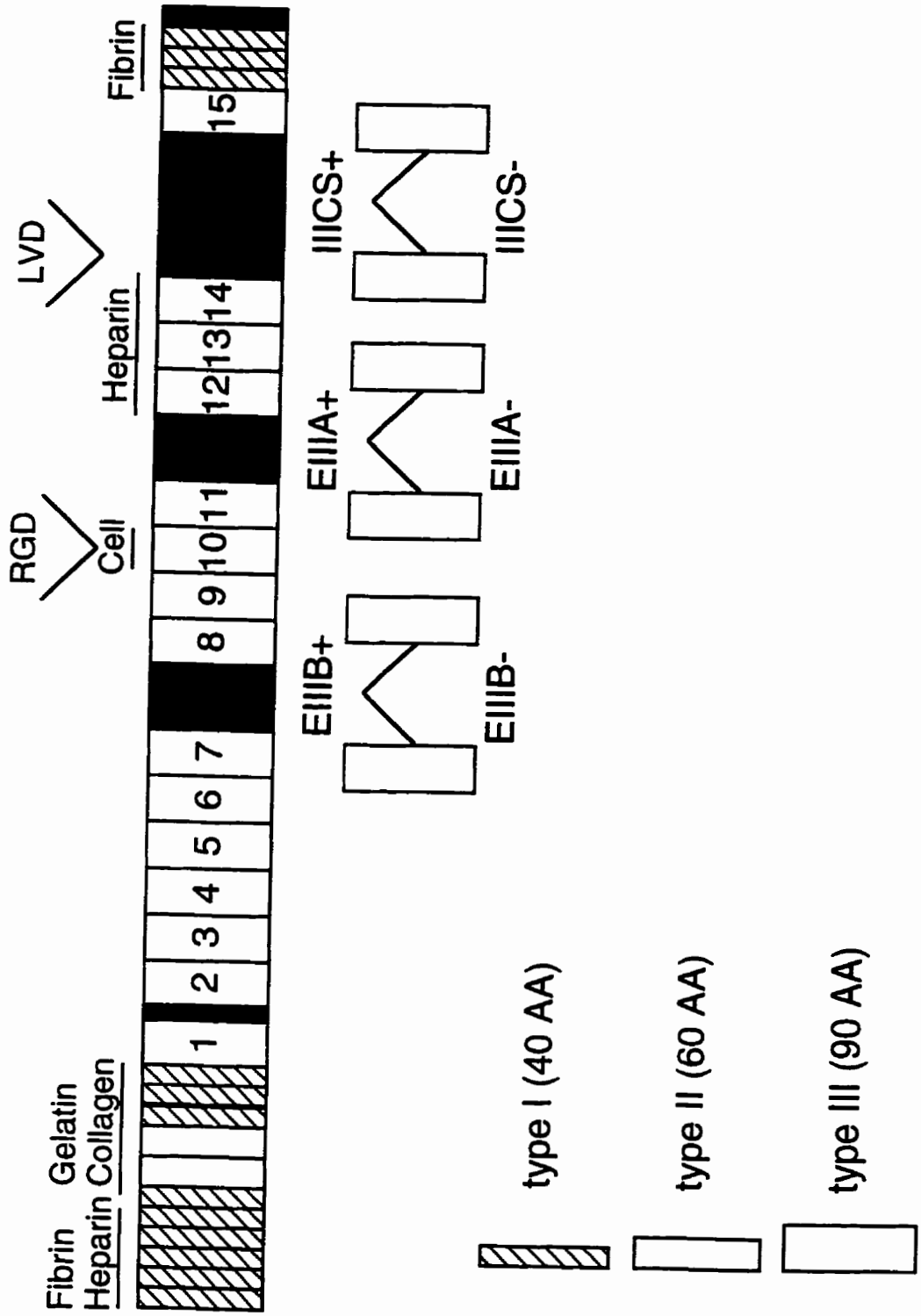
Fibrin
Heparin
Gelatin
Collagen
1
2
3
4
5
6
7
8
9
10
11
RGD
Cell
12
13
14
Heparin
LVD
15
Fibrin
EIIIB+
EIIIB-
EIIIA+
EIIIA-
IIICS+
IIICS-
type I (40 AA)
type II (60 AA)
type III (90 AA)

Figure 6

Figure 6. FN structures and variants

Schema of the primary sequence of the various forms of FN. The sequence is made up of a series of repeats of the three types with internal homologies. Each repeat is separated from its neighbour in the gene by introns (not shown in the diagram). On the top, the constitutive (RGD), alternatively spliced (LDV) cell-binding sites, and functional domains for matrix assembly are indicated. At the bottom, the alternatively spliced segments in the type III repeat region including two type III repeats, EIIIA and EIIIB, and the third segment with various length and no homology to other segments, which was referred to as the type III connecting segment (IIICS). Type III repeats are numbered from 1 to 15, excluding the EIIIA and EIIIB (Modified from Kornblihtt A.R., *et al.* FASEB J, 10:248-257, 1996).

characteristic of lymphoid cells (Guan and Hynes, 1990; Mould *et al.*, 1990). Thus, most cells would utilize mostly the integrin receptor $\alpha 5\beta 1$ for adhesion and for spreading on a FN matrix, whereas certain cell types, such as melanoma, lymphocytes, and monocytes, likely use $\alpha 4\beta 1$ receptor to bind the alternative spliced LDV sequence.

Expression of Fibronectin during Cardiovascular Development

Successful organogenesis requires migration of mesenchymal cells on ECM. The temporal and spatial expression of FN during cardiovascular development have been well documented (Icardo and Manasek, 1983; Icardo and Manasek, 1984; Linask and Lash, 1986; ffrench-Constant and Hynes, 1988; Linask and Lash, 1988; Armstrong and Armstrong, 1990; Roman and McDonald, 1992; Samuel *et al.*, 1994). Quantitative and qualitative alterations in FN distribution are observed during cardiac development (Icardo and Manasek, 1983); and high FN expression is specifically present in migratory cells involved in the formation of the cushion tissue mesenchyme in the embryonic heart (Icardo and Manasek, 1984). Consistent with these features, FN mRNA levels are abundant in the migrating mesenchymal cells of the outflow tract and in the endocardial cushion cells (ffrench-Constant and Hynes, 1988). The importance of FN for successful embryonic development is conclusively illustrated by the lethal effect of the mouse FN null mutation, in which lack of normal vasculogenesis is one of the major defects observed in this knockout mouse (George *et al.*, 1993). Temporal expression of FN EIIIA and EIIIB variants was addressed in fetal and post-natal development of the human Ao (Glukhova *et al.*, 1990). This study showed that FN expressed in Ao during early fetal development (8 to 12 week) contains both EIIIA and EIIIB variants, but these isoforms are decreased by 20-25 weeks of gestation. In contrast, the medial layer of the adult Ao produces FN which contains neither EIIIA nor EIIIB domains, whereas the SMC in the thickened intima of an atherosclerotic plaque express FN containing the EIIIA variant.

Effect of Fibronectin on Cardiovascular Development

During embryonic development, vascular precursors migrate from an undifferentiated site of origin to their eventual tissue or organ of destination. This migration is a slow, orderly process. in which matrix FN provides a migratory tract (Hynes and Lander, 1992). Upon binding to FN. integrin receptor molecules cluster and transmit this spatial orientation across the cell membrane and the intracellular cytoskeleton, allowing the actin locomotory apparatus to follow the preset FN gradient (Chen *et al.*, 1986). For example, avian precardiac cells migrate on a FN matrix, and the direction of their movement is dependent on the FN gradient (Linask and Lash, 1986; Linask and Lash, 1988; Armstrong and Armstrong, 1990), since antibodies to FN or excessive RGD-containing synthetic peptides inhibit, in a dose-dependent manner, migration of these cells and subsequent heart development. Capillaries are also associated with an abundant FN-enriched matrix (Risau and Lemmon, 1988), and microvascular EC adhesion is significantly enhanced by FN (Clark and Folkvord, 1986). In the FN knockout mouse, lack of a FN gradient, which is produced normally by vascular EC (Risau and Lemmon, 1988; ffrench-Constant *et al.*, 1989) to support recruitment and differentiation of mesenchymal cells, results in impaired vasculogenesis (George, *et al.*, 1993).

Altered Fibronectin Expression in Vascular Intimal Thickening

Increased FN expression has been observed in the neointima of human atherosclerotic plaques (Shekhonin *et al.*, 1987). Further studies identified the embryonic EIIIA FN variant as the main FN component in the intimal lesion, whereas it was not detected in the medial layers or normal vessel (Glukhova *et al.*, 1989; Glukhova, *et al.*, 1990). The expression of the EIIIA variant by SMC is phenotype-dependent, that is, it is a characteristic of 'synthetic' SMC versus 'contractile' SMC, as both FN EIIIA protein and mRNA expression were observed in synthetic cultured SMC derived from atherosclerotic lesions, but not in contractile cells derived from the medial layers of the vessel wall (Glukhova, *et al.*, 1989).

Elevated FN synthesis has also been found in restenotic human coronary arteries after

atherectomy or percutaneous balloon angioplasty (Clausell *et al.*, 1995), as well as in neointimal lesions in coronary arteries after experimental cardiac transplantation in piglets (Clausell *et al.*, 1993) and in the thickened intima induced by endothelial denudation (Madri *et al.*, 1989; Ishiwata *et al.*, 1994; Kim, *et al.*, 1995). The FN induced in neointima after endothelial denudation includes the EDIIIA and EDIIIB domains (Bauters *et al.*, 1995; Dubin *et al.*, 1995), but their functional significance is not known. In addition, upregulated FN expression is observed in the Ao of the hypertensive rat (Takasaki *et al.*, 1994), the thickened intima of hypertensive pulmonary arteries in the human (Botney *et al.*, 1992), and in the rat (Jones *et al.*, 1997). The embryonic FN EDIIIA variant is expressed in the vascular thickened intima in hypertensive arteries mainly associated with intimal hyperplastic 'immature' or 'synthetic' SMC (Pauletto, *et al.*, 1994).

Role of Fibronectin in Development of Vascular Neointima

Several roles have been attributed to FN during the formation of the vascular neointima. This glycoprotein has been shown to modulate SMC in primary cultures from a contractile to a synthetic phenotype, associated with loss of myofilaments, formation of a widespread rough endoplasmic reticulum and prominent Golgi bodies, and increased RNA and protein synthesis (Hedin and Thyberg, 1987; Hedin *et al.*, 1988). The RGD cell-binding motif in FN appears to be important in this phenotypic transition since incubation of cultured SMC with RGD peptides blocks the FN effect and SMC maintain their contractile phenotype in the cultures (Hedin, *et al.*, 1988). In contrast, substrate containing RGD peptides promotes the SMC switch from a contractile to a synthetic phenotype (Hedin *et al.*, 1989). Thus, interaction of FN with its receptor, $\alpha 5\beta_1$, on the surface of vascular EC and SMC *in vivo* is likely to modulate their synthetic phenotype, thereby elevating synthesis of ECM components, growth factors, and their receptors (Pauletto, *et al.*, 1994).

Fibronectin has also been implicated in the mechanism regulating SMC migratory behavior, a prominent feature of neointimal formation. Since migration of SMC during neointimal formation is non-random, it has been presumed that there is a specific FN gradient along which cells migrate

via interaction with $\alpha 5\beta 1$ integrins (Thyberg *et al.*, 1990), which, in a sense, recapitulates the migration observed in embryogenesis (Linask and Lash, 1986; Linask and Lash, 1988; Armstrong and Armstrong, 1990; Choy, *et al.*, 1990; George, *et al.*, 1993). This notion is supported by the fact that FN synthesis is increased shortly after vascular injury and is deposited mainly in the immediate subendothelium where the radially oriented SMC are directed to migrate (Jones, *et al.*, 1997).

Since FN is important in cell adhesion, a process involving attachment, spreading, organization of cytoskeletal filaments, and formation of focal adhesion contacts (Couchman and Hook, 1983), its role in cell migration must require the breaking, as well as formation of attachments. Thus, the net effect of FN on cell migration depends on adhesive forces and traction for movement. Studies of DiMilla and colleagues (1993) demonstrated that the initial adhesive strength determines migration speed and the maximal migration of human SMC on FN and type IV collagen occurs at an intermediate level of cell-matrix adhesiveness. Several factors contribute to this intermediate level of adhesiveness, depending on the cell type, and these include the production of proteolytic enzymes, the presence of FN in a soluble form versus its rapid deposition in the matrix, as well as the number and, perhaps most important, the availability of cell surface integrin and non-integrin matrix receptors which interact with other matrix molecules, such as hyaluronan (Bauer *et al.*, 1992; Clyman, *et al.*, 1992). Thus, the FN receptor $\alpha 5\beta 1$ can either mediate firm ECM attachment or cell migration depending on the microenvironment (Albelda and Buck, 1990; Darribere *et al.*, 1990).

Regulation of Fibronectin Expression

The molecular mechanisms regulating FN have been studied in embyrogenesis, wound repair, and tissue remodeling, i.e., conditions in which increased expression is observed. In contrast, decreased FN expression is a feature of oncogenically-transformed cells and the mechanisms involved have also been broadly studied.

Down-regulation of FN in Oncogenic Transformation. One of the pioneering observations in matrix biology is differences in (Buck, *et al.*, 1971) or the loss of cell surface glycoprotein (Grahmberg and Hakomori, 1973; Hynes, 1973a) in tumor virus transformed cells. This feature actually led to the identification of cellular FN (Mosesson, *et al.*, 1975; Chen *et al.*, 1976; Engvall and Ruoslahti, 1977; Hynes and Destree, 1977; Yamada *et al.*, 1977). Until now, it is still the most striking example of regulation of FN expression. Reduced FN expression has been observed in cells transformed with tumor viruses, such as human cytomegalovirus, Rous sarcoma virus (RSV), and adenovirus (Olden and Yamada, 1977; Yamada, *et al.*, 1977; Vaheri and Mosher, 1978; Hayman *et al.*, 1981; Pande *et al.*, 1990), or transfected with viral oncogenes, such as adenovirus early region 1A (E1A), Ha-ras, and v-mos (Roberts *et al.*, 1985; Setoyama *et al.*, 1985; Sistonen *et al.*, 1987; Chandler and Bourgeois, 1991; Nakajima *et al.*, 1992; Nakamura *et al.*, 1992; Chandler *et al.*, 1994). Decreased FN synthesis has also been seen in cell lines derived from malignant tumors (Pearlstein *et al.*, 1976; Marshall *et al.*, 1977; Yang *et al.*, 1980; Oliver *et al.*, 1983; Tai *et al.*, 1983; Steele *et al.*, 1988).

Many studies demonstrated that the loss of FN expression in tissue cultures correlates with their tumorigenesis *in vivo* (Chen, *et al.*, 1976; Ali *et al.*, 1977; Gallimore *et al.*, 1977; Marshall, *et al.*, 1977; Chen *et al.*, 1979; Der and Stanbridge, 1980; Der and Stanbridge, 1981; Lawrence and Singer, 1986; Steele, *et al.*, 1988). Thus, cells selected by growth in suspension or by passage in immunodeficient mice are often FN negative (Gallimore, *et al.*, 1977; Der and Stanbridge, 1980; Lawrence and Singer, 1986). Reduction of FN synthesis also contributes to their invasiveness and metastatic potential (Chen, *et al.*, 1979; Schalken *et al.*, 1988). Moreover, addition of purified FN to various transformed cells induces cell adhesion, promotes reorganization of the cytoskeleton, and allows the cell to adopt a more normal morphology (Chen, *et al.*, 1976; Yamada *et al.*, 1976; Ali, *et al.*, 1977). More recently, overexpression of recombinant FN in HT1080 cells has been shown to reduce their migration, and suppress their proliferation on soft agar, as well as their growth in nude mice (Akamatsu *et al.*, 1996). In addition, induction of FN synthesis in transformed or tumor cells by a variety of pharmacological reagents, such as cAMP (Nielson and

Puck, 1980), butyrate (Hayman *et al.*, 1980), dexamethasone (Furcht *et al.*, 1979a; Furcht *et al.*, 1979b), and oxamflatin (Sonoda *et al.*, 1996), by the tumor suppresser gene *krev-1* (Noda *et al.*, 1989), or by MP41, a gene regulated by the circadian clock (Kondo *et al.*, 1996) is also associated with a 'reverse transformed' cell phenotype that resembles normal cells.

Multiple mechanisms may contribute to reduced cell surface FN upon oncogenic transformation. In Rous sarcoma virus transformed chicken embryo fibroblasts, impaired FN biosynthesis, i.e., a 3- to 6-fold drop compared to the normal parent cells, is associated with a 5- to 6-fold reduction in cell surface FN (Olden and Yamada, 1977). *In vitro* translation studies using RNA extracted from normal and transformed chicken embryo fibroblasts demonstrate that FN mRNA levels are reduced in transformed cells (Fagan *et al.*, 1979), and this has been confirmed by northern blot analyses (Fagan *et al.*, 1981; Norton and Hynes, 1987). Nuclear run-on studies indicate that the reduction in FN mRNA level is due to decreased transcription (Tyagi *et al.*, 1983). However, the mechanism of how the Rous sarcoma virus oncoprotein, src, represses FN gene transcription is still unclear. In adenovirus E1A oncoprotein transformed rat fibroblasts, the reduction of FN gene transcription is through the induction of a nuclear repressor activity related to G10BP (G10 binding protein) (Nakamura, *et al.*, 1992). This nuclear factor binds to a string of 10 Gs present at -239 of the rat FN promoter, and two GC boxes at -105 and -54. The recognition sequences of G_{10}BP and transcription factor Sp1 overlap in the two GC boxes. Site-direct mutagenesis studies demonstrated that all of these elements are important in transcriptional activation, whereas the downstream GC box plays a primary role (Suzuki *et al.*, 1995). Since the nuclear factor G_{10}BP has a stronger affinity for the downstream GC box and G_{10} stretch than Sp1, binding of G_{10}BP replaces Sp1, thereby repressing FN gene expression. Post-transcriptional mechanisms can also regulate reduced FN expression in tumor cells. For example, in HT1080 fibrosarcoma cells, Ha-*ras* oncoprotein reduces either nuclear processing or nuclear stability of processed FN mRNA (Chandler, *et al.*, 1994).

Upregulation of FN: Transcriptional Mechanisms. Growth factors, cytokines,

hormones, and serum factors upregulate FN expression in a variety of cell types. Treatment of serum-starved 3T3 cells with epidermal growth factor (EGF) increases FN matrix deposits (Chen *et al.*, 1977) by increasing FN synthesis (Thorne *et al.*, 1987; Seebacher *et al.*, 1988) through gene transcription (Blatti *et al.*, 1988; Seebacher, *et al.*, 1988). Other growth factors, such as TGF-β (Dean, *et al.*, 1988; Kahari, *et al.*, 1991; Kahari, *et al.*, 1992), PDGF (Blatti, *et al.*, 1988; Zhang and Lo, 1995), and cytokines, such as interferon-γ (INF-γ) (Czaja *et al.*, 1987; Diaz and Jimenez, 1997), serum (Blatti, *et al.*, 1988; Dean, *et al.*, 1988; Ryseck *et al.*, 1989), and steroid hormones (Nimmer *et al.*, 1987; Dean, *et al.*, 1988) also induce FN synthesis in many cell types via transcriptional activation. As well, cytokines, such as IL-1β and tumor necrosis factor (TNF)-α stimulate FN gene transcription (Clausell and Rabinovitch, 1993; Molossi *et al.*, 1995) in vascular SMC.

The mechanisms involved in stimulating FN gene transcription have been investigated and transcriptional factors that bind to specific *cis* elements in FN promoter have been identified. There is, in fact, high identity between the human (Dean *et al.*, 1987), rat (Patel *et al.*, 1986), and mouse (Polly and Nicholson, 1993) FN promoter. Analysis of the human promoter in transient transfection studies using promoter-reporter constructs has identified TGF-β1, serum, and cAMP response elements (Dean, *et al.*, 1988; Dean *et al.*, 1989). The cAMP responsive element (CRE) is the *cis* element of serum stimulation in that it can by itself confer serum responsiveness to a neutral promoter (Dean *et al.*, 1990), and CRE binding activities have been demonstrated in nuclear extracts of diverse cell lines (Dean, *et al.*, 1989; Muro *et al.*, 1992). More recently, a tissue-specific transcriptional enhancer element has been reported in the rat FN gene (Sporn and Schwarzbauer, 1995). Gel mobility shift assays demonstrated fibroblast-specific binding of a nuclear factor(s) to this element and DNase I footprinting indicated the binding site contains a 27 bp sequence at -1688 of the rat FN gene. However, the effect of this enhancer element on endogenous FN gene transcription has not been examined.

Post-transcriptional Regulation. Post-transcriptional mechanisms also regulate FN

expression (Raghow *et al.*, 1987; Dean, *et al.*, 1988; Chandler and Bourgeois, 1991; Wrana, *et al.*, 1991; Chandler, *et al.*, 1994; Eckes *et al.*, 1996; Diaz and Jimenez, 1997). For example, despite elevated FN gene transcription, TGF-β1 also stabilizes FN mRNA (Raghow, *et al.*, 1987). As well, the synthetic glucocorticoid dexamethasone stabilizes FN mRNA selectively in a human fibrosarcoma cell line, HT1080 (Dean, *et al.*, 1988). Reduction of FN steady-state mRNA levels and FN synthesis in non-tumorigenic human osteosarcoma cells transfected with Ha-*ras*, as well as malignant human fibrosarcoma, HT1080, is not accompanied by decreased FN gene transcriptional activities and is linked to the activation of the Ha-*ras* oncogene (Chandler and Bourgeois, 1991; Chandler, *et al.*, 1994). The reduction is rather due to a mechanism that would alter nuclear FN mRNA stability and/or processing (Chandler, *et al.*, 1994).

Post-transcriptional regulation of FN may also involve alterations in the efficiency of mRNA translation as has been documented in early *Xenopus* development (Lee *et al.*, 1984). Temporal and spatial upregulation of FN expression observed shortly after the midblastula transition is related to translational activation of masked maternal FN mRNA, since transcriptional blockade by inhibition of RNA polymerase II dependent RNA synthesis with α-amanitin had no effect on the increased FN synthesis. Repression of FN synthesis has also been observed in fetal and postnatal development of the heart in which FN gene transcription is activated but the translation of the mRNA into protein is always poor (Samuel, *et al.*, 1994). In addition, prematurely senescent cultured Werner syndrome fibroblasts produce more FN than normal fibroblasts, due to both augmentation of FN mRNA levels and enhanced efficiency of FN mRNA translation (Rasoamanantena *et al.*, 1994). As well, the antiproliferative reagent IFN-γ modulates FN synthesis by stimulating FN gene transcription, destabilizing FN transcripts (Diaz and Jimenez, 1997), and repressing FN mRNA translation by a mechanism that inhibits translational elongation (Levine *et al.*, 1990).

Our previous studies on the mechanisms related to fetal DA intimal cushion formation demonstrated that cultured DA SMC produce up to 3-fold increased FN synthesis compared to Ao SMC after serum stimulation (Boudreau and Rabinovitch, 1991; Boudreau, *et al.*, 1992). Further

assessment of FN steady-state mRNA levels indicated that this feature was not associated with increased FN mRNA levels. Rather a 50% decrease in DA compared to Ao SMC levels was observed (Boudreau, *et al.*, 1992). In addition, there are no differences in FN mRNA stability or mRNA splicing between DA and Ao SMC (Boudreau, *et al.*, 1992). Together, these data indicated an enhanced translational efficiency of FN mRNA in DA versus Ao SMC, and the FN mRNA translational efficiency in DA SMC was estimated to be about 6-fold of that in Ao SMC (Figure 7).

Role of 3' AU-rich Elements in mRNA Translation

The importance of AU-rich elements (AREs) in the 3'UTR in the post-transcriptional regulation of eukaryotic gene expression was first noted in experiments in which oncogenic forms of the c-*fos* gene were found to have lost a 67-nt AT-rich sequence in the 3'UTR which was present in non-oncogenic forms of the gene (Meijlink *et al.*, 1985). When added to the 3'UTR of β-globulin mRNA, the ARE of c-*fos* (Treisman, 1985) and GM-CSF (Shaw and Kamen, 1986) destabilize otherwise stable β-globulin-reporter mRNA. Subsequent observations made by Caput and colleagues (Caput *et al.*, 1986) discovered that the ARE, particularly the octanucleotide UUAUUUAU sequence, is frequently present in the 3'UTR of inflammatory mediators or immediate early response genes, such as cytokines, oncogenes, as well as FN. Since then, the presence of the ARE has been shown to destabilize a large number of labile mRNAs, including c-*myc* (Jones and Cole, 1987), c-*fos* (Wilson and Treisman, 1988), INF–β (Whittemmore and Maniatis, 1990), IL-3 (Wodnar-Filipowicz and Moroni, 1990), and the human tissue factor (Ahern *et al.*, 1993). Recent studies have indicated that degradation of mRNA mediated by ARE is coupled to ongoing translation (Savant-Bhonsale and Cleveland, 1992; Aharon and Schneider, 1993; Winstall *et al.*, 1995). The ARE can either reduce or increase mRNA translational efficiency, but this likely depends on its interaction with tissue-specific cytoplasmic proteins (Kruys *et al.*, 1987; Kruys *et al.*, 1988; Kruys *et al.*, 1989; Han *et al.*, 1990a; Han *et al.*, 1990b; Grafi *et al.*, 1993; Kruys *et al.*, 1993; Jain *et al.*, 1997).

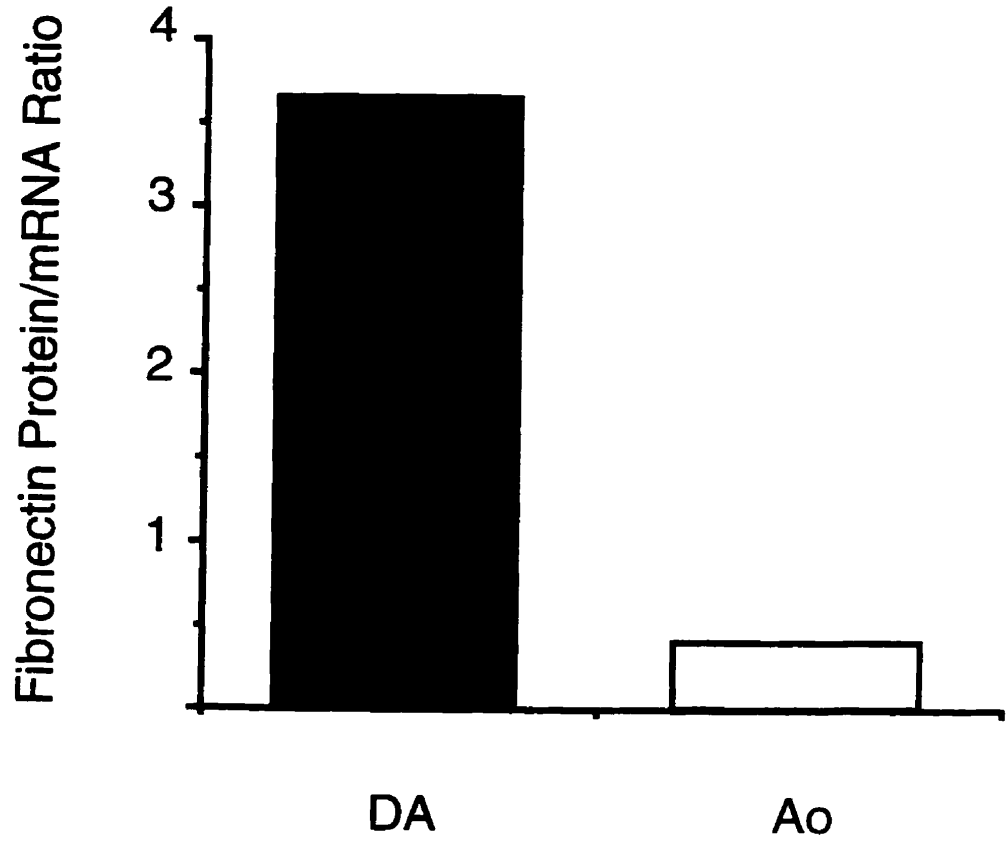

Figure 7

Figure 7. Increased FN mRNA translation in DA vs Ao SMC

Measurement of the ratio of the newly-synthesized FN protein to the steady-state levels of FN mRNA indicates an up to 6-fold increase in FN mRNA translational efficiency in cultured DA compared to Ao SMC (Modified from Boudreau N. *et al.*, Lab Invest 67:350-359, 1992).

Effect of AREs of 3'UTR on mRNA Translation

In studies addressing the regulation of human IFN-β gene expression, Kruys and colleagues (Kruys, *et al.*, 1987) observed that the presence of the AREs in the 3'UTR of the mRNA greatly suppressed mRNA translation in both *Xenopus* oocytes and in the reticulocyte lysate, since removal of the AREs from the 3'UTR of IFN-β mRNA increased its translation up to 100-fold in *Xenopus* oocytes and 10-fold in the reticulocyte lysate without affecting mRNA stability (Kruys, *et al.*, 1988). Further studies demonstrated that significant translational inhibition could be achieved in *Xenopus* oocytes injected with the IFN-β mRNA containing only one copy of the octanucleotide. The level of inhibition was enhanced when the copy number was increased, and the presence of three copies affects the mRNA translation to a level comparable to that of the 3'UTR of natural IFN-β mRNA (Kruys, *et al.*, 1989). Subsequently, AREs containing the octanucleotide derived from c-*fos* and GM-CSF have been shown to have the same inhibitory effects on mRNA translation (Kruys, *et al.*, 1989).

Translational suppression mediated by the AREs was also observed in somatic cells, including RAW 264.7 macrophages (Han, *et al.*, 1990a), rat L929 fibroblast cells, and NIH3T3 cells (Kruys, *et al.*, 1993). For example, in the studies with L929 cells and NIH3T3 cells, 3'UTR regulated-reporter constructs were generated in such a way that the reporter gene, chloramphenicol acetyl transferase (CAT) was driven by the cytomegalovirus (CMV) promoter, whereas the CAT 3'UTR was replaced by either the TNF-α 3'UTR containing the AREs or human growth hormone (hGH) 3'UTR without the AREs. Assessment of CAT activities (protein levels), as well as CAT mRNA levels in stable transfectants, revealed that cells transfected with the CAT construct containing the TNF-α 3'UTR produce 100-fold less CAT protein than the cells transfected with the CAT construct containing the hGH 3'UTR, while the CAT mRNA level is comparable. However, when the AREs were deleted from the TNF 3'UTR, the translational efficiency was increased. These results strongly suggest that, in addition to their function as destabilizing elements, AREs can also modulate translational efficiency.

AREs are not always associated with suppression of mRNA translation. In RAW 264.7

macrophages, the AREs of TNF 3'UTR normally inhibit TNF mRNA translation (Han, *et al.*, 1990a). However, lipopolysaccharide (LPS)-induced TNF-α expression is related to ARE-dependent enhanced mRNA translation. Dexamethasone, which inhibits TNF-α production by activated macrophages, greatly represses the ARE-dependent translational activation induced by LPS (Han, *et al.*, 1990b).

Mechanisms of Translational Modulation Mediated by the AREs

The mechanisms by which AREs affect mRNA translation are relatively unexplored since most studies have focused on ARE functions related to their mRNA destabilizing properties, although as discussed previously, these functions may be interdependent. For example, several independent studies have shown that the c-*fos* and GM-CSF AREs rely on ongoing translation to exercise their mRNA destabilizing functions (Savant-Bhonsale and Cleveland, 1992; Aharon and Schneider, 1993; Winstall, *et al.*, 1995). In a study carried out by Savant-Bhonsale and Cleveland (1992) inhibition of mRNA translation by mutation of the ATG initiator codon resulted in a 10-fold accumulation of chimeric RNA with GM-CSF ARE inserted downstream of the coding region compared with the non-mutated transcripts. They also showed that mRNA degradation mediated by the 3'UTR ARE was independent of the length of coding region. On the other hand, if the ARE is placed within the coding region, i.e., upstream of the stop codon, then its mRNA degrading property is lost. By further analysis of sucrose gradients, larger than average mRNPs were found only with 3'UTR ARE-containing transcripts, due to an extra divalent cation-independent complex (> 20S) and this suggested that there were ARE-binding proteins creating this complex. The formation of this complex is also dependent on ongoing mRNA translation and requires an intact ARE downstream of the stop codon. Studies of Aharon and Schneider (1993) demonstrated that insertion of a strong stem-loop into the 5'UTR of a chimeric mRNA containing GM-CSF AREs downstream of the coding region results in a 20- to 30-fold inhibition of translation, as well as a corresponding 15-fold enhanced accumulation of steady-state mRNA levels and mRNA half-life. Further studies using the same strategy revealed that insertion of this translation-blocking

secondary structure at any position upstream, but not downstream, of the ARE inhibits the degradation of chimeric mRNA. In studies by Winstall and colleagues (Winstall, *et al.*, 1995), the properties of the iron-response element (IRE) were used to shuttle mRNA from ribonucleoproteins (RNPs) to polyribosomes in response to cellular iron concentration. An IRE was inserted into the 5'UTR of chimeric mRNA, which contains either c-*fos* or GM-CSF AREs at the 3'UTR. Upon depletion of intracellular iron, chimeric mRNA was sequestered in the RNPs and concomitantly stabilized, whereas supply of iron by addition of hemin induced translation of chimeric mRNA toward polyribosomes and restored their rapid degradation.

In contrast, two other studies using similar methods have shown that decay of mRNAs containing 3'UTR c-*fos* or GM-CSF AREs is not coupled with ongoing translation (Koeller *et al.*, 1991; Chen *et al.*, 1995). It is therefore hard to offer a unifying explanation that could reconcile these differences, except to say that there may be differences in the mRNA decay pathways in different cells, or under different growth conditions, or with different reporter mRNAs (Chen and Shyu, 1995). Nevertheless, these data suggest that, under certain conditions, mRNA decay mediated by the AREs may be induced by their interaction with the translating ribosomes and may also require factors other than ribosomes.

Few experiments have been yet designed to address specifically the mechanisms by which the AREs decrease or increase mRNA translation. Kruys and colleagues (1990) have shown that, in a cell-free translation assay with a reticulocyte lysate, IFN-β mRNA containing its ARE is translocated onto polyribosomes to a much lower extent than the construct lacking the ARE, suggesting a sluggish translational initiation or inhibition of the 80S monosome formation in the presence of the 3'UTR ARE. Studies by Grafi and colleagues (1993) demonstrated that the addition of a poly (A) tail to IFN-β greatly decreases its translational efficiency in a reticulocyte lysate. However, shortening the poly (A) tract or removal of the 3'UTR ARE markedly improves translational efficiency. These observations were consistent with the distribution of IFN-β mRNA on the polysome profile. That is, the poly (A) rich IFN-β mRNA failed to form large polysomes, while its counterparts bearing short poly (A) tract recruit more efficiently into large polysomes.

While the direct effect of removal of the ARE on the polysomal distribution of IFN-β was not addressed in this study, the interaction of the ARE with the poly (A) tract was supported by the experiments showing that the presence of the poly (A) tail specifically inhibits binding of cytoplasmic factors to the ARE and a shortened transcript is created after RNase H treatment which cleaves double-stranded RNA. Physical interaction of the poly (A) tail with the ARE might inhibit mRNA translation by masking the poly (A) tail, thereby preventing its translation-promoting functions (Sachs and Davis, 1989; Munroe and Jacobson, 1990; Tarun and Sachs, 1995; Tarun and Sachs, 1996). It is therefore conceivable that, depending on the nature of the cell or the condition under which it is being studied, the binding of a tissue-specific or induced cytoplasmic factor to the ARE could release the poly (A) tail, thereby triggering mRNA translation (Grafi, *et al.*, 1993), and promoting rapid poly (A) shortening and RNA decay (Brewer and Ross, 1988; Wilson and Treisman, 1988; Shyu *et al.*, 1991; Grafi, *et al.*, 1993).

ARE-binding Proteins and their Functions

Although the mechanisms by which AREs exert their effect on mRNA stability and translation are obscure, their functional complexity may reflect dynamic changes in their binding proteins. Malter (1989) first identified an ARE-binding protein in lymphocyte cytoplasmic extracts. In this study, gel mobility shift assay showed one protein-RNA binding complex which was only present with ARE-containing synthetic mRNA, and the cytoplasmic factor was denoted the adenosine-uridine binding factor (AUBF). UV-crosslinking assay revealed that the molecular weight of the binding complex is 28 to 45 kD under denaturing but non-reducing conditions, whereas a set of three subunits of molecular weight at 15, 17, 19 kD was resolved under reducing conditions. It appears that the 15 kD subunit binds to RNA more rapidly and, more specifically, to the ARE or has higher affinity for the ARE. Further studies demonstrated that the AUBF binds to ARE-containing labile mRNAs, including GM-CSF, IL-3, INF-γ, c-*fos*, and v-*myc*, and the binding is ARE-dependent. Although the minimal length of ARE and the exact binding site have not been determined, it has been shown in this study that a synthetic 23-base ARE containing 4

repeats of AUUUA pentanucleotides or an intact UUAUUUAU sequence binds to AUBF, and replacement of the middle uridine of AUUUA with guanosine but not cytosine greatly inhibits its binding activity. This protein binding assay is consistent with two other independent studies in which the minimal length sequence of ARE required to direct mRNA decay has been determined to be UUAUUUA(U/A)(U/A) (Lagnado *et al.*, 1994; Zubiaga *et al.*, 1995). AUBF is inactive in resting lymphocytes but can be activated by 12-*O*-tetradecanoylphorbol-13-acetate (TPA) or calcium ionophore (Malter and Hong, 1991), which are known to induce labile mRNA stabilization (Shaw and Kamen, 1986 1986; Akashi *et al.*, 1989; Yamato *et al.*, 1989). The AUBF is a phosphoprotein, and its ARE binding activity is regulated by its phosphorylation status and by a redox switch of its disulfide bonds (-S-S-) to free sulfhydryl groups (-SH).

Numerous cytoplasmic proteins that bind ARE-containing 3'UTRs have since been identified in a variety of cells or tissues (Bohjanen *et al.*, 1991; Brewer, 1991; Rondon *et al.*, 1991; Vakalopoulou *et al.*, 1991; Bickel *et al.*, 1992; Bohjanen *et al.*, 1992; Port *et al.*, 1992; Stephens *et al.*, 1992; Levine *et al.*, 1993; Zhang *et al.*, 1993; Katz *et al.*, 1994; Nagy and Rigby, 1995; Nakagawa *et al.*, 1995; Chung *et al.*, 1996; Ma *et al.*, 1996), but their functions are largely unknown. Some appear to be similar to AUBF, are inducible, and are functionally related to labile mRNA stabilization (Bohjanen, *et al.*, 1991; Vakalopoulou, *et al.*, 1991; Bickel, *et al.*, 1992; Bohjanen, *et al.*, 1992; Stephens, *et al.*, 1992). With other ARE-binding proteins, expression or ARE-binding activity is correlated with rapid mRNA degradation (Brewer, 1991; Zhang, *et al.*, 1993). In addition, cellular localization of ARE-binding proteins does not necessarily correlate with mRNA stability. Some ARE-binding proteins appear to be located in both the nucleus and the cytoplasm, suggesting that they may have functions related to the formation of mRNP complexes in the nucleus, the processing of premRNA or mRNA transport from nucleus to cytoplasm (Brewer, 1991; Zhang, *et al.*, 1993; Nakamaki *et al.*, 1995). Indeed, several nuclear proteins are known to have RNA-binding activity, such as hnRNP A1, A0, and C (Myer *et al.*, 1992; Hamilton *et al.*, 1993; Katz, *et al.*, 1994; Nakamaki, *et al.*, 1995), and embryonic lethal abnormal vision (Elav)-like proteins, such as Hel-N1 and Hu-R (Levine, *et al.*, 1993; Chung, *et al.*, 1996; Ma, *et*

al., 1996). Surprisingly, there are also other groups of ARE-binding proteins known to have enzymatic activities in intermediary metabolism, such as thiolase (Nanbu *et al.*, 1993), enoyl-CoA hydratase (Nakagawa, *et al.*, 1995), glyceraldehyde-3-phosphate dehydrogenase (GAPDH) (Nagy and Rigby, 1995). The significance of such dual function proteins in mRNA decay or translational efficiency is unknown.

Several ARE-binding proteins have been purified and cloned. They include two Elav-like proteins, Hel-N1 (Levine, *et al.*, 1993) and Hu-R (Ma, *et al.*, 1996), and AUF1 (Zhang, *et al.*, 1993), and AUH (Nakagawa, *et al.*, 1995). The availability of their recombinant proteins or cDNAs makes it possible to gain insights into their function in mRNA decay or translational efficiency. This was shown with the two ARE-binding proteins, AUF1 and Hel-N1.

AUF1 was initially identified to be involved in c-*myc* mRNA degradation in a cell-free mRNA decay system (Brewer and Ross, 1988; Brewer and Ross, 1989; Brewer, 1991; Nakagawa, *et al.*, 1995). The decay of c-*myc* mRNA requires mRNA-polysome association (Brewer and Ross, 1988) and is facilitated by factors present in a 130,000 x g post-ribosomal supernatant (S130) (Brewer and Ross, 1989). These factors are present as a 25S complex in low-salt buffer or a 7S complex in high salt (0.5 M) condition (Brewer and Ross, 1989). The mRNA degradation activities are related to two polypeptides of 37 and 40 kd copurified from the 7S complex and bound to 3'UTR of c-*myc* and GM-CSF mRNA as well as poly (U) (Brewer, 1991). The two polypeptides, referred to as AUF1, were then purified from S130 cytoplasmic extracts of human erythroleukemia K562 cells (Zhang, *et al.*, 1993). They are immunologically cross-reactive, phosphorylated, and associated with other polypeptides in a complex. The cDNA of the 37 kDa polypeptide cloned from a Hela cell expression library contains two RNA recognition motifs and domains that potentially mediate protein-protein interactions (Zhang, *et al.*, 1993).

Several lines of evidence suggest that AUF1 targets decay of ARE-containing mRNA *in vivo*. For example, a previously described 35 kD ARE-binding protein in SMC associated with β-adrenergic agonist-induced downregulation of β-adrenergic receptor mRNA (Port, *et al.*, 1992), appears to be the AUF1. Upregulation of AUF1 occurs by β-adrenergic receptor stimulation in

SMC and correlates with increased decay of some ARE-containing RNAs (Pende *et al.*, 1996). Conversely, a slow decay rate of ARE-containing mRNA, such as GM-CSF mRNA is associated with reduced AUF1 expression (Buzby *et al.*, 1996). The binding affinity of AUF1 *in vitro* to the ARE is proportional to the rate of mRNA decay mediated by the ARE *in vivo*, whereas mutations in the ARE stabilize mRNA *in vivo* and decrease RNA-binding affinity of AUF1 (DeMaria and Brewer, 1996). More recently, monocyte adherence, which induces rapid stabilization of IL-1 and GROα (growth related oncogene α) mRNA, is associated with a decrease in protein-RNA complex formation related to AUF1 and the ARE. In contrast, monocyte deadhesion results in rapid mRNA degradation and enhanced RNA-AUF1 binding complex formation (Sirenko *et al.*, 1997). Thus, since it was first identified, there has been a growing literature supporting AUF1 as one of the ARE-binding factors involved in mRNA decay mediated by the 3'UTR ARE. Whether this factor at the same time increases mRNA translation has not been addressed, albeit there is some evidence suggesting that its correlation with mRNA decay also depends on ongoing translation under certain circumstances (Brewer and Ross, 1989; Buzby, *et al.*, 1996).

Hel-N1 is a member of Elav-like proteins which bind RNA *in vitro* (Gao *et al.*, 1994; Chung, *et al.*, 1996; Gao and Keene, 1996; Ma, *et al.*, 1996). Hel-N1 possesses an 80-amino acid consensus element, termed the RNA recognition motif (RRM) (Query *et al.*, 1989), which forms the core of a functional RNA-binding domain. It is interesting that members of the Elav family have a high affinity and selectivity for the ARE in the 3'UTR of cytokines and proto-oncogene mRNAs (Gao, *et al.*, 1994; Chung, *et al.*, 1996; Ma, *et al.*, 1996). Hel-N1 and its alternative form, Hel-N2 have been shown to bind to poly $(A)^+$ mRNA in granular RNP structures and to be involved in mRNA metabolism in human medulloblastoma cells and embryonic carcinoma P19 cells (Gao and Keene, 1996). Their expression is upregulated during neuronal cell differentiation of P19 cells (Gao and Keene, 1996). More recently, a study by Antic and Kneene (submitted, 1997) demonstrated that differentiation of NTera-2 cell (human embryonic carcinoma cells) induced by retinoic acid exhibits increased expression of Hel-N1 protein which co-localizes with mRNPs associated with polysomes, suggesting that Hel-N1 may affect mRNA translation.

Indeed, ectopic expression of Hel-N1 in 3T3-L1 adipocytes greatly increases glucose transporter (GLUT1) expression (Jain, *et al.*, 1997). This increased GLUT1 expression is associated with a relatively prolonged mRNA half life (7.0 ± 0.5 hours) in Hel-N1 transfectants compared to parent cells (4.8 ± 0.7 hours). Moreover, polysomal distribution of GLUT1 mRNA in Hel-N1 transfectants is exclusively located in the heavy polysomal region whereas GLUT1 mRNA in non-transfected cells has a broad distribution ranging from ribosome subunits to polysomes. This indicates that expression of Hel-N1 in 3T3-L1 adipocytes also results in enhanced GLUT1 mRNA translation via a rapid translational initiation. It was not addressed, however, in this study, whether Hel-N1 protein is also associated with mRNPs containing GLUT1 mRNA, rather an *in vitro* gel shift assay was used to show that the recombinant Hel-N1 protein binds to a U-rich region in the 3'UTR of GULT1 mRNA.

Other studies have also demonstrated that quiescent 3T3-L1 preadipocytes have a low level of GLUT1 expression and glucose transport activity that could be upregulated by TNF-α, phorbol esters, okadaic acid, and 8-brom-cAMP (Cornelius *et al.*, 1990; Cornelius *et al.*, 1991; Stephens, *et al.*, 1992; Jain, *et al.*, 1997). These conditions are associated with the accumulation of GLUT1 mRNA resulting from increased mRNA stability. There is a corresponding increase in AUBF activity specific for the AU-rich sequence in the 3'UTR of GLUT1 mRNA (Stephens, *et al.*, 1992), suggesting that AUBF increases GLUT1 mRNA stability. The main criteria used to identify the ARE-binding protein as the AUBF was visualizing a ~38 to 42 kD crosslinked ARE-binding complex on a sodium dodecyl sulfate-polyacrylamide gel electrophoresis (SDS-PAGE). A ubiquitously expressed ~36 kD Elav-like protein, HuR, has been cloned from Hela cells and has a high affinity and selectivity for the ARE in 3'UTR of c-*fos*, c-*myc*, N-*myc*, and IL-3 mRNAs (Ma, *et al.*, 1996). The possibility that this 'AUBF' in 3T3-L1 preadipocytes is related to HuR, the non-neuronal homologue of Hel-N1, could not be excluded.

Thus, ARE-binding proteins functionally fall into two categories: one group includes RNA-binding proteins, such as AUF1, whose ARE-binding activities correlate with rapid mRNA decay that may or may not depend on ongoing translation; the other group, represented by Hel-N1.

contains proteins whose ARE-binding activities are associated with stabilization of labile mRNAs. as well as enhanced mRNA translation.

Models of 3'UTR Modulating mRNA Stability and Translation

Translation itself is a process starting from initiation and proceeding to elongation. and termination. This process was extensively studied a decade ago, and translational initiation was recognized as the limiting step and the most important site of regulation (Hershey *et al.*, 1996; Pain, 1996). A scanning model for translational initiation was then proposed (Kozak, 1986a; Kozak, 1986b). The scanning model states that the 43S ribosomal subunit (carrying Met-tRNAi^{met} and various translational initiation factors) binds initially at the 5' end of mRNA and then migrates, stopping at the first AUG codon in a favorable context (Kozak consensus sequence) for initiating translation. After this, the 60S ribosomal unit joins to the 40S translational initiation complex and completes the assembly of the ribosome, followed by peptide chain elongation. The scanning model has since been shown to be operational for some 90 to 95% of mRNAs in eukaryotic cells (Kozak, 1987b; Kozak, 1987a; Kozak, 1989; Kozak, 1991).

A central aspect of the scanning model is that the 5' mRNA cap structure is the interaction site for the recruitment of the 43S small ribosomal subunit complex (i.e., the 40S ribosomal unit and its associated translational initiation factors) to eukaryotic mRNA. More recently, studies have shown that the 43S ribosomal subunit could also be recruited onto mRNA by an internal ribosome entry site (IRES) or by the interaction of 3' poly (A) tail with 5' end (Jacobson, 1995; Jacobson and Peltz, 1996; Sachs *et al.*, 1997). Thus, the 5' mRNA cap structure is no longer the exclusive requirement for the 43S recruitment. This suggests that different RNAs may potentially have different mechanisms related to their translational initiation. Even more interesting is that a given RNA may have diverse ways to initiate translation. Figure 8 shows a recently proposed revised

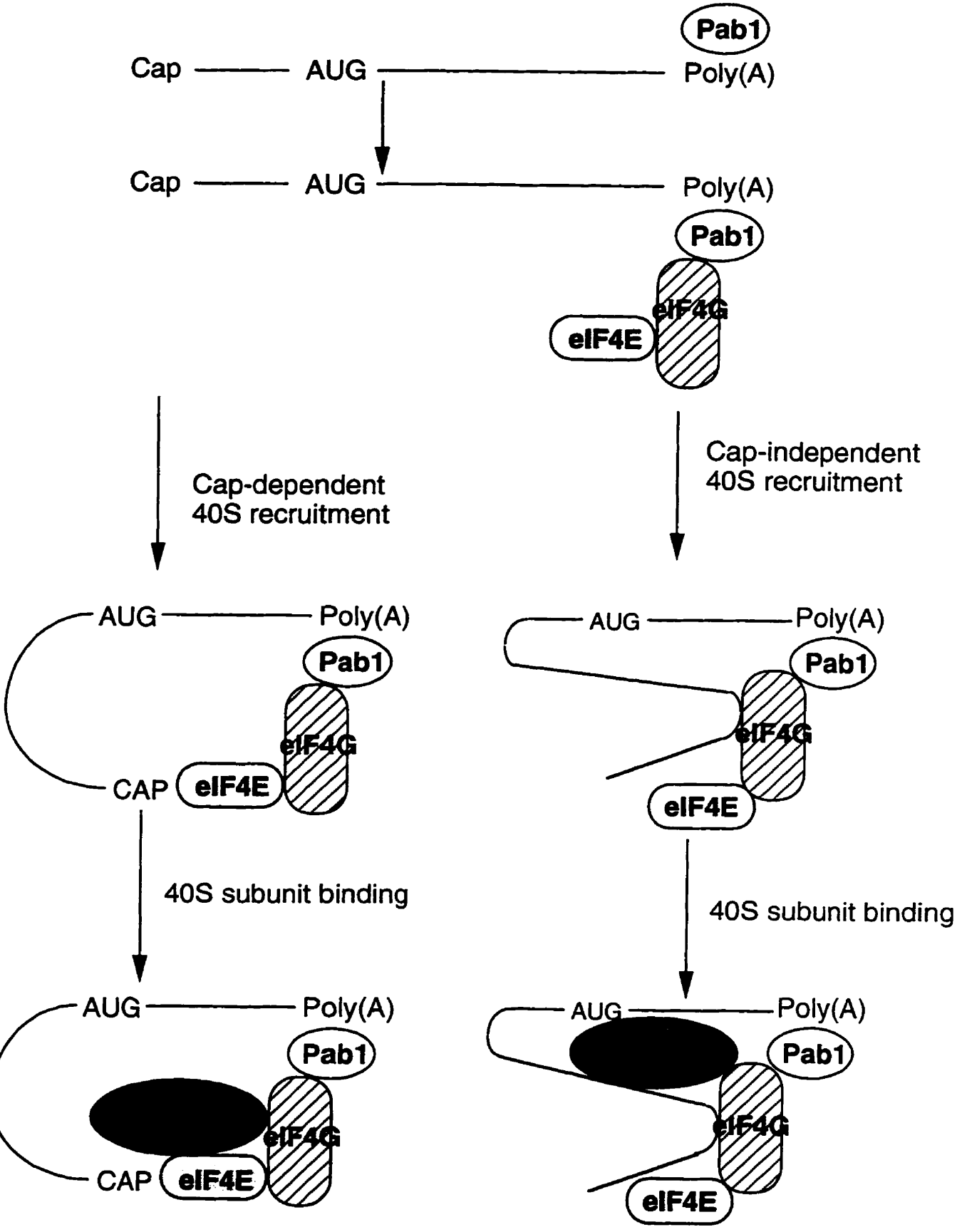
Pab1
Cap
AUG
Poly(A)
Cap
AUG
Poly(A)
Pab1
eIF4G
eIF4E
Cap-dependent
40S recruitment
Cap-independent
40S recruitment
AUG
Poly(A)
Pab1
eIF4G
CAP
eIF4E
AUG
Poly(A)
Pab1
eIF4G
eIF4E
40S subunit binding
40S subunit binding
AUG
Poly(A)
Pab1
eIF4G
CAP
eIF4E
AUG
Poly(A)
Pab1
eIF4G
eIF4E

Figure 8

Figure 8. Model of 5' and 3' closed loop in mRNA translational control

This model states that the poly (A) tail can promote mRNA translation by facilitating 40S recruitment through either 5' cap-dependent or independent mechanisms. It hypothesizes that the poly (A) tail could bring the 40S subunit to the 5' end through a circularized mRNA structure by interaction of a poly (A) binding protein, Pab1, and mRNA-associated initiation factor eIF4F that consists of two core subunits, eIF4E and eIF4G. Subsequently, the 40S ribosomal subunit is docked onto the cap structure due to its high affinity for the cap binding protein eIF4E. For cap-independent translation, the 40S ribosomal unit is loaded onto mRNAs through the interaction of eIF4G and an IRES (not indicated in the diagram) (Modified from Sachs A.B. *et. al.*, Cell 89: 831-838, 1997).

model of translational initiation (Sachs, *et al.*, 1997). This model states that both mRNA 5' cap structure and the poly (A) tail can determine 43S ribosomal subunit recruitment. While the cap structure has the exclusive role of docking the 43S ribosomal subunit onto a unique site in the RNA, due to its high affinity for the cap binding protein eIF4E, the poly (A) tail could also bring the 43S subunit to the 5' end via a circularized mRNA structure by interaction of a poly (A) binding protein, Pabl, and mRNA-associated initiation factor eIF4F that consists of two core subunits, eIF4E and eIF4G. Thereafter, the 43S subunit could be loaded onto mRNAs through either binding of eIF4E to the 5' cap structure or binding of eIF4G to an IRES. Whether this model could be the 'prototype' for interaction of other RNA-binding proteins with *cis* elements in the 3'UTR, such as the ARE and its binding protein, in translational control is currently unclear.

Broadly, translation could also be modulated by factors outside of the translational process itself, such as access of mRNA to translational machinery. During early development of *Drosophila* and *Xenopus* embryos, or in neuronal cells, translation of many mRNAs is regulated by their transport and localization (Singer, 1992; St Johnston, 1995). Transport and localization of mRNAs requires cytoskeletal elements, such as microtubules (MTs) and actin filaments. The signals that determine the mRNA localization are found (thus far) exclusively in the 3'UTR. 3'UTR RNA-binding proteins which also attach to MTs have been reported and implicated in modulating mRNA transport and localization (Elisha *et al.*, 1995; Han *et al.*, 1995; Schumacher *et al.*, 1995). Translational regulation via RNA transport and localization is mostly described in mRNAs encoding cytoskeletal or cytoplasmic proteins. The sorting of mRNAs encoding secreted proteins to endoplasmic reticulum (ER) was thought to depend on their signal peptide, but spatial distribution of mRNAs that encode secreted proteins, such as matrix proteins, FN (Lee, *et al.*, 1984), and collagens (Mansour *et al.*, 1988), an estrogen-dependent oviduct secretory protein (Murry and DeSouza, 1995), or a membrane-bound glycoprotein, lactase (Rings *et al.*, 1992; Rings *et al.*, 1994b) has also been reported. It is also likely that docking of mRNAs onto membrane-bound polysomes could be facilitated by cytoskeletal structures as compared to simple diffusion of large mRNA-RNP particles (Rings *et al.*, 1994a).

The AU-rich Element in 3'UTR of Fibronectin mRNA

As discussed before, the increased expression of FN in DA SMC appears to result from an enhanced translational efficiency. The question now is which mechanism is responsible for this tissue-specific elevated FN mRNA translation? Study of 3'UTR of FN mRNA revealed a UUAUUUAU sequence aforementioned, which is also conserved among different animal species (Kornblihtt, *et al.*, 1983; Schwarbauer, *et al.*, 1983; Caput, *et al.*, 1986). The function of the FN ARE has not yet been addressed. Given the overwhelming evidence indicating a role for the ARE in other mRNA 3'UTR in mRNA stability and translation in a variety cell types, including SMC, it would be logical to speculate that the ARE in the 3'UTR of FN mRNA may also function to modulate mRNA translation in vascular SMC. The difference in the ability to translate FN mRNA in DA versus Ao SMC might be due to differences in cytoplasmic factors which could bind to the ARE in the 3'UTR of FN mRNA.

Rationale, Feasibility, and Outline of the Present Studies

Previous studies in our laboratory (Rabinovitch, *et al.*, 1988; Zhu, *et al.*, 1990) and by others (Gittenberger-de Groot, *et al.*, 1985; de Reeder, *et al.*, 1988; Rabinovitch, *et al.*, 1988; de Reeder, *et al.*, 1989; de Reeder, *et al.*, 1990; Zhu, *et al.*, 1990) demonstrated that, morphologically, the natural occurring DA intimal cushion has features that are similar to those of the neointima which results from vascular injury. In view of the importance of TGF-β1 and FN (Boudreau, *et al.*, 1992; Boudreau and Rabinovitch, 1991; Boudreau, *et al.*, 1991), both in the pathogenesis of the vascular neointima and in the development of intimal cushions in the DA (Figure 7), this thesis investigates mechanisms involved in modulating their expression in vascular cells during intimal cushion formation in the DA.

Primary cultured EC and SMC isolated from fetal lamb DA and Ao tissues at different gestation times have been used in most of the studies presented in this thesis. These primary tissue cultures have been established and characterized as homogeneous EC or SMC populations

(Rabinovitch, *et al.*, 1988), maintaining the tissue-specific cell phenotype observed *in vivo* (Boudreau, *et al.*, 1991). The consistent and reproducible differences in tissue-specific and developmentally-related gene expression (Rabinovitch, *et al.*, 1988; Rabinovitch, *et al.*, 1989; Boudreau and Rabinovitch, 1991; Boudreau, *et al.*, 1992) in these cells allows us to identify regulatory mechanisms enhancing TGF-β1 and FN expression related to the intimal cushion formation in DA. Once uncovered, these mechanisms can be extrapolated to other cell systems and, in the case of this thesis, to the behavior of a tumor cell line which is impaired in its production of FN.

In this thesis, the first chapter describes tissue-specific and developmentally-related expression patterns of DA EC TGF-β1 and determines its levels of regulation. The next chapter demonstrates that interaction of an ARE in the 3'UTR of FN mRNA with its binding factor(s) is the mechanism responsible for the upregulating FN mRNA translation in DA SMC. Chapter three addresses the purification and functional characterization of a 15 kD ARE-binding protein that we identified as light chain 3 (LC3) of microtubule-associated protein 1; the fourth chapter addresses the involvement of microtubule structures in LC3-mediated FN mRNA translation; and the last chapter provides evidence that a tumor cell line (HT1080 fibrosarcoma), which shows little FN production and no immunodetectable LC3 can revert to a slower growing cell line with well assembled microtubules and abundant FN production following stable transfection of LC3. Moreover, we determine that the mechanism whereby LC3 upregulates FN mRNA translation is related to enhanced ribosome recruitment.

HYPOTHESIS

1. Upregulation of DA endothelial hyaluronan is a reflection of a developmental and tissue-specific regulated expression of TGF-β1.

2. Differences in cytoplasmic factors, which bind the ARE in 3'UTR of FN mRNA are responsible for the increased FN mRNA translation in DA versus Ao SMC.

3. Microtubules are important in FN mRNA translation modulated by the FN ARE-binding protein.

4. Reduction in FN production in HT1080 cells is related to loss of the FN ARE-binding protein.

OBJECTIVES

1. Define tissue-specific expression of TGF-β1 in DA EC during intimal cushion formation.

2. Determine the function of FN ARE in mRNA translation.

3. Purify, identify, and functionally characterize the FN ARE-binding factor.

4. Evaluate whether microtubule structures are involved in enhancement of FN mRNA translation.

5. Address whether reduction of FN production in HT1080 cells is due to a lack of the FN ARE-binding factor. If so, use these cells to further define the mechanism by which this factor regulates FN mRNA translation.

MATERIALS AND METHODS

I. Assessment of TGF-β1 Expression and its Regulation in DA EC

Immunohistochemistry

The distribution and expression of TGF-β was evaluated by immunohistochemical staining of DA and Ao tissue sections prepared from 100-day and 138-day gestation fetal lambs. Tissues were fixed with 4% paraformaldehyde and paraffin-embedded sections were dewaxed in xylene and rehydrated through standard graded ethanol solutions. Sections were stained according to the method of Heine *et al.* (1987) with a neutralizing antibody against TGF-β (1:100 of a stock solution of 10 mg/ml; R&D Systems, Minneapolis, Minnesota). This antibody was purified IgG and raised in rabbit by injection of highly-purified native porcine TGF-β1. The antibody is also cross-reactive with TGF-β2 with less sensitivity. The sections were visualized using Vectastain ABC Kit (Vector Laboratories Inc, Burlingame, CA) with goat anti-rabbit antibody and hematoxylin blue counterstain. Control experiments were performed by replacing the primary antibody with normal rabbit IgG (Dako Corp. Carpinteria, CA). The stained tissue sections were assessed qualitatively, independently, and in a blinded fashion by 3 co-workers and there was no discrepancy.

Cell Culture

Fetal Rambouillet lambs were delivered by Caesarian section on day 100 or 138 of a 145-day timed gestation. Fetal lambs were maintained in a 100% nitrogen environment to prevent breathing and maintain patency of the DA. DA and Ao were removed *en bloc* as previously described (Rabinovitch, *et al.*, 1988), and the vessels were separated, opened and rinsed in phosphate buffered saline (PBS) containing 3% antibiotics/antimycotics (GIBCO, Burlington, Ontario, Canada). Endothelial cells were harvested by scraping the luminal surface with a No. 11 scalpel blade (Ryan *et al.*, 1978) and maintained in Medium 199 (M199; GIBCO) containing 20% heat-inactivated fetal bovine serum (FBS, GIBCO) and 1% antibiotics/antimycotics. Endothelial

cells were characterized by a contact-inhibited 'cobblestone' morphology and positive staining for factor VIII (Rabinovitch, *et al.*, 1988), and used at passages 2 or 3. The animal work involved in this study is approved by the Research Institute of Hospital for Sick Children in Toronto, Ontario.

Immunoprecipitation

Subconfluent cultures of either DA or Ao EC were labeled with 100 μCi/ml [^{35}S]-cysteine and methionine (Amersham, Boston, MA) for 24 h in medium containing 25% of the normal concentration of cysteine and methionine and 5% FBS. Culture medium was removed in the presence of proteinase inhibitors (aprotinin, leupeptin, and pepstatin, Sigma Co., St Louis, MO), added in a final concentration of 1 μg/ml of each. To activate TGF-β, aliquots of 1 ml medium were transiently acidified by adding 25 μl of 5 M HCl for 2 h at room temperature, followed by neutralization with 35 μl of 0.7 M Hepes (pH 7.0) supplemented with 1.4 M NaOH (Assoian, *et al.*, 1987). The samples were then precleared 2 rounds on ice for 30 min with 100 μg/ml normal rabbit IgG. The precleared supernatants were then incubated with the TGF-β neutralizing antibodies which recognizes TGF-β (1:1000 of the stock solution, 10 mg/ml) at 4°C overnight, followed by addition of 100 μl of protein A agarose (Sigma) for 1 h. The samples were washed four times with immunoprecipitation buffer (50 mM Tris-HCl, pH 7.5, 150 mM NaCl, 1 mM EDTA, 1 % Triton-X 100, 1 % sodium deoxycholate, 0.1% SDS, and 0.005% thimerosal) (Colletta *et al.*, 1991). The final pellets were resuspended in 50 μl of Laemmli sample buffer (Laemmli, 1970), heated to 90°C for 10 min, and then resolved on a 12.5% SDS-PAGE under non-reducing conditions. The gel was treated with En^{3}Hance (Dupont, Boston, MA) for 30 min, dried, and exposed to Kodak X-Omat AR-5 film for one week at -70°C. Using the autoradiograph as a template, the prominent band at 25 kD corresponding to TGF-β, was cut from the gel and counted by liquid scintillation spectrometry. To standardize values for cell number, DNA content was determined as the mean of duplicate cell suspension aliquots, using the fluorescent dye, bisbenzamide (Hoescht Reagent H3313, Calbiochem) as previously described (West *et al.*, 1985). Results are expressed as cpm/100 ng DNA. Total protein was also assessed in these series of

experiments by total TCA-precipitated proteins found in the conditioned medium.

Western Immunoblot Analysis

To confirm the positive identification of TGF-β, western immunoblots were also carried out. Flasks (T-25) of subconfluent DA or Ao EC were incubated in 2 ml serum-free M199 for 24 hr. Conditioned medium was prepared by dialyzing against 1 M acetic acid for 72 hr with 2 changes, followed by dialysis against water and lyophilization. Equal amount of proteins (20 μg) were solublized by boiling in 40 μl of non-reducing Laemmli sample buffer for 5 min and resolved on a 12.5% polyacrylamide gel. After electrophoresis, proteins were transferred from the polyacrylamide gel to a nitrocellulose membrane. The membrane was blocked by 5% dried milk in PBS containing 0.5% Tween-20 for 2 h and incubated for 1 h with TGF-β antibody diluted at 1:1000 of the stock solution (10 mg/ml), followed by incubating for 1 h with goat anti-rabbit horseradish peroxidase conjugated IgG diluted at 1: 3000 (Bio-Rad Laboratories, Richmond, CA). Blots were visualized by staining with 3, 3'-diaminobenzidine tetrahydrochloride (Dako) and photographed.

Northern Blot Analysis

Total RNA was prepared from subconfluent DA and Ao EC harvested from 100- and 138-day gestation lambs by the phenol-chloroform extraction method (Chomczynski and Sacchi. 1987). Samples of 30 μg of total RNA were then separated on a 1% agarose gel containing formaldehyde and transferred to Hybond nylon membranes (Amersham, Arlington, IL) by capillary transfer for 16 h and fixed by exposure to short wave ultraviolet irradiation. A 0.9 kb HindIII and SmaI porcine TGF-β1 cDNA fragment excised from pTGFB-Ch119 (a gift from Dr. M.B. Sporn; NIH, Bethesda, Maryland) and a 1.2 kb cDNA probe for Glyceraldehyde-3-phosphate dehydrogenase (GAPDH) were labeled with [^{32}P] dCTP using a random primer kit (Amersham, Oakville, ON) and purified with NucTrap^{TM} push column (Stratagene, La Jolla, CA). Prehybridization and hybridization were performed for 16 h at 42°C. Blots were washed twice at

60°C in 2 x SSC (1 x SSC = 15 mM sodium citrate, 150 mM NaCl), 0.1% SDS for 1 h and once in 0.1 x SSC, 0.1% SDS for 30 min. Autoradiographs of RNA blots were analyzed by relative densitometric scanning. Values were standardized to mRNA levels of GAPDH to correct for any differences in total RNA loaded onto gels.

Stability of TGF-β1 mRNA

DA and Ao EC were cultured to subconfluence in the 100-mm dishes in M199 and 10% FBS. Actinomycin D was then added to the cultures at a concentration of 2.5 μg/ml and cell were incubated for various times from 4 to 12 h before extraction of total RNA. Northern blot analyses were then carried out on each sample as described above. Autoradiographs of blots were analyzed by relative densitometric scanning.

Statistical Analysis

Statistical analysis was performed using a computerized software, SuperANOVA with Duncan's New Multiple Range test to compare differences among the groups. Data reported in the figures are mean ± SD. $p < 0.05$ denotes significant difference. TGF-ß1 mRNA half-life was estimated as previously described (Johnson, *et al.*, 1995). After correction for any differences in total RNA loading by standardizing to mRNA levels of GAPDH, TGF-ß1 mRNA signals were graphically plotted as a function of time. Simple linear regression was used to determine mRNA half-life. The differences in TGF-ß1 mRNA half-life between cultured DA and Ao cells isolated from both 100-d and 138-d gestation lambs were assessed by two factor ANCOVA. The number of animals compared in each group is indicated in the corresponding figure legend.

II. Functional Assessment of an AU-rich Element in FN 3'UTR

Cell Culture

Primary DA and Ao SMC cultures were prepared as follows. Fetal Rambouillet lambs were delivered by Caesarian section on day 100 of a 145-day timed gestation period, as previously

described (Rabinovitch, *et al.*, 1988). Ductus arteriosus and Ao SMC were propagated by tissue explant after scraping endothelial layers and removing the adventitia (Ross, 1971). Smooth muscle cells were cultured in M199 with 10% FBS and identified morphologically by phase-contrast light microscopy [Nikon Diaphot microscope (Nikon)] as having a "hills and valleys" phenotype and by positive immunofluorescence using an antibody for smooth muscle α-actin. In serum stimulation experiments, test cells were serum-starved for 20 h after which adding 20% FBS was added for 4 h, while control cells were serum-starved for 24 h.

Plasmid Construction and Site-directed Mutagenesis

Three different chloramphenicol acetyltransferase (CAT) reporter constructs were made for *in vitro* transfection studies. Plasmid pECE-CAT was generated by insertion of a BglII-KpnI fragment from pBL-CAT2 (Luckow and Schütz, 1987) containing full-length CAT cDNA and SV40 small *t* intron into the same unique site of pECE (Ellis *et al.*, 1986) in the correct orientation with respect to the SV40 early promoter. Plasmid pECE-CAT-FN which included the FN 3'UTR was constructed in several steps. The CAT cDNA without its 3'UTR was obtained by digesting pBL-CAT2 with BglII and ScaI, and the coding sequence was repaired using synthetic oligonucleotides flanked upstream by a ScaI site and downstream immediately following the stop codon by a HindIII site. This full-length CAT coding sequence was inserted into pECE at the BglII and HindIII sites and the plasmid was named pECE-CAT3'UTR$^-$. A 717-bp KpnI-EcoRI rat FN fragment from a plasmid SP65 (pFN) (kindly provided by Dr. R. Hynes, Center for Cancer Research, Massachusetts Institute of Technology, Cambridge, MA), containing the full-length 3'UTR of FN, except for a 60-bp sequence upstream of the polyadenylation signal and including a single copy ARE, UUAUUUAU (which is 81-bp upstream from the 3' flanking end), was inserted into pECE-CAT 3'UTR$^-$ at the same site downstream of CAT coding sequence.

Site-directed mutation of the ARE was carried out using the PCR method. A pair of oligonucleotides carrying mismatched base pairs corresponding to the ARE were used. The upper primer was 5'-CCTGGGAGGGAGCAATTTTTCCC-3' and the lower primer was 5'-

GCTCCCTCCCAGGTAAGAGAAAG-3' (mutated ARE shown underlined). A 5'-end primer GTTCTGCTTTCTTTGC-3' located upstream of the mutated site and a downstream 3'-end primer 5'-ATCAACTGCATACAAAG-3' were also used. A 199-bp product with mutated ARE was generated by PCR and subcloned into pECE at SmaI site. A 170-bp PstI-XbaI fragment containing the mutated ARE was further released and used to replace the corresponding fragment within pECE-CAT-FN, and the new construct was designated pECE-CAT-FNΔ. All constructs were confirmed by restriction enzyme mapping and the mutation was verified by DNA sequencing.

Templates for *in vitro* synthesis of antisense RNA probes for RNase protection assays were as follow. pBSKS$^-$-CAT was constructed by ligating a 260-bp XhoI-EcoR1 CAT fragment from pBL-CAT2 into the same sites of phagemid Bluescript II KS$^-$ (pBSKS$^-$, Stratagene). When linearized with XhoI and transcribed with T7 RNA polymerase, a full-length 329-nt probe was generated of which the protected CAT mRNA fragment was 260-nt. pBSKS$^-$-β-gal, consisted of a 289-bp ClaI-EcoRV fragment of β-gal from pSV-β-gal (Promega Corp., Madison, WI) which was cloned into the same sites of pBSKS$^-$. When digested with XhoI and transcribed by T7 RNA polymerase, a full-length 377-nt probe was generated of which the protected β-gal RNA fragment was 289-nt.

The full-length FN 3'UTR containing wild or mutated ARE for use in gel mobility shift assays was obtained by insertion of the HindIII-XbaI fragment from pECE-CAT-FN or pECE-CAT-FNΔ into the same sites of pBSKS$^-$ and transcribed by T3 RNA polymerase after linearization with XbaI.

In Vitro Transcription

Antisense RNAs for RNase protection assay and full-length FN 3'UTR probe for gel shift assay were synthesized by *in vitro* transcription reactions in the presence of [α-^{32}P]-UTP. DNA templates were removed with DNase I digestion and the full-length probes were obtained by 6% acrylamide/8 M urea gel purification.

Fibronectin mRNA oligonucleotide containing the ARE (underlined), 5'-ACCUG-

UUAUUUAUCAAUU-3' or irrelevant oligonucleotide containing non-ARE from the FN coding region, 5'-AGAGCGGGAGCAGGAAGU-3', were generated by a method previously described (Milligan *et al.*, 1987). A 35-bp oligonucleotide template, 5'-AATTGATAAATAA CAGGT-TATAGTGAGTCGTATTA-3' (ARE consensus sequence and T_7 polymerase promoter, respectively, are underlined), was synthesized by G & D, Center for Biomaterials, The Hospital for Sick Children, Toronto. A 17-bp oligonucleotide, 5'-TAATACGACTCACTATA-3', was used as a primer to generate a T_7 polymerase promoter after annealing with the complementary oligonucleotide. Eighteen-mer transcripts containing the ARE were then generated by *in vitro* transcription reactions using 2.5 mM of ATP, CTP, GTP, UTP and 20 units of T_7 RNA polymerase. The DNA template was removed by adding RNase-free DNase I. The product of the reaction was extracted by mixing with phenol:chloroform (1:1), and the full-length transcript was purified on a 19% acrylamide/8 M urea denaturing gel and eluted with 1 mM EDTA, 0.1% SDS, and 0.5 M ammonium acetate. Labeled RNA transcripts were produced by end-labeling with [γ-^{32}P]-ATP using T_4 polynucleotide kinase (Boehringer Mannheim Biochemicals, Indianapolis, IN). The unincorporated labels were removed using NucTrap™ Push Columns (Stratagene).

Transfection and CAT assay

Transient transfection was performed using the calcium phosphate method (Sambrook *et al.*, 1989). Twenty-four h prior to transfection, cells were plated at a density of 1 x 10^6/100mm dish. Cells were fed with fresh medium (M 199) 4 h prior to transfection. Twenty µg of plasmid DNA were used to transfect each dish. Five µg of the plasmid pSV-β-Gal (Promega) were co-transfected with each experiment as a control for transfection efficiency. The cells were shocked with 10% glycerol for 1 min, then fed with fresh medium, cultured for 48 h, and harvested. In each assay, β-galactosidase activity was measured by colorimetry, and cell lysates containing similar amounts of activity were mixed with 0.1 µCi [^{14}C] chloramphenicol (58.2 µCi/mmol, ICN Biomedicals) and 20 µl of 4 mM acetyl coenzyme A (Sigma), in a total volume of 105 µl of 0.6 M Tris-HCl, pH 7.5 and incubated at 37°C for 1 h. The reaction was stopped by extraction of the

acetylated products with 1 ml of ethyl acetate. The acetylated products were dried by speed vacuum for 1 h, redissolved in 20 µl of ethyl acetate and chromatographed on thin layer plates in 95% chloroform: 5% methanol for 30 min. The plates were exposed to Kodak X-AR film for 24 h after air-drying. The CAT activity was counted using a scintillation counter and expressed as a percent conversion of total added [^{14}C] chloramphenicol after correction for background. Values for mock transfected cells were subtracted as background counts.

Additional experiments were carried out to improve efficiency of transfection with a 'component system' which included adenovirus, polylysine, and plasmid (Kohout *et al.*, 1996). The replication-deficient human adenovirus type 5 mutant, Ad5dl312, (generously provided by Dr. Frank Graham, McMaster University, Hamilton, Ontario) was propagated in the human embryonic kidney cell line, HEK 293 (ATCC, Rockville, MD), harvested, and purified as previously described (Kohout, *et al.*, 1996). Cells at passage one were seeded onto 25-mm^2 glass coverslips in Petri dishes at a density of 10^6 cells 24 h before transfection and transfected with 5 µg of each CAT constructs in a final vol of 2 ml media. Three days after transfection, the cells were fixed and stained for CAT or FN protein.

RNase protection assay

CAT mRNA levels in cells transfected with different CAT constructs were determined by RNase protection assay. As an internal control for both transfection efficiency and loading conditions, mRNA level of co-transfected β-gal plasmid was also examined. RNase protection assays were carried out using an Ribonuclear Protection Assay II Kit (RPA II, Ambion, Danvers, MA) following the manufacturer's instructions. For each reaction, $8x10^4$ cpm CAT and β-gal probes were hybridized with 10 µg total RNA overnight at 45°C. An equal amount of yeast RNA was used as a negative control. After RNase T1/RNase A digestion for 30 min at 37°C, the protected probes were separated by 6% acrylamide/8 M urea gel. Quantitative analysis was achieved by densitometric measurement of intensity of radioactive bands corresponding to predicted size of protected probe and CAT mRNA level was expressed as relative densitometric

unit after normalized to β-gal mRNA level.

Indirect immunofluorescence

To visualize cells with positive expression of CAT, 2 x 10^3 cells were immediately split into chamber slides after transfection and glycerol shock and cultured for 48 h. Cells were washed twice in PBS and fixed using ice-cold 100% methanol for 30 min at -20°C. After preincubation in blocking solution containing 10% normal goat serum, 2% bovine fraction V (Boehringer) for 1 h at room temperature, slides were incubated with a polyclonal rabbit anti-CAT antibody (IgG; 5'-3' Inc., Boulder CO) at 1:100 dilution overnight at 4°C. Slides were then washed four times with PBS and incubated for 1 h at room temperature with 1:50 diluted goat anti-rabbit IgG antibody conjugated with tetramethylrhodamine isothiocyanate (TRITC, Sigma) in blocking solution. After washing the slides 4 times with PBS, cell nuclei were stained with 1:10,000 diluted 4', 6-diamidino-2-phenylindole (DAPI, Sigma) in PBS for 10 min. Fluorescence microscopy was performed with an Olympus AHBT3 Research Photomicrographic Microscope System (Olympus). In 3 different experiments, the CAT positive cells were counted and analyzed according to morphology (stellate versus elongated) and cell surface expression of FN (positive or negative immunoreactivity). For double-staining of CAT and FN protein, a monoclonal mouse anti-FN antibody (Chemicon International Inc., Temecula, CA) was also used at a 1:100 dilution, followed by probing with goat anti-rabbit IgG conjugated with Texas red and goat anti-mouse IgG conjugated with fluorescein isothiocyanate (FITC).

Preparation of S-100 Cytoplasmic Extracts

Confluent cells were collected by scraping into 15 ml Falcon tubes, and spun at 2000 rpm for 10 min. Pellets were resuspended in twice the volume of hypotonic buffer (25 mM Tris-HCl, pH 7.9, 0.1 mM EDTA) with proteinase inhibitors, aprotinin, pepstatin, and leupeptin (1 μg/ml each) and lysed by 3 repetitive cycles of freeze-thaw. After a 1-h centrifugation at 100,000 g at 4°C, the supernatants were dialyzed against RNA binding buffer (15 mM Hepes, pH 7.9, 100 mM

KCl, 10% glycerol, 5 mM $MgCl_2$, 0.2 mM DTT) overnight at 4°C and stored at -70°C. The concentration of protein was determined using the Bio-Rad protein assay kit (Bio-Rad).

RNA Gel Mobility Shift Assays

In a standard reaction, 40 µg of cytoplasmic extracts from DA and Ao SMC were incubated with 10^5 cpm full-length 3'UTR probes or 10^4 cpm of FN RNA oligonucleotide probes in RNA binding buffer of a total volume of 20 µl containing 2 µg of *E. coli* tRNA for 30 min at 30°C. RNase T_1 was added in a concentration of 1 unit/µl, and incubation continued for 1 h for full-length 3'UTR probes or for 10 min for the oligonucleotide probes. The reaction mixtures were resolved by electrophoresis on a 1-h prerun 6% native polyacrylamide gel in 0.25 x TBE (Tris-borate-EDTA) buffer in the cold room at 120 volts for 4 h. The gel was dried and exposed for 24-48 h to Kodak X-AR film with 2 intensifying screens.

Characterization of Binding Complex Formation

Selective ARE-binding of cytoplasmic factors in DA SMC were determined by comparing binding complex formations with ARE-containing or ARE-mutated FN 3'UTR probe, as well as oligonucleotide. Competition studies were also carried out by incubation the cytoplasmic extract for 10 min with 10 to 200-fold excess unlabeled ARE-containing or irrelevant RNA oligonucleotides before adding the labeled RNA transcript. Dose-dependent binding of cytoplasmic factors to RNA probes was assessed by incubating increased concentrations (2.5 µg to 40 µg) of cytoplasmic lysates with RNA probes. Binding kinetics was studied by performing the binding reactions with a various times ranging from 5 to 60 min.

UV-crosslinking assay

Cytoplasmic lysates (40 µg) were added to the RNA probe (10^5 cpm) in a final volume of 20 µl. The binding reaction was carried out as previously described. The reaction mixtures were placed onto a parafilm sheet and crosslinked by 254 nm UV radiation (Stratalinker™ 1800,

Stratagene) under auto cross link setting. Samples were then boiled in 2 volumes of 2 x SDS sample buffer (Laemmli, 1970) for 10 min and analyzed on 8-16% gradient SDS-polyacrylamide gel electrophoresis (SDS-PAGE) under reducing or nonreducing conditions. The gel was dried and exposed to film at -70°C for 48 h. In some UV-crosslinking studies, the cytoplasmic extracts were incubated with 1 μg/μl proteinase K (Boehringer Mannheim Biochemica), 2% β-mercaptoethanol (β-ME), 10 mM DTT, 10 mM *n*-ethylmaleimide (*n*-EM), respectively, or the probe was treated with RNase T_1 for 30 min at 37°C prior to the binding reaction, followed by UV-crosslinking and SDS-PAGE.

III. Purification and Characterization of a 15 kD FN ARE-binding Protein

Preparation of S-100 Extract

S-100 extract was prepared from the media of 21 sheep Ao (weight 98.91 g) after removing adventitia and homogenized in homogenization buffer (10 mM Tris-HCl, pH 7.5; 100 mM KCl; 10 mM β-ME; 0.2 mM PMSF; 0.5 mM EDTA and 1μg/ml each of aprotinin, pepstatin, leupeptin) and centrifuged at 100,000 rpm for 90 min. The final volume of the S-100 extract was 220 ml with a protein concentration of 4.3 mg/ml.

Purification and Identification of FN mRNA Binding Protein

The extract was extensively dialyzed against column running buffer (Tris-HCl, 10 mM, pH 7.5/KCl 10 mM/EDTA 1 mM/β-ME 1mM) and run through a DEAE-Sepharose column after the column was equilibrated with running buffer. Flow-through from the DEAE-Sepharose (250 ml, 0.32 mg/ml) column was loaded onto a phosphocellulose column after the column was equilibrated with running buffer. A one-step 1 M KCl eluate was collected (130 ml, 0.16 mg/ml) from the phosphocellulose column. The sample was extensively dialyzed with heparin running buffer (20 mM Tris-HCl, pH 8.0; 100 mM KCl), then loaded onto a heparin agarose column connected to a liquid chromatography apparatus (ConSep LC100; Millipore, Bedford, MA) and eluted using a KCl gradient (80-800 mM). Fractions were collected and assayed for protein content using SDS-

PAGE and mRNA binding activity, using gel shift assays and UV-crosslinking. Fraction 19 containing a peak 15 kD RNA binding activity (judged by UV-crosslinking), was concentrated to 20 µl by ultrafiltration using centricon-10 (Ambion). The concentrated sample was resolved by SDS-PAGE. The gel was then electroblotted onto a polyvinyldifluoride transfer membrane (PVDF, Amersham) and the membrane was stained with Coomassie blue. The 15 kD band was excised and the sequence of the first 10 amino acids of the purified protein determined (Biotechnology Service Center, University of Toronto, Ontario, Canada).

Western Blotting

Western blot analyses of LC3 in S-100 extracts (10 µg) were carried out as described in Section I with rabbit anti-LC3 antiserum (generated by Dr. J. Hammarback, Dept. of Neurobiology and Anatomy, The Bowman Gray School of Medicine, Winston-Salem, NC). The blot was developed using an enhanced chemiluminescence (ECL) kit (Amersham). The intensity of immunoreactive bands was analyzed using NIH image software.

Indirect Immunofluorescence

For immunostaining of LC3, as well as MTs, 100-day DA SMC (10^5) were seeded onto 2.2-cm^2 coverslips, and cultured for 3 days. Cells were washed twice in PBS and fixed using ice-cold 100% methanol for 30 min at -20°C. After preincubation in blocking solution containing 10% normal goat serum (Sigma), 2% bovine fraction V for 1 h at room temperature. Fluorescent labeling for tubulin or LC3 was carried out using a monoclonal mouse anti-tubulin IgG (dilution 1:1000; Sigma) and a rabbit anti-LC3 antiserum (dilution 1:100). Cells were incubated with first antibody overnight at 4°C. After washed four times with PBS, cells were labeled with 1:100 diluted rhodamine-conjugated goat anti-rabbit or goat anti-mouse IgG (all dilutions 1:100) for 1 h at room temperature. After washing the slides 4 times with PBS, cell nuclei were stained with 1:10,000 diluted DAPI, in PBS for 10 min.

Fluorescence In Situ Hybridization (FISH)

For co-localization of LC3 and FN mRNA, a digoxigenin-labeled FN DNA probe was generated following manufacturer's recommendations (Boehringer) by random priming a 0.6 kb human FN KpnI/EcoRI fragment excised from pHF (a gift from Dr. R. Hynes, Center for Cancer Research, Massachusetts Institute of Technology, Cambridge, MA). Hybridization was performed by a method of Bassell et al (1994). Labeling LC3 was then carried out with rabbit-anti-LC3 antiserum as above. Detection of digoxigenin-labeled nucleotides was accomplished by using a rhodamine-conjugated sheep-anti-digoxigenin antibody (1:20 dilution; Boehringer). Fluorescein-conjugated goat-anti-rabbit IgG was used to detect LC3. For control experiments. normal immunoglobulin was used instead of primary antibodies. Controls for *in situ* hybridization included cells pretreated with RNase A 200 μg/ml in PBS for 1 h in 37°C.

Immunohistochemistry

The distribution and expression of FN and LC3 protein was evaluated by immunohistochemical staining of sections prepared from DA and Ao tissues from 2 different 100-day and 138-day gestation fetal lambs. Tissues were fixed with 4% paraformaldehyde and paraffin-embedded sections were dewaxed in xylene and rehydrated through standard graded ethanol solutions. Sections were stained with rabbit-anti-LC3 antiserum (1:100 dilution) or a rabbit polyclonal antibody against FN (1: 200 dilution; Chemicon) using a Vectastain ABC kit according to manufacturer's instructions. Sections were then counterstained with hematoxylin blue. Control experiments were carried out using normal rabbit IgG as a substitute for primary antibodies. The stained tissue sections were assessed qualitatively, independently, and in a blinded fashion by 2 co-workers and there was no discrepancy.

Expression of Recombinant LC3 and RNA Binding

The LC3 coding region was amplified by PCR using pCR-LC3 plasmid as a template (provided by Dr. J. Hammarback, Dept. of Neurobiology and Anatomy, the Bowman Gray

School of Medicine, Winston-Salem, NC). The 5' primer (5'-CAGGATCCCATATG-CCGTCCGAGAAGACC-3') led by BamHI and NdeI sites and 3' primer (5'-CTGGATCCGAATTCAAGCATGGCTCTCTTCC-3') led by BamHI and EcoRI sites were used in the PCR. The PCR products were digested with BamHI and EcoRI and cloned into pGEX-2T (Pharmacia-LKB Biotechnology, Piscataway, NJ) at the same sites. The GST-LC3 fusion protein was purified using a glutathione-agarose column (Sigama) and the recombinant LC3 was released from the column by adding thrombin to the column to cleave glutathione S-transferase. The purified recombinant LC3 protein was verified by SDS-PAGE and western blotting.

Overexpression of LC3 in DA and Ao SMC

Cultured 100-day DA and Ao SMC were transfected with pCR3-LC3 plasmid using a adenovirus 'component system' described above with reference to transfection of the CAT plasmids in Section II. Cells at passage one were plated onto 17-mm well dishes at a density of 10^6 cell per well 24 h before transfection and transfected with two different doses of pCR-LC3 (1.67 or 5 μg/ml/well). Twenty-four h after transfection, cells were labeled with [^{35}S]-methionine (10 μCi/ml) and incubated for 20 h with medium (2 ml/well) mixed by adding 3 vol of methionine-free with 1 vol of complete DMEM containing 20% FBS.

Measurement of FN Synthesis

The newly synthesized FN protein was assessed as previously described (Wrana *et al.*, 1988) by incubating conditioned media containing equal counts of total TCA precipitated protein ($5x10^5$ cpm/ml) with 50 μl of Gelatin 4B-Sepharose (Pharmacia). After washing with PBS, FN retained on the beads was eluted by boiling for 5 min in 100 μl of SDS-sample buffer and resolved by 6% SDS-PAGE under reducing conditions. Gels were treated with En^{3}Hance, dried, and exposed to the film. Using the autoradiograph as a template, the corresponding bands were cut from the gel and the radioactivity determined by liquid scintillation spectrometry. Quantitative analysis of data from 4 different experiments was carried out using computerized SuperANOVA

software.

RNA Extraction and Northern Blotting

Total RNA extraction and northern blot analyses were carried out with 10 μg of total RNA with a [^{32}P]-dCTP random labeled (10^6 cpm/ml) 0.6 kb human FN cDNA excised from pHF at sites of KpnI/EcoRI .as described in Section **I.**

IV. Assessment of MT Effect on FN mRNA Translation

In Vitro Transcription and Translation

Translation of mRNAs transcribed from the fusion plasmid was carried out using the TNT rabbit reticulocyte lysate (Promega) according to the protocol of the supplier. The fusion plasmids CAT-FN3'UTR and CAT-FN3'UTRΔ were constructed by removing a XhoI and BamHI fragment from pECE-CAT-FN or pECE-CAT-FNΔ (See Section **II**) which contains the CAT coding region, 3'UTR of rat FN cDNA with wild or mutated UUAUUUAU sequence (indicated by Δ) and a poly-A tail and inserting it into the phagemid Bluescript II KS$^-$ (Stratagene) at the same sites. *In vitro* transcription and translation reactions were carried out using equal amounts (0.5 μg) of purified fusion constructs in the presence of 5 μCi of [^{35}S]-UTP and 10 μCi of [^{35}S]-methionine for 1 h at 30°C in a final volume of 25 μl. In some reactions, 0.5 or 2 μg of purified recombinant LC3 protein were added to the reaction mixtures. At the end of each reaction, the transcribed fusion RNAs were recovered from the reticulocyte lysate by phenol extraction and resolved on a 7 M urea-polyacrylamide gel. The CAT protein product was resolved on SDS-PAGE and analyzed by autoradiograph as well as western immunoblot.

Cell Culture

Primary SMC cultures were prepared as described in Section **II.** In the experiments to examine the effect of MT structure on FN synthesis, 2 x 10^6 DA SMC were seeded into 6-well dishes and cultured for 24 h, followed by a 2-h treatment with 10 μM colchicine (Sigma), a MT

depolymerizing agent. After washing with methionine-free media, cells were labeled with [^{35}S]-methionine (100 μCi/ml) in 1 ml serum- and methionine-free media containing colchicine in the above concentrations for an additional 2 h. At the end of labeling, the cells were photographed under a phase-contrast microscope before removal of the conditioned media. The conditioned media were collected for FN extraction and cells were lysed and extracted for total RNA.

Indirect Immunofluorescence

For double-immunofluoresence staining of LC3 and tubulin, 10^5 cells were plated on coverslips and cultured for 3 days. After treatment with colchicine for 2 h, cells were fixed by 4% paraformaldehyde in MT stabilizing buffer (100 mM Pipes, pH 6.9, 4 mM $MgSO_4$, 1 mM EGTA) for 20 min at room temperature and permeabilized with 0.1% Triton X-100 in PBS for 2 min on ice. Fluorescent labeling for tubulin and LC3 was carried out as described in Section **III** using a monoclonal mouse anti-α-tubulin IgG (1:1000; Sigma) and a rabbit anti-LC3 antiserum (1:100). Secondary antibodies used were fluorescein-conjugated goat-anti-mouse IgG and Texas-red-conjugated goat-anti-rabbit IgG (all dilutions at 1:100). Normal rabbit IgG and secondary antibody alone were used as controls. Cell nuclei were stained with 1:10,000 diluted DAPI in PBS for 10 min.

Fibronectin Synthesis

Measurement of FN protein production was performed as described in Section **III**, by incubating conditioned media containing equal counts of total TCA precipitated protein (10^5 cpm/ml) with 50 μl of Gelatin 4B-Sepharose. Fibronectin retained on the beads was eluted by boiling for 5 min in 100 μl of SDS-sample buffer and resolved by 6% SDS-PAGE under reducing conditions.

RNA Extraction and Northern Blot

Total RNA extraction and northern blot analyses were carried out with 10 μg of total RNA

and [^{32}P]-dCTP random labeled 1.4 kb human FN cDNA (GIBCO) (10^6cpm/ml) as described in Section III.

Cell Fractionation

Normal cultured DA SMC or cells treated with 10 μm colchicine for 4 h were washed in PBS and scraped into 14 ml Falcon tube in 5 ml PBS. After centrifugation at 500 g for 5 min, the cell pellets were extracted 5 min on ice with 1 ml lysis buffer [10 mM Tris-HCl, pH 7.4, 0.15 M NaCl, 5 mM $MgCl_2$, 0.1 mM PMSF, 10 mM DTT, 100 μg of cyclohexamide/ml, 100 units of RNAguard (Pharmacia)/ml, 0.5% Nonidet P-40 (v/v), and lysed with a Dounce homogenizer, type B pestle. After removal of nuclei by centrifugation at 1000 g for 5 min, the lysate was centrifuged at 16,000 g for 30 min. RNA was extracted from the supernatant containing free and cytoskeletal-bound polysomes and the pellet containing membrane-bound polysomes (Hesketh and Pryme. 1991) and analyzed for FN mRNA by northern blot analysis.

Polysome Profile Analysis

Analyses of polysome profiles by sucrose gradient fractionation were performed using 2 x 10^7 confluent cells as previously described (Chen, *et al.*, 1995). Cells were harvested and homogenized with lysis buffer (10 mM Tris-HCl, pH 7.4, 100 mM NaCl, 5 mM $MgCl_2$, 200 U/ml RNasin, 100 μg/ml cyclohexamide, 0.5% NP-40). Nuclei were pelleted by centrifugation at 4°C and 12, 000 g for 3 min. Two hundred μl of resulting supernatant were layered on 4.5 ml of 15-40% sucrose gradient, centrifuged at 42, 000 rpm for 2 h at 4°C in a Beckman SW 50.1 rotor. Following centrifugation, 17 fractions (0.25 ml each) were collected from top to bottom and the absorbency of the fractions was measured at 254 nm. Proteins and RNA were extracted from each fraction using Trisol (GIBCO) according to the manufacturer's instructions. Further analyses of the distributions of LC3 protein and FN mRNA were done by western immunoblotting and RNase protection assay. The results were analyzed by NIH image program, and used for graphic presentation.

RNase Protection Assays

The construct used in *in vitro* synthesis of the antisense sheep-specific FN RNA probe for the RNase protection assay was made using a standard RT-PCR method. One μg of total RNA harvested from cultured lamb Ao SMC cells was primed with a synthetic oligonucleotide, 5'-TGTTCGGTAATTAATGGAAATTGG-3', which complemented with the 3' end of human FN exon 7, and the reaction was driven by the MMLV reverse transcriptas (GIBCO). The PCR reaction was then carried out by adding the 5' primer, 5'-TTTCTGATGTTCCGAGGGACC-3'. which is homolgous to the 5' end of human FN exon 6. The 221-bp PCR product containing sheep FN exons 6 and 7 were cloned into a pCR®2.1 vector (Invitrogen Co., San Diego, CA). After linearizing by SacI, a 329-nt antisense RNA was generated by an *in vitro* transcription reaction using T7 RNA polymerase. The expected protected FN mRNA was 221-nt. RNase protection assays were carried out as described in Section **II**.

Western Immunoblotting

Western immunoblot analysis of LC3 was performed as described in Section **I** using S-100 extracts (10 μg). The blot was developed using an enhanced chemiluminescence (ECL) kit according to the supplier's instructions.

V. Assessment the Role of LC3 in Fibronectin mRNA Translation in HT1080 cells

Cell culture

All cell lines, including rat embryonic aortic smooth muscle cells (A10), mouse NIH3T3 cells (3T3), Chinese hamster ovary cells (CHO), SV40 transformed African Green monkey kidney cells (Cos7), human fibrosarcoma cell line (HT1080), and normal human skin fibroblasts (CCD-973SK), were obtained from ATCC (American Type Culture Collection, Rockville, MD), and cultured with EMEM with 10% FBS and 1% antibiotics. For all comparative studies, cells were passaged at the same time and plated at the same density. To assess morphologic differences, the cultures were photographed with a phase-contrast microscope (Nikon Inc. Garden City, NY).

Transfection

Twenty-four hours prior to transfection, HT1080 cells were plated at a density of 10^6/100-mm dish. HT1080 cells were stably transfected using the calcium phosphate precipitation method (Sambrook, *et al.*, 1989). Ten μg of plasmids pCR3-LC3 or vector pCR3 were used to transfect each dish for 8 h. The cells were then shocked with 10% glycerol for 1 min and fed with fresh complete medium containing the aminoglycoside G418 (200 μg/ml, GIBCO). The media were changed every two days with gradually increasing concentrations of G418 up to 800 μg/ml. Fourteen clones transfected with pCR3-LC3 were selected on the basis of resistance to G418 (800 μg/ml) by selective trypsinization and screened for LC3 expression using western immunoblot analysis. Eight clones with verified stable expression of LC3 and four vector-transfected clones were expanded individually and passaged at least 3 times before use. Where applicable, as indicated in the Methods of Section **V**, cells expanded from the entire pools of eight LC3-transfected clones or four vector-transfected clones were studied.

Western Immunoblot Analysis

Western blot analyses of LC3 in S-100 extracts (10 μg) or polysomal fractions were carried out as described in Section **I** with rabbit anti-LC3 antiserum. The blot was developed using an enhanced chemiluminescence (ECL) kit.

Cell Growth Curve

HT1080 cells individually expanded from each of eight clones with stable expression of LC3 or four vector-transfected clones were plated on 6-well dishes at the density of 2×10^5 cells/well. The media containing G418 were changed every two days. Cells were trypsinized every 24 h and the cell number was determined using an improved Neubauber hemacytometer (American Opitcal Scientific Instrument Division, Buffalo, NY) by averaging two separate counts for each well.

Indirect Immunofluorescence

HT1080 cells were plated on 2.2 cm^2 coverslips at a density of 10^5 cells/well and cultured for 3 days. Immunofluoresence staining of tubulin and FN were carried out as described in Section **II** and **III** using a monoclonal mouse anti-α-tubulin IgG (1:1000 dilution) or a polyclonal rabbit anti-FN IgG (1:100 dilution). Secondary antibodies were FITC-conjugated goat-anti-mouse IgG or goat-anti-rabbit IgG (dilution at 1:100). After staining, cells were mounted with antifade reagent (Molecular Probes Inc., Eugene, OR). For negative controls, normal mouse or rabbit IgG was used instead of first antibodies.

Fibronectin Biosynthesis

HT1080 cells individually expanded from each of eight clones with stable expression of LC3 or four vector-transfected clones were plated on 6-well dishes at a density of 10^6 cells/well. After 24 h, cells were labeled with [^{35}S]-methionine (10 μCi/ml) for 20 h in 2 ml media mixed with 3 vol of methionine-free and 1 vol of complete MEM containing 20% FBS. The conditioned media were collected for analysis of FN protein and the cells were used to extract total RNA and to assess steady state levels of FN mRNA. Measurement of FN protein production in conditioned media with equal amount of total TCA precipitated protein ($5x10^5$cpm/ml) was performed as described in Section **III**.

Fate of Newly-synthesized Fibronectin

HT1080 cells expanded from pools of eight clones with stably expressed LC3 or four vector-transfected clones were used in these experiments. Twenty-four hours after plating HT1080 cells into 6-well dishes at a density of 10^6 cells/well, the cells were washed twice with methionine-free MEM and labeled with [^{35}S]-methionine (100 μCi/ml) for 2 h in 2 ml methionine-free MEM. The cultures were chased by replacing complete MEM containing 10% FBS for various times ranging from 30 to 240 min. The conditioned media, as well as cell lysates, containing $5x10^5$cpm/ml were collected for analysis of FN synthesis and secretion, as previously

described. Cell-associated FN was solubilized in PBS containing 0.1% SDS and 0.5% NP-40.

RNA Isolation and Northern Blot Analysis

Northern blot analyses of FN mRNA were carried out using 10 µg total RNA extracted from the cells as described in Section **III**.

RNA decay analysis

HT1080 cells expanded from the pools of eight LC3-transfected or four vector-transfected clones were cultured at 50% confluence in the 100-mm dishes in EMEM and 10% FBS. Actinomycin D was then added to the cultures at a concentration of 2.5 µg/ml and cells were incubated for various times from 4 to 24 h before extraction of total RNA. Northern blot analyses were carried out as described in Section **III**.

Polysome profile analysis

HT1080 cells expanded from pools of eight clones with stably expressed LC3 or four vector-transfected clones were used in these experiments. Analyses of polysome profiles by sucrose gradient fractionation were performed as described in Section **IV**. Proteins and RNA were extracted from each fraction using Trisol reagent. Further analyses of the distributions of LC3 protein and FN mRNA were done by western immunoblotting and RNase protection assays.

RNase protection assays

RNase protection assays were carried out as described in Section **II**. The construct used in *in vitro* synthesis of the antisense human-specific FN RNA probe for the RNase protection assay was generated as described in Section **IV**.

Northwestern blot analysis

Northwestern blot analysis was carried out as previously described (Chen *et al.*, 1993)

with modifications. Protein samples were resolved under non-reducing conditions on a 10-20% tricine gel and electroblotted onto a nitrocellulose membrane at 4°C. Proteins were renatured in RNA-binding buffer (10 mM Tris-HCl, pH 7.9, 100 mM KCl, 5 mM $MgCl_2$, 1 mM EDTA, 0.2 mM DTT, 1 x Denhardt's solution) overnight at 4°C. After blocking with RNA-binding buffer containing 100 µg/ml tRNA for 1 h at room temperature, radiolabeled 3'UTR of rat FN mRNA (717-nt) containing either intact or mutated UUAUUUAU consensus sequence (generated by *in vitro* transcription reactions and purified by polyacrylamide/urea gels electrophoresis) were added at a concentration of 10^7 cpm/ml and membranes were incubated at room temperature for 1 h. Membranes were then washed with RNA-binding buffer without tRNA until desired signals were reached (typically 200 - 400 cpm by Geiger Counter) and exposed to film. Identical membranes were also used for western immunoblot analysis of LC3.

CHAPTER ONE

TISSUE-SPECIFIC AND DEVELOPMENTAL REGULATION OF TRANSFORMING GROWTH FACTOR-β EXPRESSION IN FETAL LAMB DUCTUS ARTERIOSUS ENDOTHELIAL CELLS

INTRODUCTION

During late gestation, the fetal ductus arteriosus (DA) undergoes morphologic changes leading to the formation of 'intimal cushions' in a variety of animal species (Yoder, *et al.*, 1978; Gittenberger-de Groot, *et al.*, 1985; de Reeder, *et al.*, 1988; de Reeder, *et al.*, 1989; de Reeder, *et al.*, 1990) and in the human (Gittenberger-de Groot, *et al.*, 1980; Silver, *et al.*, 1981; Slomp, *et al.*, 1992). These structures partially occlude the DA lumen and assure that the vessel closes completely when it constricts post-natally (Clyman, 1987; Coceani, *et al.*, 1988). Structurally, intimal cushions are associated with smooth muscle cell (SMC) migration into a subendothelium enriched in glycosaminoglycans, especially hyaluronan (Gittenberger-de Groot, *et al.*, 1985; de Reeder, *et al.*, 1988). We studied the mechanism of intimal cushion formation in the fetal lamb, a process which takes place largely between 100 and 138 days of a 145-day gestation period. Using cultured endothelial cells (EC) and SMC from the DA and aorta (Ao) at 100 and 138 days gestation, we have shown that the DA EC are responsible for the increased synthesis of hyaluronan and that this feature is manifested in cells from 100-day gestation lambs (Boudreau and Rabinovitch, 1991). In DA EC harvested from 138 day gestation tissues, when the intimal cushions are formed, hyaluronan production is reduced to the levels observed in Ao cells.

The role of increased DA endothelial hyaluronan production during the intimal cushion formation was further elucidated when we showed the relationship of this feature to SMC migration into the subendothelium. Using 3-dimensional collagen gel assays, DA SMC showed enhanced migration as well as a streamlined elongated mobile phenotype when compared with Ao SMC (Boudreau, *et al.*, 1991). The migratory phenotype of DA SMC was related to their increased production of fibronectin and increased expression of a cell surface specific hyaluronan binding protein, the receptor for hyaluronan mediated motility (RHAMM) (Hardwick *et al.*, 1992). This receptor is particularly evident at the leading edges of the DA SMC and is associated with their enhanced migration in response to a hyaluronan-enriched matrix.

The increased production of DA endothelial hyaluronan appears to be regulated by transforming growth factor-β (TGF-β) in that neutralizing antibodies to TGF-β reduce its

synthesis to levels observed in the Ao (Boudreau, *et al.*, 1992). Thus, the increased production of endothelial hyaluronan in DA compared to Ao and its downregulation between early and late gestation might also be accompanied by similar changes in the expression of TGF-β. Indeed, we have documented that there is an increased intensity of immunostaining for TGF-β1 in 100-day DA compared with Ao tissues (Boudreau, *et al.*, 1992). However, the endothelial-specific expression of TGF-β has not been addressed. Increased expression of TGF-β has also been found in the DA during its post-natal closure (Tannenbaum, *et al.*, 1996).

TGF-β is a homodimeric peptide with a molecular weight of 25 kD. TGF-β is synthesized and secreted by cells as a latent complex that requires activation to gain binding activity to its cell surface receptors. Of the three isoforms (TGF-β1, β2, and β3) that have been characterized in mammals, the expression of TGF-β1 has been shown to be tightly regulated during development in embryos (Heine, *et al.*, 1987; Lehnert and Akhurst, 1988) and developing hearts (Potts and Runyan, 1989). TGF-β1 is required for normal cardiogenesis (Letterio, *et al.*, 1994) and vasculogenesis (Dickson, *et al.*, 1995). Upregulation of TGF-β1 expression is associated with vascular intimal thickening resulting from hypertension (Sarzani, *et al.*, 1989), atherosclerosis (Ross, 1993), and angioplasty (Majesky, *et al.*, 1991; Nikol, *et al.*, 1992). Both transcriptional (Kim, *et al.*, 1989a; Kim, *et al.*, 1989b; Kim *et al.*, 1989c; Birchenall-Roberts *et al.*, 1990; Kim, *et al.*, 1990; Kim, *et al.*, 1991) and post-transcriptional mechanisms are involved in the regulation of TGF-β1 (Wager and Assoian, 1990; Kim, *et al.*, 1992; Romeo, *et al.*, 1993; Scotto and Assoian, 1993; Wager *et al.*, 1994).

In this chapter, we investigated both, *in vivo* and *in vitro*, whether there were changes in the production of endothelial TGF-β in the DA compared to the Ao in early and late gestation fetal lambs. We found, by immunohistochemical assessment, an increase in TGF-β in DA compared to Ao endothelium from 100-day gestation fetal lambs and a reduction to comparable levels of expression in tissue from 138-day gestation lambs. In keeping with these observations, the production of TGF-β is increased significantly in cultured 100-day DA compared with Ao EC and decreased in 138-day DA EC whereas no site-related differences were seen. Northern blot analysis

demonstrated that TGF-β1 mRNA levels were slightly but not significantly increased in 100-day DA comparing with Ao EC although the half life was shorter, suggesting increased transcription and translation of a relatively unstable mRNA. TGF-β1 mRNA levels were reduced in 138-day DA and Ao EC related to reduced mRNA transcription and stability respectively. Thus we have uncovered differences in the levels of regulation of DA endothelial TGF-β which determine its tissue-specific and developmental patterns of expression.

RESULTS

Increased Expression of TGF-β in 100-day gestation DA tissue

TGF-β1 expression in 100-day gestation fetal lamb DA and Ao tissues was studied previously using immunostaining (Boudreau, *et al.* 1992). Positive staining was observed in the subendothelium and throughout the media and adventitia layers of DA tissue. There was relatively less dense immunostaining in the corresponding Ao tissue. This study confirmed and extended our previous observations. Tissue sections prepared from DA and Ao tissue from 3 different 100-day and 138-day gestation fetal lambs were evaluated by immunohistochemical staining using a rabbit anti-TGF-β neutralizing antibody, visualized using a Vectastain ABC Kit, and counter-stained by hematoxylin blue. Control experiments were performed by replacing the primary antibody with normal rabbit IgG. The findings were consistent and reflected similar tissue specific and developmentally regulated changes in all samples examined. As shown in Figure 9, positive staining for TGF-β was associated with EC in 100-day DA tissues (**A**), but not appreciated in the endothelial lining in tissues from the 100-day gestation Ao or 138-day gestation DA and Ao (**B**, **C**, **D**, respectively). The negative control shows only background staining (**E**). Thus, there appears to be a tissue-specific increased expression of TGF-β in 100-day DA EC, which is developmentally regulated. In addition to its endothelial expression, TGF-β was also observed in the medial SMC in all the tissues examined (Figure 10). However, SMC in 100-day DA tissues exhibited the highest intensity of staining (**A**) compared to 100-day Ao (**B**) or 138-day DA and Ao tissues (**C** and **D**, respectively). Control tissues using normal rabbit IgG showed no staining (**E**).

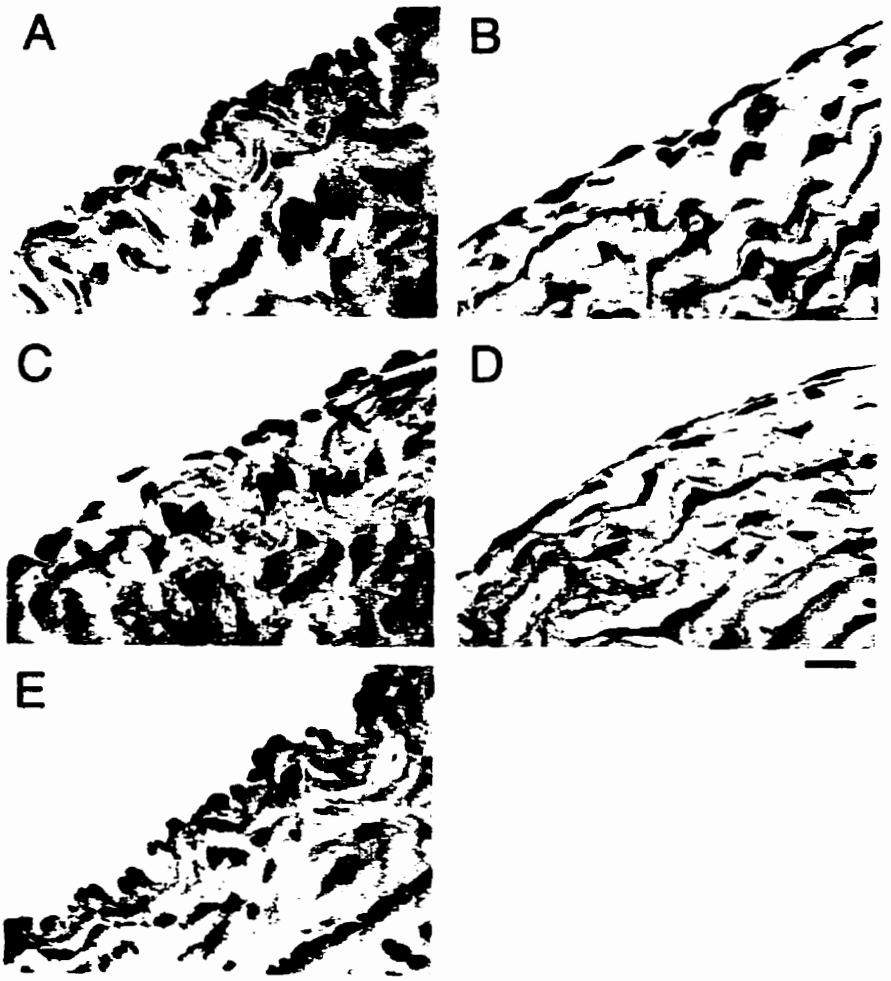

Figure 9

Figure 9. Increased expression of endothelial TGF-β in 100-day gestation DA tissues

Representative immunostaining of tissues from DA and Ao showing positive staining for TGF-β was seen in EC from 100-day DA tissues (**A**), but not in the endothelial lining in tissues from the 100-day Ao (**B**) or 138-day DA and Ao (**C** and **D**, respectively). Negative control shows only background staining (**E**). Comparison is representative of vessels from 3 different animals at each time-point.

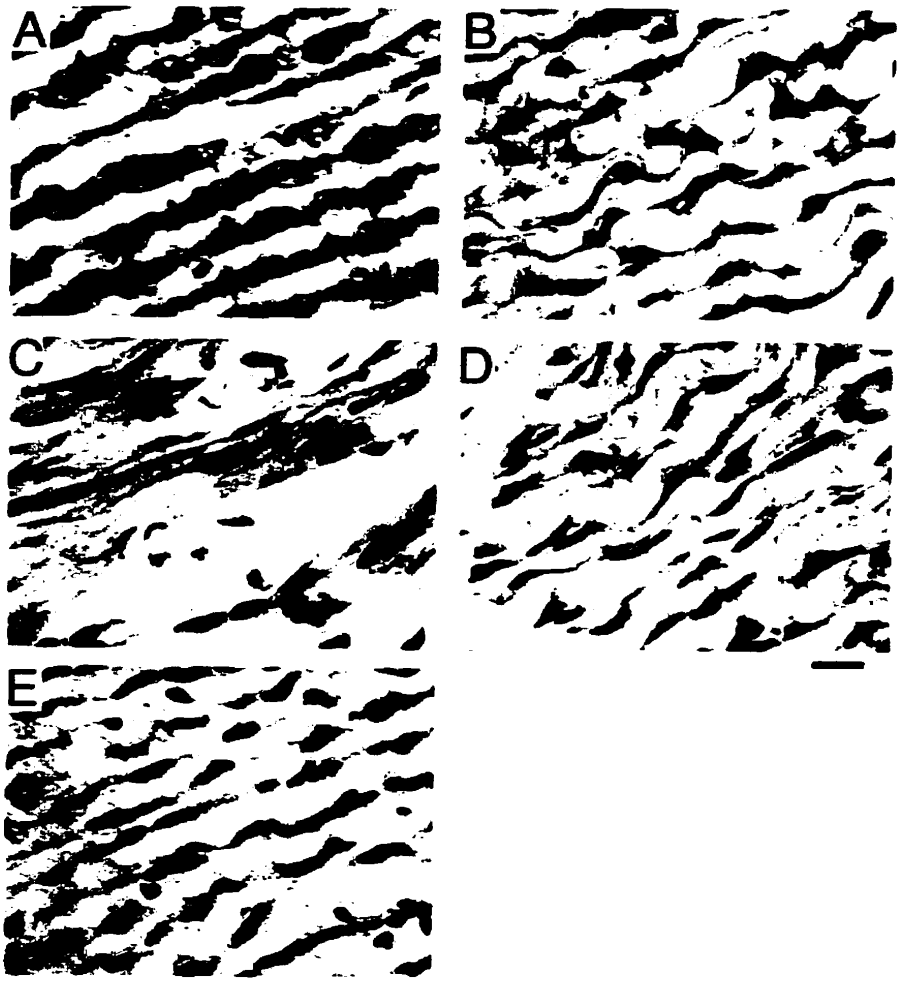

Figure 10

Figure 10. Increased TGF-β expression in medial SMC in 100-day gestation DA tissues

Representative immunostaining of tissues from DA and Ao showing increased TGF-β expression in medial SMC from 100-day gestation DA tissues (**A**) with less intense staining found in 100-day Ao (**B**) or 138 DA and Ao SMC (**C** and **D**, receptively). Control tissues using normal rabbit IgG are negative for immunostaining (**E**). Comparison is representative of vessels from 3 different animals at each time-point.

Increased TGF-β Synthesis in cultured 100-day gestation DA EC

Primary cultures of EC from both 100-day and 138-day gestation lambs were then established and used for assessment of biosynthesis of TGF-β. Subconfluent cultures of either DA or Ao EC were labeled with [^{35}S]-cysteine and methionine for 24 hr. Conditioned media were collected and the newly-synthesized TGF-β was immunoprecipitated with TGF-β neutralizing antibodies. The proteins were resolved by SDS-PAGE and values were normalized for total DNA content. Results are expressed as cpm/100 ng DNA. Figure 11 summarizes the immunoprecipitation studies. Figure 11**a** shows a representative autoradiograph of these studies and Figure 11**b** is quantitative analysis of data from all harvests.

TGF-β was synthesized and secreted by both DA and Ao EC cultured from 100-day and 138-day gestation fetal lambs. The majority of newly-synthesized TGF-β was secreted in the culture medium while small amounts remain cell-associated (data not shown). Thus, analysis of biosynthesis of TGF-β could be achieved by measuring TGF-β secreted in the culture media. As shown in the Figure 11, a significant one-fold increase in newly-synthesized TGF-β is secreted by 100-day DA EC compared to Ao EC (lane 1 versus 2, $p < 0.05$), while no significant increase in TGF-β production is found in 138-day DA EC compared to 138-day Ao EC (lane 3 versus 4). TGF-β synthesis thus decreases significantly in DA EC from 138-day compared to 100-day gestation lambs (lane 1 versus 3, $p < 0.05$), while comparable amounts of TGF-β were found in 100-day and 138-day Ao EC.

Western immunoblot analysis confirmed the specificity of TGF-β antibodies. The immunoreactive band from conditioned media co-migrated in 12.5% nonreducing SDS-PAGE gels with a purified TGF-β1 peptide (R&D) at the position of 25 kD (data not shown), confirming that the band detected by immunoprecipitation from EC conditioned media is TGF-β. Furthermore, increased secretion of TGF-β in 100-day DA compared to 100-day Ao EC is also evident qualitatively by western immunoblot (Figure 12).

We next established whether any changes in TGF-β synthesis reflected differences in total protein synthesis. Total protein was also assessed in this series of experiments by the amount of

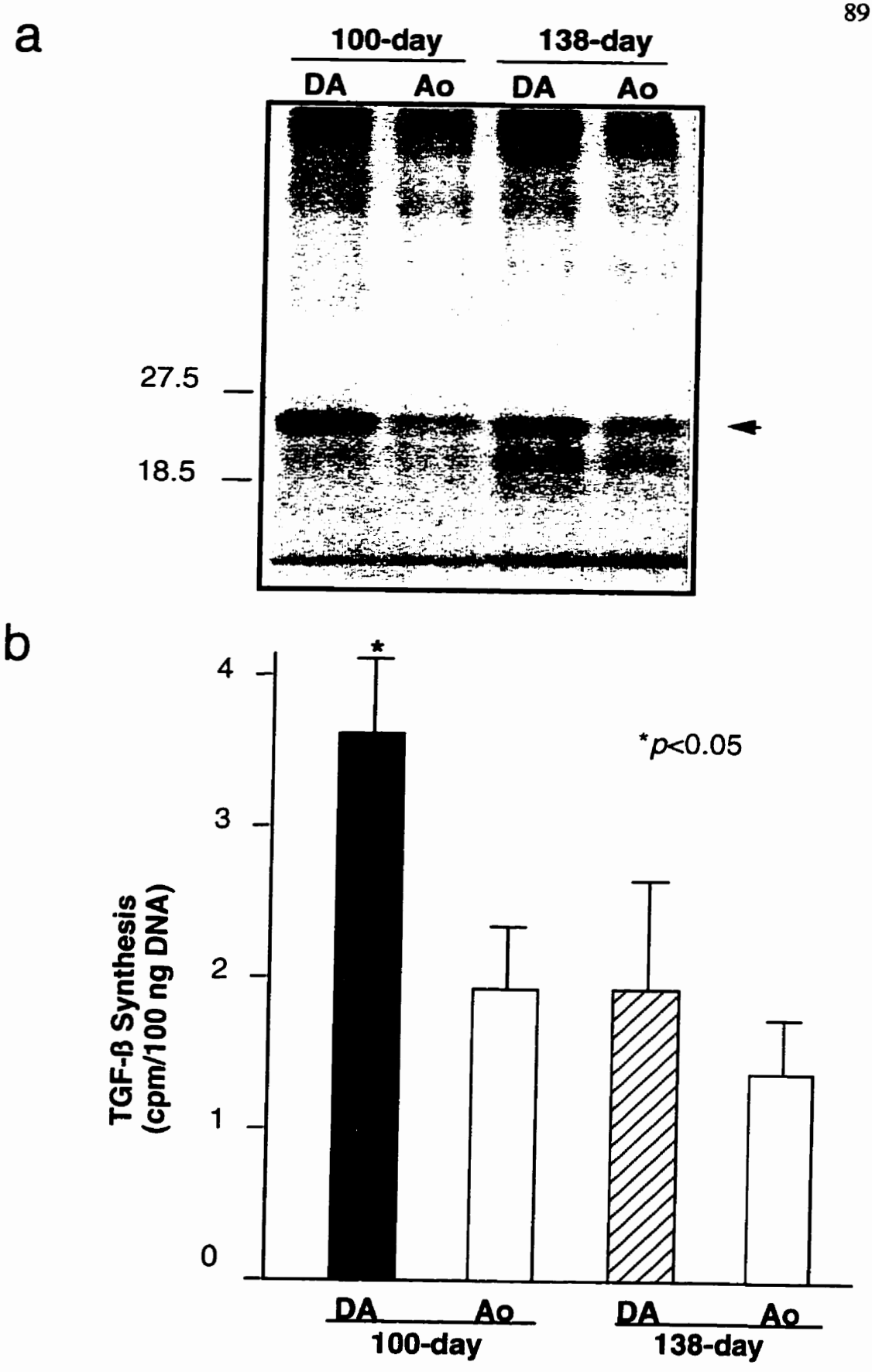
a
100-day
138-day
DA
Ao
DA
Ao
27.5
18.5
b
*p<0.05
TGF-ß Synthesis
(cpm/100 ng DNA)
4
3
2
1
0
DA
Ao
DA
Ao
100-day
138-day

Figure 11

Figure 11. Increased TGF-β synthesis in cultured 100-day gestation DA EC

(**a**) A representative autoradiograph of immunoprecipitation studies showing TGF-β was synthesized and secreted by both DA and Ao EC cultured from 100-day and 138-day gestation fetal lambs. Arrow indicates the 25 kD TGF-β protein. (**b**). Statistical analysis of immunoprecipitation studies indicates a significant one-fold increase in newly-synthesized TGF-β secreted by 100-day DA EC compared to Ao EC. TGF-β synthesis also decreases in 138-day DA EC compared to 100-day DA cells, but no differences were found between 100-day and 138-day Ao EC. Bar reflects mean ± SD. * indicates $p < 0.05$. n = 7, for number of comparisons from different lambs at 100 days, and n = 5, for comparisons at 138 days.

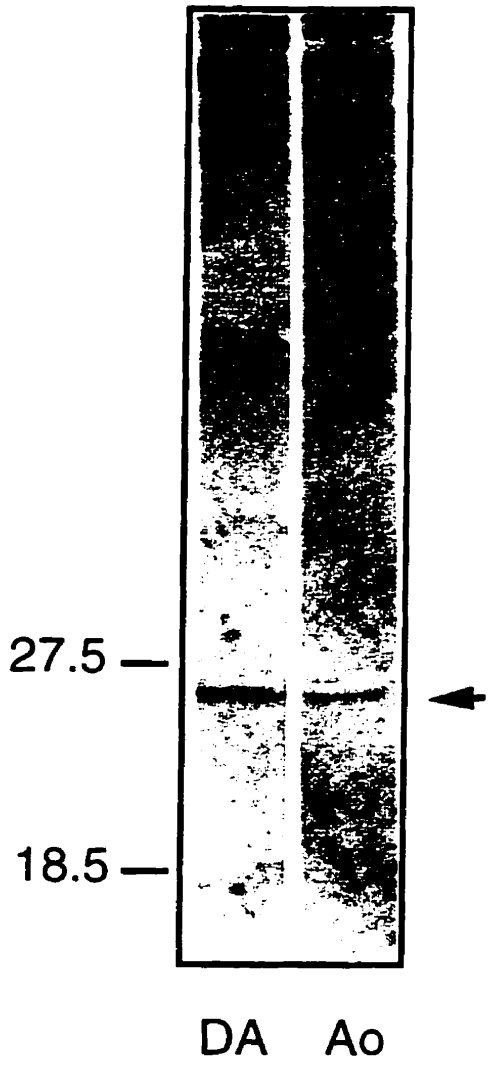

Figure 12

Figure 12. A western immunoblot analysis of TGF-β1

Increased production and secretion of TGF-β was found in media collected from cultured DA compared to Ao EC assessed by western immunoblot. Arrow indicates the 25 kD TGF-β protein.

total TCA-precipitated proteins found in the conditioned medium and normalized for DNA contents. Figure 13 shows quantitative studies of 3 experiments using cells from 3 different lambs. Similar values for total protein synthesis and secretion was observed in cultured DA and Ao EC at both gestation time-points.

Increased levels of TGF-β1 mRNA in cultured 100-day DA EC

We next measured the steady-state levels of TGF-β1 mRNA to determine whether there were corresponding changes, as the antibody that we used would recognize mostly the TGF-β1 isoform. The pattern of TGF-β staining using this antibody is consistent with our previous studies in which we showed that an increase in expression of TGF-β1 in 100-day DA compared to Ao tissues using a highly specific anti-TGF-β1 antibody (Boudreau, *et al.*, 1992). Using northern blot analyses, expression of TGF-β1 mRNA was detected in both cultured DA and Ao EC from 100- and 138-day gestation fetal lambs, and this appears as a single message of 2.4 kb (Figure 14). In contrast to the protein synthesis, TGF-β1 mRNA levels in 100-day DA compared to Ao EC are slightly but not significantly increased. There is, however, a significant fall in TGF-β1 mRNA levels in 138 day DA EC ($p < 0.05$). In Ao EC steady-state mRNA levels are also decreased in cells from 138 day compared to 100 day tissue ($p < 0.05$).

Analysis of stability of TGF-β1 mRNA

To study the mechanism for the lack of significant increase in the steady-state levels of TGF-β1 mRNA in 100-day DA compared to Ao EC and its developmental decrease in late gestation, we carried out experiments to examine the stability of TGF-β1 mRNA in these cells. Transcription was inhibited by actinomycin D and the remaining synthesized TGF-β1 mRNA was chased for various times ranging from 4 to 12 h. Compared to 100-day Ao EC, the levels of TGF-β1 in 100-day DA EC decreased relatively more rapidly (Figure 15**a**). The estimated mRNA half-life is approximately 9.5 h for 100-day DA EC and 20 h for 100 day Ao EC TGF-β1 (Figure 15**b**). TGF-β1 mRNA decay was relatively comparable in late gestation DA and Ao EC, where the half

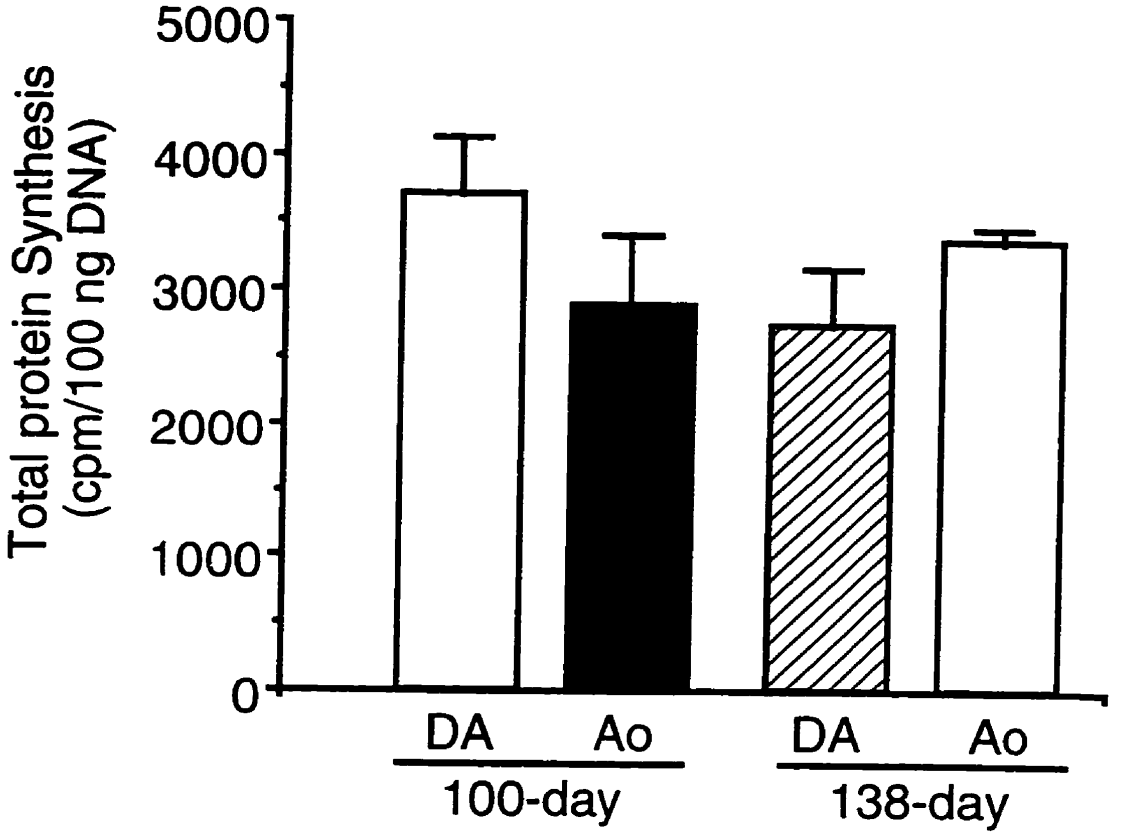
Total protein Synthesis
(cpm/100 ng DNA)
5000
4000
3000
2000
1000
0
DA
Ao
DA
Ao
100-day
138-day

Figure 13

Figure 13. Total protein synthesis and secretion in cultured DA versus Ao EC

The specificity of the differences in TGF-β produced by cultured DA and Ao EC is reflected in similar values for total newly synthesized proteins in tissues from both 100- and 138- day gestations. Bar represents mean ± SD. n = 3, for comparisons number of comparisons of different lambs from both gestation time points.

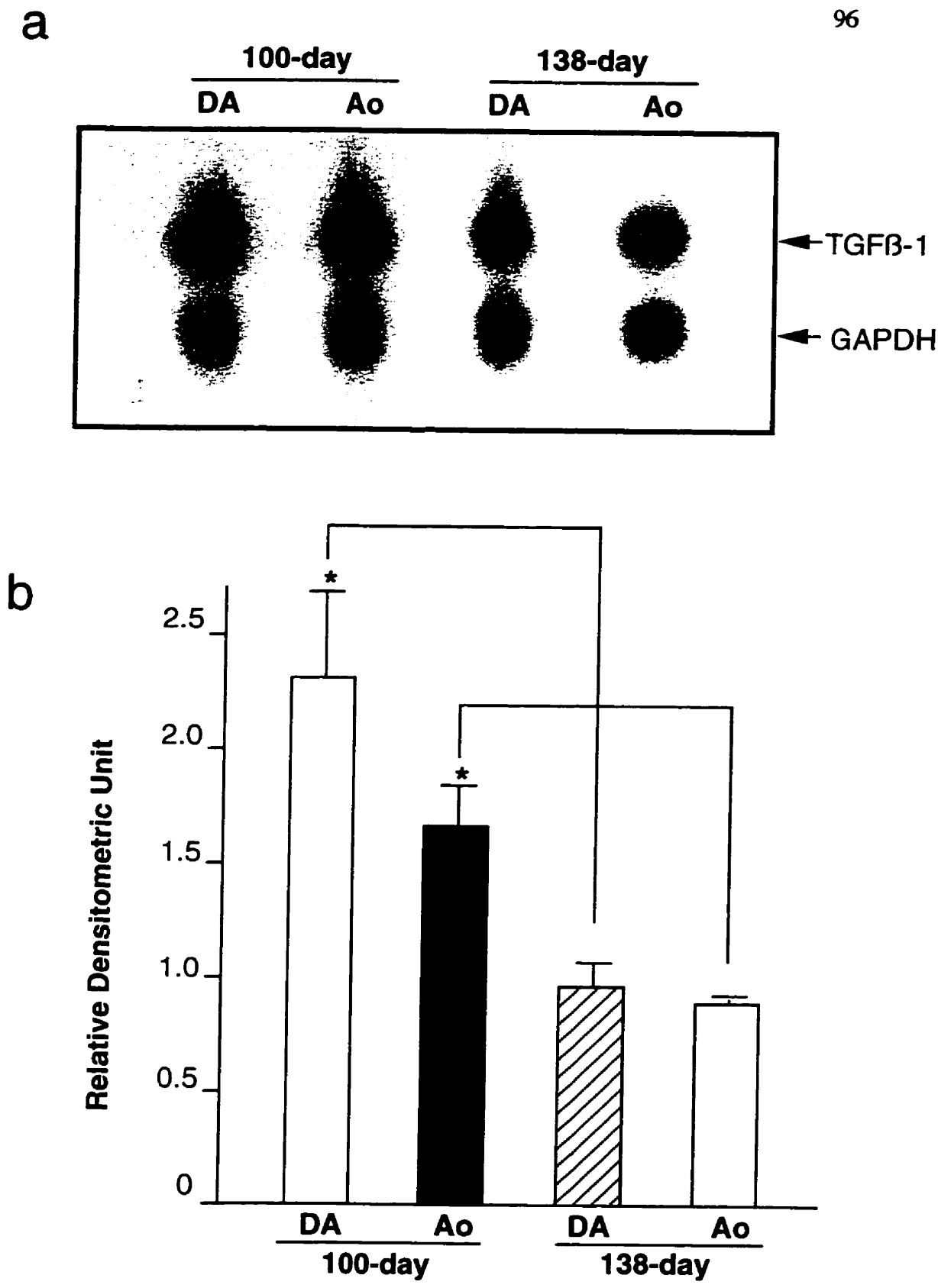
a
100-day
138-day
DA
Ao
DA
Ao
TGFß-1
GAPDH
b
Relative Densitometric Unit
2.5
2.0
1.5
1.0
0.5
0
*
*
DA
Ao
DA
Ao
100-day
138-day

Figure 14

Figure 14. Northern blot analysis of steady-state TGF-β1 mRNA levels.

(**a**) A representative northern blot analysis. Arrows indicate TGF-β1 mRNA or GAPDH. (**b**) Quantitative studies show that TGF-β1 mRNA levels in 100-day DA compared to Ao EC are not significantly increased while there is a significant fall in TGF-β1 mRNA levels in both DA and Ao EC comparing cells from 100- and 138-day gestation lambs. Bar represents mean ± SD from assays from 4 different animals at each time-point. * indicates $p < 0.05$.

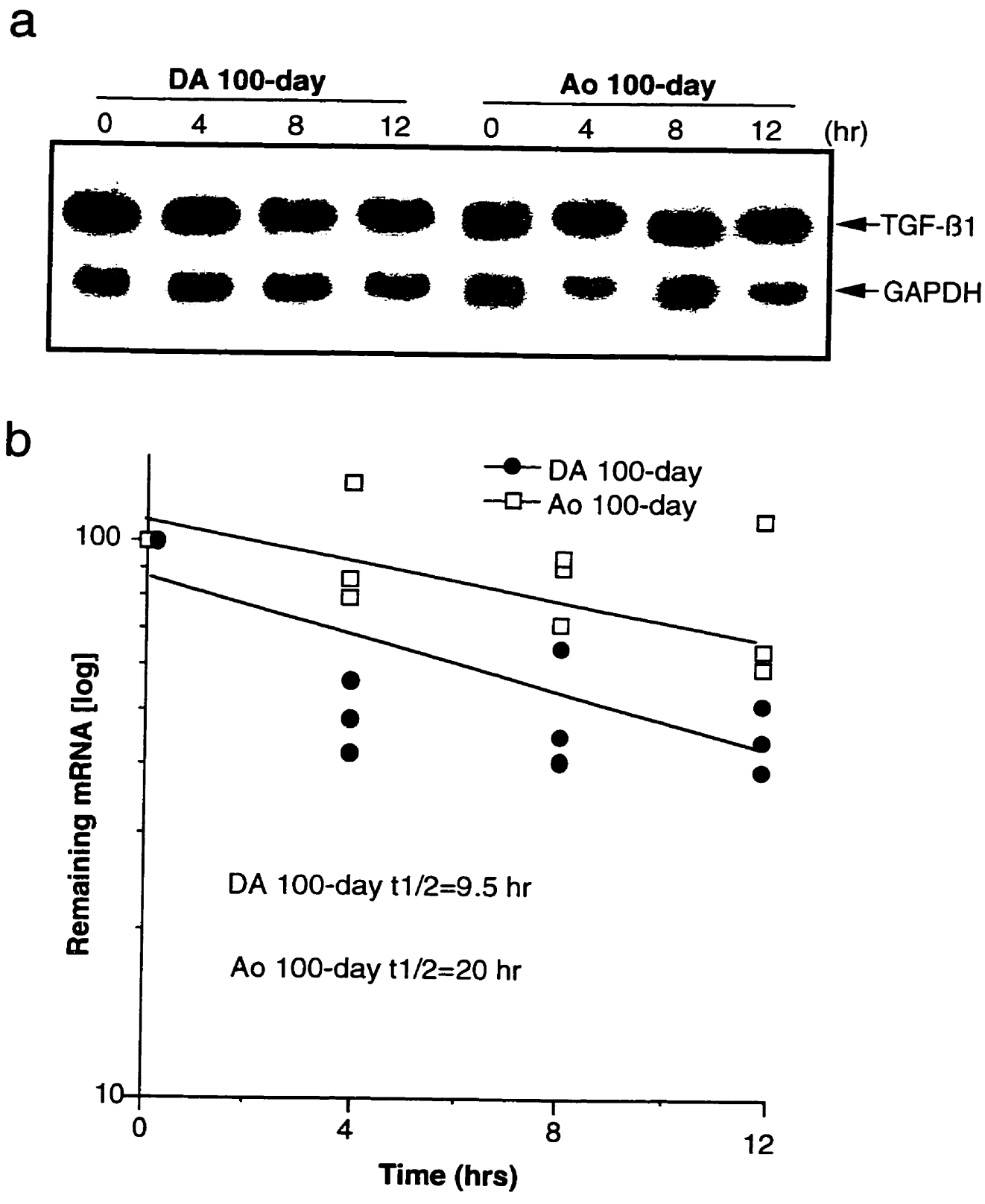
a
DA 100-day
Ao 100-day
0
4
8
12
0
4
8
12
(hr)
TGF-β1
GAPDH
b
DA 100-day
Ao 100-day
100
10
Remaining mRNA [log]
DA 100-day t1/2=9.5 hr
Ao 100-day t1/2=20 hr
0
4
8
12
Time (hrs)

Figure 15

Figure 15. Northern blot analysis of stability of TGF-β1 mRNA in 100-day DA and Ao EC

(**a**) is the representative autoradiograph of northern blots from 3 different experiments and (**b**) represents mRNA decay curves generated by plotting the remaining mRNA of three experiments to related time-point. After correcting for any differences in total RNA loading by standardizing to mRNA levels of GAPDH, TGF–ß1 mRNA signals were plotted semi-logarithmically as a function of time. Simple linear regression was used for determination of mRNA half-life. The difference in TGF-ß1 mRNA half-life between DA and Ao cells is represented by the difference in slopes of the curves as assessed by two factor ANCOVA, and $p = 0.0248$.

life of the mRNA was approximately 13 h and 9 h, respectively (Figure 16). Taken together these data suggest increased transcription and translation of a relatively unstable TGF-β mRNA in 100-day DA EC, and a reduction in transcription in the 138-day DA and in the mRNA stability in Ao EC.

DISCUSSION

Our previous studies have shown that the EC from 100-day gestation fetal lamb DA produce a matrix rich in hyaluronan and the corresponding SMC produce significantly greater amounts of fibronectin than cells from the Ao (Boudreau and Rabinovitch, 1991). These changes in DA extracellular matrix production appear to be developmentally-regulated and the increased endothelial hyaluronan and SMC fibronectin synthesis early in gestation has been further related to DA SMC migration by *in vitro* three-dimensional collagen gel assays (Boudreau, *et al.*, 1991), suggesting a mechanism for the DA intimal cushion formation observed *in vivo* (Gittenberger-de Groot, *et al.*, 1985; de Reeder, *et al.*, 1988). That is, the increase in the synthesis and accumulation of hyaluronan in the subendothelium of the DA in early gestation seems to provide a suitable environment for subsequent SMC migration during the intimal cushion formation by late gestation.

It is likely that certain growth factors may be responsible for inducing the extracellular matrix changes, which set the stage for the whole process of intimal cushion formation. TGF-β1 is likely the growth factor involved, as it is known to be the predominant TGF-β isoform upregulated in remodeling vessels (Sarzani, *et al.*, 1989; Majesky, *et al.*, 1991; Nikol, *et al.*, 1992; Ross, 1993) and the most potent activator for extracellular matrix production (Sarzani, *et al.*, 1989; Nikol, *et al.*, 1992; Ross, 1993). Infusion of TGF-β1 or direct transfer of the TGF-β1 gene into the vessel wall induce intimal hyperplasia due to extracellular matrix production (Nabel, *et al.*, 1993; Kanzaki, *et al.*, 1995). Conversely, antibodies against TGF-β1 suppress intimal hyperplasia in an acutely injured vessel associated with reduced extracellular matrix production (Wolf, *et al.*, 1994).

a

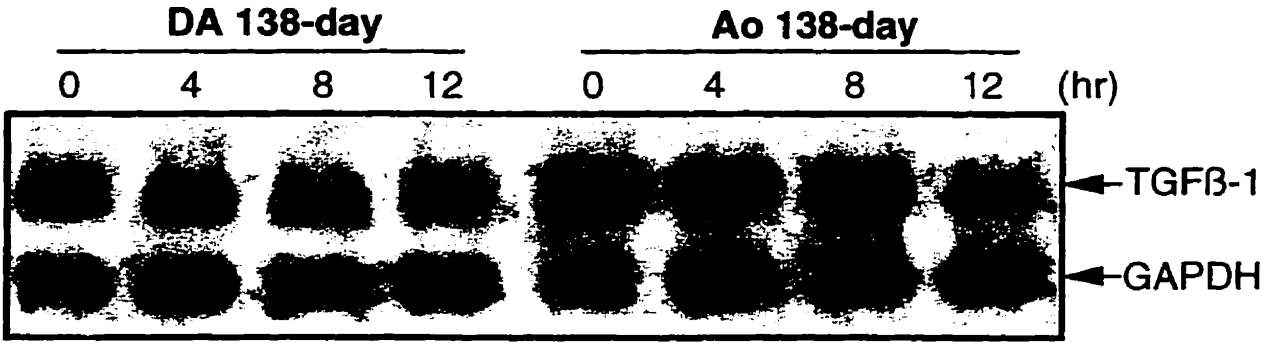
DA 138-day
Ao 138-day
0
4
8
12
0
4
8
12
(hr)
TGFß-1
GAPDH

b

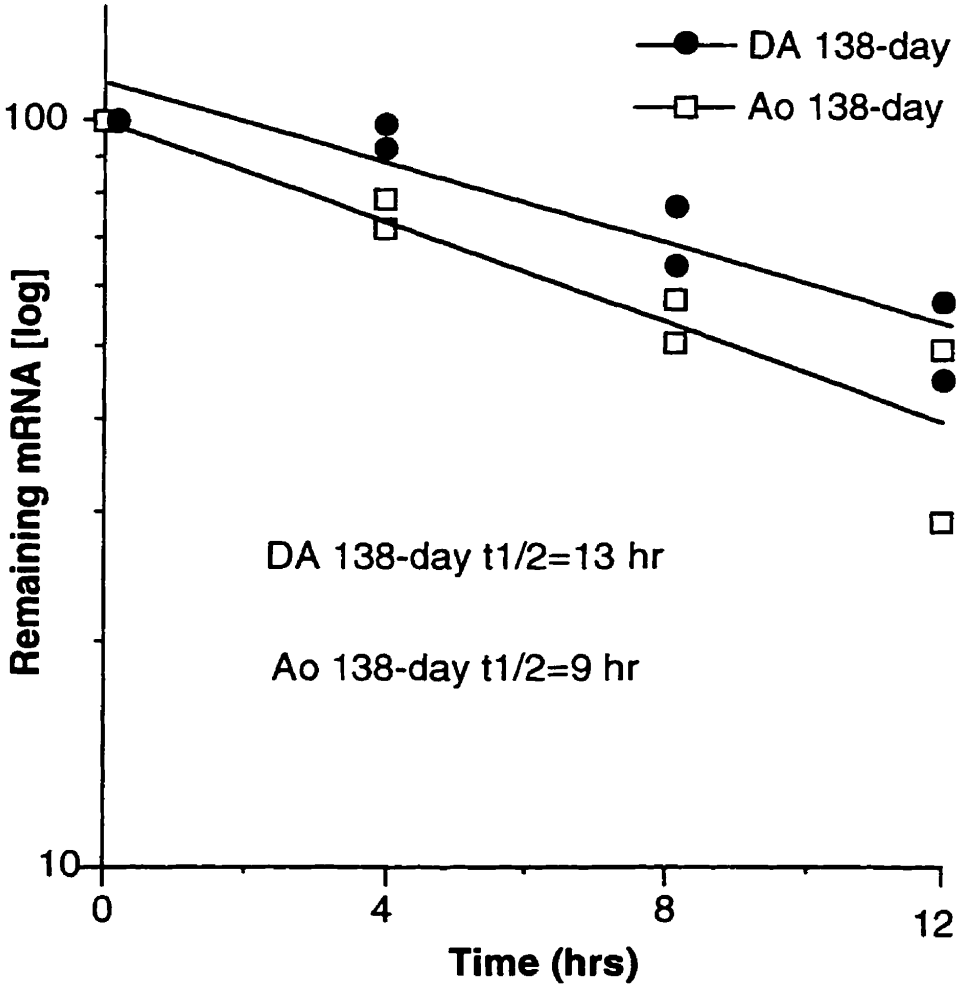
DA 138-day
Ao 138-day
100
10
Remaining mRNA [log]
DA 138-day t1/2=13 hr
Ao 138-day t1/2=9 hr
0
4
8
12
Time (hrs)

Figure 16

Figure 16. Northern blot analysis of stability of TGF-β1 mRNA in 138-day DA and Ao EC

(**a**) shows representative autoradiographs of northern blots from 2 different experiments and (**b**) indicates the curves generated by plotting remaining mRNA of two experiments to the related time-point. Half-life of mRNA was calculated as described in Figure 15.

In previous studies, we showed that the increase in DA endothelial hyaluronan is TGF-β-dependent, since the addition of neutralizing antibodies to TGF-β in 100-day DA EC cultures decreased synthesis of hyaluronan to the level of that seen in the Ao cells (Boudreau, *et al.*, 1992). We also demonstrated by immunohistochemical staining that increased amounts of TGF-β1 are associated with 100-day gestation DA compared to Ao tissues (Boudreau, *et al.*, 1992). We have extended these observations in this study, first by comparing the presence of TGF-β in the tissue at 100- and 138-day gestation time-points with the expression of TGF-β in cultured cells as judged by protein synthesis and mRNA levels.

Our data show site-related differences in the expression of TGF-β in DA cells reflected in an increase in protein synthesis when compared to that in the Ao at 100-day gestation. In addition, there is a developmentally-associated downregulation of TGF-β synthesis in DA cells between the 100-day and 138-day gestation time-points. Since the antibody that we used in the immunostaining and immunoprecipitation studies would detect mostly the TGF-β1 isoform, and since similar changes in the cellular localization of the different isoforms of TGF-β are reported in the closing of the lamb ductus arteriosus (Tannenbaum, *et al.*, 1996), we studied the regulation of TGF-β expression by assessing steady-state levels of TGF-β1 mRNA. There were, however, no significant differences in mRNA levels comparing DA with Ao EC at both gestation time points but there was a developmental decrease in TGF-β1 mRNA level in both DA and Ao cells.

The stability of TGF-β1 mRNA was then studied and TGF-β1 mRNA half-life was estimated based on three (100-day cells) or two (138-day cells) sets of experiments. The half-life of TGF-ß1 mRNA in 100-day DA cells was short compared to that in 100-day Ao cells, indicating TGF-ß1 mRNA is relatively unstable in 100-day DA cells. Variability is to be expected in this type of experiment, and so it would be best to further confirm our observations by increasing experimental sample sizes and time points. It would be of further interest then to explore the mechanism and to determine if there are similar features related to those described for other cytokines. For example, previous observations have shown that the reduced stability of growth factor or cytokine mRNAs bearing AU-rich elements consisting of the UUAUUUAU octamer are

coupled with their increased translational efficiency (Savant-Bhonsale and Cleveland, 1992; Aharon and Schneider, 1993; Winstall, et al., 1995).

There is likely also increased transcription of mRNA in 100-day DA EC cells, as the levels of steady-state TGF-β1 mRNA in 100-day DA EC were similar to that observed in Ao cells despite its shorter half life in DA EC. Technical features related to the inability to culture sufficient numbers of EC from the DA that would maintain the phenotypic characteristics of this vessel, limited our ability to assess rates of transcription of mRNA by nuclear run-on. Thus, our results indicate that both transcriptional and post-transcriptional mechanisms may be involved in the upregulation of 100-day DA TGF-β1 synthesis in our primary EC culture system. The reduced TGF-β synthesis at 138 days gestation in the DA EC is associated with decreased steady-state mRNA levels suggesting decreased mRNA transcription. In the Ao EC however, there is little decrease in TGF-β synthesis at 138 days suggesting that the decrease in the steady-state level of TGF-β1 mRNA and in its stability is likely accompanied by heightened efficiency of mRNA translation.

Previous studies concerned with the regulation of TGF-β1 expression have shown that the human TGF-β1 promoter contains two transcription start sites and several binding domains for known transcription factors (Kim, *et al.*, 1989a; Kim, *et al.*, 1989b). For example, phorbol ester-responsive elements have been identified in both the upstream and downstream domains of the gene, and seem to be important in regulating TGF-β1 expression at the transcriptional level (Kim, *et al.*, 1989b; Scotto, *et al.*, 1990). Moreover, the transcription of TGF-β1 has been shown to be stimulated by the product of the retinoblastoma gene through specific retinoblastoma response elements (Kim, *et al.*, 1991).

There is also a growing accumulation of evidence indicating that expression of TGF-β1 may be also regulated post-transcriptionally (Assoian, *et al.*, 1987; Wager and Assoian, 1990; Ahuja, *et al.*, 1995; Cosgaya and Aranda, 1995). For example, nerve growth factor induces TGF-β1 expression partly due to an increase in its mRNA half life from 6 h to 30 h in PC12 cells (Cosgaya and Aranda, 1995). The immunosuppressant cyclosporine has also been shown to

prolong the half life of TGF-β1 mRNA in activated human T lymphocytes (Ahuja, *et al.*, 1995). Although the mechanisms of the post-transcriptional control of TGF-β1 expression are not well known, several studies have demonstrated that the GC-rich sequence in the 5' untranslated region (UTR) may play a role in controlling TGF-β1 production from mRNA (Kim, *et al.*, 1992). Computer analysis showed that this region of the 5'UTR contains a stable secondary stem-loop structure between sequences +49 to +76. This stem-loop region alone is sufficient to inhibit expression of the growth hormone gene, suggesting that it may contain a *cis* element which plays an important role in the post-transcriptional regulation of TGF-β1 gene expression. Moreover. Scotto and Assoian (Scotto and Assoian, 1993) have been able to show that a GC-rich domain in the 3'UTR of can have a bifunctional effect on the overall protein expression; it may decrease the steady-state TGF-β1 mRNA while increasing its protein production by improving the efficiency of translation. The relative contributions of these inhibitory and stimulatory bifunctional elements to TGF-β1 protein production may result from temporal or cell-specific expression of certain *trans*-acting factors (Scotto and Assoian, 1993). It would be interesting to investigate whether or not these *cis* elements including the aforementioned AU-rich-like element in the 3'UTR of TGF-β1 mRNA are responsible the regulation of expression of TGF-β1 in the DA EC.

Since we had previously identified that the increased FN synthesis in the DA SMC is regulated at a post-transcriptional level, we next went on to evaluate the mechanisms involved with the view that it might ultimately also provide new insight into regulation of other gene expression.

CHAPTER TWO

POST-TRANSCRIPTIONAL MECHANISM REGULATING FIBRONECTIN SYNTHESIS IN DUCTUS SMOOTH MUSCLE CELLS RELATED TO AN 3'UTR AU-RICH ELEMENT AND ITS BINDING PROTEIN

INTRODUCTION

We observed a developmentally-regulated increase in synthesis of FN in cultured DA compared to aorta (Ao) SMC isolated from 100-day gestation lambs (Boudreau and Rabinovitch, 1991). This increased FN synthesis was further related to the DA elongated migratory SMC phenotype (Boudreau, *et al.*, 1991). These features contribute to the SMC migration observed *in vivo*, from the inner media of the vessel wall into a subendothelium enriched in glycosaminoglycans. SMC migration contributes the intimal cushion formation that partially occlude the vessel lumen and assure that the vessel closes completely when it constricts post-natally (Gittenberger-de Groot, *et al.*, 1985; de Reeder, *et al.*, 1989). Study of the regulation of FN synthesis revealed that the increased FN synthesis in DA SMC was not associated with increased FN mRNA levels or stability or with differences in mRNA splicing (Boudreau, *et al.*, 1992), suggesting enhanced translational efficiency of FN mRNA in DA versus Ao SMC. Other studies from our laboratory using piglets to study the development of the neointima in coronary arteries after experimental cardiac transplant suggest that there may also be post-transcriptional regulation of the increased FN synthesis by donor coronary artery EC (Molossi *et al.*, 1993).

Fibronectin, a large extracellular matrix glycoprotein with M_r of 220 kD, functions as a molecule involved in cell adhesion, migration, and differentiation (Hynes, 1990). Fibronectin synthesis is regulated by growth factors (Dean, *et al.*, 1988; Penttinen *et al.*, 1988; Seebacher, *et al.*, 1988), cytokines (Clausell, *et al.*, 1993), or serum stimulation (Dean, *et al.*, 1990) through increasing mRNA levels due to transcriptional activation. Post-transcriptional mechanisms have been also reported involving in upregulating FN protein production (Dhawan *et al.*, 1991; Rasoamanantena, *et al.*, 1994; Chou *et al.*, 1995). Dhawan *et al.* (Dhawan, *et al.*, 1991) reported that cell adhesion modulates FN synthesis at the post-transcriptional level without a change of mRNA stability. Prematurely senescent cultured Werner syndrome fibroblasts produce more FN than normal fibroblasts due to both augmentation of FN mRNA levels and enhanced efficiency of FN mRNA translation (Rasoamanantena, *et al.*, 1994). In addition, Chou and colleagues (1995) demonstrated that increased FN synthesis and secretion in human fibroblasts by altering the

substratum surface topography, which is accompanied with enhanced mRNA stability.

A number of investigators have shown that regulatory elements in the 5' as well as the 3' untranslated region (UTR) of mRNA modulate mRNA stability and/or translational efficiency (Kruys, *et al.*, 1987; Rouault *et al.*, 1988; Klausner and Harford, 1989). Caput *et al.* (1986) reported a consensus sequence (UUAUUUAU) present in the 3'UTR of cytokine-derived mRNAs, such as tumor necrosis factor-α (TNF-α), granulocyte macrophage colony-stimulating factor (GM-CSF), interleukin-1 (IL-1), and interferons (IFN), which is also present in the 3'UTR of FN mRNA (Kornblihtt, *et al.*, 1983; Schwarbauer, *et al.*, 1983; Caput, *et al.*, 1986). In most studies, this AU-rich element (ARE) in the 3'UTR of labile mRNAs, such as c-*myc* (Jones and Cole, 1987), GM-CSF (Shaw and Kamen, 1986), and c-*fos* (Wilson and Treisman, 1988; Shyu, *et al.*, 1991) correlates with rapid mRNA turnover. However, the ARE also regulates mRNA translation (Kruys, *et al.*, 1987; Kruys, *et al.*, 1988; Kruys, *et al.*, 1989; Han, *et al.*, 1990a; Han, *et al.*, 1990b; Grafi, *et al.*, 1993; Kruys, *et al.*, 1993; Marinx *et al.*, 1994). Recent studies have indicated that degradation of mRNA mediated by GM-CSF ARE is coupled with ongoing translation (Savant-Bhonsale and Cleveland, 1992; Aharon and Schneider, 1993; Winstall, *et al.*, 1995) and this appears to be related to translational-dependent assembly of a >20S degradation complex (Savant-Bhonsale and Cleveland, 1992).

Trans-acting factors in the cytoplasm may alter mRNA stability or translational efficiency through binding to the ARE. Malter (Malter, 1989) first reported a cytosolic protein, termed adenosine-uridine binding factor (AUBF), which binds specifically to AUUUA motifs. Bohjanen *et al.* identified three factors which bind to the ARE with different binding affinities and specificities (Bohjanen, *et al.*, 1991; Bohjanen, *et al.*, 1992). The ARE found in the 3'UTR of FN mRNA (Kornblihtt, *et al.*, 1983; Schwarbauer, *et al.*, 1983; Caput, *et al.*, 1986) may also function to modulate DA and Ao SMC FN mRNA stability and translational efficiency. In this study, by using a combination of transfection and immunofluorescence studies with site-directed mutagenesis, we have been able to show that the FN ARE is of functional significance in enhancing mRNA translation in vascular cells. We then demonstrated that the degree of mRNA

translation may be related to intracellular differences in the FN ARE-binding factors in DA and Ao SMC cytoplasmic extracts. We further identified, through UV-crosslinking studies, three binding complexes of M_r of approximately 60, 30 and 15 kD.

RESULTS

The ARE in FN 3'UTR is an mRNA Translational Enhancer in Vascular Cells

Our previous studies suggested that the increased synthesis of FN in DA compared to Ao SMC is due to an increased translational efficiency of FN mRNA. Messenger RNAs of many cytokines, proto-oncogenes, and adhesion molecules contain an ARE in their 3'UTR. This element has been documented as an mRNA destabilizing element (Shaw and Kamen, 1986; Jones and Cole, 1987; Wilson and Treisman, 1988) or a modulator of translational efficiency (Kruys. *et al.*, 1987; Kruys, *et al.*, 1988; Kruys, *et al.*, 1989; Han, *et al.*, 1990a; Han, *et al.*, 1990b; Kruys. *et al.*, 1993; Marinx, *et al.*, 1994). One copy of UUAUUUAU is also within an AU-rich region in the FN 3'UTR (Kornblihtt, *et al.*, 1983; Schwarbauer, *et al.*, 1983; Caput, *et al.*, 1986) with unknown function. To determine whether the FN ARE may be involved in the augmentation of FN mRNA translational efficiency in primary cultured DA versus Ao SMC, we first generated a 3'UTR regulatory CAT construct (Figure 17) containing the CAT coding sequence, an upstream SV40 early promoter and a downstream FN 3'UTR bearing the intact ARE, UUAUUUAU, followed by a poly-A sequence (defined as pECE-CAT-FN). The ARE was mutated as GGAGGGAG and the mutated plasmid was defined as pECE-CAT-FNΔ. The plasmid (pECE-CAT) containing CAT and its own 3'UTR was used as a control. Transfection studies were then carried out with these three constructs and the level of CAT protein (activity) as well as mRNA were measured. Table I summarizes the data illustrated in Figure 18 using cells from 3 different fetal lambs.

Figure 18a demonstrated that DA SMC transfected with pECE-CAT-FN showed a 2.4-fold increase in CAT activity compared to pECE-CAT-FNΔ with mutated ARE ($p < 0.05$) and a relatively smaller 1.3-fold increase was observed in Ao cells ($p < 0.05$). RNase protection studies

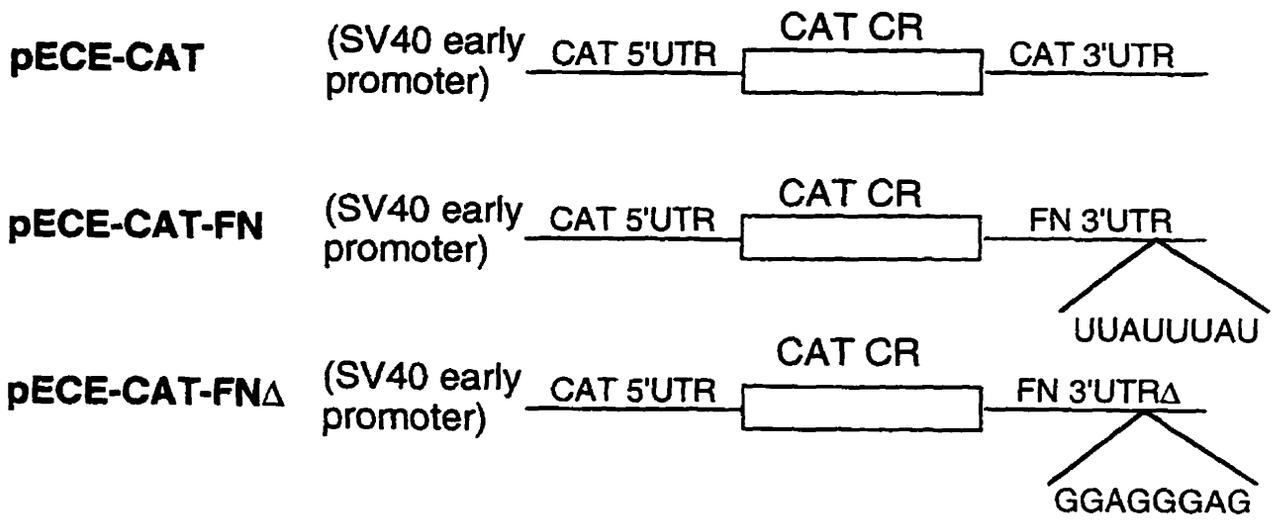
pECE-CAT
(SV40 early promoter)
CAT 5'UTR
CAT CR
CAT 3'UTR
pECE-CAT-FN
(SV40 early promoter)
CAT 5'UTR
CAT CR
FN 3'UTR
UUAUUUAU
pECE-CAT-FNΔ
(SV40 early promoter)
CAT 5'UTR
CAT CR
FN 3'UTRΔ
GGAGGGAG

Figure 17

Figure 17. Schematic representation of the CAT constructs

CAT transcription is driven by the SV40 early promoter. The CAT coding region (CR) is followed by its own 3'UTR or FN 3'UTR containing either wild type or the mutated UUAUUUAU generated by site-directed mutagenesis.

Table I. Measurements of CAT activity, mRNA, and ratio of CAT activity to mRNA

Transfectant	CAT activity (n = 6)	CAT mRNA (n = 3)	CAT activity/mRNA
DA/pECE-CAT	30.678 ± 4.396	2.223 ± 0.075	13.800
DA/pECE-CAT-FN	19.272 ± 4.622*	1.117 ± 0.074*	17.253
DA-pECE-CAT-FNΔ	5.745 ± 0.847	3.963 ± 0.154	1.450
Ao/pECE-CAT	18.330 ± 2.218	1.830 ± 0.190	10.016
Ao/pECE-CAT-FN	11.078 ± 1.923*	1.143 ± 0.046*	9.692
Ao/pECE-CAT-FNΔ	4.915 ± 0.523	3.783 ± 0.202	1.299

Values are mean ± SEM; n = number of experiments. * $p < 0.05$, compared to the group above and below by SuperANAOVA and Duncan New Multiple Range test.

showed a significant decrease in CAT mRNA levels in both DA (50%) and Ao SMC (38%) transfected with pECE-CAT-FN compared to pECE-CAT after normalization using β-gal mRNA levels (Figure 18**b**). This is in agreement with the level of CAT activities found in these cells, suggesting that the 3'UTR of FN mRNA may decrease CAT mRNA stability relative to the native CAT 3'UTR. The CAT mRNA levels were, however, greatly decreased (~70%) in both DA and Ao cells transfected with pECE-CAT-FN compared to pECE-CAT-FNΔ ($p < 0.05$). This result suggests that the ARE in the 3'UTR of FN mRNA has mRNA destabilizing properties as has been described for the ARE in other mRNA species (Shaw and Kamen, 1986; Jones and Cole, 1987; Wilson and Treisman, 1988). Using the ratio of CAT activity to mRNA level as an index of translational efficiency (Table I), we noted that the translation of pECE-CAT-FN mRNA was more efficient than that of pECE-CAT-FNΔ in both DA (increased 10.9-fold) and Ao SMC (increased 6.5-fold). Thus, the ARE in the 3'UTR of FN mRNA may serve as an enhancer of mRNA translation with this function perhaps amplified in DA compared to Ao SMC.

Alteration of Cell Shape and Reduction of FN production in DA SMC Transfected with pECE-CAT-FN

Having evidence indicating that FN ARE is responsible for increased CAT mRNA translational efficiency in DA compared to Ao SMC, the following studies were carried out to verify the functional presence of FN ARE-binding factors in SMC, and their potential effects on FN production. As transient transfection of pECE-CAT-FN would result in abundant FN 3'UTR in transfected cells, the ARE in pECE-CAT-FN fusion transcripts could be expected to sequester the putative ARE-binding factors and reduce their binding to the ARE of endogenous FN mRNA. If the interaction of the cytoplasmic factors and the FN ARE promotes endogenous FN expression, the decoy of ARE-binding factors would decrease the expression of FN protein in the cells that express exogenous AREs, and alter the FN-dependent elongated migratory cell shape (Boudreau, *et al.*, 1991). To determine whether this does in fact occur, we examined CAT-positive cells by immunostaining and correlated the cell shape and the expression of FN with transfected plasmids.

a

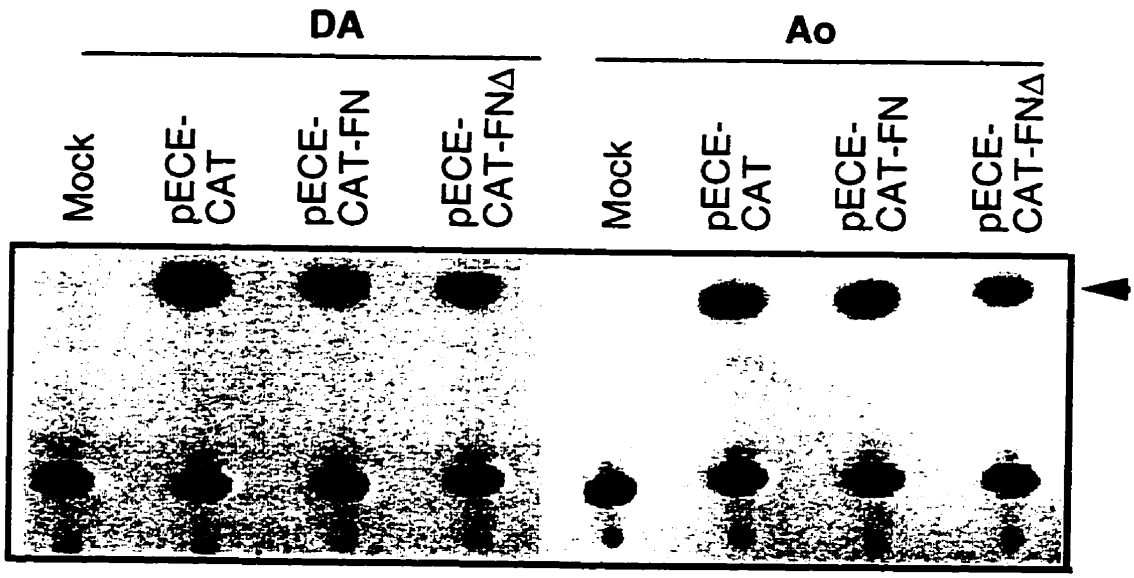
DA
Ao
Mock
pECE-CAT
pECE-CAT-FN
pECE-CAT-FNΔ
Mock
pECE-CAT
pECE-CAT-FN
pECE-CAT-FNΔ

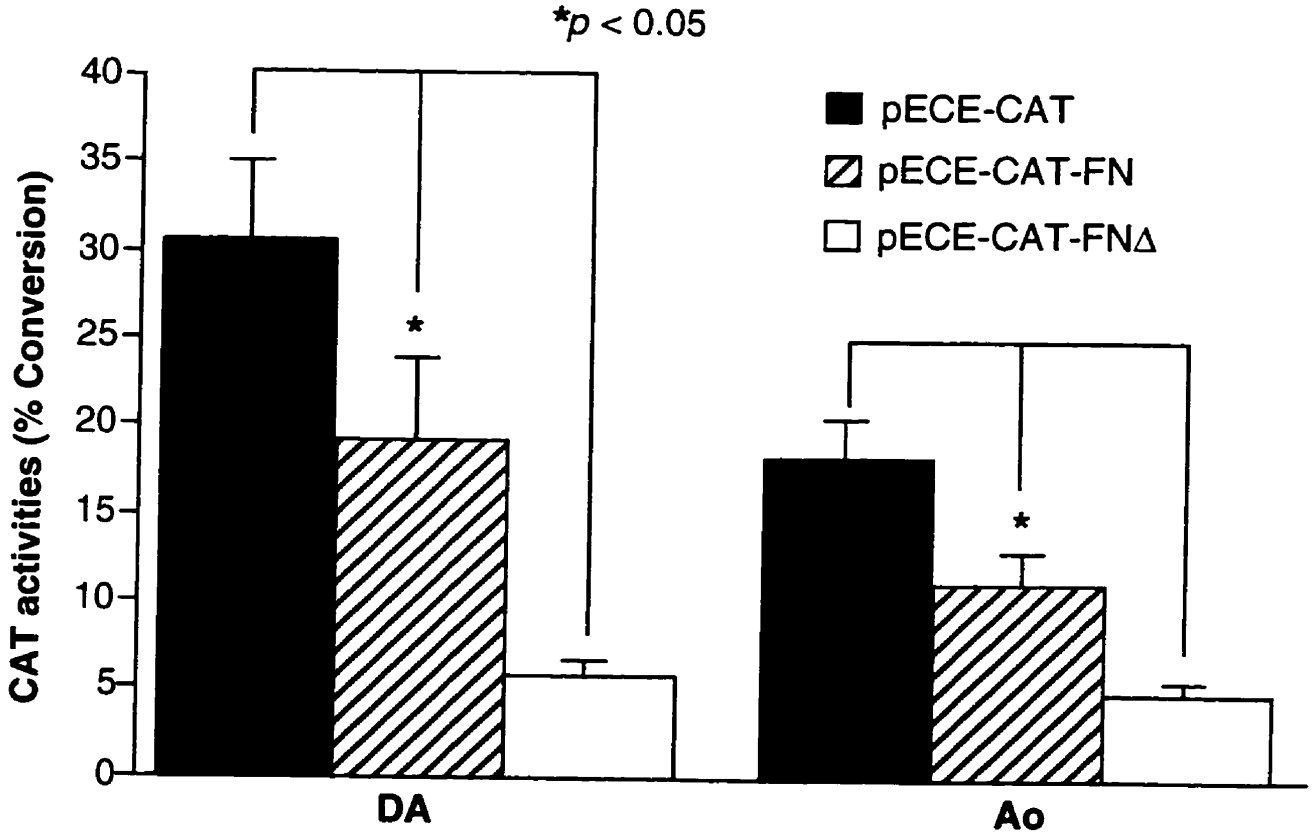
*p < 0.05
CAT activities (% Conversion)
40
35
30
25
20
15
10
5
0
pECE-CAT
pECE-CAT-FN
pECE-CAT-FNΔ
*
*
DA
Ao

Figure 18a

Figure 18a. The ARE in the 3'UTR of FN mRNA enhances translation

Top is a representative autoradiograph of CAT assays using thin layer chromatography; bottom is the quantitative results of CAT assays from 6 separate transfection studies using control plasmid (pECE-CAT), plasmid containing wild type ARE (pECE-CAT-FN), and plasmid containing mutated ARE (pECE-CAT-FNΔ). Mock transfected cells show radiolabeled non-acetylated chloramphenicol only, whereas the acetylated product is observed in cells transfected with CAT constructs (arrow). The CAT activity is significantly decreased in either DA (37%) or Ao cells (40%) transfected with the plasmid pECE-CAT-FN compared to pECE-CAT ($p < 0.05$. SuperANOVA and Duncan New Multiple Range test of multiple comparisons). However, there is a significance increase in CAT activity in both DA (2.4-fold) and Ao cells (1.3-fold) transfected with pECE-CAT-FN compared to pECE-CAT-FNΔ ($p < 0.05$), suggesting that the FN ARE is functionally involved CAT expression.

b

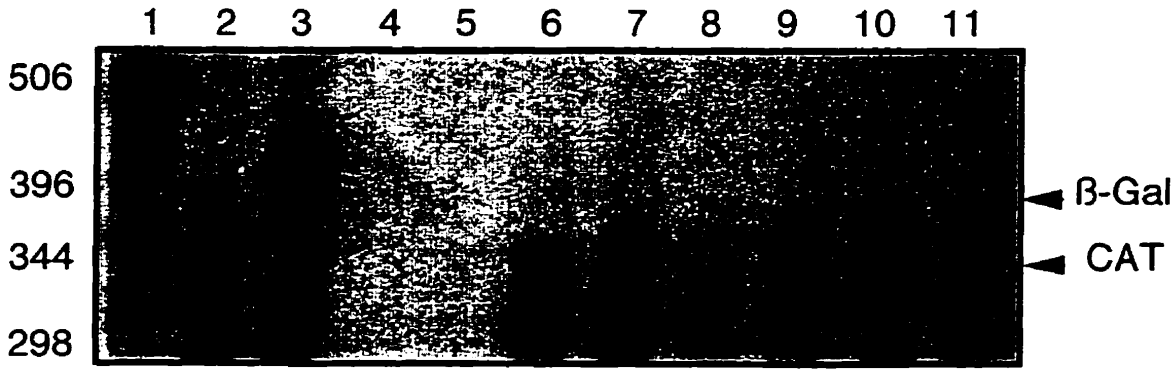
1 2 3 4 5 6 7 8 9 10 11
506
396
344
298
ß-Gal
CAT

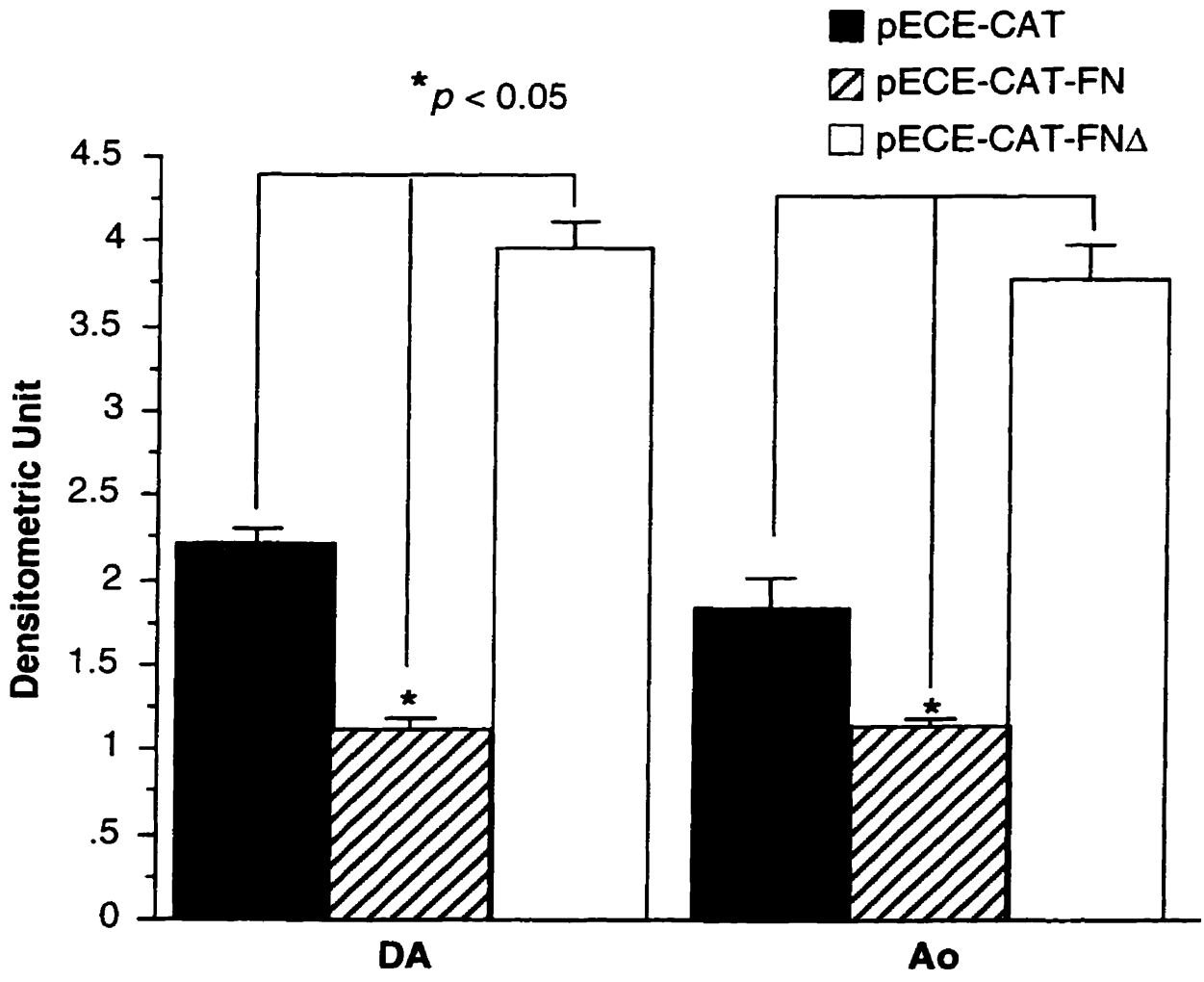
pECE-CAT
pECE-CAT-FN
pECE-CAT-FNΔ
*p < 0.05
Densitometric Unit
4.5
4
3.5
3
2.5
2
1.5
1
.5
0
*
*
DA
Ao

Figure 18b

Figure 18b. The ARE in the 3'UTR of FN mRNA enhances translation

Top is a representative autoradiograph of RNase protection assay and bottom is a densitometric analyses of three different experiments. Lane 1 shows 1 kb DNA ladder as a marker. Lanes 2 and 3 show only the full-length CAT (325 bp) and β-gal (378 bp) probes, respectively. Lanes 4 and 5 are negative controls using CAT and β-gal probe to hybridize with yeast RNA, respectively, showing no protected RNA fragment. Lanes 6-8 show RNA from DA SMC and lanes 9-11 RNA from Ao SMC transfected with different CAT constructs (lanes 6 and 9 = pECE-CAT; lanes 7 and 10 = pECE-CAT-FN; lanes 8 and 11 = pECE-CAT-FNΔ) hybridized with CAT, as well as β-gal probe. The protected CAT (260 bp) and β-gal (289 bp) probe are indicated by arrows on the right (an RNA fragment will run a slightly slower than a DNA fragment of the same size). Densitometric studies show a significant decrease in the level of CAT mRNA in both DA (50%) and Ao SMC (38%) transfected with pECE-CAT-FN compared to pECE-CAT which is consistent with the decreases in CAT activities. When compared to cells transfected with pECE-CAT-FNΔ however, a remarkable decrease in the CAT mRNA level is found in both DA (72%) and Ao SMC (70%) which is not associated with decreased but rather increased CAT activities. The CAT mRNA level was normalized with β-gal mRNA which was used to control for transfection efficiency and loading conditions.

Figure 19**a** shows that of a total number of CAT-positive cells transfected with control plasmid pECE-CAT (mean = 25, range 19-30), 82% (range = 72-89%) had an elongated phenotype. In CAT-positive cells transfected with wild type plasmid pECE-CAT-FN (mean = 21, range 15-30), however, only 54% (range 47-60%) showed the elongated phenotype. In CAT-positive cells transfected with mutated plasmid pECE-CAT-FNΔ (mean = 18, range 16-20), 77% (75-80%) were elongated. The decrease in the percentage of elongated cells following transfection with pECE-CAT-FN was significant ($p < 0.05$). Figure 19**b** is a representative photograph of cells from these experiments. The CAT-positive cells (red staining) were identified as cells in which there was cytoplasmic staining with a rhodamine-tagged anti-CAT antibody. The CAT-positive cells transfected with control plasmid pECE-CAT showed an elongated phenotype (**A**). The switch from elongated (**A**) to stellate phenotype was observed in cells transfected with wild type plasmid containing intact ARE (pECE-CAT-FN) (**B**), but not in cells transfected with ARE-mutated plasmid (pECE-CAT-FNΔ) (**C**). Moreover, consistent with the CAT assay, CAT-positive cells transfected with ARE-mutated plasmid pECE-CAT-FNΔ (**C**) showed a decrease in intensity of CAT immunostaining compared to cells transfected with pECE-CAT-FN (**B**).

Since transient transfection using the calcium phosphate method had only a 1-2% transfection efficiency and cells were cultured at low density to visualize cell morphology, it was difficult to assess FN production. To overcome this limitation, we used a more efficient method of adenovirus transfection (see Materials and Methods, Section **II**). This system had been shown to allow more than 70% of primary cultured cardiac cells to express transfected genes (Kohout, *et al.*, 1996). We applied double-immunofluorescence using both a Texas-red-tagged antibody to visualize CAT expression (Figure 19**c**, **A**, **C**, **E**), as well as a FITC-labeled antibody to examine the FN expression (**B**, **D**, **F**). While almost all the cells transfected with CAT constructs showed positive staining for CAT, we observed a consistent decrease in the accumulation of FN in the cell cultures transfected with pECE-CAT-FN (**D**) compared to pECE-CAT (**B**) or pECE-CAT-FNΔ (**F**), which also seem to correlate with a stellate compared to an elongated phenotype. Negative control using normal IgG showed that almost all the fluorescence signal was abolished (**G**).

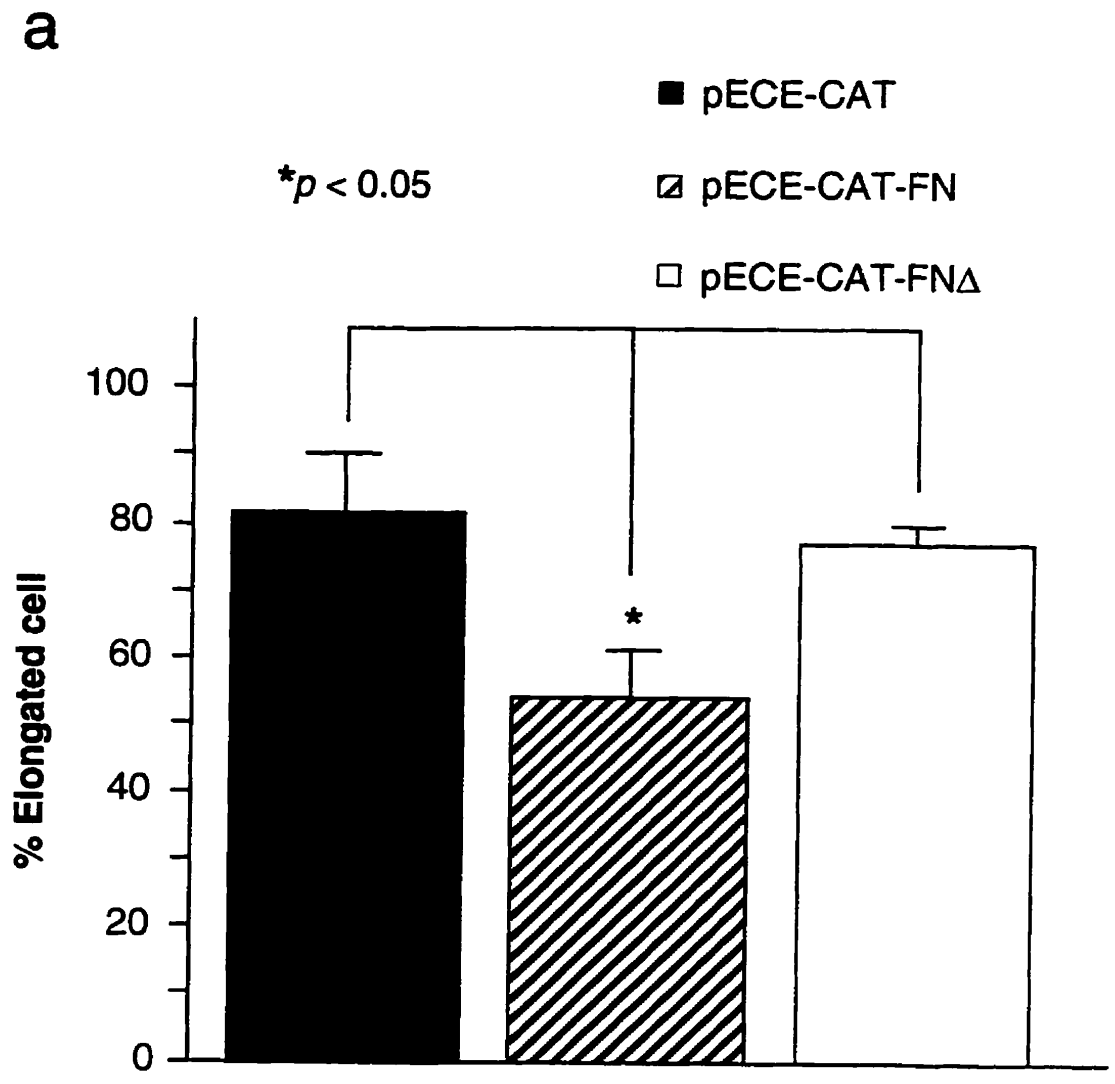
a
pECE-CAT
*p < 0.05
pECE-CAT-FN
pECE-CAT-FNΔ
% Elongated cell
100
80
60
40
20
0
*

Figure 19a

Figure 19. Expression of pECE-CAT-FN altered cell shape and decreased FN

(**a**) A graph summarizes the quantitative analysis of the change of cell shape in CAT-positive cells from three different experiments. The bar value equals the mean percentage of cells with elongated shape ± SEM. *Significant difference, $p < 0.05$, by SuperANOVA and Duncan Multiple Range test. As seen in the graph, the percentage of cells with elongated shape is reduced significantly in cells transfected with pECE-CAT-FN compared to cells transfected with other two plasmids.

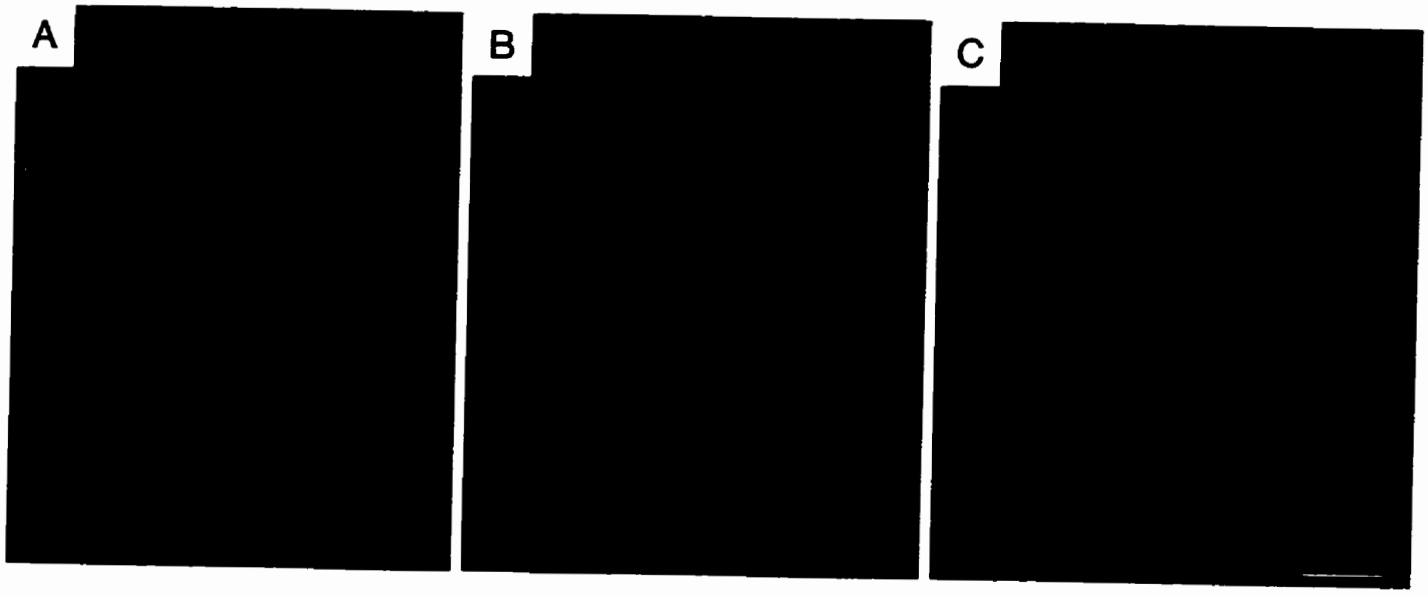

Figure 19b

Figure 19. Expression of pECE-CAT-FN altered cell shape and decreased FN

(**b**) A representative photomicrograph showing cells transfected with control plasmid pECE-CAT (**A**), ARE-containing plasmid pECE-CAT-FN (**B**) or ARE-mutated plasmid pECE-CAT-FNΔ (**C**) using calcium phosphate method. The cells were stained for CAT with rhodamine-conjugated secondary antibody and nuclei were stained with DAPI. Compared to pECE-CAT (**A**) or pECE-CAT-FNΔ (**C**), overexpression of pECE-CAT-FN (**B**) altered cell shape from elongated to stellate.

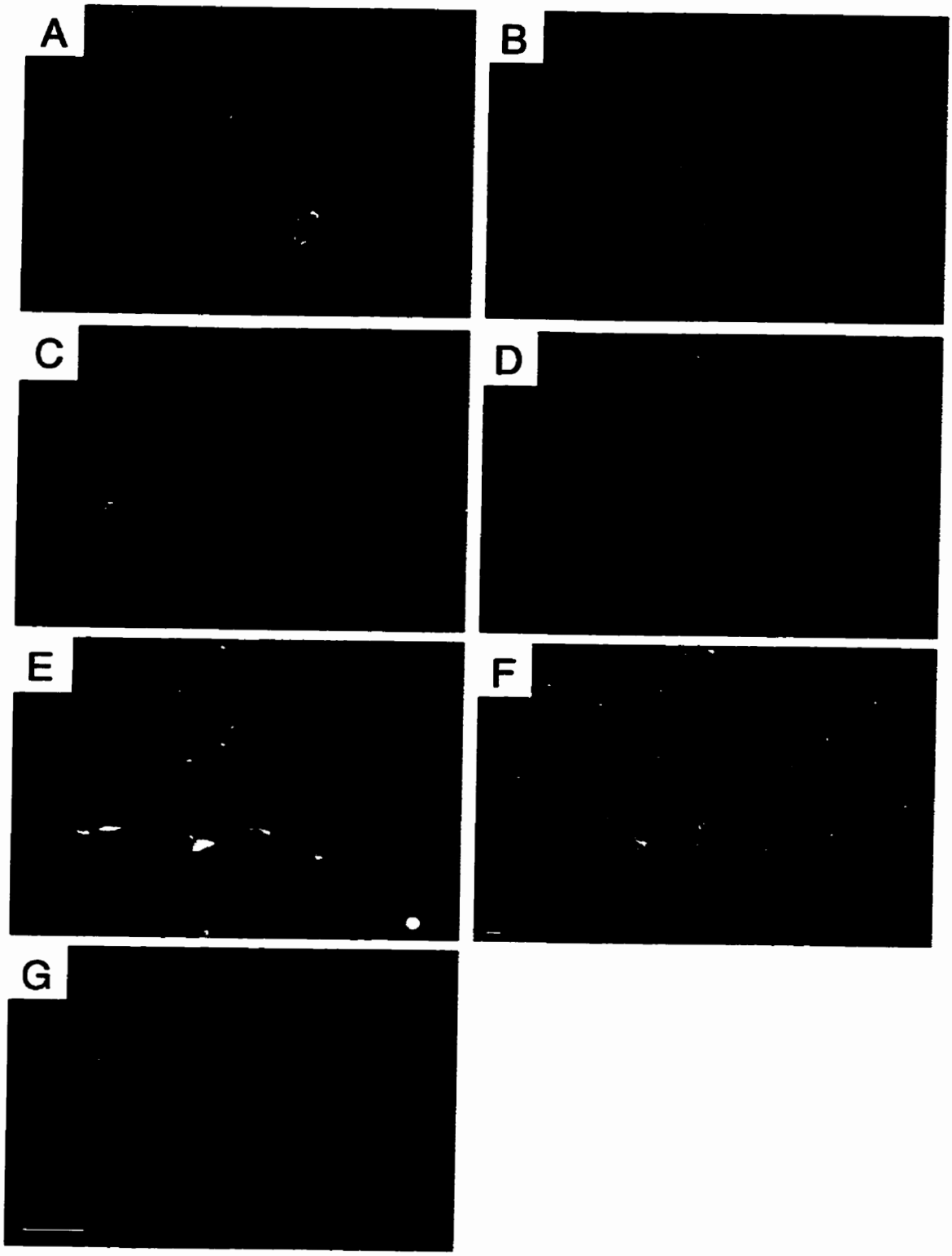

Figure 19c

Figure 19. Expression of pECE-CAT-FN altered cell shape and decreased FN

(c) A representative simultaneous immunofluorescence staining of CAT (**A**, **C**, **E**) and FN protein (**B**, **D**, **F**) in transfection studies using a 'component' adenovirus delivery system (see Materials and Methods, Section **II**). Almost all the cells stain positive for CAT by Texas red-conjugated secondary antibody. The staining for FN reveals as cell surface fibrous deposits by FITC-conjugated secondary antibody. Qualitatively, the staining for FN is less intense in cells transfected with pECE-CAT-FN (**D**) compared to either control plasmid pECE-CAT (**B**) or ARE-mutated plasmid pECE-CAT-FNΔ (**F**). Control using normal IgG shows that almost all the fluorescence signal was abolished (**G**). Bar = 10 μm.

Identifying FN ARE-Binding Activity in SMC

Studies were next undertaken to identify a cytoplasmic factor(s) with FN 3'UTR ARE-binding properties. Gel mobility shift assays were carried out in which S-100 cytoplasmic extracts prepared from cultured DA or Ao SMC were incubated with a [^{32}P]-labeled full-length FN 3'UTR with intact or mutated ARE. While probe alone showed no binding complex formation (Figure 20**a**, lanes 1 and 3), three retarded bands were found in DA S-100 extracts with wild type FN 3'UTR probe (lane 2). However, the major retarded band was not observed when using the ARE-mutated probe (lane 4). This indicated that there are cytoplasmic factors which could bind to the FN 3'UTR and that at least one of these RNA-cytoplasmic factor interactions is related to the ARE.

The specificity of this interaction was further assessed by competition experiments using an ARE-containing FN oligonucleotide probe, as well as an irrelevant probe (without ARE) of the same size. Two binding complexes (top binding complex appears to be doublet bands) were observed on a gel shift using the specific ARE-containing probe (SP) (Figure 20**b**, lane 2; lane 1 containing probe only as a control). They may represent the same binding factor with differing degrees of aggregation or different binding factors. No binding complex formation was found with the irrelevant probe (IP) (lane 3). Preincubation of unlabeled SP (10, 50, and 200-fold of radiolabeled SP) with S-100 extracts shows inhibition of radiolabeled SP binding (lanes 4-6), but the unlabeled IP was inefficient in blocking radiolabeled SP binding (lanes 7-9), indicating that the protein-RNA interaction is ARE-probe specific.

Further gel shift assays revealed formation of a similar binding complex between ARE-containing oligonucleotides and S-100 extracts from cultured both DA and Ao SMC, but a consistent increase in binding complex formation was found with S-100 extracts from DA SMC in 5 of the 6 different experiments. Since DA SMC FN synthesis has been shown to increase following serum stimulation without a parallel increase in mRNA level (Boudreau, *et al.*, 1992), we then determined whether this feature correlated with increased mRNA binding activity of the cytoplasmic factor(s). As shown in Figure 20**c**, an increase in the intensity of binding complex formation with DA compared to Ao cytosols was observed even under serum-free conditions (lane

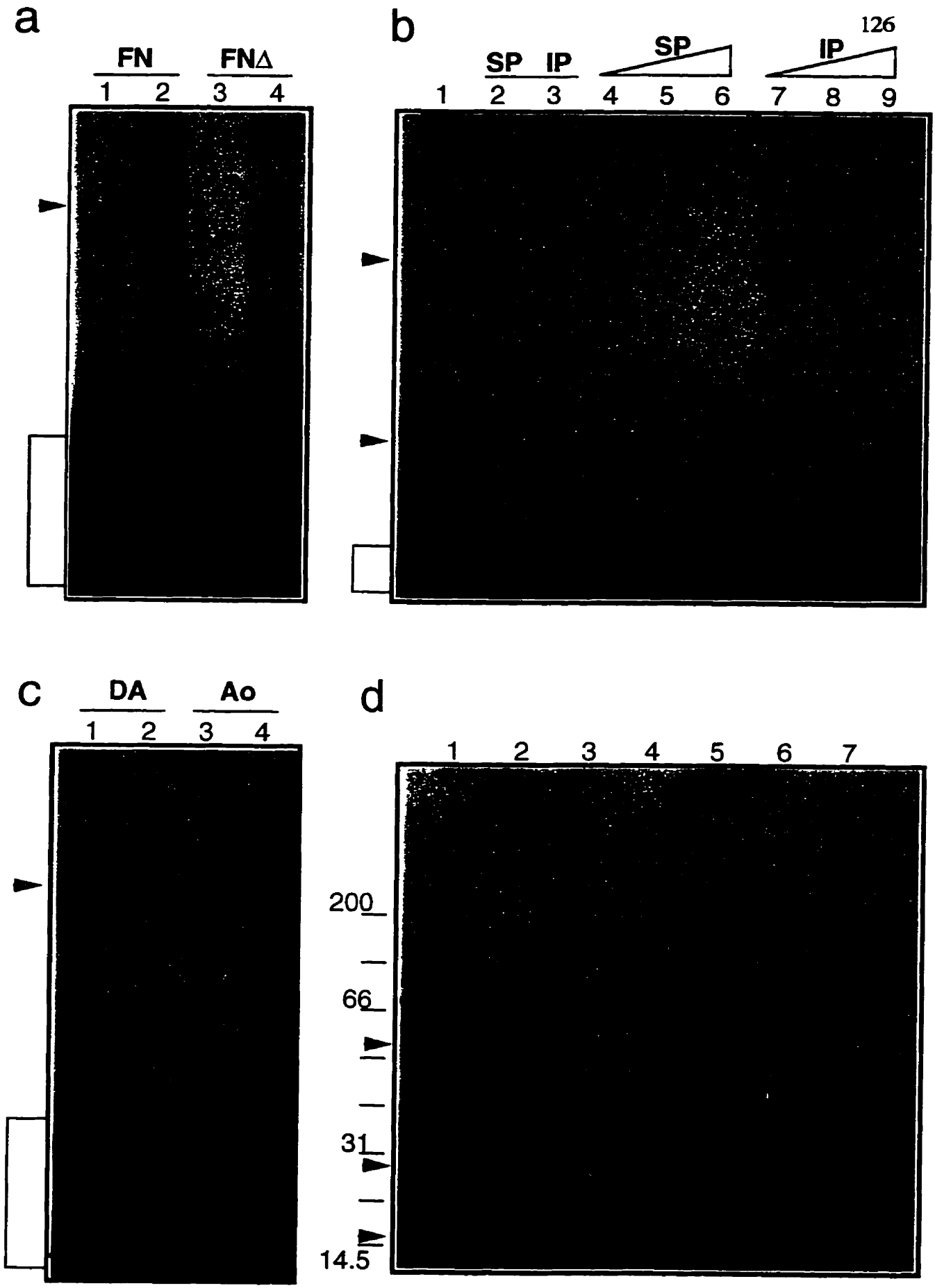
a
FN
FNΔ
1 2 3 4
b
126
SP IP
SP
IP
1 2 3 4 5 6 7 8 9
c
DA
Ao
1 2 3 4
d
1 2 3 4 5 6 7
200
66
31
14.5

Figure 20

Figure 20. Binding complex formation between the FN ARE and SMC cytoplasmic factors

(**a**) A representative autoradiograph of a gel shift assay using DA SMC S-100 cytoplasmic extracts and radiolabeled full-length FN 3'UTR containing wild type (FN) (lane 2) or mutated ARE (FNΔ) (lane 4). Lanes 1 and 3 are controls without S-100 extracts. Arrow shows the binding complex is specifically related to wild type FN 3'UTR (compare lane 2 with 4). The free probe is indicated by the bracket. (**b**) A gel shift assay with the oligonucleotide containing the ARE (SP) or irrelevant probe (IP). Lanes 1 is radiolabeled probe alone; lane 2 is SP + S-100 extracts, showing binding complexes indicated by arrows; lane 3 is IP + S-100 extracts, showing no binding complex formation. A preincubation of an increased amount of unlabeled SP (10, 50, and 200-fold, lanes 4-6) with S-100 extracts prevented binding complex formation in a does-dependent manner but not IP with the same order of concentrations (lanes 7-9). The variabilities in lanes 7-9 may result from unequal loading. (**c**) shows a gel shift assay using S-100 extracts from cultured DA (lanes 1 and 2) and Ao SMC (lanes 3 and 4) under serum-free conditions (lanes 1 and 3) or following serum-stimulation (lanes 2 and 4). Compared to Ao S-100 extracts, an increased binding complex formation is evident with DA S-100 extracts in both serum-free and serum-stimulation conditions. (**d**) a UV-crosslinking assay of the cytoplasmic factors with radiolabeled FN ARE-containing oligonucleotide. Lane 1, binding complexes run under non-reducing conditions. Lane 2, binding complexes run under reducing conditions. Lane 3, S-100 extracts incubated with 1 μg/μl proteinase K for 30 min at 37°C before the binding reaction. Lane 4, the oligonucleotide probe was treated with 1 u/μl RNase T_1 before incubation with the S-100 extracts. Lanes 5-7, the S-100 extracts were pretreated with 2% β-ME, 10 mM DTT, or 10 mM *n*-EM for 30 min at 37°C, respectively, before incubation with the oligonucleotide. The protein molecular weight markers are indicated on the left. The M_r of the binding complexes were estimated at ~60, 30, and 15 kD (arrows).

1 vs 3). After serum stimulation, increased mRNA binding activities were seen in cytoplasmic extracts from both DA and Ao SMC, but there was a greater increase binding with S-100 extracts from DA SMC (lane 2 vs 4).

Additional studies were carried out to determine whether the binding complex consists of several subunits and whether the binding requires free sulfhydryl groups, as suggested for the iron-response element-binding protein (IRE-BP) (Hentze *et al.*, 1989) or the AUBF (Malter and Hong, 1991). In two different experiments, we treated the cytoplasmic extracts with reducing reagents, β-mercaptoethanol (β-ME), dithiothreitol (DTT), or the alkylating reagent, *n*-ethylmaleimide (*n*-EM), prior to the binding reaction. The binding complexes were then UV-crosslinked and resolved by SDS-PAGE. In the absence of pretreatment with reducing or alkylating agents, three radioactive bands migrated at positions related to M_r of approximately 60, 30, and 15 kD (Figure 20**d**, lanes 1 and 2, gel run under non-reducing and reducing conditions, respectively). To confirm that the components of the binding complex were proteins and RNA, cytoplasmic extracts were treated with proteinase K or the radiolabeled probes were pretreated with RNase T_1 before the binding reaction (lanes 3 and 4, respectively). Both conditions prevented the binding complex formation originally observed, confirming a protein-RNA interaction. A weak 40 kD band observed could be attributed to incomplete digestion with proteinase K.

Of particular interest, however, was the observation that the binding complex was resolved as an intense band at 15 kD after pretreatment of the extracts with reducing reagents, β-ME (lane 5) or DTT (lane 6), as well as an alkylating reagent, *n*-EM (lane 7). The relative differences observed in the intensity of the 15 kD band may be related to differences in reducing capacity of β-ME and DTT in the doses used. Both reducing and alkylating conditions prevent disulfide bond formation. Since *n*-EM also alkylates irreversibly reduced sulfhydryl groups and pretreatment of cytoplasmic extracts with *n*-EM did not inhibit the 15 kD binding complex formation, free sulfhydryl groups seem not to be required for direct binding of the ~15 kD protein to RNA. Thus, the higher M_r binding complexes may be due to disulfide bond-dependent interactions between multimers of the ~15 kD protein, or between the 15 kD protein and other proteins, or disulfide bond dependent

RNA binding of two different proteins with the M_r of ~30 kD and 60 kD.

Time-course, and Dose-dependent Binding of Complex Formation

To determine whether the factor binding to the mRNA might occur under biological conditions, we studied the binding kinetics of the complex. Binding reactions were carried out for various times before the addition of RNase T_1. Incubations as short as 5 min yielded the same amount of binding activity as 60 min incubations (Figure 21**a**), indicating a similar profile to that of an AUUUA binding factor (AUBF) of different molecular weight previously described (Malter, 1989; Malter and Hong, 1991). Thus, the binding of the factor to the probe appears to occur quickly and likely precedes the degradation of the mRNA by the exonuclease-mediated shortening of the polyadenylated tail (Wilson and Treisman, 1988). This stable binding would favor a mechanism required for efficient protein translation.

We next determined whether the binding was dose-dependent by using increasing concentrations of DA cytoplasmic extracts. Increased binding activities were found to correlate with increasing amount of extracts used in the binding reaction (Figure 21**b**). Together, these data suggest that there is a cytoplasmic factor(s) existing in DA and Ao SMC which binds the ARE in the 3'UTR of FN mRNA, and the greater binding activity in DA SMC extracts may result from an increase in the concentration of the factor(s) or in its binding affinity.

DISCUSSION

In this chapter we addressed whether the mechanism of post-transcriptional regulation of FN in the DA may involve the FN ARE. We first related the mechanism of post-transcriptional regulation of FN expression to the ARE by transfecting constructs containing the CAT coding region and downstream FN 3'UTR into primary cultured SMC. A significant increase in CAT mRNA translational efficiency in both DA (10.9-fold) and Ao SMC (6.5-fold) transfected with pECE-CAT-FN containing wild type ARE as opposed to pECE-CAT-FNΔ bearing mutated ARE supported the ARE as being critical to the mechanism of increased fusion mRNA translation. A

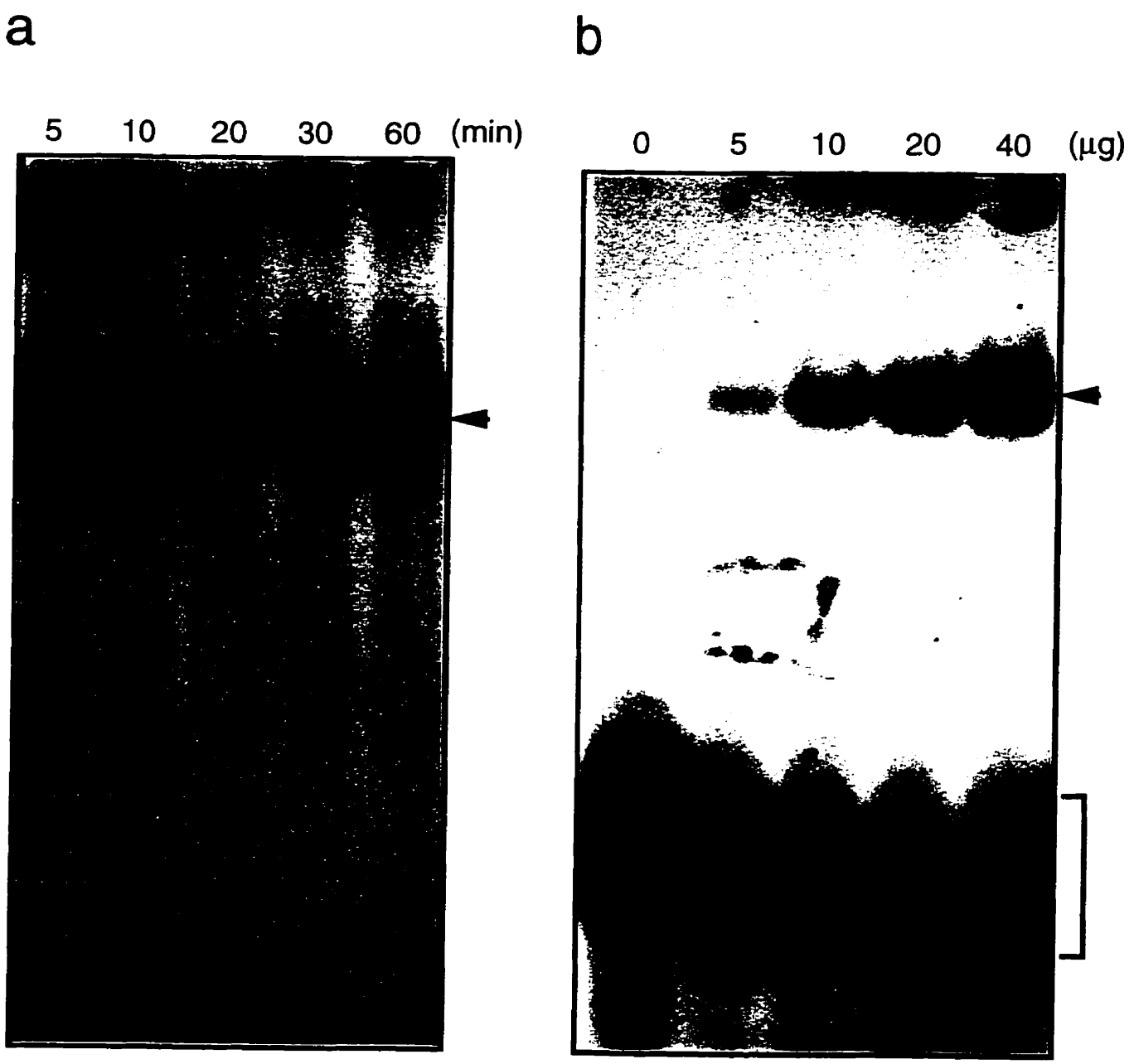

Figure 21

Figure 21. Binding of cytoplasmic factor ARE probe is rapid, stable, and dose-dependent

(**a**) The binding reaction was performed for different times [indicated as (in minutes) at the top of each lane] before the addition of RNase T1. Lower shifted bands may be related to the properties of the binding complex elucidated by the UV cross-linking studies shown in Figure 20**d**. (**b**) Gel-shift assays with increasing concentration of DA SMC cytoplasmic extracts as indicated at the top of each lane. The position of the band-shifted complex is shown by the arrow while the free RNA probe is shown by the bracket.

decrease in CAT-FN3'UTR fusion mRNA in SMC transfected with pECE-CAT-FN but not pECE-CAT-FNΔ suggested that the ARE also functions as an mRNA destabilizing element. although we did not specifically measure CAT mRNA stability.

The decrease in CAT mRNA by the wild-type ARE may be coupled with the increase in CAT mRNA translation. There are studies indicating that destabilization of mRNA mediated by the ARE is associated with mRNA translation, since degradation of mRNA directed by the GM-CSF and c-*fos* ARE is coupled to ongoing translation or ribosome binding (Savant-Bhonsale and Cleveland, 1992; Aharon and Schneider, 1993; Winstall, *et al.*, 1995) and is related to translational-dependent assembly of a >20s degradation complex (Savant-Bhonsale and Cleveland. 1992). Alternatively, these may represent independent events, as suggested by study of Chen and colleagues (1995) which showed that mRNA decay mediated by the GM-CSF and c-*fos* ARE is independent of ongoing translation of an RNA.

Since others have described the ARE as a repressor of mRNA translation (Kruys, *et al.*. 1987; Kruys, *et al.*, 1988; Kruys, *et al.*, 1989; Han, *et al.*, 1990a; Han, *et al.*, 1990b; Grafi, *et al.*. 1993; Kruys, *et al.*, 1993; Marinx, *et al.*, 1994), the difference between our findings and theirs may be due to several factors. First, our experimental system used primary cultured vascular SMC and investigated the ARE function in the entire 3'UTR of FN mRNA. Second, the ARE may function as a repressor or an enhancer of translation, depending on binding of tissue-specific cytoplasmic factors.

The functional existence of ARE-binding factors was suggested when we compared FN expression and cell shape in DA SMC transfected with CAT-FN3'UTR fusion constructs bearing wild type or mutated AREs. Since the elongated 'mobile' phenotype of DA cells is dependent on the increased FN expression (Boudreau and Rabinovitch, 1991; Boudreau, *et al.*, 1991), we reasoned that the alteration of cell shape may be due to a reduction of FN expression by sequestering ARE-binding factors that would otherwise influence endogenous FN mRNA translation (Later studies in Chapters 4 and 5 showed that, if sequestering ARE-binding factors indeed happens, it may only apply for a subset of ARE-binding factors). We could not, however.

rule out the possibility that decoy of these putative factors would also prevent binding to other endogenous ARE-containing mRNAs. This could also affect their stability or translation, thereby causing a change in cell phenotype. The change in cell phenotype may also be due to effect of plasmids (difference in copy number of transfected wild type versus mutant plasmid) on protein synthesis, although we have no reason to suggest why this would occur.

Indeed, using gel mobility shift assays, we observed that the cytoplasmic proteins in SMC form three binding complexes with the full-length FN 3'UTR, but only one of them is specifically related to the ARE. Consistently, a cytoplasmic protein(s) in DA and Ao SMC selectively form a binding complex with the ARE-containing oligonucleotides. There was increased binding complex formation in DA compared to Ao SMC, especially after serum stimulation when we used the ARE-containing oligonucleotide probes. This suggests that the increased binding to the ARE may be responsible for the increased translation of mRNA in DA SMC, since serum-stimulation upregulates FN protein synthesis in DA but not Ao SMC without changing its mRNA level (Boudreau, *et al.*, 1992). In further UV-crosslinking studies, we identified three binding complexes with molecular weights at ~15, 30, and 60 kD. The main binding factor appears to be 15 kD protein, which may, in fact, forms a protein complex by itself or with other protein peptides through disulfide bonds. Disruption of disulfide bonds by β-ME or DTT, as well as *n*-EM, increased the lowest molecular mass complex formation, while the highest molecular binding complex disappeared completely and the middle one was partially retained. This feature suggested that the structural conformation of this FN ARE-binding protein as a monomer or a protein complex may influence its binding affinity, but this remains to be proven. This would seem worth pursuing, however, since there is evidence for alterations in intracellular redox in DA compared to Ao related to decreased superoxide dismutase levels (Frazer and Brady, 1978), with the potential for increased superoxide production reducing disulfide bonds (Peterson *et al.*, 1994). In addition, since disruption of sulfhydryl groups by an alkylating reagent does not impair but rather increases the low molecular weight binding complex formation, it is therefore noteworthy that, unlike other RNA binding proteins such as IRE-BP (Hentze, *et al.*, 1989) and AUBP (Malter and Hong,

1991), the binding complex formation does not depend on free sulfhydryl groups. Taken all together, these data suggest a unique protein or a unique interaction that differs from other ARE-binding proteins previously described (Malter, 1989; Bohjanen, *et al.*, 1991; Brewer, 1991; Malter and Hong, 1991; Rondon, *et al.*, 1991; Vakalopoulou, *et al.*, 1991; Bickel, *et al.*, 1992; Bohjanen, *et al.*, 1992; Port, *et al.*, 1992; Stephens, *et al.*, 1992; Hamilton, *et al.*, 1993; Levine, *et al.*, 1993; Zhang, *et al.*, 1993; Katz, *et al.*, 1994; Nakagawa, *et al.*, 1995; Chung, *et al.*, 1996; Ma, *et al.*, 1996).

The ARE-binding factor previously described requires at least 3 AUUUA motifs to interact with RNA (Gillis and Malter, 1991; Bohjanen, *et al.*, 1992). However, our experiments indicated that the UUAUUUAU sequence is the basic binding element for the FN mRNA binding protein. In our studies, probes containing only one copy of the conserved consensus sequence, UUAUUUAU, resulted in specific and stable binding to a cytoplasmic factor. A possible interpretation is that 3 motifs of AUUUA (AUUUAUUUAUUUA) actually contains only one repeat of the conserved consensus sequence, UUAUUUAU, as underlined. Recent studies based upon functional activity of various AREs and sequence comparisons have indicated that the key ARE motif within the AU-rich sequence is the nonamer UUAUUUA(U/A)(U/A) (Lagnado, *et al.*, 1994) or UUAUUUAUU (Zubiaga, *et al.*, 1995).

Our results expand previous findings that the ARE plays an important role, not only in regulating the stability and translational efficiency of transient mRNAs coding for cytokines and proto-oncogenes, but also in controlling the translation of the more stable mRNA, FN mRNA that encodes a major extracellular matrix protein. Since FN plays a critical role in vascular development and in diseases related to the control of SMC growth, differentiation, and migration, understanding the molecular basis of its regulation is of critical importance. Also, by using primary cell cultures which maintain distinct phenotypic properties *in vitro*, we have provided evidence that a *trans*-acting factor may contribute the high levels of expression of FN in the DA SMC. Purification of the protein will be necessary to identify it and further characterize its function.

CHAPTER THREE

PURIFICATION AND FUNCTIONAL CHARACTERIZATION OF A FIBRONECTIN AU-RICH ELEMENT RNA-BINDING PROTEIN IN VASCULAR SMOOTH MUSCLE CELLS

INTRODUCTION

We have shown that the ARE found in the 3'UTR of FN mRNA functions to enhance mRNA translation. Using RNA gel shift and UV-crosslinking assays, we have also isolated three RNA-protein complexes of M_r of approximately 60, 30 and 15 kD. The 15 kD protein may be the principal binding factor, since the high molecular binding complexes appear to be formed by several protein subunits through disulfide bonds. Two lines of evidence suggest that the interaction of the ARE-binding factors with FN ARE may promote FN mRNA translation in DA SMC. First, compared to Ao SMC, the increased FN ARE-binding activities found in DA SMC correlates with an enhanced FN mRNA translation (Boudreau and Rabinovitch, 1991). Second. decoy of ARE-binding factors by exogenous AREs reduced FN synthesis in DA SMC and altered their FN-dependent elongated motile phenotype (Boudreau, *et al.*, 1991). More definitive evidence requires purification of the ARE-binding factors.

This study is therefore, designed to purify the 15 kD FN ARE-binding protein using sequential ion-exchange and heparin-affinity chromatography. We purified a 15 kD protein with ARE-dependent mRNA binding activity, and sequenced its first 10 N-terminal amino acids. The revealed peptide sequence indicated that the purified 15 kD ARE-binding protein is related to the light chain 3 (LC3) of microtubule-associated protein 1 (MAP1). Using western immunoblot, we confirmed that the purified peptide is LC3, and demonstrated that its expression is increased in DA compared to Ao SMC. Recombinant LC3 protein was then generated and shown to bind the FN 3'UTR in an ARE-dependent manner. Overexpression of LC3 in Ao SMC optimizes FN mRNA translation, suggesting that binding of LC3 to FN mRNA may increase FN mRNA translational efficiency.

RESULTS

Purification and Identification of the 15 kD FN ARE-binding Protein

The aim of the purification procedure was to identify the nature of the 15 kD ARE-binding protein. We designed a large-scale purification scheme based on sequential ion exchange and

heparin chromatography (Figure 22). Gel shift and UV-crosslinking assays were used to detect RNA binding activity and to monitor the purification process. Most of the FN mRNA binding activity in the S-100 extract from sheep Ao tissue was initially resolved as a slow migrating band on gel shift assay (Figure 23**a**, lane 1; P = probe alone) and a ~60 kD band on UV-crosslinking assay (**b**, lane 1). A weak ~50 kD band was inconsistently present. It was conceivable that the majority of the ~15 kD binding protein in the S-100 extract was present as a protein complex due to the high protein concentration of the starting material. This may explain why two separate RNA-binding complexes were subsequently found on gel shift using the flow-through fraction from the DEAE-sepharose (1st column in **a**, lane 2), as well as on UV-crosslinking assay (~15 kD and 30 kD; **b**, lane 2), while we confirmed that the 60 kD binding activity remained bound (data not shown). Interaction with the DEAE-column appeared to dissociate the high molecular weight binding complex, as well as separate the high and low molecular weight binding activities.

The flow-through fraction of the DEAE-column containing the 15 kD and 30 kD RNA binding activities was loaded onto the phosphocellulose-column (2nd column) and the bound material eluted by 1 M KCl. The eluate containing the 15 kD, as well as 30 kD RNA-binding activities (**a** and **b**, lane 3) was further purified by heparin chromatography. Twenty-one fractions were eluted using an 80-800 mM KCl gradient. Aliquots of fractions 7-21 were tested by gel shift (**a**, lanes 4-18) and UV-crosslinking assays (**b**, lanes 4-18). The SDS-PAGE gels of the UV-crosslinking assay were also stained by Coomassie blue (**c**). Fractions 17-20 (lanes 14-17 in **a** and **b**) contained the majority of the binding activity evident as a smear band between 30 and 40 kD and a more clearly resolved radioactive band at ~15 kD. In fraction 20, weak ~21 kD binding activity was also observed (**b**, lane 17). On Coomassie blue staining a 15 kD protein was evident corresponding to the ~15 kD complex (compare **c** to **b**, lanes 14-17). The peak ~15 kD binding activity corresponded to fraction 19 (**a**, lane 16) which was eluted at a salt concentration of about 700 mM.

Fraction 19 (F19) was concentrated, separated by SDS-PAGE, and blotted onto a PVDF

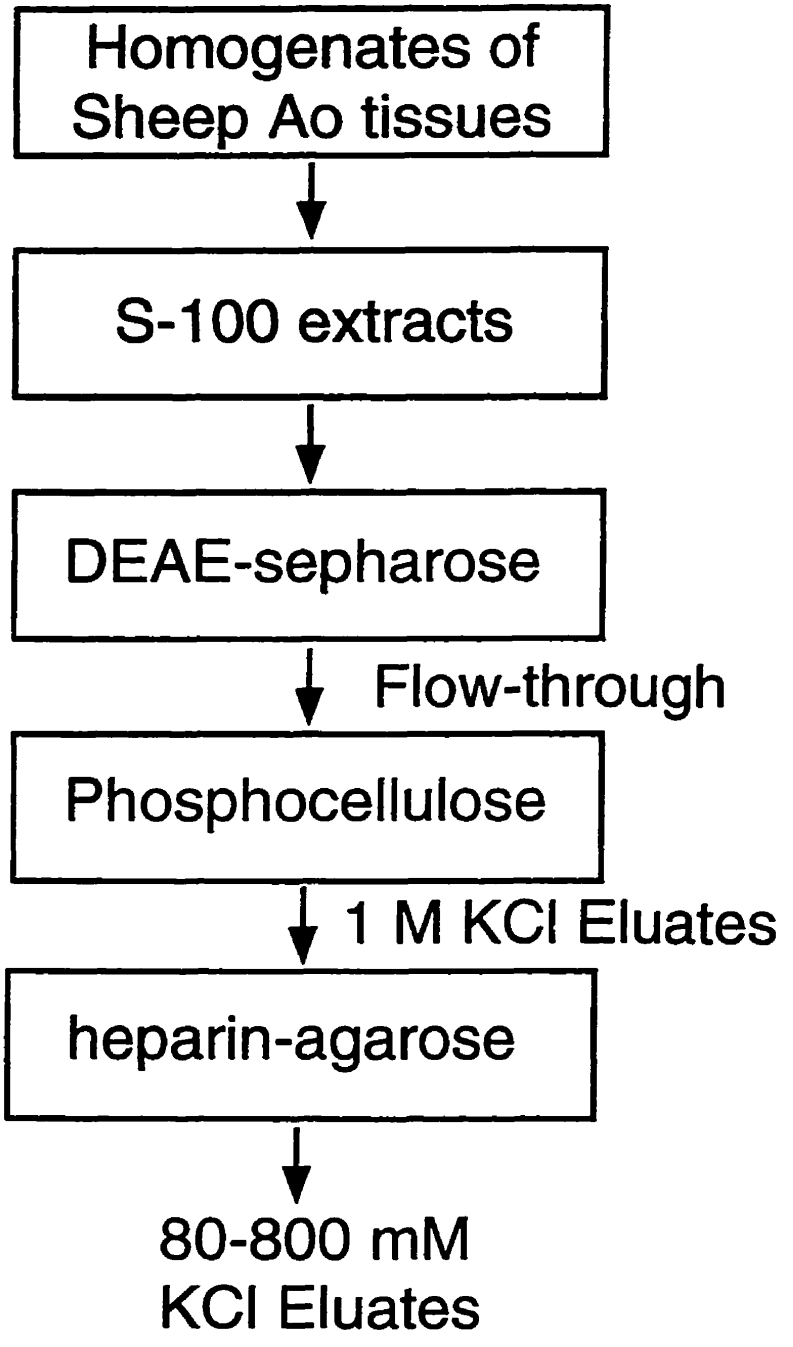
Homogenates of Sheep Ao tissues
S-100 extracts
DEAE-sepharose
Flow-through
Phosphocellulose
1 M KCl Eluates
heparin-agarose
80-800 mM KCl Eluates

Figure 22

Figure 22. A scheme of the purification procedure

Gel shift and UV-crosslinking assays were applied to monitor the purification procedure and to determine the ARE-binding activities in samples collected from each purification step.

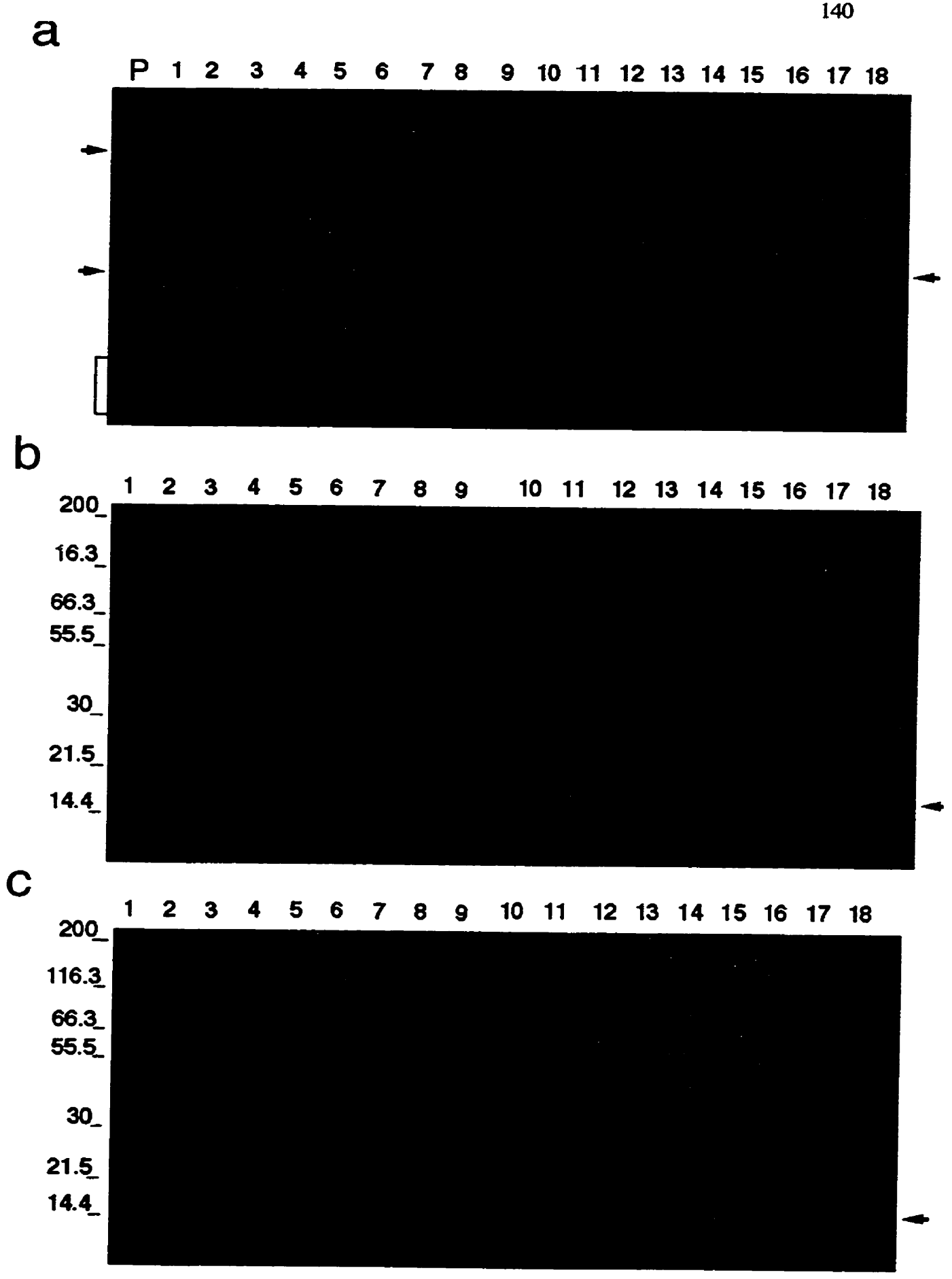
a
P 1 2 3 4 5 6 7 8 9 10 11 12 13 14 15 16 17 18
b
1 2 3 4 5 6 7 8 9 10 11 12 13 14 15 16 17 18
200
16.3
66.3
55.5
30
21.5
14.4
c
1 2 3 4 5 6 7 8 9 10 11 12 13 14 15 16 17 18
200
116.3
66.3
55.5
30
21.5
14.4

Figure 23

Figure 23. Purification of FN ARE-binding protein

The purification procedure was monitored by (**a**) gel shift assay and (**b**) UV-crosslinking assay using ARE-containing FN oligonucleotide probes. The protein contents in each sample were stained by Coomassie blue (**c**). P = probe only as control. Bracket denotes free probe. ARE-binding activities in S-100 extracts were revealed on gel shift as a major binding complex (**a**, lane 1), and ~60 kD radioactive band on UV-crosslinking (**b**, lane 1). Lane 1 in **c** shows dense protein staining of S-100 extracts. The binding activities were present in the DEAE-unbound materials as two separate binding complexes indicated by gel shift (**a**, lane 2) with the M_r of ~15 kD and 30 kD on UV-crosslinking and SDS-PAGE (**b**, lane 2). The DEAE flow-through was loaded onto the phosphocellulose column and 1 M KCl eluates which contain RNA binding activities were collected (**a** and **b**, lane 3). The eluates of the phosphocellulose-column were further applied to a heparin chromatography and eluted with an 80-800 mM KCl gradient. Twenty-one fractions were collected in total. Aliquots of fractions 7-21 were tested by gel shift (**a**, lanes 4-18) and UV-crosslinking assay (**b**, lanes 4-18), and stained with Coomassie blue (**c**, lanes 4-18). Only fractions 17-20 (**a**, lanes 14-17) contained detectable binding activity at about 15 kD (**b**, lanes 14-17), which corresponded with protein staining (**c**, lanes 14-17). Arrow indicates the binding complexes or an approximately ~15 kD protein band.

membrane. The 15 kD Coomassie blue stained band was excised (Figure 24**a**). The sequence of the first 10 amino acids (after the first methionine) of this purified protein was determined as PSEKTFKQRR. A Genbank data base search revealed that the sequence is identical to the rat MAP1 LC3 (light chain 3 of microtubule-associated protein 1), a ~16 kD protein previously found to be expressed predominantly in the rat brain and to a lesser extent in testis (Mann and Hammarback, 1994). Western immunoblot analysis was carried out using rabbit anti-LC3 antiserum to corroborate the immunological identity of the purified 15 kD FN mRNA-binding protein as LC3 and to examine its expression in DA versus Ao SMC. The purified 15 kD protein in fraction 19 is immunoreactive with the LC3 antibody as expected (**b**). Moreover, the major protein in DA or Ao S-100 extracts which reacted with the LC3 antibody is 15 kD. Also noted is that DA S-100 cytoplasmic extracts contain more than twice the amount of the 15 kD protein which immunoreacts with LC3 antibodies when compared with Ao extracts. These findings are consistent with the results of the previous gel shift assays showing more FN mRNA-binding complex formation with DA compared to Ao SMC S-100 extracts.

Binding of Recombinant LC3 to FN ARE

To examine the RNA binding activity of LC3, we expressed rat LC3 in *Escherichia coli* as a GST-LC3 fusion protein. The purified recombinant LC3 protein was verified by SDS-PAGE and Coomassie blue staining (Figure 25**a**) and western immunoblotting (**b**). We then used the gel mobility shift assay to examine the binding activity of recombinant LC3 to the FN mRNA 3'UTR (named FN; **c**). Three retarded binding complexes were found on the gel, the formation of which were not evident using the ARE-mutated FN 3'UTR probe (FNΔ). This study indicated that the RNA-LC3 interaction was ARE-dependent and that the three binding complexes may represent the interaction of RNA with different aggregates of LC3. The specificity of ARE-binding of LC3 was further determined by competition assays using unlabeled ARE-mutated (AREΔ) or ARE-containing oligonucleotides (ARE) (**d**). Incubation of AREΔ oligonucleotides with LC3 (molar ratio = 100:1) before adding radiolabeled FN 3'UTR was inefficient in blocking formation of the

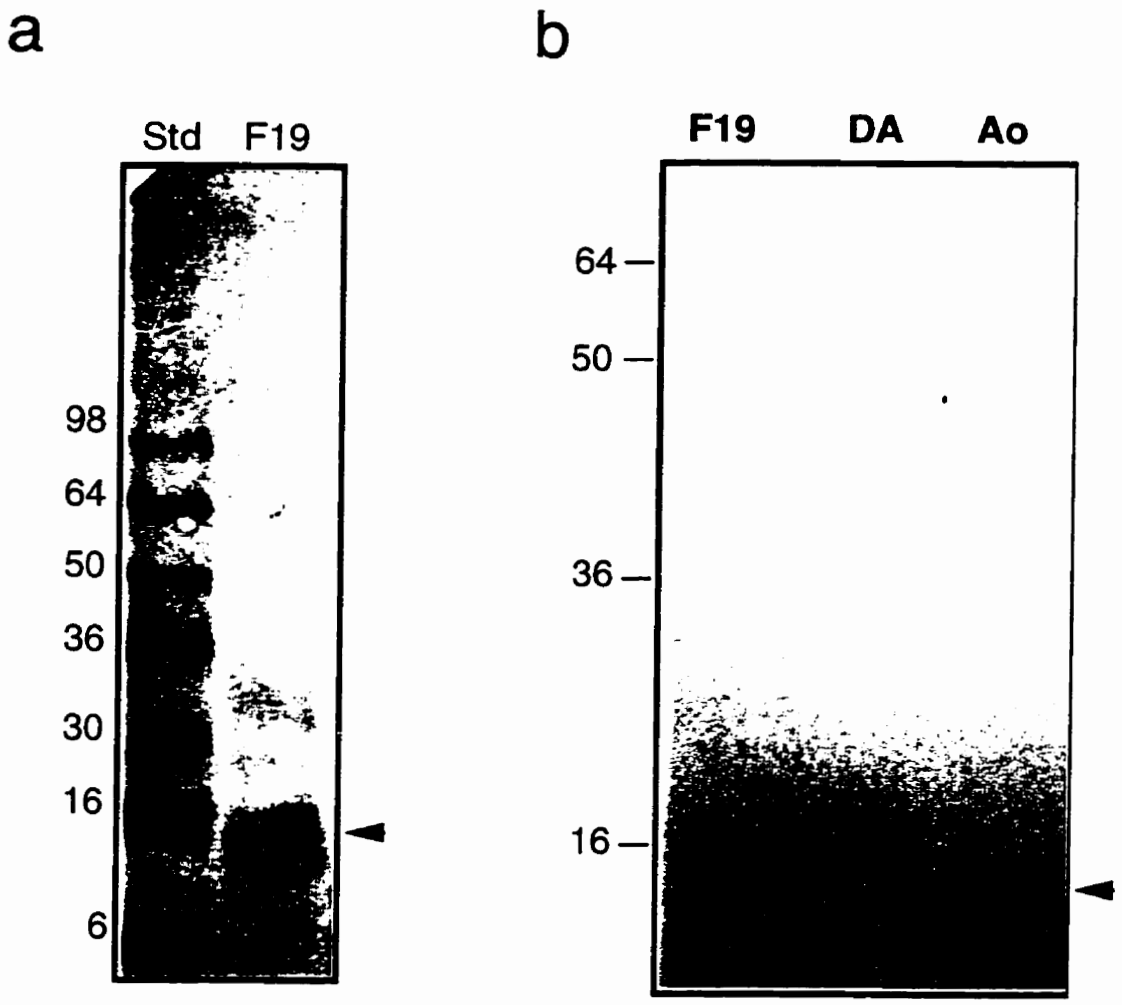

Figure 24

Figure 24. Identification of a 15 kD FN ARE-binding protein

(**a**) Coomassie blue staining of a PVDF membrane. Fraction-19 (F19) containing the peak ~15 kD RNA-binding activity (See lane 16 in Figure 3-2) was concentrated, separated by SDS-PAGE, and electroblotted onto a PVDF membrane. The ~15 kD protein band stained with Coomassie blue was excised and the sequence for first 10 amino acids was determined. The sequence is PSEKTFKQRR which is identical to rat MAP1 LC3. (**b**) Western blot analysis using rabbit anti-LC3 antibody pointing the identities of the purified FN mRNA-binding protein as LC3, and provides quantitative data concerning its levels in DA versus Ao SMC S-100 extracts.

Figure 25. Recombinant LC3 binds to the ARE in the 3'UTR of FN mRNA

(**a**) A Coomassie blue stained gel showing purified recombinant LC3. Arrows indicate GST-LC3 fusion protein (~44 kD) in the bacterial lysates and the recombinant LC3 (~15 kD) in the eluates after cleavage of the GST-tag (see Methods and Materials, Section **III**). The high molecular weight band (~70 kD) may be related to a protein product of the *E. coli* gene dnaK which is involved in the degradation of "abnormal" protein in *E. coli*.. (**b**) A western blot demonstrates that the recombinant LC3 reacts to anti-LC3 antibody. (**c**) shows that recombinant LC3 binds to FN 3'UTR with wild type ARE (FN) but not to FN 3'UTR with mutated ARE (FNΔ) on the gel shift assay. Three binding complexes were found (indicated by arrows). Binding reactions were carried out with 0.1 μg purified recombinant LC3 protein and 10^5 cpm radiolabeled FN 3'UTR with intact (FN), or mutated ARE (FNΔ). (**d**) Competition study with ARE-containing FN oligonucleotides (ARE), or ARE-mutated oligonucleotides (AREΔ, all the U's in ARE was replaced by G's). The unlabeled oligonucleotides were preincubated with LC3 at molar ratio 100:1 for 10 min before addition of radiolabeled FN 3'UTR (10^5 cpm).

complexes. However, preincubation of ARE-containing oligonucleotides with LC3 completely abolished the binding complex formation.

Co-distribution of LC3 and FN in the Fetal Lamb DA

We next examined whether LC3 is differentially expressed in DA and Ao tissues and whether it co-localizes with FN protein. In 100-day gestation DA (term = 145 days), LC3 was observed in the EC and in the SMC exhibiting a motile phenotype in the subendothelium and in the adjacent inner medial SMC where the structure of the intimal cushion is emerging (Figure 26**a**). Staining of FN from the same tissue showed a similar pattern of intense staining, although the cytoplasmic staining was evident throughout the media (**a**). In contrast, in 100-day gestation tissues from the Ao, LC3 immunostaining was barely detectable (**c**), and FN SMC cytoplasmic staining was somewhat less marked than in the DA SMC (**d**).

Distribution of LC3 and FN mRNA in Cultured SMC

Since LC3 binds tubulin directly in an *in vitro* microtubule-assembly assay with purified rat brain tubulin and co-localizes with MAP1B in cultured rat neurons (Mann and Hammarback, 1994), immunofluorescent staining was performed to study the intracellular distribution of LC3 and FN mRNA in cultured SMC. Staining for microtubules with anti-tubulin antibodies was also carried out to exclude artifacts due to the effects of fixation and staining the microtubule structure. In cells showing well maintained microtubule structures (Figure 27**B**), immunostaining for LC3 was evident especially in the perinuclear area but also extended throughout the cytoplasm (**A**). Negative controls using normal IgG showed no immunofluorescence (**C** and **D**). In the simultaneous immunostaining of LC3 protein and FN mRNA (Figure 28), both LC3 (**A**, FITC), and FN mRNA (**B**, rhodamine) were observed in greatest density in the perinuclear region where co-localization was observed in a small subset of these molecules (**C**) suggesting a potential for co-localization with less intense staining apparent toward the leading edges of the cell. Negative controls using normal IgG and cells pretreated with RNase A (**D**) showed no immunofluorescence.

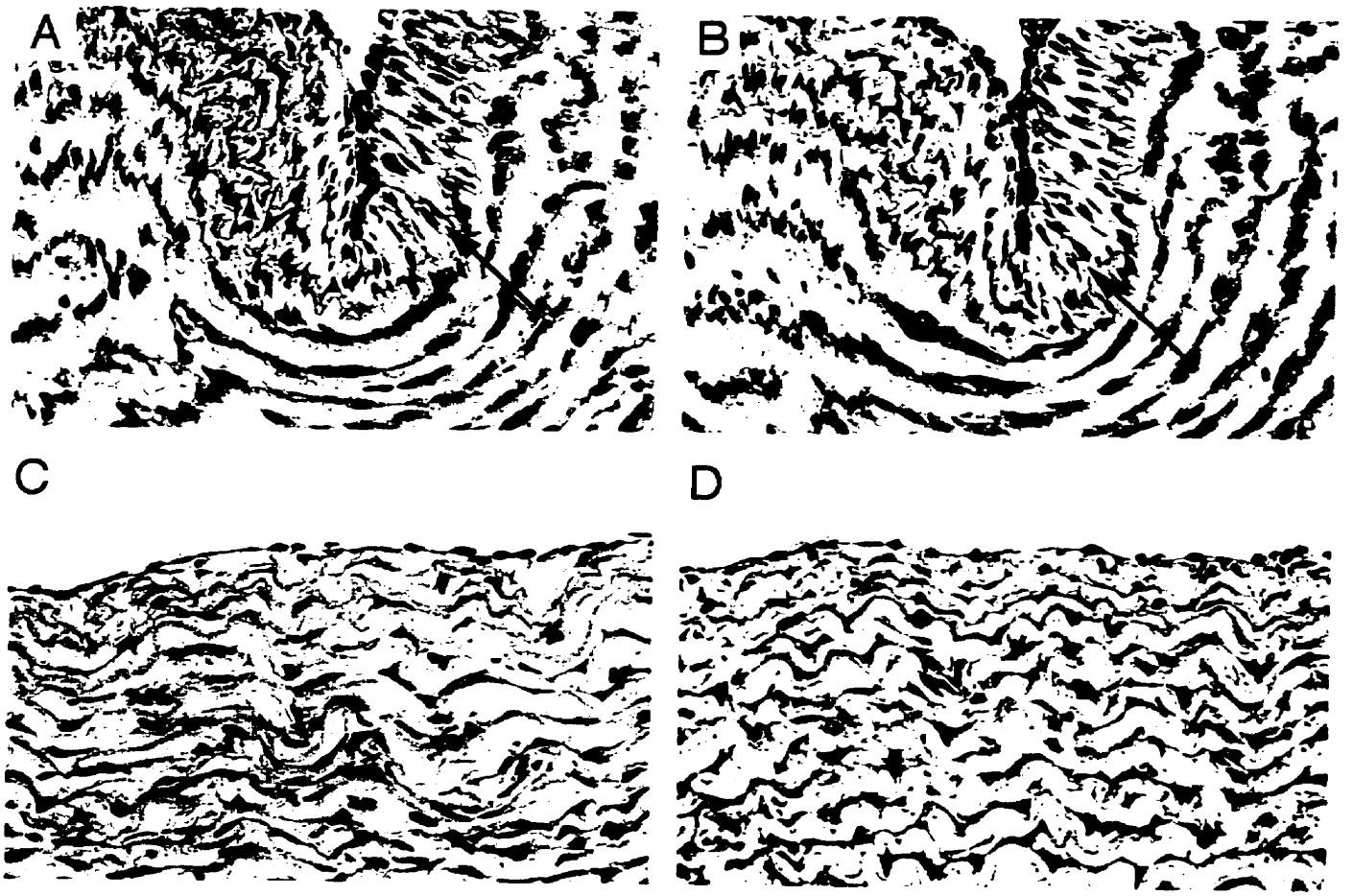

Figure 26

Figure 26. Co-distribution of LC3 with FN protein in DA tissues

Staining for LC3 is observed in **a** and **c**, and for FN in **b** and **d**. In 100-day gestation DA tissue (**a** and **b**; term = 145 days), LC3 was observed in EC, in the subendothelial intimal SMC exhibiting a motile phenotype (indicated by arrow), and to some extent in adjacent inner medial SMC where the structure of the intimal cushion is appearing (**a**). Staining of FN from the same tissue showed a similar pattern (**b**) with staining extended into the inner media. In contrast, in tissues from Ao of the same animals, LC3 was not detected (**c**), whereas cytoplasmic staining for FN was present, but less intense (**d**).

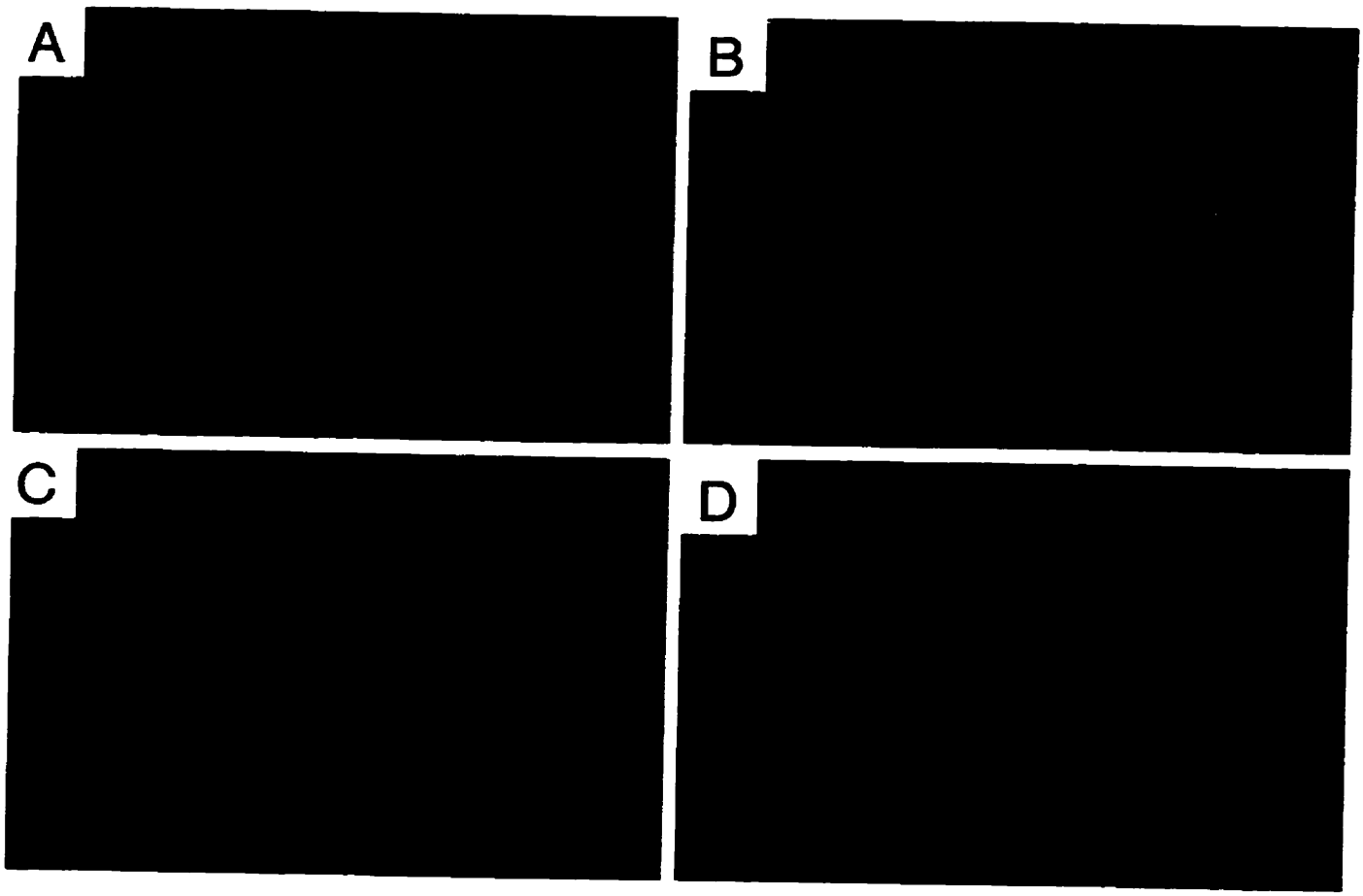

Figure 27

Figure 27. Immunofluorescent staining of LC3 and tubulin

Cultured DA SMC were stained for LC3 and MTs using anti-LC3 and anti-tubulin antibodies, and rhodamine-conjugated secondary antibodies. LC3 staining is observed in the perinuclear region (**A**) in cells with well preserved MTs (**B**). Negative controls for LC3 (**C**) and tubulin (**D**) with normal IgG show no fluorescence staining.

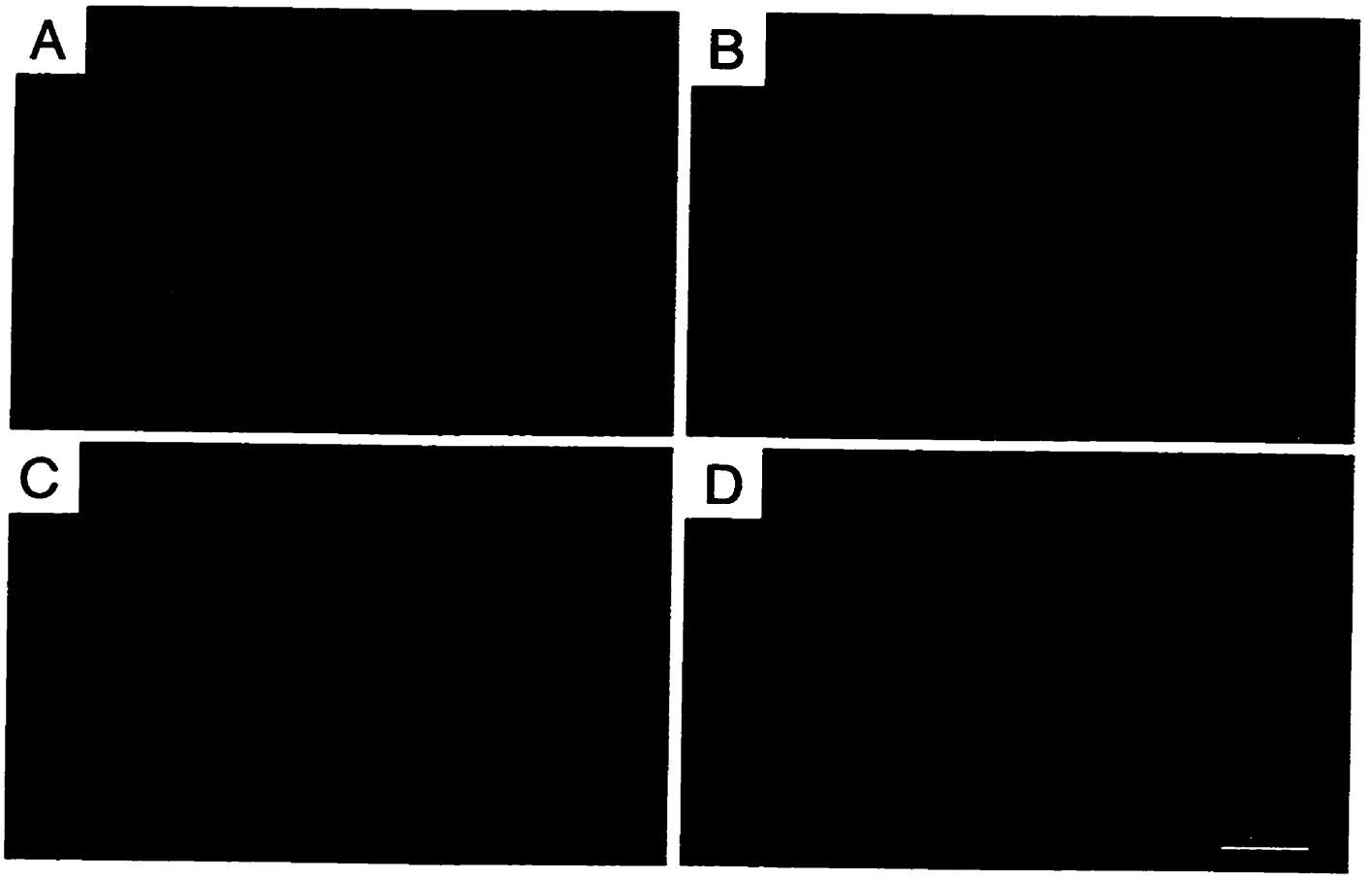

Figure 28

Figure 28. Dual-staining of LC3 and FN mRNA in cultured DA SMC

Dual-staining of LC3 (**A**, FITC) and FN mRNA (**B**, rhodamine) in cultured DA SMC. Like LC3, the majority of FN mRNA staining was also found in the perinuclear area. Under the dual filter, a small subset of two signals somewhat overlap (**C**). Controls for LC3 staining using normal IgG and for RNA staining by predigestion of RNA with RNase A show only nuclear staining by DAPI (**D**). Bar = 10 μm.

Overexpression of LC3 in Ao Cells Enhances FN mRNA Translation

To define the role of LC3 in the regulation of FN mRNA translation, we used adenovirus transfection to overexpress this protein in cultured DA and Ao SMC. As shown in Figure 29. there is a significant decrease in the basal level of newly-synthesized FN in Ao compared to DA cells ($p < 0.05$). Transfection with LC3 plasmid in Ao cells increased LC3 production (Figure 29**a**, top) and FN synthesis (**a**, bottom and **b**) in a dose-dependent manner to the level observed in the control DA cells. Transfection of DA cells with increasing doses of LC3 plasmid, however. did not result in a further increase in FN synthesis, suggesting that the mechanism may be operating at maximum efficiency. Since there was no change in FN mRNA levels following LC3 transfection in either DA or Ao cells (**c**), the results support the role of LC3 in enhanced translation of FN mRNA.

DISCUSSION

Our study was directed at studying the interaction of FN ARE and its binding protein as the mechanism involved in enhanced FN mRNA translation in DA versus Ao SMC. To this end we have purified, sequenced, and identified the transacting factor as LC3 of MAP1. Several lines of evidence led us to believe that binding of LC3 to the ARE in FN mRNA is functionally involved in its translation. First, the ARE is involved in CAT-FN3'UTR fusion mRNA translation. Second. there is increased ARE-binding activity and coincidentally higher expression of LC3 in DA compared to Ao SMC associated with increased FN mRNA translation. Third, LC3 co-distributes with FN mRNA in the perinuclear region of cells. Finally, overexpression of LC3 in Ao SMC enhances FN mRNA translation to levels observed in the DA SMC.

The 15 kD ARE-binding factor was purified using sequential ion-exchange and heparin chromatography. N-terminal sequence analysis of 10 amino acids after the methionine start site revealed a peptide sequence with identity to rat MAP1 LC3 (Mann and Hammarback, 1994) that is further supported by western immunoblot. Although further information, such as peptide digest and complete amino acid sequence analysis, is necessary to define this RNA-binding protein as

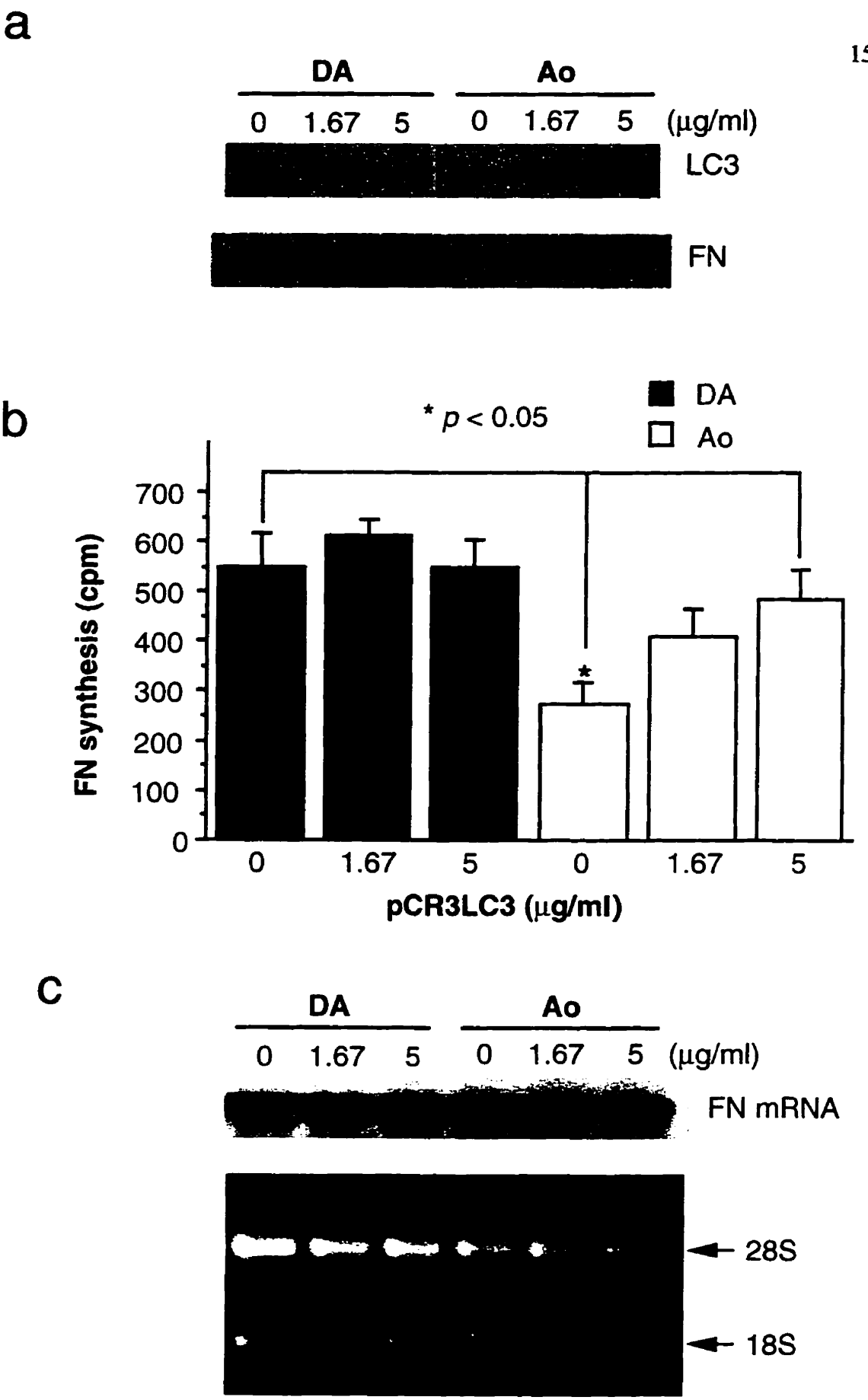
a
DA
Ao
0 1.67 5 0 1.67 5 (μg/ml)
LC3
FN
b
* p < 0.05
DA
Ao
FN synthesis (cpm)
700
600
500
400
300
200
100
0
0 1.67 5 0 1.67 5
pCR3LC3 (μg/ml)
c
DA
Ao
0 1.67 5 0 1.67 5 (μg/ml)
FN mRNA
28S
18S

Figure 29

Figure 29. Overexpression of LC3 in Ao SMC enhances FN mRNA translation

(**a**) A representative western blot shows that transfection of LC3 by the 'adenovirus component system' (Methods and Materials, Section **III**) increased LC3 production in a dose-dependent manner. This was especially evident in Ao but not in DA cells (**top**). The overexpression of LC3 in Ao cells also augmented FN synthesis to the levels observed in the DA cells, whereas this was not associated with a significant increase in FN synthesis in DA cells (**bottom**). The concentration of plasmid, pCR-LC3, used in the transfection is indicated at the top. (**b**) is a graph of quantitative assessments of FN synthesis from 4 different experiments showing that there is a significant decrease in the basal level of newly-synthesized FN in Ao compared to DA cells ($p < 0.05$. SuperANOVA and Duncan's test of multiple comparisons). However, the new synthesis of FN in Ao cells is increased after transfection with pCR-LC3 to a significant level ($p < 0.05$) in a dose-dependent manner ($p < 0.05$)). (**c**) A northern blot analysis indicating that there is no change in the level of FN mRNA following LC3 in either DA or Ao cells. The loading condition is demonstrated by ethidium bromide staining of 18s and 28s ribosomal RNA.

LC3 or a related protein (a member of a family proteins), we went on to investigate whether in fact the rat LC3 had features that corresponded to those attributed to the ARE-binding proteins in vascular smooth muscle cells, e.g., RNA binding and mRNA translation. LC3 is a different protein from other AUBFs purified or cloned thus far (Levine, *et al.*, 1993; Zhang, *et al.*, 1993; Nakagawa, *et al.*, 1995; Ma, *et al.*, 1996). Similar to AUH, an ARE-binding protein purified using an (AUUUA)6 affinity column (Nakagawa, *et al.*, 1995), computer analysis (MOTIFS/GCG) failed to identify RNA-binding motifs in LC3 protein that are present in other RNA-binding proteins, including small nuclear RNP, hnRNP, AUF1, and Elav-like RNA-binding proteins. However, LC3 is a basic protein with a predicted pI of 9.2 and arginine-rich sequences similar to arginine-rich RNA-binding proteins (Burd and Greyfuss, 1994). The arginine-rich sequence (**RRSFEQRVEDVRLIR**) close to the N-terminal may form an RNA-binding site.

We used purified bacterial-expressed recombinant LC3 to confirm its binding to the 3'UTR of FN mRNA. Moreover, LC3 appears to bind the 3'UTR in an ARE-dependent manner. The fact that LC3 co-expresses with FN protein in the 'motile' SMC in DA tissues, and overexpression of LC3 in Ao SMC optimizes FN mRNA translation supports the interaction of LC3 with the ARE as being the mechanism responsible for upregulation of FN mRNA translation in DA SMC.

Our results extend previous findings that the ARE in the 3'UTR plays an important role in regulating the stability and translation of labile mRNAs, such as cytokines and proto-oncogenes, by showing that this element modulates translational efficiency of more stable mRNAs encoding extracellular matrix proteins. By using primary cell cultures which maintain distinct phenotypic properties *in vitro*, we have identified LC3 as a *trans*-acting factor which appears to regulate the high levels of FN synthesis in migratory DA SMC and which was previously not known to have RNA binding properties. This study thus elucidates the role of a microtubule binding protein in mRNA translation and provides new insights into the molecular basis regulating expression of FN, a glycoprotein with numerous functions related to cell growth, differentiation, and migration in development and disease.

CHAPTER FOUR

MICROTUBULE INVOLVEMENT IN TRANSLATIONAL REGULATION OF FIBRONECTIN mRNA BY LIGHT CHAIN 3 OF MICROTUBULE-ASSOCIATED PROTEIN 1 IN DUCTUS SMOOTH MUSCLE CELLS

INTRODUCTION

Microtubules (MTs) have been implicated in the targeting, storage, sorting, and translational control of mRNAs in a variety of cells (Singer, 1992; Steward and Banker, 1992; Suprenant, 1993; Wilhelm and Vale, 1993; Ferrandon *et al.*, 1994; St Johnston, 1995). Signals that direct intracellular localization of mRNAs via MTs are found within the 3'UTR of mRNAs (Macdonald and Struhl, 1988; Gottlieb, 1992; Gravis and Lehman, 1992; Mowry and Melton, 1992). Interactions between MTs and mRNA may be mediated by factors which could recognize both consensus sequences in RNAs, as well as bind to MTs. Microtubule-associated proteins are good candidates for these factors. Several *trans*-acting factors that both recognize a *cis* element in 3'UTR of RNA and also bind to MTs have been reported (Kwon and Hecht, 1993; Elisha, *et al.*, 1995; Han, *et al.*, 1995; Schumacher, *et al.*, 1995). These include a spermatid perinuclear RNA-binding protein (Spnr) in mouse male germ cells (Schumacher, *et al.*, 1995), a rat testis/brain RNA-binding protein (Han, *et al.*, 1995), and Vgl RNA-binding protein (Vgl RBP) in *Xenopus* oocytes (Elisha, *et al.*, 1995).

While a wealth of evidence indicates cytoskeletal structures, such as MTs, are functionally involved in modulating the fate of localized mRNAs which encode cytoskeletal or cytoplasmic proteins, sorting of mRNAs encoding secreted proteins to the endoplasmic reticulum (ER) was thought to depend on their signal peptide. However, some studies demonstrated the spatial distribution of mRNAs that encode secreted proteins such as FN (Lee, *et al.*, 1984) and collagen (Mansour, *et al.*, 1988) or a membrane glycoprotein, lactase (Rings, *et al.*, 1994b). Thus, cytoskeletal structures may also influence the spatial localization of mRNA encoding secreted proteins. In addition, docking of mRNAs onto membrane-bound polysomes could be facilitated by cytoskeletal structures as opposed to simple diffusion of large mRNA-RNP particles (Rings, *et al.*, 1994a). LC3, which was initially cloned from a rat brain cDNA library, co-localizes with MTs in cultured rat neuronal cells, and co-precipitates with *in vitro* assembled MTs (Mann and Hammarback, 1994). The dual function of LC3 as an RNA-binding protein, as well as a MT-associated protein suggests that MTs may play a role in the translational regulation of FN mRNA

by LC3.

In this chapter, we will address the role of LC3 in regulating FN mRNA translation in the context of MT. We show that, in contrast to our previous finding in cell cultures (Chapter Two). LC3 represses translation of chimeric mRNA containing the CAT coding region and FN 3'UTR in cell-free reticulocyte lysates. The discrepancy between *in vivo* and *in vitro* studies suggests that LC3-mediated translational enhancement might require an intact cytoskeletal network and other factors. This is supported by further experiments in which disruption of MTs in cultured DA SMC by colchicine treatment inhibits FN mRNA translation. Analysis of intracellular distribution of FN mRNA and LC3 protein by cellular fractionation and polysomal profile demonstrated a concomitantly decreased association of FN mRNA and LC3 protein with membrane-bound polysomes in cells following colchicine treatment. We therefore propose that LC3-mediated FN mRNA translational enhancement is facilitated by MTs.

RESULTS

LC3 Suppresses Translation of CAT-FN3'UTR Fusion RNA in a Cell-free System

Since LC3 is a MT-associated protein (Mann and Hammarback, 1994), its function in FN mRNA translation could be associated with its role as a MT-associated protein. To test this hypothesis, we first examined the effect of LC3 on RNA translation in the absence of MT. We applied an *in vitro* cell-free transcription and translation assay using fusion constructs containing the CAT coding region and the FN 3'UTR with the wild type or mutated ARE. No LC3 was detected in the reticulocyte lysates (40 μg) by western immunoblot (data not shown). Equal amounts (0.5 μg) of purified fusion constructs (CAT-FN3'UTR and CAT-FN3'UTRΔ) were used for the cell-free transcription and translation assay. In experiments with addition of LC3 protein, there was no evidence of enhanced mRNA translation in this cell-free system. In fact, repression was observed, which was related at least in part to an interaction between LC3 and ARE. Figure 30 shows autoradiographs for CAT in the above experiments with **a** and **b** representing addition of 0.5 and 2.0 μg LC3 protein, respectively. The negative control without addition of plasmid (lane 1

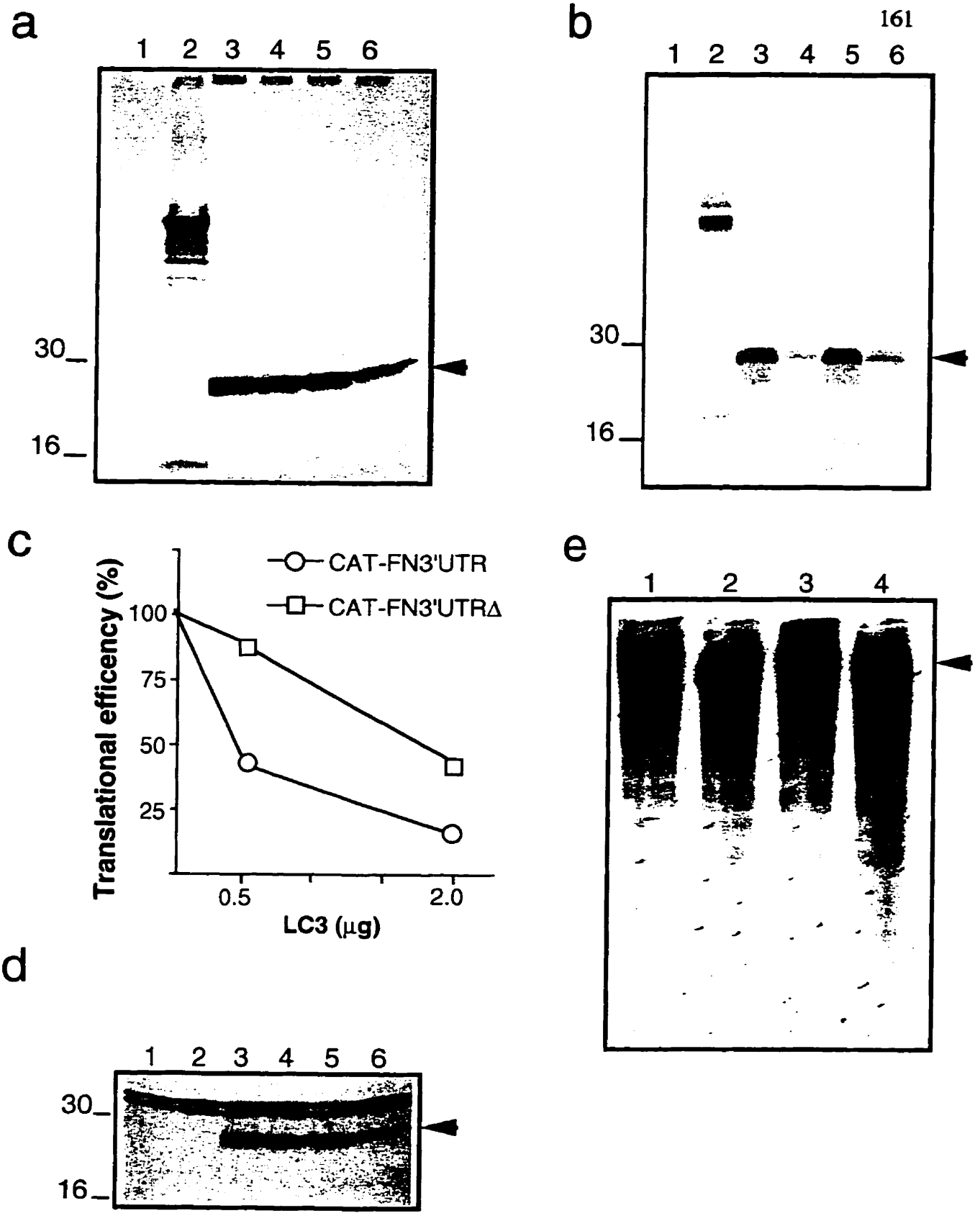
a
1 2 3 4 5 6
30
16
b
1 2 3 4 5 6
30
16
c
CAT-FN3'UTR
CAT-FN3'UTRΔ
Translational efficency (%)
100
75
50
25
0.5
2.0
LC3 (μg)
d
1 2 3 4 5 6
30
16
e
1 2 3 4

Figure 30

Figure 30. LC3 suppresses translation in a cell-free transcription and translation assay

Transcription and translation reactions were carried out as described in Materials and Methods (Section **IV**). In (**a**) and (**b**), lane 1 is negative control without addition of plasmid, lane 2 is a positive control with 0.5 μg hGH plasmid (Promega) showing a hGH protein product. Lanes 3 and 4 are reactions with purified CAT-FN3'UTR, and lanes 5 and 6 with CAT-FN3'UTRΔ. 0.5 μg (**a**) or 2 μg (**b**) LC3 protein were added to the reaction mixture (lanes 4 and 6). (**c**) A graph summarizing quantitative data from two independent experiments. (**d**) A representative western immunoblot comparable to (**a**) showing the CAT product (arrow) using a rabbit polyclonal antibody. (**e**) Assessments of fusion mRNA using CAT-FN3'UTR (lanes 1 and 2) or CAT-FN3'UTRΔ fusion constructs (lanes 3 and 4) without addition of LC3 protein (lanes 1 and 3) or with addition of 0.5 μg LC3 protein (lanes 2 and 4).

in **a** and **b**) shows no radiolabeled protein products, whereas the positive control with 0.5 µg hGH plasmid (Promega) shows a major protein product (lane 2 in **a** and **b**). Reactions with 0.5 µg purified CAT-FN3'UTR (lane 3 in **a** and **b**), or CAT-FN3'UTRΔ (lane 5 in **a** and **b**) produced approximately equal amounts of CAT protein (indicated by arrow). Thus, the presence of the ARE alone does not seem to alter *in vitro* translation of CAT mRNA. Addition of 0.5 µg LC3 protein into the reaction mixtures repressed production of CAT protein in reactions with both CAT-FN3'UTR (lane 4 in **a**), or CAT-3'UTRΔ (lane 6 in **a**), but a greater reduction in CAT production was observed in reactions using the ARE-mutated construct. Increasing the dose of LC3 to 2 µg results in a further decrease in CAT production in reactions with both constructs (**b**, lanes 4 and 6), but still a relatively greater difference is observed with the wild type construct (**b**, lane 4). Densitometric analysis of data from two independent experiments (**c**) revealed that a 57% repression of CAT production is found by adding 0.5 µg LC3 protein to the reaction with wild type fusion construct (CAT-FN3'UTR) compared to only a 16% decrease with the ARE mutated construct (CAT-FN3'UTRΔ). At higher concentrations of LC3 protein (2 µg/2.5 mg reticulocyte lysate), there was an 83% decrease of CAT production with CAT-FN3'UTR compared to a 55% decrease using CAT-FN3'UTRΔ. Western blot analysis using a polyclonal anti-CAT antibody (5'-3' Inc.) confirms the protein product as CAT (**d**).

Assessment of fusion RNA levels indicates that the decrease in CAT production is likely due to translational suppression, since approximately equal amounts of full-length mRNAs were found in the reaction mixtures transcribed from either wild type constructs (**e**, lane 1) or ARE-mutated CAT-FN3'UTRΔ fusion constructs (lane 3) at the end of the reaction. Addition of the LC3 protein to the reaction mixture had no effect on the transcription of either wild type (**e**, lane 2) or mutated fusion construct (**e**, lane 4). This suggests that the transcription rates of the two constructs were the same and independent of LC3. Similar amounts of short transcripts were also found in all reactions, which may be due to either premature termination of the reaction or degradation of full-length transcripts. This study suggests that, in the cell-free transcription and translation system, LC3 suppresses mRNA translation, but the effect may not be exclusively

dependent on the ARE, especially as evident with higher concentrations of LC3.

Intact MT Structures are Important for FN Synthesis

The results of the cell-free transcription and translation study suggest that an intact MT system might be necessary for LC3-mediated upregulation of mRNA translation. To test this *in vivo*, colchicine was applied to disrupt MT structures in cultured DA SMC and FN synthesis was examined. Treatment of cells with 10 μM colchicine for 2 h induced changes in cell shape related to alterations in MT structures (Figure 31); those treated with colchicine looked foreshortened with fragmentation of MTs, which appeared as condensations in the perinuclear region, as well as at the cell edge (**B** vs **A**). The distribution of LC3 in colchicine-treated and control cells was similar in its perinuclear distribution and punctate appearance. Cells probed with normal IgG instead of primary antibody and DAPI were used as negative controls and showed only nuclear staining for DAPI (**C**).

Cells were then labeled with [^{35}S]-methionine for 2 h and conditioned media were collected for FN extraction. Fibronectin extracted from conditioned media (normalized by total TCA precipitated protein) was reduced by 80% in DA cells treated with colchicine compared to control cells (Figure 32**a**, $p < 0.01$). The selective reduction in FN secretion following colchicine was unlikely explained solely on the basis of blocked secretion. There is little retention of newly-synthesized FN within the cells, although slightly more under colchicine-treated condition (Figure 32**b**). Northern blot analysis indicated that the steady-state levels of FN mRNA were not changed in cells treated with colchicine compared to control conditions (**c**). This is consistent with the reduction of FN synthesis by disruption of MTs being related to a suppression of mRNA translation.

We confirmed that cells were seeded at the same density, and cell lifting and loss was not observed during the treatment of colchicine (Figure 33). Since the time frame of the experiment was only 4 hrs while the doubling time of these primary DA and Ao SMC is approximately 72 h, the reduction in FN synthesis following colchicine treatment was not due to mitotic arrest. We also

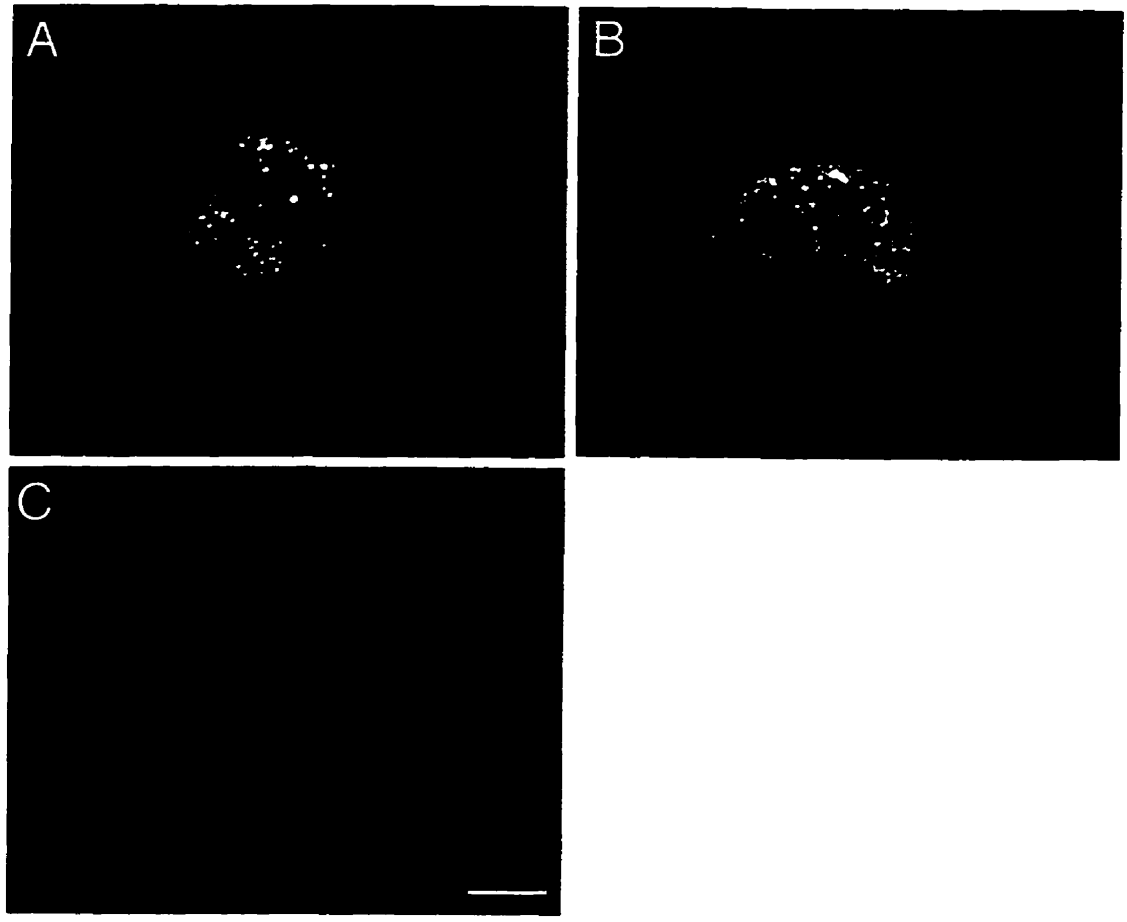

Figure 31

Figure 31. Disruption of MTs alters SMC shape

Cultured DA SMC were treated with colchicine for 2 h, fixed, and immunostained for tubulin and LC3 using a monoclonal mouse anti-tubulin IgG and a rabbit anti-LC3 antiserum as described in Materials and Methods. Secondary antibodies used were FITC-conjugated goat-anti-mouse IgG and Texas-red-conjugated goat-anti-rabbit IgG. Cell nuclei were stained with DAPI. Normal rabbit IgG and secondary antibody alone served as controls. Compared to normal cultured cells (**A**), cells treated with colchicine (**B**) are foreshortened with fragmentation of MTs (FITC staining) which appear as prominent condensations at the cell edge. In the perinuclear region. LC3 appears particulate and its co-distribution with tubulin results in a yellow color (overlap of Texas-red with FITC). Control specimen (**C**) using normal IgG shows only DAPI staining for nuclei. Bar = 20 μm.

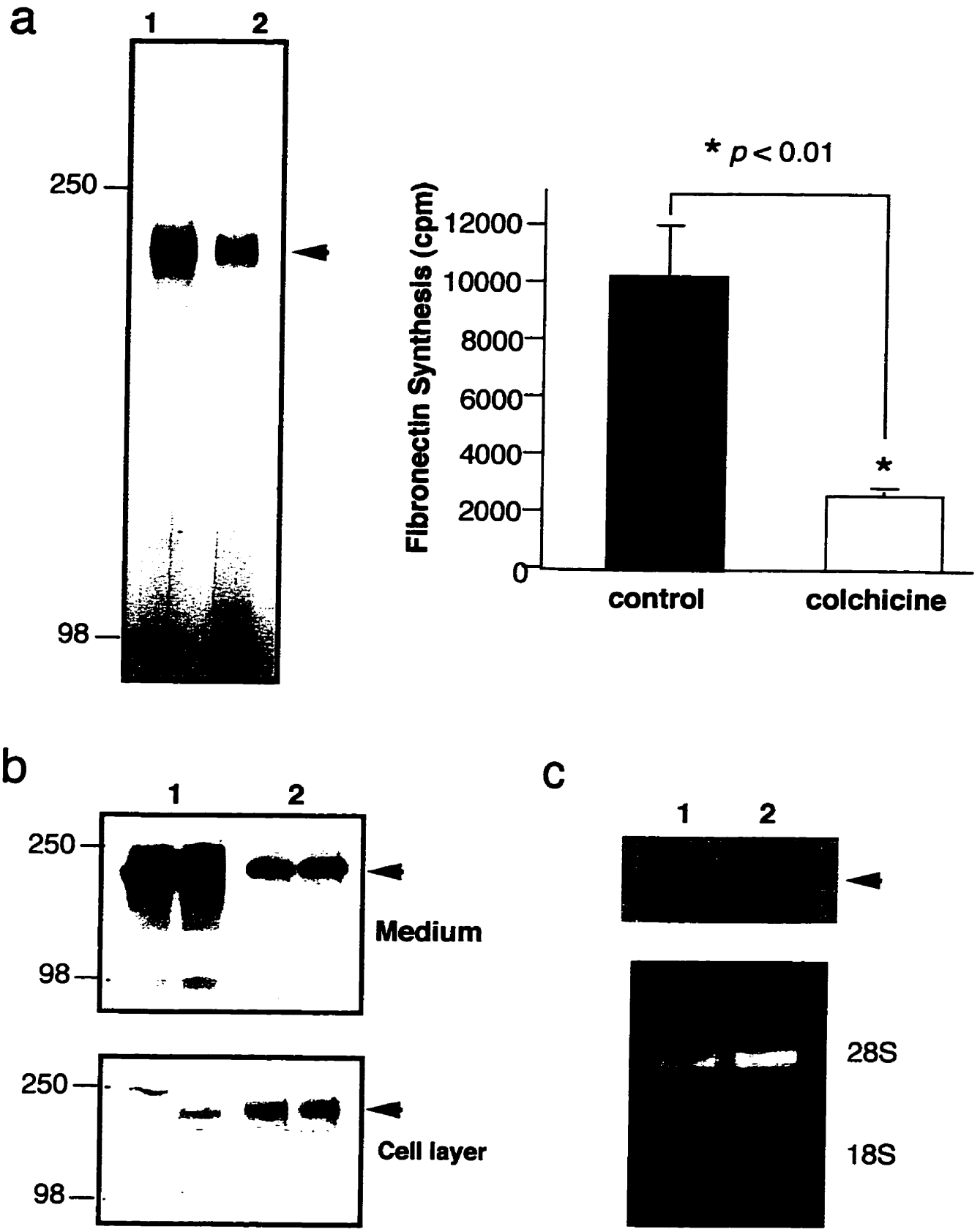
a
1
2
250
98
* p < 0.01
Fibronectin Synthesis (cpm)
12000
10000
8000
6000
4000
2000
0
*
control
colchicine
b
1
2
250
98
Medium
250
98
Cell layer
c
1
2
28S
18S

Figure 32

Figure 32. Disruption of MT by colchicine inhibits FN mRNA translation

(**a**) Left is a representative autoradiograph of newly-synthesized FN extracted from conditioned media of normal cells (lane 1) or colchicine-treated cells (lane 2). The same amount of total secreted proteins, as judged by total TCA precipitated protein counts was used for FN extraction. Right is a quantitative analysis from 4 different experiments. Compared to normal cultured cells, FN synthesis was significantly decreased in cells treated with colchicine ($*p < 0.01$, by Student t test). (**b**) an autoradiograph of newly-synthesized FN extracted from conditioned media (top) and cell layers (bottom) of normal cells (lanes 1 and 2) or colchicine-treated cells (lanes 3 and 4) from two separate experiments. The majority of newly-synthesized FN was found in the media under both normal or colchicine-treated cultures. Only a small amount was associated with cells under both conditions, but this did appear to increased slightly following colchicine treatment. (**c**) A representative northern blot analysis shows that the steady-state level of FN mRNA remain the same when normal (lane 1) and colchicine-treated (lane 2) SMC are compared. 28S and 18S RNA are shown to confirm equal loading conditions. Three different experiments showed similar results.

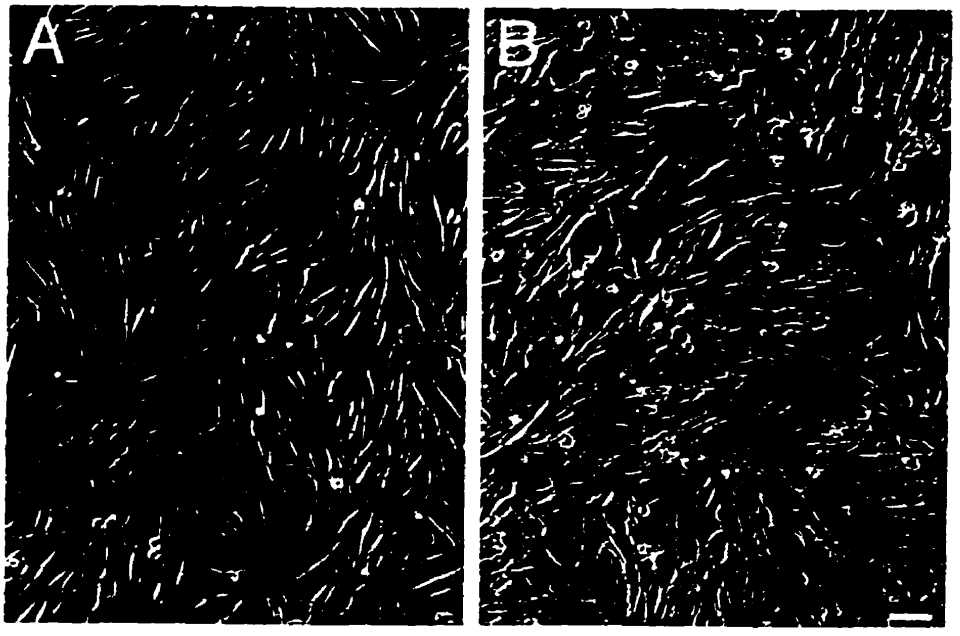

Figure 33

Figure 33. Phase contrast light microscopy of DA SMC treated with colchicine

Compared to control cells in (**A**), there is no lifting or loss of cells 4 h after colchicine treatment (**B**), although the cells appear less elongated after colchicine treatment. Bar = 40 μm.

confirmed by western immunoblot that the decreased FN synthesis following colchicine treatment was not reflected in a decrease in LC3 (data not shown).

Sorting of FN mRNA to Membrane-bound Polysomes Requires MTs

We next examined whether disruption of MTs alters FN mRNA distribution, i.e. its association with membrane-bound polysomes. Cultured DA SMC were lysed with non-ionic detergent, Nonidet P-40, and fractionated into soluble and insoluble portions. The soluble fraction of the cytoplasmic extract contains free polysomes and polysomes released from the cytoskeleton; while the insoluble fraction contains ER membrane-associated polysomes. RNA was extracted from both fractions, and distribution of FN mRNA was determined by northern blot analysis. As shown in the Figure 34, in normal cultured cells, approximately equal amounts of FN mRNA were found in the insoluble fraction containing membrane-bound polysomes (lane 1), and soluble fractions containing free polysomes (lane 2). However, in cells treated with colchicine, FN mRNA associated with membrane-associated polysomes was reduced (lane 3), and appeared to be 'shifted' in the soluble fraction (lane 4). Indeed the ~60% reduction in membrane-associated FN mRNA after colchicine treatment could account for the ~80% reduction in FN synthesis (Figure 32). Since FN is a secreted glycoprotein, the signal peptide would direct FN mRNA to the ER, where FN protein is translated. Thus, the colchicine-induced reduction of FN mRNA in membrane-bound polysomes implicates involvement of MTs in RER sorting of FN mRNA.

Polysome Profile Analysis

To determine more specifically whether the effect of MTs on FN mRNA translation likely involves LC3, we applied a polysome profile analysis to compare the distribution of FN mRNA and LC3 protein under conditions where LC3 and FN synthesis were increased (DA versus Ao cells), or where MTs were disrupted (DA cells treated with colchicine versus control). Post-nuclei cell lysates were loaded onto a 15-40% sucrose gradient.

In both DA and Ao cells (Figure 35, **a** and **b** respectively), most of FN mRNA was found

a

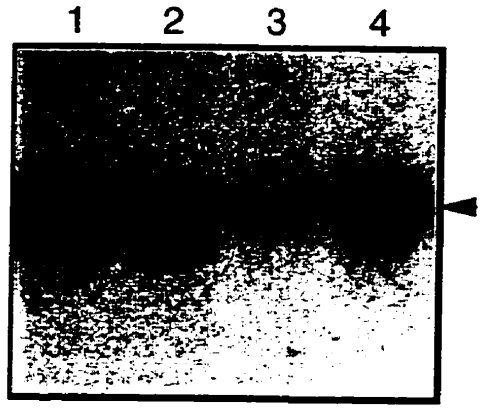

b

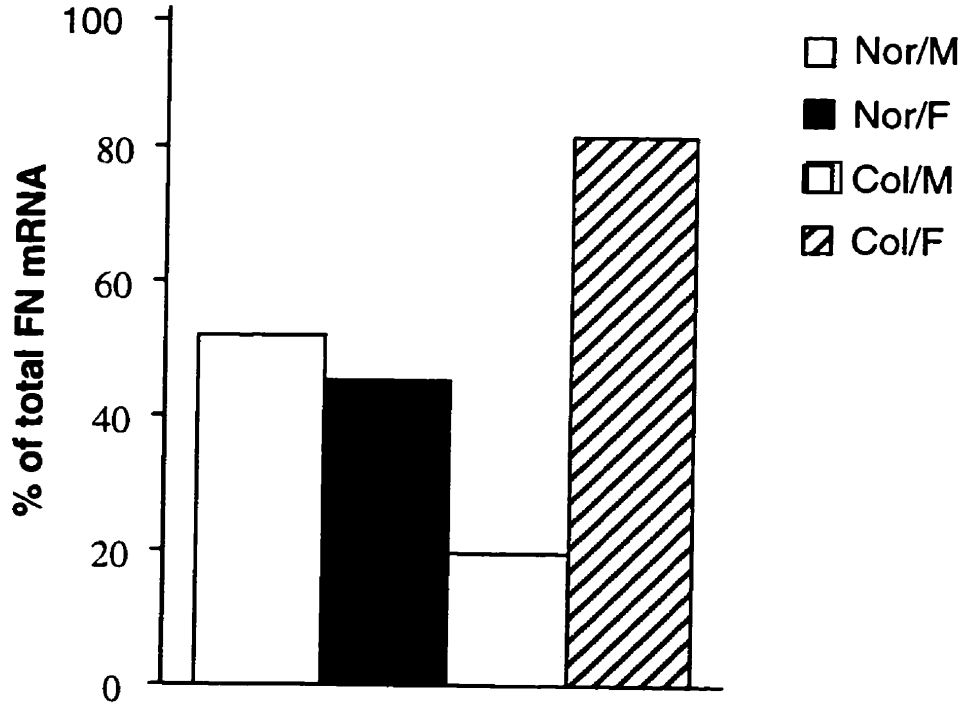

Figure 34

Figure 34. Alteration of FN mRNA distribution in DA SMC by disrupting MT structure

(**a**) A northern blot analysis of FN mRNA distribution. DA SMC were cultured under normal (lanes 1 and 2) or colchicine-treated conditions (10 μM for 4 h) (lanes 3 and 4). Cells were extracted with lysis buffer containing 0.5% NP-40, mRNA associated with cytoskeleton or free RNPs (lanes 1 and 3) were separated from mRNA associated with membrane-bound polysomes (lanes 2 and 4) by one step centrifugation at 16,000g for 30 min. Distribution of FN mRNA was then assessed northern blot analysis. (**b**) A corresponding graphic presentation of distribution of FN mRNA (% of total cellular mRNA) in free RNPs or cytoskeletal fractions (**F**) versus membrane-bound polysome fractions (**M**) under normal (**Nor**) or colchicine-treated (**Col**) conditions is shown.

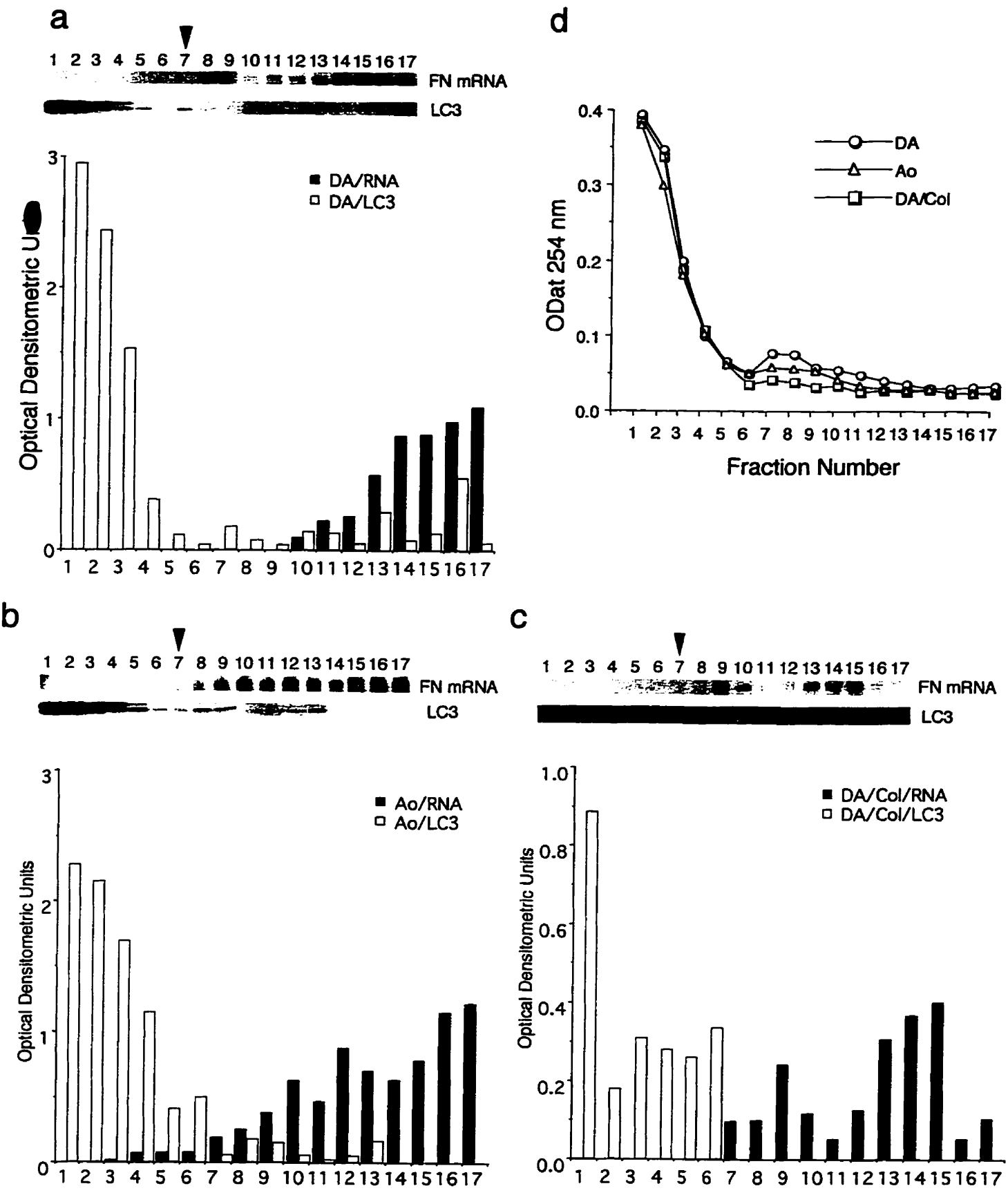
a
1 2 3 4 5 6 7 8 9 10 11 12 13 14 15 16 17
FN mRNA
LC3
DA/RNA
DA/LC3
Optical Densitometric U
d
DA
Ao
DA/Col
ODat 254 nm
Fraction Number
b
Ao/RNA
Ao/LC3
Optical Densitometric Units
c
DA/Col/RNA
DA/Col/LC3
Optical Densitometric Units

Figure 35

Figure 35 Polysomal distribution of FN mRNA and LC3 protein

Polysomal distribution of FN mRNA and LC3 protein in DA (**a**), Ao SMC (**b**), and DA SMC treated with colchicine (**c**) is assessed. Post-nuclei cell lysates were layered on a 15-40% sucrose gradient, centrifuged at 42, 000 rpm for 2 h at 4°C in a Beckman SW 50.1 rotor, and fractionated from top to bottom. Analyses of the distributions of FN mRNA and LC3 protein were done by RNase protection assay and western immunoblotting as described in the Materials and Methods (Section **IV**). Top is the photograph of RNase protection assay and western immunoblot that represents one of two reproducible studies (arrow indicates the position of 80S monosome); and bottom shows the graphic representation of the corresponding densitometric analyses using NIH image program. (**d**) A graph shows the ribosomal distribution assessed by the OD at 254 nm. which is similar in DA and Ao cells or DA cells treated with colchicine (DA/Col).

in the polysome region and there was no detectable FN mRNA the ribosome subunit region in DA cells. Little, if any, FN mRNA in Ao cells associated with ribosome subunits (arrow indicates the position of 80S monosome). This suggests that most of FN mRNA in both cells is translationally activated. While comparable amounts of FN mRNA were found in the polysome profiles of both cells, the polysome-associated FN mRNA in DA SMC was largely concentrated in the last 5 fractions (**a**, 12-17), which were located at the bottom of sucrose gradient. In contrast, there was a broader distribution of polysome-associated FN mRNA in Ao cells, from fractions 9 to 17 (**b**). In general, the association of mRNA with heavier polysomes could be due to two different mechanisms: enhanced translational initiation or decreased elongation. Since the translation of FN mRNA into protein in DA SMC is greater than that in the Ao cells (Boudreau and Rabinovitch, 1991), the location of FN mRNA in heavier polysomes in DA versus Ao SMC suggests an increase in efficiency of FN mRNA translation. Furthermore, since there were equal amounts of FN mRNA in the polysome profiles of both cells and no FN mRNA was associated with translationally inactive ribosome subunits, the increased FN mRNA translation in DA SMC was likely related to an enhanced recruitment or reinitiation of ribosomes.

LC3 appeared as a doublet in most fractions and had a dual cellular distribution. The majority of LC3 was found at the top of the gradient (**a** and **b**), which is consistent with LC3 as a MT-associated protein, since MT are largely dissociated as soluble tubulin monomers during the process of homogenization of cells. The LC3 protein, however, also appeared in the polysomal fractions which contained the majority of FN mRNA, especially in DA cells (compare **a** to **b**). For example, LC3 was apparent in fractions 11-16 in the DA cells and in fractions 8-13 in the Ao cells. A similar dual distribution of LC3 protein was observed in our study in which expression of LC3 in HT1080 cells that lack LC3 protein promotes ribosome recruitment to FN mRNA and enhance its translation (See Chapter Five for details).

The effect of colchicine on the polysome profile of FN mRNA and LC3 in cultured DA SMC further supported the role of MTs in LC3 function related to FN mRNA translation. Compared to normal cultured DA cells (**a**), the distribution of FN mRNA in those treated with

colchicine was shifted into fractions in the sucrose gradient associated with lighter polysomes (**c**, fractions 9-15). Moreover, LC3 was associated with fractions containing ribosome subunits or RNPs and not with polysome fractions (**c**, fractions 1-7). The overall distribution of polysomes, however, was similar in normal cultured DA, Ao, and colchicine-treated DA SMC (**d**). These data suggest that disruption of MTs interferes with the interaction of FN mRNA with LC3, and impedes docking of FN mRNA-RNP complexes onto membrane-bound polysomes.

DISCUSSION

In Chapter 3, we demonstrated that a FN mRNA ARE-binding protein is LC3 of MAP1. The work described in this Chapter was undertaken to examine whether the mechanism of LC3 regulation of FN mRNA translation involved MTs. We report three different experimental approaches to support the involvement of MTs in the translational regulation of FN mRNA by LC3. First, we show that the addition of LC3 to a cell-free translation system lacking an intact cytoskeletal network represses mRNA translation. We next demonstrate that disruption of MTs by colchicine results in the repression of FN mRNA translation in DA SMC. We further demonstrate by cellular fractionation and polysome profile analysis of FN mRNA and LC3, that an accelerated recruitment of FN mRNA-RNP complexes onto membrane-bound polysomes is likely the mechanism by which LC3 enhances FN mRNA translation in DA SMC, and this feature might require or be optimized by intact MT structures.

To our knowledge, our findings provide the first evidence for a coordinated function of MTs and a specific MT-associated protein (LC3), in regulating translation of a translationally-activated mRNA encoding a secreted protein. It has previously been shown that cytoskeleton involves anchoring, sorting, and translation of mRNAs encoding cytoskeletal structural proteins and spatially localized cytoplasmic proteins (Singer, 1992; Steward and Banker, 1992; Suprenant, 1993; Wilhelm and Vale, 1993; Ferrandon, *et al.*, 1994; St Johnston, 1995). Signals that direct intracellular transport and localization of mRNAs are within the 3'UTR of mRNAs (Macdonald and Struhl, 1988; Gottlieb, 1992; Gravis and Lehman, 1992; Mowry and Melton, 1992). In

Xenopus oocytes, Vgl RNA-binding protein (Vgl RBP) mediates the association of Vgl mRNA with MT and Vgl RBP itself binds to MT (Elisha, *et al.*, 1995). In rat male germ cells, spermatid perinuclear RNA-binding protein (Spnr), which binds to the 3'UTR of spermatid-specific protamine-1 (Prm-1) mRNA, is localized to MTs and is proposed to be functionally involved in RNA transport or translational activation (Schumacher, *et al.*, 1995). In mouse, a testis/brain RNA-binding protein attaches both to translationally repressed transcripts such as protamine-2 (Prm-2), tau, and myelin basic protein containing conserved sequences (*Y* and *H* elements) in the 3'UTR (Han, *et al.*, 1995).

In previous studies, colchicine has been used to depolymerize MT to establish their pivotal role in the transport or localization of mRNA. In our studies, we used colchicine to determine that MT were critical to FN mRNA translation. Others have reported that colchicine treatment inhibits synthesis of collagen (Mansour, *et al.*, 1988), stearoyl-CoA desaturase and fatty acid synthetase (Kasturi *et al.*, 1984) without affecting total protein synthesis, but the mechanism was unexplored. Colchicine has also been demonstrated in hepatectomized rats to inhibit general translation of mRNA without affecting cell proliferation, by inducing a global dissociation of membrane-bound polysomes (Walker and Whitfield, 1984; Walker and Whitfield, 1985). However, this mechanism cannot explain the selective inhibition of FN mRNA translation by colchicine in our study, since the overall polysome profile was unchanged in colchicine treated cells compared to normal cultures, yet the association with FN mRNA was altered. The difference may be related to the experimental model: whole hepatectomized animal and rapidly proliferating hepatic cells versus relatively quiescent cultured SMC in our studies.

It is also interesting that the staining of LC3 in the SMC appears 'particulate' around the perinuclear region, even in non-colchicine treated DA cells. This suggests that LC3 may associate with FN mRNA as an RNP complex which contains segregated MT elements or tubulin as described previously by others (Suprenant, 1993). Since there were no changes in LC3 protein or FN mRNA levels after disruption of MTs by colchinine, or in the LC3 perinuclear distribution pattern, we speculate that the decreased translation of FN mRNA is due to an inability of LC3, in

the absence of MTs, to influence sorting of FN mRNA onto membrane-bound ribosomes. Similarly, in the cell-free translation system, the failure of LC3 to enhance rather than to repress CAT-FN3'UTR fusion mRNA translation may also be due to the lack of a MT 'tract'. However, it is also necessary to consider other mechanisms unrelated specifically to MTs. For example, the abundance of ribosomes available for translation in the cell-free system may bypass the fine tuning (enhanced ribosome recruitment) provided by LC3 in cell culture where competition among RNAs for ribosome binding would be expected. Alternatively, the high concentration of exogenous LC3 in the *in vitro* system may mask mRNA so that it has less access to translational machinery.

We attempted to elucidate the mechanism by which LC3 regulates FN mRNA translation in the context of MTs by comparing intercellular distribution of both FN mRNA and LC3 protein in DA versus Ao or colchicine-treated DA SMC. Colchicine treatment diminishes membrane-associated FN mRNA, suggesting that sorting of FN mRNA onto the ER membrane was impaired. Further polysome profile studies indicate that the FN mRNA is translationally activated in both DA and Ao SMC. However, FN mRNA was associated with heavier polysomes in DA than in Ao SMC, suggesting an enhanced recruitment of FN mRNA-ribosome complexes onto the ER membrane. In addition, while the majority of LC3 protein was distributed with the translationally-inactive subunits in both DA and Ao SMC, a small fraction of LC3 was associated with FN mRNA on the polysomes. The LC3 in the translationally-inactive fraction would be likely due to dissociation of MTs following homogenization of the cells on the ice. However, we could not exclude the possibility that LC3 is associated with other mRNAs containing AREs in the complex of RNPs or is directly associated with ribosome subunits. The overlap of distribution of FN mRNA and LC3 protein in DA and Ao SMC suggests that LC3 may associate with ribosomes through binding of FN mRNA. A similar observation has been made in 3T3-L1 preadipocytes in which ectopic expression of Hel-N1, another ARE-binding protein, increases glucose transporter (GLUT1) expression due to marked acceleration of progression from the preinitiation complex to heavy polysomes (Jain, *et al.*, 1997). However, the association of Hel-N1 with translational machinery (polysome profile) was not addressed in that study.

The polysomal distribution of FN mRNA and LC3 protein in colchicine-treated cells provides additional experimental evidence that intact MT structures are required for the interaction of LC3 and FN mRNA, and docking of FN mRNA-RNP complexes onto polysomes. Disruption of MTs by colchicine shifts FN mRNA into fractions in the sucrose gradient associated with fewer polysomes, and LC3 was only detected in the translationally-inactive fractions. The finding strongly suggests that there were two functionally distinct pools of LC3, one binds MTs, and the other binds FN mRNA. MTs may affect FN mRNA translation by providing a 'track' for mRNA transport to ER, thus incorporating the dual function of LC3 both as an MT and as an mRNA-associated protein. Alternatively, the LC3 in the translationally-inactive compartment may represent a storage pool, and modification of MT-associated LC3 e.g., by phosphorylation (our unpublished data), is necessary for its function in promoting polysome recruitment of FN mRNA. Alterations in phosphorylation status are of functional significance in other ARE-binding proteins (Malter, 1989), and the testis/brain RNA binding protein which also binds MT (Kwon and Hecht, 1993).

While we have focused on the relationship between LC3 and FN expression in the context of MTs, it is likely that LC3 regulates other mRNAs, particularly those with AREs. For example, cytokines, such as tumor necrosis factor-α and interleukin 1β, have AREs in their 3'UTR, and are upregulated in vascular SMC in association with neointimal formation (Clausell and Rabinovitch, 1993; Clausell, *et al.*, 1995; Molossi, *et al.*, 1995). In summary, our data show that the effect of LC3 on translational regulation of FN mRNA is likely at the level of ribosome recruitment and is mediated by intact MTs. How binding of LC3 to 3'UTR of FN mRNA impacts on ribosome recruitment and how MTs influence the interaction of LC3 and FN mRNA will be of great interest in future studies.

CHAPTER FIVE

LIGHT CHAIN 3 OF MICROTUBULE-ASSOCIATED PROTEIN 1, AN AU-RICH ELEMENT RNA-BINDING PROTEIN, INCREASES FIBRONECTIN mRNA TRANSLATION IN HUMAN FIBROSARCOMA CELLS

INTRODUCTION

This study was designed to determine whether LC3 enhances FN mRNA translation in other cells by a similar mechanism observed in DA SMC. We therefore screened several cell lines for expression of LC3. Unlike normal human fibroblasts, we could not detect expression of LC3 in a human fibrosarcoma cell line, HT1080. It was of further interest that this cell line has reduced FN synthesis and diminished cell surface deposits of FN (Oliver, *et al.*, 1983; Dean, *et al.*, 1988). Upon stable transfection of HT1080 cells with LC3, FN synthesis was enhanced and cell surface deposits of FN were observed. This was accompanied by a morphologic alteration to a flattened cell shape consistent with a 'revertant' phenotype (Paterson *et al.*, 1987), a rearrangement of MTs. and a slower growth rate. Polysome profile analysis demonstrated that FN mRNA in LC3 transfectants was more compressed in heavy polysomes compared to vector transfectants, and LC3 protein expressed in LC3-transfectants co-distributed with FN mRNA. These data suggest that LC3 upregulates FN mRNA translation by a mechanism involving enhanced ribosome recruitment.

RESULTS

Selection of LC3 transfectants and verification of the presence of LC3 expression

To understand the functional relationship between LC3 and FN expression, we carried out experiments using a human fibrosarcoma HT1080 cell line (Rasheed *et al.*, 1974). Like other transformed or neoplastic cells (Rasheed *et al.*, 1974; Yamada, *et al.*, 1977; Vaheri and Mosher, 1978; Steele, *et al.*, 1988; Varani *et al.*, 1991), HT1080 has reduced or absent cell surface-associated FN (Oliver, *et al.*, 1983; Dean, *et al.*, 1988). When we screened S-100 cytoplasmic extracts from different cell lines for the presence of LC3 by western immunoblotting using a rabbit-anti-LC3 antiserum, A10, NIH3T3, CHO, and Cos7, were all positive, whereas HT1080 cells had no detectable 16 kD LC3 (data not shown). Instead, a ~40 kD protein immunoreactive with the anti-LC3-antibody was evident. Further comparison of HT1080 cells (HT) with a more normal counterpart, human skin fibroblast cells (HF), CCD-973SK, revealed a 16 kD protein immunoreactive with anti-LC3 antiserum only in the human skin fibroblast cells and a ~40 kD

immunoreactive protein in both cells (Figure 36**a**). A ~110 kD protein in HT1080 cells was found cross-reactive to anti-LC3 antibodies.

Stable HT1080 transfectants expressing LC3 were then generated by the calcium phosphate precipitation method. G418-resistant clones were individually isolated and expanded. After three passages, the presence of recombinant LC3 protein in LC3 transfectants and its absence in vector transfectants was confirmed by western immunoblot. As shown in Figure 36**b** (a representative western blot analysis examining LC3 expression in LC3 transfectants), a ~16 kD protein immunoreactive with LC3 antiserum and consistent with the size of recombinant LC3 protein was present in three of five G418 resistant LC3 transfectants (lanes 1, 3, 5). The high molecular weight immunoreactive protein was also found in all the transfectants. As expected, cells transfected with vector alone had no LC3 expression (data not shown). A total of eight HT1080 clones with stable expression of LC3 protein and 4 vector-transfected clones were used to assess growth properties and FN expression.

Characterization of stable HT1080 transfectants expressing LC3

During their preparation, we noted that LC3 stable transfectants had a flattened shape and grew slowly in comparison to control vector stable transfectants. To confirm this observation, we correlated cell shape with growth. Cells were plated on dishes at the same density and the number of cells was determined at different time points ranging from one to 7-days. Cell morphology was also recorded at different time points during the first 3 days under subconfluent conditions. As shown in Figure 37 (a representative photograph of similar findings from all the transfectants), stable HT1080 transfectants expressing LC3 were more spread than vector-transfected cells at 24 h after plating (**B** versus **A**). By day 2 (48 h) and day 3 (72 h), LC3 transfectants (D and F, respectively) exhibited similar epithelioid morphology but appeared to be somewhat more spread and flattened and less phase-dense than vector-transfected cells (**C** and **E**). At 72 h, reduced cell density was also noted with LC3 transfectants (**F**) compared to vector-transfected cells (**E**), suggesting a slower proliferation rate associated with LC3 expression. This observation was

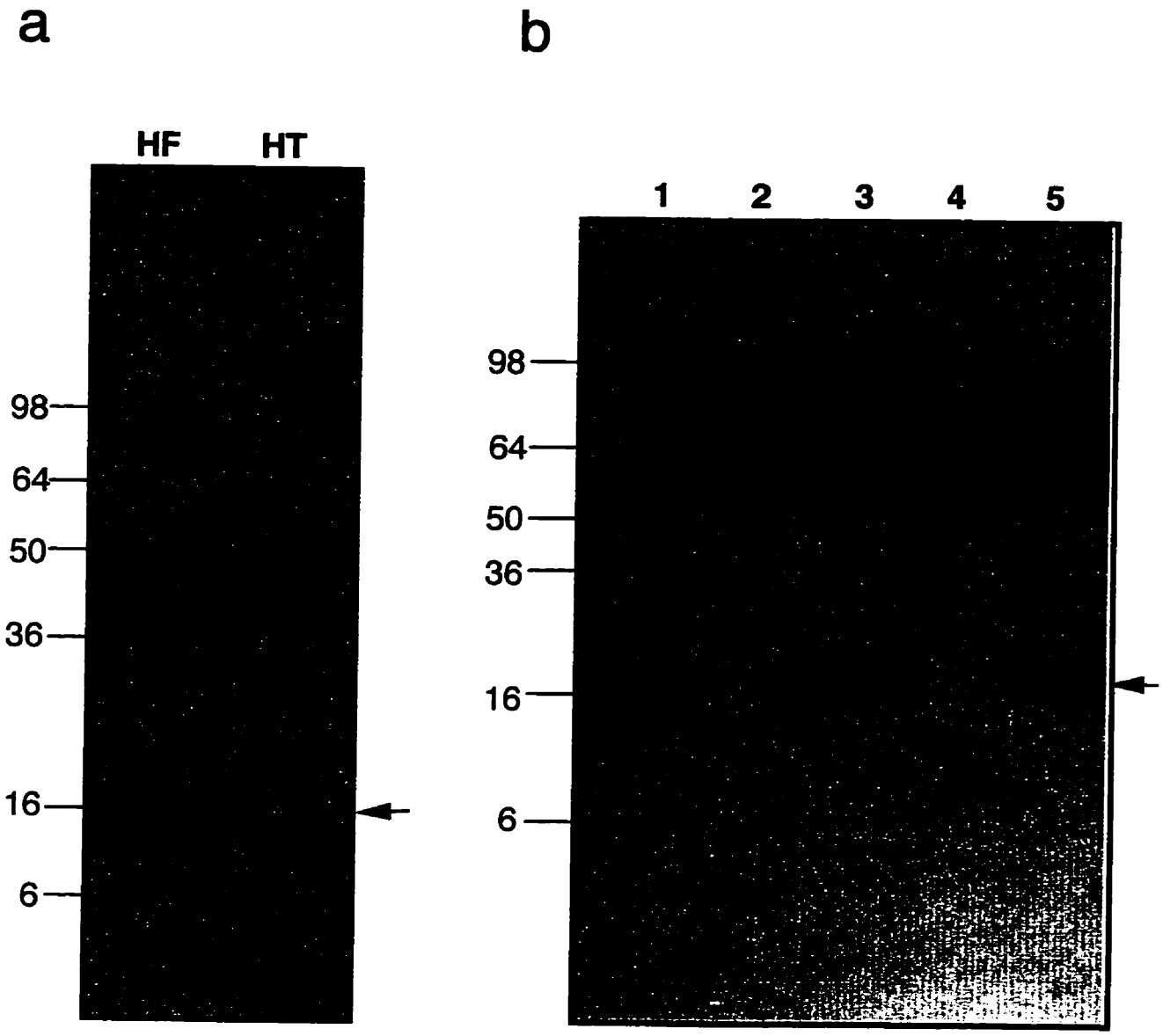

Figure 36

Figure 36. Expression of LC3 in stable HT1080 transfectants

(**a**) A representative western immunoblot of S-100 extracts from human fibroblasts and HT1080 cells shows expression of ~16 kD LC3 (arrow) in human fibroblasts (HF) but not in HT1080 cells (HT), while both cell lines have a ~40 kD protein immunoreactive with the LC3 antibody. (**b**) A representative western immunoblot shows that three of five LC3 stable transfectants express LC3 (lanes 1, 3, 5) as evidenced by the presence of a ~16 kD immunoreactive band (arrow). A higher molecular weight protein ~60 kD immunoreactive with the LC3 antibody is seen in all transfectants and may represent a modified form of the ~40 kD immunoreactive protein seen in the parent HT1080 cells.

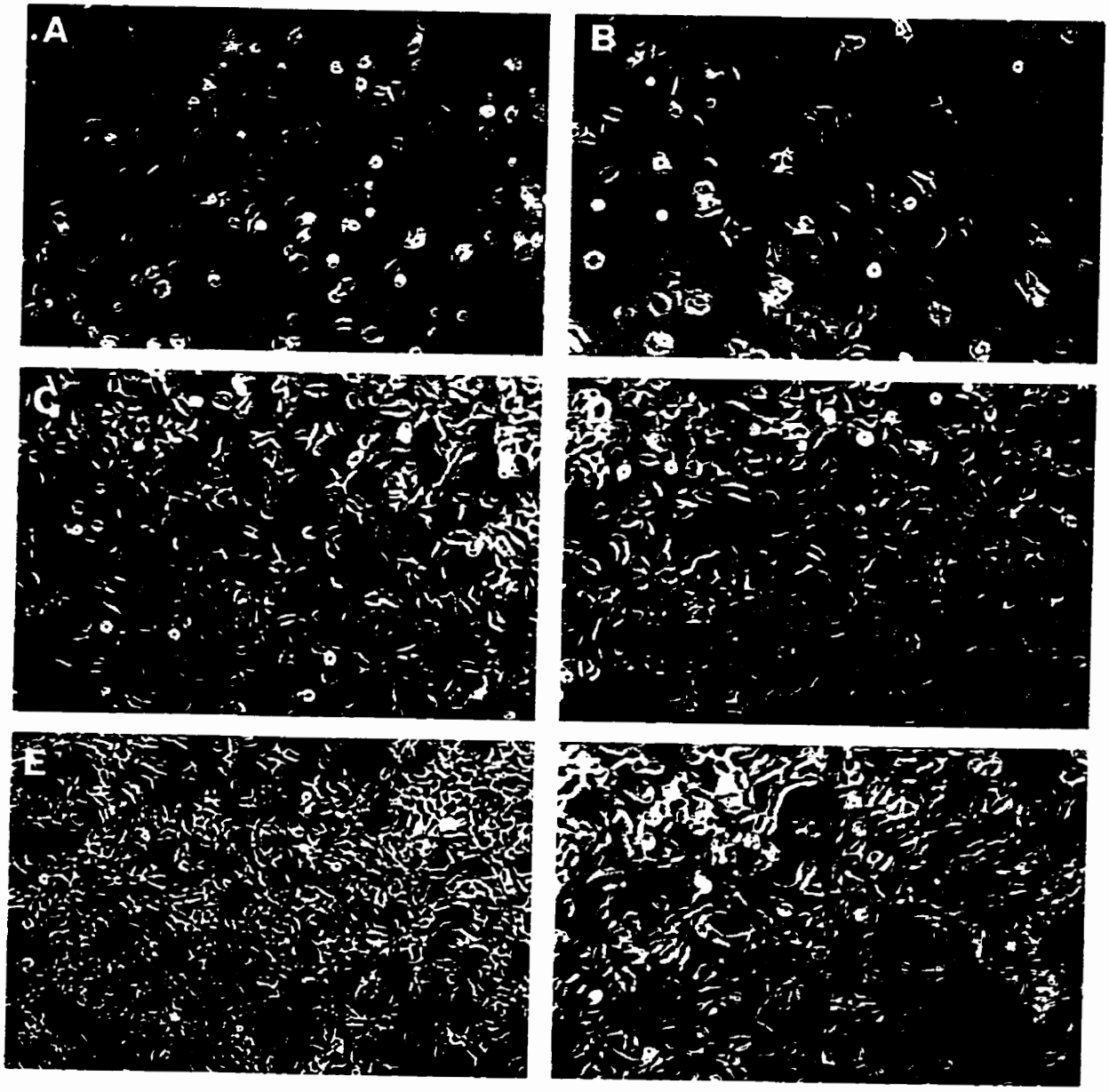

Figure 37

Figure 37. Effect of expression of LC3 on HT1080 cell morphology and growth

A representative phase-contrast photographs of cultured HT1080 cells at various times after plating. Compared to vector transfectants at 24 h (**A**), 48 h (**C**), and 72 h (**E**) following plating. LC3 transfectants show a flattened in morphology at each time point (**B**, **D**, **F**) and a reduced density of LC3 transfectants is also appreciated at 72 h (**F** vs **E**). Bar = 200 μm.

confirmed by growth curves (Figure 38). Statistically significant accelerated growth in vector-compared to LC3-transfected cells is observed starting from the third day after plating (Student's *t* test $p < 0.05$).

Effects of LC3 expression on FN matrix deposition

Previous studies have shown that HT1080 cells synthesize small amounts of FN and do not show cell surface FN matrix deposits. However, treatment of HT1080 cells with dexamethasone increased their rate of FN biosynthesis, and this was associated with FN matrix deposits and changes in cell adhesion and morphology (Rasheed, *et al.*, 1974; Yamada, *et al.*, 1977; Vaheri and Mosher, 1978; Oliver, *et al.*, 1983; McKeown-Longo and Etzler, 1987; Dean, *et al.*, 1988; Steele, *et al.*, 1988; Varani, *et al.*, 1991). Since these morphologic changes are similar to those of LC3 transfectants, we assessed whether the LC3 transfectants were also associated with increased cell surface FN matrix deposits using indirect immunofluorescent staining with anti-FN antibodies. Cell morphology was further visualized by indirect immunofluorescence of MTs with an anti-α-tubulin antibody. Figure 39 illustrates a representative photomicrograph of the transfected cells. Consistent with previous phase-contrast microscopic studies (Figure 37), LC3 transfectants were elongated, more spread, and flattened, and this was associated with well aligned arrays of MTs (**B**) when compared to vector transfectants (**A**). A FN filamentous matrix could also be seen on the cell surface of LC3 transfectants (**D**) but not the vector transfectants which exhibited sparse punctate staining on the cell surface (**C**).

Biosynthesis of FN in the stable transfectants expressing LC3

To confirm that FN biosynthesis was increased in LC3 transfectants, cells were labeled with [^{35}S]-methionine and culture media containing equal amounts of proteins determined by TCA precipitation were used for estimate of the rate of FN biosynthesis and secretion. Figure 40**a**, an autoradiograph of SDS-PAGE shows the 220 kD FN protein purified from four vector transfectants (V1-4) and eight LC3 transfectants (L1-8) using gelatin-4B sepharose extraction

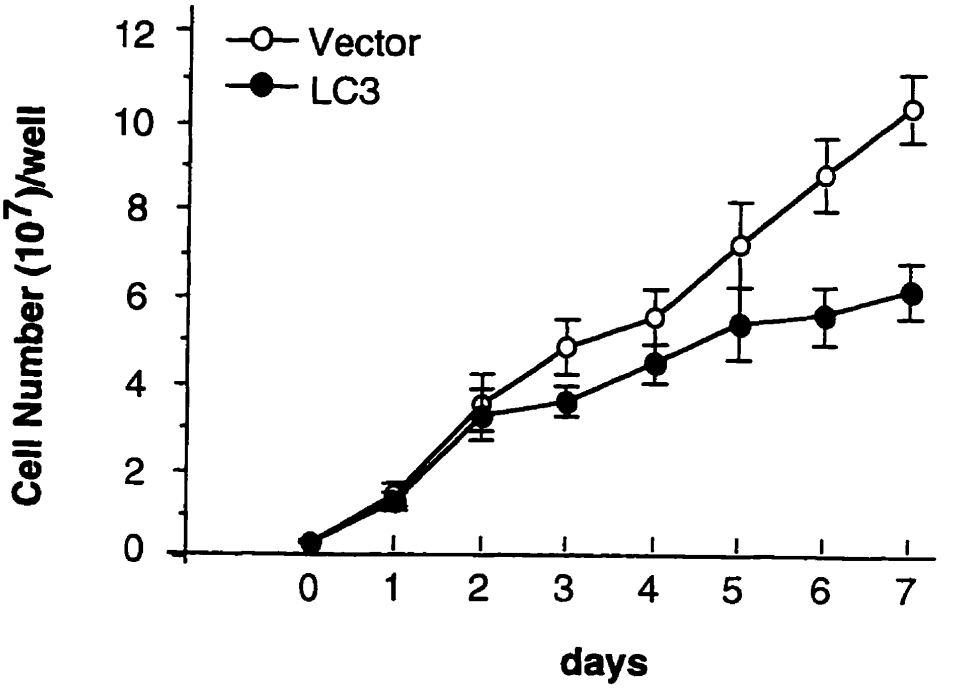

Figure 38

Figure 38. Growth curve of HT1080 cells

There is significantly reduced growth of LC3-transfectants compared to vector transfectants appreciated from day 3 after plating. This difference is $p < 0.05$ by Student's t test. Bars reflect standard deviations from n = 4 vector transfectants and n = 8 LC3 transfectants.

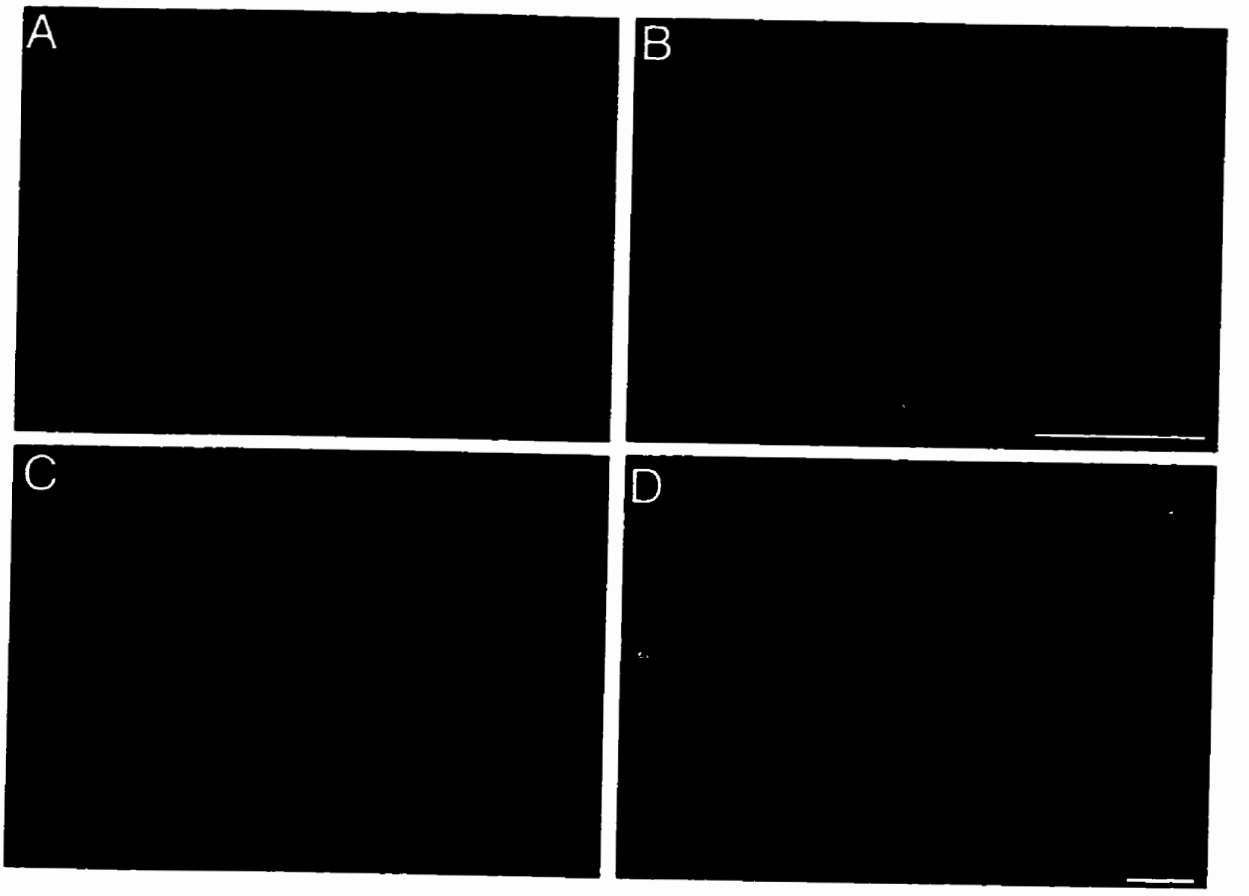

Figure 39

Figure 39. Immunofluorescent staining for MTs and FN in vector- and LC3-transfected HT1080 cells

Compared to vector-transfected cells (**A**) which show a round phenotype and less intense MT immunostaining, cells stably transfected with LC3 (**B**) show an elongated flattened phenotype with dense MT arrays. At the same time, vector-transfected cells (**C**) which exhibit little cell surface FN immunostaining, whereas a similar density of LC3-transfected cells (**D**) produce intense filamentous matrix deposits of FN on the cell surfaces. Bar = 40 μm

method. The FN bands were cut from the gel and the radioactivities were determined. Figure 40**b** shows a four-fold increase in newly synthesized and secreted FN in LC3 transfectants compared to control vector transfectants. The difference is significant by Student's *t*-test ($p < 0.01$).

To establish that the rate of biosynthesis was truly increased, we also carried out protein pulse-chase studies to determine the kinetics of FN secretion. Cells combined from all LC3 or vector transfectants were labeled for 2 h with [^{35}S]-methionine and then chased by replacement with fresh complete media. FN associated with cell layer, as well as secreted in the media was assessed at various time-points from 30 to 240 minutes. As shown in the Figure 41, in both vector and LC3 transfectants, starting from 30 min after chasing, most of newly-synthesized FN protein was secreted into the media while very little was found associated with or retained within cells. An increased amount of FN in LC3 compared to vector transfectants was observed as early as 30 minutes after chasing, reflecting a higher rate of biosynthesis. In addition, no degradation of FN protein was noted during the chase.

Analysis of FN mRNA levels and its stability

Total cellular RNA from eight stable LC3 and four vector transfectants was isolated and steady-state levels of FN mRNA were analyzed by northern blot. As shown by Figure 42, no apparent changes in FN mRNA levels were observed between vector and LC3 transfectants (V1-4 vs L1-8). Further examination of the stability of FN in vector- and LC3-transfected cells (pool of four vector and eight LC3 transfectants), using actinomycin D to block transcription, showed no alterations of FN mRNA stability in either vector- or LC3-transfected cells whereas the levels of control GAPDH mRNA decreased gradually after inhibition of transcription (Figure 43). These data suggest that the regulation of increased FN expression does not reside at transcriptional or post-transcriptional levels related to mRNA stability. Rather, an enhancement of FN mRNA translation in LC3 transfectants is the likely mechanism.

a

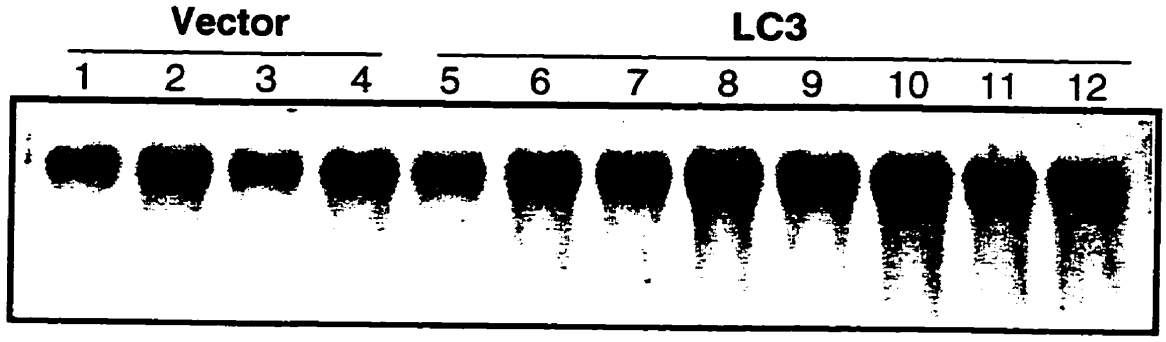
Vector
LC3
1 2 3 4 5 6 7 8 9 10 11 12

b

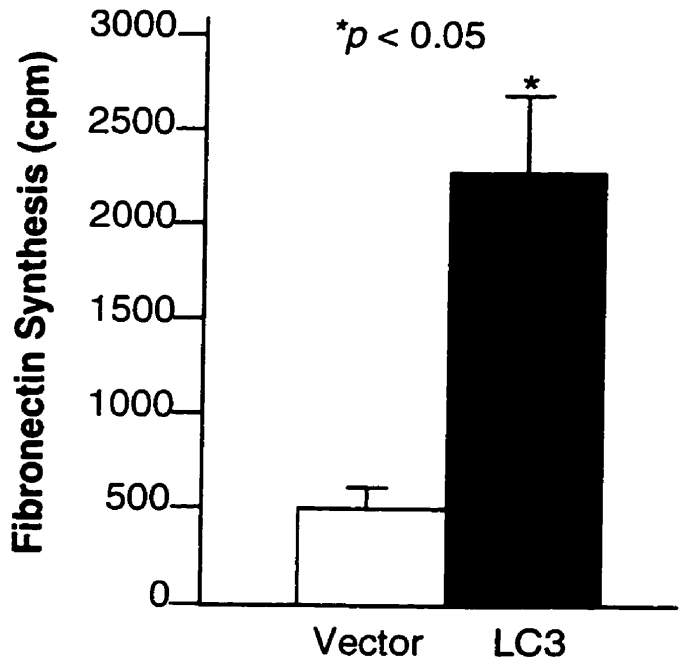
*p < 0.05
Fibronectin Synthesis (cpm)
3000
2500
2000
1500
1000
500
0
*
Vector
LC3

Figure 40

Figure 40. Expression of LC3 in HT1080 cells enhances FN synthesis

(**a**) An autoradiograph showing newly synthesized FN extracted from culture media of 4 vector-transfected (lanes 1 to 4) and 8 LC3-transfected clones (lanes 5-12). (**b**) A graph showing quantitative comparison of FN production in vector-transfected cells versus LC3-transfected cells as described in the Methods. LC3-transfected cells have a four-increase in FN production compared to vector-transfected cells ($p < 0.05$, Student *t*-test).

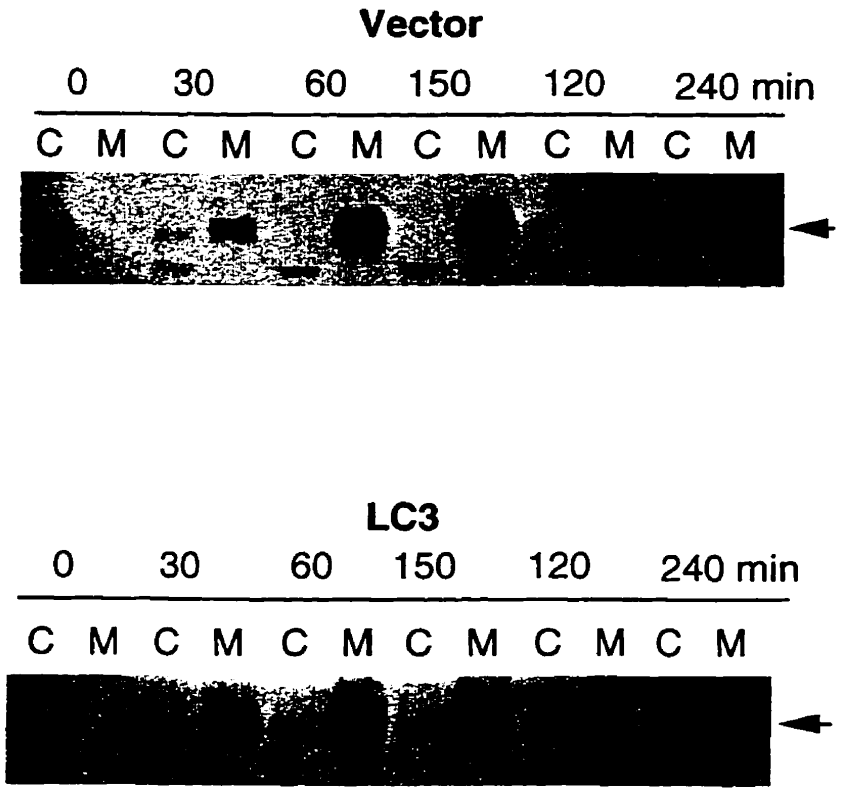
Vector
0 30 60 150 120 240 min
C M C M C M C M C M C M
LC3
0 30 60 150 120 240 min
C M C M C M C M C M C M

Figure 41

Figure 41. Kinetics of FN secretion in HT1080 vector and LC3-transfectants

HT1080 cells were pulse-labeled for 2 h with [^{35}S]-methionine and chased for increasing periods of time as described in the Methods. Cell-associated FN (**C**) and FN secreted in media (**M**), were separately extracted and resolved by SDS-PAGE. No appreciable differences in retention of FN is observed between LC3 and vector transfectants. After 2 h labeling with [^{35}S]-methionine, FN is appreciated in greater amounts in the cell lysate of LC3 versus vector-transfectants, whereas after a 30 minute chase, a greater amount of FN in both cell layer and media is appreciated in LC3 transfectants. The increased amount of FN after chase reflects continuous synthesis using [^{35}S]-methionine in the cell.

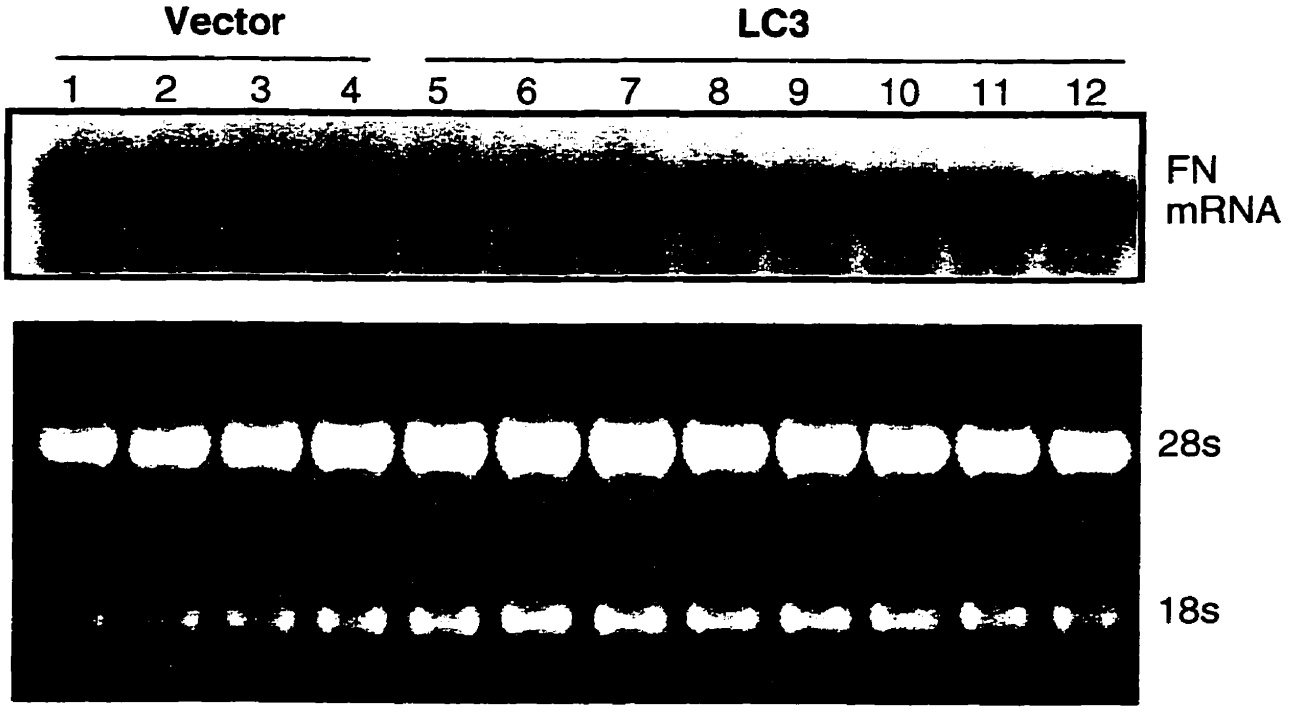

Figure 42

Figure 42. Steady-state levels of FN mRNA in stable HT1080 LC3 transfectants

A northern blot analysis shows a comparable amount of steady-state FN mRNA levels in vector-transfected cells (lanes 1 to 4) and LC3-transfectants (lanes 5 to 12). Ethidium bromide staining of 28S and 18S ribosome RNAs served as control for loading conditions.

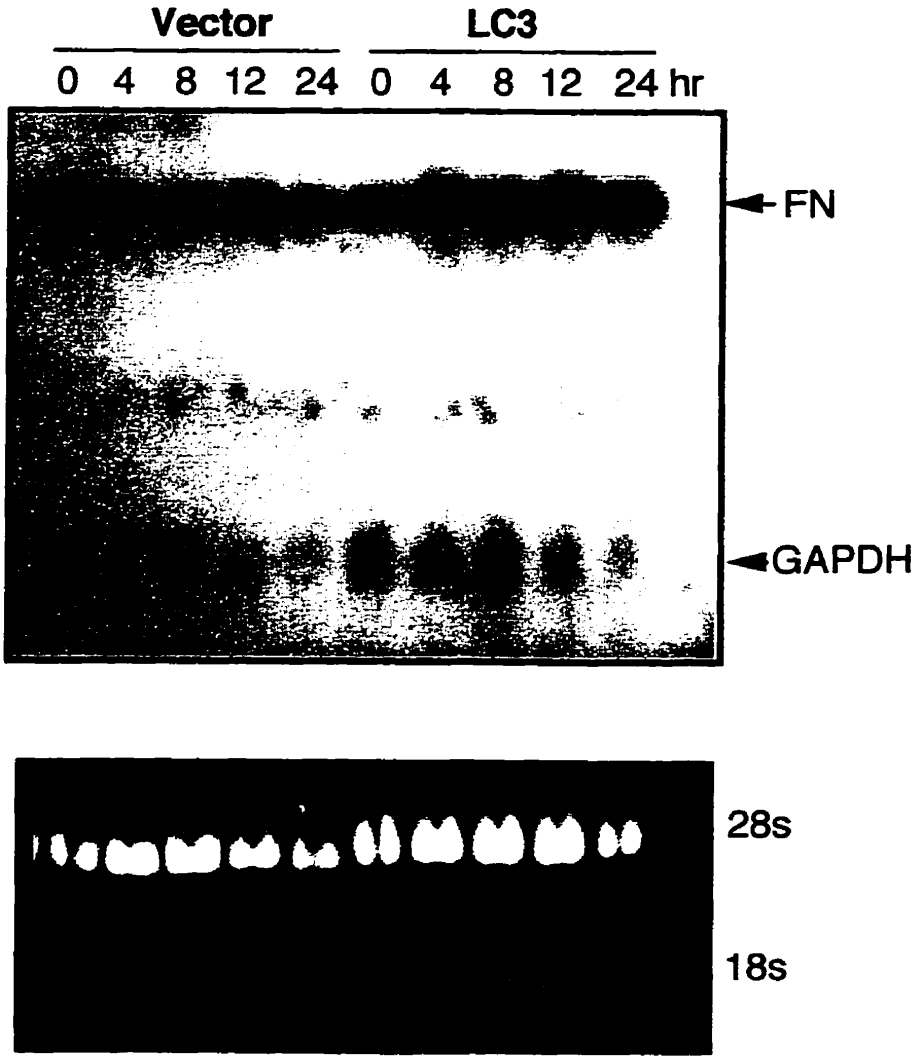

Figure 43

Figure 43. FN mRNA stability in stable HT1080 LC3 transfectants

A representative northern blot analysis of two separate experiments with similar results of FN mRNA at different time points following actinomycin D treatment as described in the Methods and Materials V. The membrane was probed with human FN cDNA as well as human GAPDH cDNA. 28s and 18s ribosome RNAs were also used to control for loading conditions. No apparent decay of FN mRNA was noted up to 24 h after blocking mRNA transcription, while the levels of control GAPDH mRNA decreased gradually over time. The increased amount of FN mRNA seen in LC3-transfected cells at 4, 8, and 12 h after actinomycin D treatment may be due to overloading.

Polysome profile analysis

To further determine whether the increased FN expression in LC3 compared to vector transfectants is due to enhanced FN mRNA translation, we applied a polysome profile analysis under identical conditions to examine the distribution of FN mRNA and LC3 protein among ribosomes and polysomes. Cell lysates with comparable amounts of total RNA from pools of four vector or eight LC3 transfectants were loaded onto a 15-40% sucrose gradient. RNA extracted from each fraction with equal volume was used in RNase protection assays for FN mRNA, as well as in agarose gel electrophoresis to determine the distribution of ribosomes and quality of mRNA. While there was a similar distribution pattern of ribosomes and polysomes in vector and LC3-transfected cells (compare bottom panels of Figure 44**a** and **b**), there was a broad distribution of FN mRNA in vector-transfected cells (**a**, fractions 6-17). In contrast, FN mRNA in LC3-transfected cells was shifted and concentrated in the fractions containing heavy polysomes (**b**, fractions 10-17). The decreased presence of FN mRNA in the lower density fractions (fractions 6-10) and the shift of FN mRNA into the higher density fractions (fractions 12-17) of the sucrose gradient is consistent with increased loading of ribosomes onto FN mRNA in the LC3-transfected cells. Thus, the polysome profiles of FN mRNA suggest that the mechanism of increased FN protein expression in LC3-transfected cells is due to enhanced translational efficiency resulting from a more rapid recruitment of ribosomes.

Analysis of LC3 protein in the gradient revealed a dual distribution pattern (**c**). The majority of LC3 protein was found at the top of the gradient (fraction 1), which is consistent with LC3 as a MT-associated protein, since MTs are largely dissociated as soluble tubulin monomers during the process of homogenization of cells. This was consistent with the presence of tubulin (fractions 1-3) confirmed by western immunoblot. LC3 was observed in fractions 2-9 which contained dissociated ribosome subunits. The peak of LC3 (fractions 5 and 6) was located at the position corresponding to 40S ribosome subunit. However, LC3 also appeared at the bottom of the gradient (fractions 14-17) where FN mRNA was present.

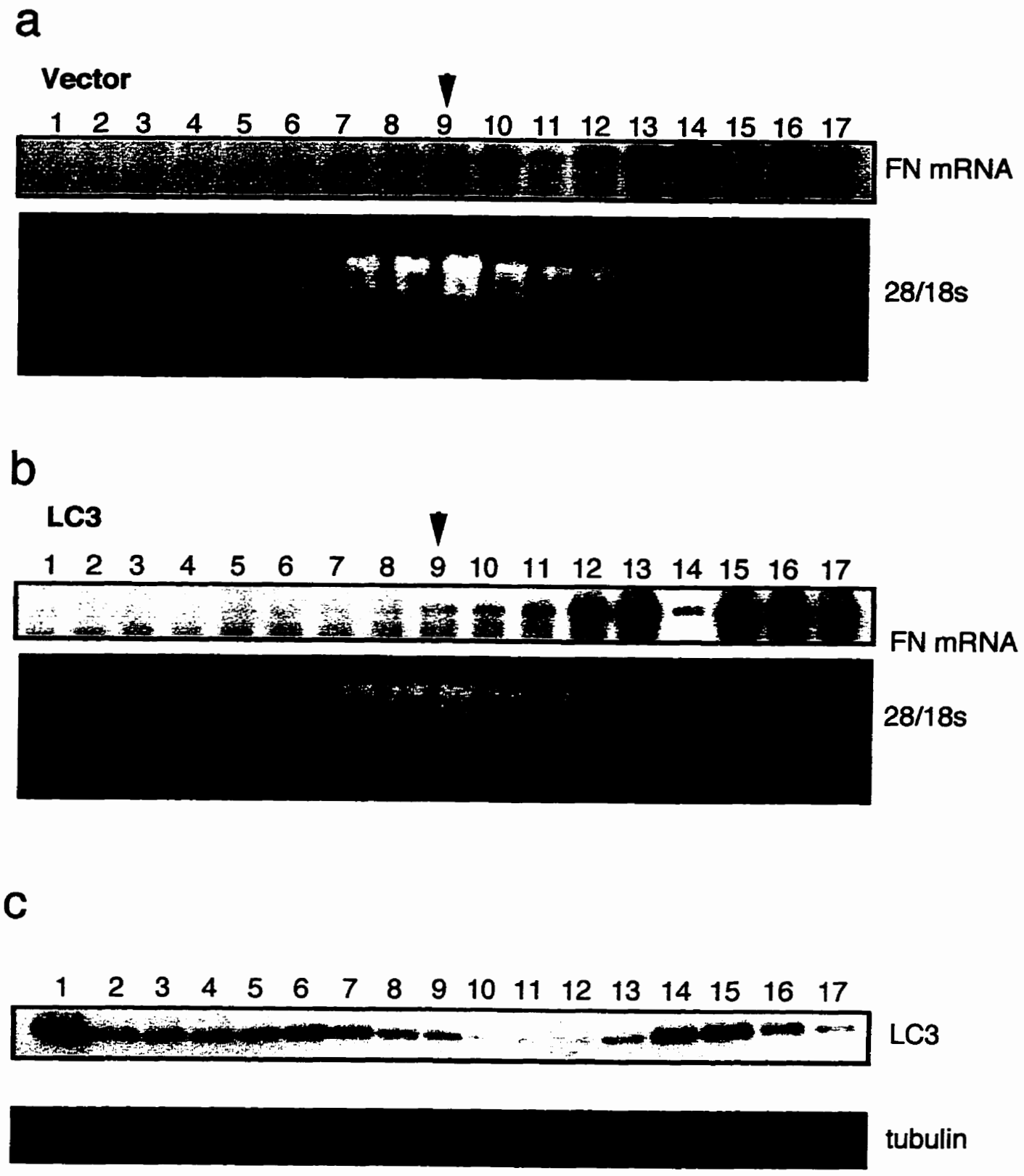
a
Vector
1 2 3 4 5 6 7 8 9 10 11 12 13 14 15 16 17
FN mRNA
28/18s
b
LC3
1 2 3 4 5 6 7 8 9 10 11 12 13 14 15 16 17
FN mRNA
28/18s
c
1 2 3 4 5 6 7 8 9 10 11 12 13 14 15 16 17
LC3
tubulin

Figure 44

Figure 44. Polysomal distribution of FN mRNA and LC3 protein in HT1080 cells

(**a**) Top is an RNase protection assay showing that there was a broad range of distribution of FN mRNA in vector-transfected cells extending from the ribosome subunit region at the top of the sucrose gradient to the polysome region at the bottom of the gradient (fractions 6-17). Most of the FN mRNA is located in the polysome region (arrow indicates 40s ribosome subunits and 80s monosome). Bottom is ethidium bromide staining of the agarose gel showing the quality of mRNA extracted from the sucrose gradient and distribution of ribosomes. (**b**) Compared to vector transfectants, all the FN mRNA in LC3 transfectants was shifted and concentrated at the very bottom of the sucrose gradient (fractions 10-17), suggesting that it is associated with the heavier polysomes, while the distribution pattern of ribosomes and polysomes is similar to that in vector transfectants. The less intense band of fraction 14 was due to underloading of RNA. (**c**) Polysome profile of LC3 protein in LC3 transfectants shows a dual distribution pattern. While most of LC3 is located from the top to middle of the gradient (fractions 1-9) containing ribosome subunits, an appreciable amount of LC3 is also located at the bottom of the gradient (fractions 12-17) containing polysomes and co-distributing with FN mRNA. Western immunoblot for tubulin shows the presence of this protein in fractions 1-3 of the sucrose gradient.

Binding of LC3 to FN mRNA LC3 transfectants

Northwestern blot analyses were subsequently performed to establish whether recombinant LC3 expressed in LC3 transfectants could bind directly to the 3'UTR of FN mRNA and whether the binding is dependent on the consensus ARE (UUAUUUAU). To this end, the 3'UTR of rat FN mRNAs with either wild type (FN3'UTR) or mutated ARE (FN3'UTRΔ) were *in vitro* transcribed in the presence of [^{32}P]-UTP, and northwestern blot analyses were performed. The results demonstrate binding of an ~18 kD protein to the 3'UTR of FN mRNA containing the wild type ARE in LC3-transfected cells but not vector-transfected cells (Figure 45, lane 2 versus lane 1). In addition, the binding of this protein appears to be specific or has a high affinity for the wild type FN 3'UTR compared to FN 3'UTR with mutated ARE (compare lane 2 to 4). The size of this protein is close to the size of recombinant rat LC3 which is predicted to be 16.3 kD but frequently exhibits a relative higher molecular mass about 18 kD on the SDS-PAGE (Mann and Hammarback. 1994). In agreement with this, western immunoblot analysis of the same membranes using LC3 anti-serum revealed a immunoreactive band of the same molecular weight in LC3 transfectants (data not shown). These data indicate that recombinant LC3 expressed in LC3 transfectants maintains its ARE-dependent RNA-binding capacity.

DISCUSSION

We have recently purified a FN mRNA ARE-binding protein and identified it as LC3 of MT-associated protein 1 (as determined by N-terminal sequence analysis and immunological recognition). The work described in this Chapter was undertaken to define the role of LC3 in regulating FN expression. Our initial screen of several cell lines for expression of LC3 showed that HT1080 cells, a human fibrosarcoma cell line (Rasheed, *et al.*, 1974), does not have detectable LC3 by western immunoblot analysis. HT1080 has also been shown to express low levels of FN and to lack cell surface FN matrix deposits (Oliver, *et al.*, 1983; Dean, *et al.*, 1988). Thus, transfection of LC3 in HT1080 cells provided us with the opportunity to investigate the function of this protein in modulating FN expression.

Expression of LC3 in HT1080 cells resulted in a 4-fold increase in newly-synthesized FN protein in culture media after a 20 h period of metabolic labeling and this was associated with dense FN matrix deposits on cell surfaces. Comparative analyses were controlled for equal amounts of metabolically labeled protein. Pulse-chase studies indicated that the increase in FN protein in the conditioned media was not associated with an altered pattern of FN protein secretion or degradation, but rather confirmed an increased rate of FN biosynthesis. Northern blot analysis revealed no increase in steady state levels of FN mRNA in the LC3 transfectants and no alteration in the stability of FN mRNA was observed after inhibition of transcription for 24 h using actinomycin D. These data suggested that the increased FN expression in LC3 transfectants was due to enhanced mRNA translation.

We then attempted to elucidate the mechanism by which LC3 regulates FN mRNA translation using polysome profile analysis. This approach permitted analysis of the association of the FN mRNA with the translational machinery, the ribosomes and polysomes, in the presence or absence of LC3. Most of the FN mRNA was found to be located in the sucrose gradient fractions containing polysomes in either vector or LC3 transfectants, suggesting that the FN mRNA is translationally activated under both conditions. However, while comparable amounts of FN mRNA were present in the sucrose gradients of vector- and LC3-transfected cells, the distribution of FN mRNA in the polysome profile demonstrated a shift to and compression in the bottom of the sucrose gradient in LC3 transfectants, indicating that FN mRNA was associated with heavier polysomes in these cells. These features are consistent with increased efficiency of ribosome recruitment and a rapid progression from the preinitiation complex to polysomes resulting in an enhancement of translation. A similar observation has been made in 3T3-L1 preadipocytes in which expression of Hel-N1, also an ARE-binding protein, increases glucose transporter (GLUT1) expression, and this is associated with accelerated movement of the GLUT1 mRNA toward the high density region of the sucrose gradient (heavy polysomes) (Jain, *et al.*, 1997). Ours is the first report in which we have shown the compatibility between microtubule association and ribosome recruitment in effecting mRNA translation.

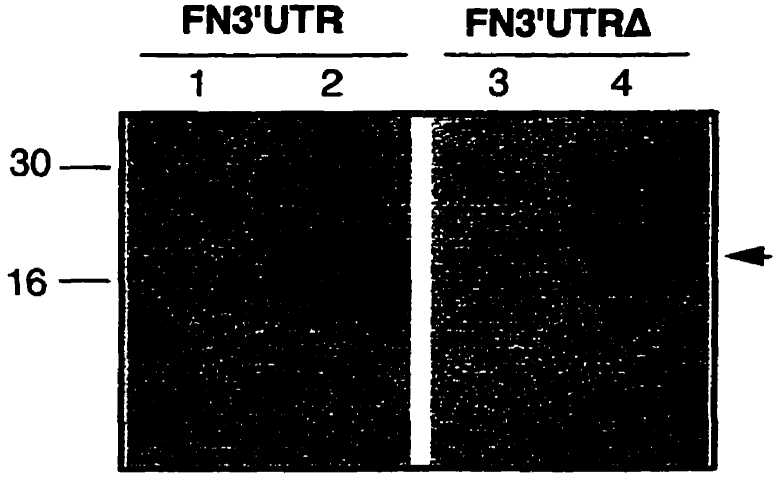

Figure 45

Figure 45. LC3 expressed in LC3 transfectants binds to the 3'UTR of FN mRNA

Northwestern blot analysis was carried out using the radiolabeled 3'UTR of FN mRNA containing wild type (FN3'UTR) (lanes 1 and 2) or mutated ARE (FN3'UTRΔ) (lanes 3 and 4) to determine RNA-binding activity of LC3 expressed in stable transfectants (lanes 2 and 4). For comparison. vector transfectants were used as a control (lanes 1 and 3). A protein at ~18 kD bound to the FN3'UTR with wild type ARE was observed in LC3 transfectants (lane 2). A band at ~20 kD with less intensity was also observed in LC3 transfectants probed with the FN3'UTRΔ containing mutated ARE (lane 4). Controls vector transfectants showed no RNA binding activities (lanes 1 and 2).

We also sought to determine the association of LC3 protein with FN mRNA in the context of translational machinery by comparing the distribution pattern of LC3 protein with FN mRNA in the polysome profile of the LC3 transfectants. The dual distribution of LC3 protein in the sucrose gradient indicated that while the majority of LC3 protein was located at the top of sucrose gradient (less dense) (Figure 44c, fractions 1-9) containing the translationally-inactive ribosome subunits. a considerable amount of LC3 protein was also found with FN mRNA at the bottom of the sucrose gradient (more dense) containing heavy polysomes (fractions 12-17) which were translationally activated. While the very soluble form of LC3 protein at the top of the gradient (fraction 1) appears to result from the dissociation of MTs following detergent lysis and homogenization of the cells. the co-migration of LC3 with 40S ribosome subunits in the sucrose gradients (fractions 5 and 6) suggests an association of LC3 with 40S ribosome subunits which requires further clarification. i.e., does this represent a separate pool or a modified, e.g., phosphorylated, LC3 protein. Furthermore, the second peak of LC3 at the bottom of gradient is not simply the co-sedimentation of LC3 with remnants of MT structures, since no tubulin protein was detected by western blot in those fractions. Rather, we suggest that the LC3 protein at the bottom of the gradient in LC3 transfectants is related to its association with ribosomes through binding of FN mRNA. as well as other mRNAs as yet unknown. This is supported by northwestern analysis in which LC3 expressed in LC3-transfected cells appears to bind the 3'UTR of FN mRNA in an ARE-dependent manner. These data suggest that the increased translational initiation and ribosome recruitment of FN mRNA in LC3 transfectants may be the result of a direct sequence-specific interaction of LC3 with the ARE in the 3'UTR of FN mRNA. This interpretation is compatible with a previous working model in which the 3'UTR interacts with 5'-end to facilitate recruitment of 40S ribosomes (Sachs, *et al.*, 1997) or acts in *cis* to increase the local concentration or transient reservoir of ribosomes for re-recruitment (Tanguay and Gallie, 1996).

While the emphasis of our studies has been on the functional analysis of the effect of LC3 on FN mRNA translation, the coincident changes of cell morphology and growth rate following expression of LC3 in HT1080 cells are also of considerable significance. The reduced expression

of FN is a common feature of neoplastic transformation in a variety of cells (Yamada, *et al.*, 1977; Vaheri and Mosher, 1978; Steele, *et al.*, 1988; Varani, *et al.*, 1991) including HT1080 cells (Oliver, *et al.*, 1983), and correlates with the metastatic property of malignant cells (Roos, 1984). Induction of FN expression and its matrix assembly by growth factors or hormones in HT1080 cells, alters their morphology (more flattened) and inhibits cell growth *in vitro* (Kahari, *et al.*, 1992; McCarthy and Kollmus, 1995). Moreover, overexpression of recombinant FN in HT1080 cells reduces their migration *in vitro* and tumorigenicity *in vivo* (Akamatsu, *et al.*, 1996). Increased FN expression in LC3-transfected HT1080 cells was similarly associated with changes in phenotype reflected by a flattened morphology and slower growth rate. Thus, the lack of LC3 expression in HT1080 cells compared to their normal counterpart, human fibroblasts, may be directly involved in the acquisition of tumorigenicity.

While we have focused on the relationship between LC3 and FN expression and conducted studies in HT1080 cells, it is important to note that LC3 was co-purified with MT-associated protein 1, cloned from a rat brain cDNA library and present in large amounts in brain tissues and neuron cells (Mann and Hammarback, 1994). The better organized MT structures in HT1080 LC3 transfectants is consistent with this previous study. The presence of high levels of LC3 and highly organized MT structures in neuron cells, as well as a dual function of LC3 related to both mRNA and tubulin binding, suggests that LC3 may function in RNA trafficking.

GENERAL DISCUSSION

Increased expression of TGF-β1 and FN is associated with the intimal cushion formations in the DA and neointimal formation as the result of various pathologic etiologies. Although the functional involvement of TGF-β and FN in SMC migration in vascular neointimal formation has been examined, little is known about their regulation. Using cultured EC and SMC isolated from DA, we have demonstrated coordinate, tissue-specific, and developmentally-regulated expression patterns of EC TGF-β1 and SMC FN that directly influence the migratory phenotype of DA SMC. These observations provide a rationale for analyzing the specific regulatory mechanisms accounting for the increased expression of TGF-β1 and FN during intimal cushion formation.

DA EC at 100 days of gestation produce more TGF-β1 than 100-day Ao or 138-day DA EC. This increased DA EC TGF-β1 expression in early gestation is likely controlled by mechanisms that increase transcription and translation of a relatively unstable mRNA. This hypothesis is in keeping with a previously described process whereby the decay of unstable cytokine and oncogene mRNAs by the 3'UTR ARE is mediated by ongoing translation (Savant-Bhonsale and Cleveland, 1992; Aharon and Schneider, 1993; Winstall, *et al.*, 1995), and is supported by the fact that an ARE-like element is present in the 3'UTR of TGF-β1 mRNA.

While the function of the ARE in 3'UTR of TGF–β1 mRNA has not been determined, the role of the FN 3'UTR ARE in FN expression has been characterized through the experimental data presented in this thesis. Consistent with previous observations (Shaw and Kamen, 1986; Jones and Cole, 1987; Kruys, *et al.*, 1987; Kruys, *et al.*, 1988; Kruys, *et al.*, 1989; Han, *et al.*, 1990a; Han, *et al.*, 1990b; Grafi, *et al.*, 1993; Kruys, *et al.*, 1993; Marinx, *et al.*, 1994; Winstall, *et al.*, 1995), the FN ARE in vascular SMC affects both mRNA stability and translational efficiency. Several lines of evidence suggest that the functional status of this ARE is modulated by changes in ARE-binding factors. First, elevated expression of the ARE-binding factor, LC3, and increased ARE-binding activities correlate with enhanced FN mRNA translation in DA SMC. Second, decoy of ARE-binding factors by exogenous AREs inhibits endogenous FN production in DA SMC.

Third, overexpression of LC3 in Ao SMC improves FN mRNA translation to the levels observed in DA SMC in a dose-dependent manner. Last, expression of LC3 in HT1080 cells, which lack LC3, greatly enhances FN mRNA translational efficiency. Therefore, the elevated levels of LC3 observed in DA compared to Ao SMC could be the underlying mechanism responsible for increase in FN mRNA translational efficiency in DA SMC.

Other genes whose expression could be regulated by LC3 include proto-oncogenes, such as c-*fos* and c-*myc*, cytokines, such as TNF-α and IL-1, and growth factors, such as TGF-β1 and VEGF. All of them are highly expressed shortly after vascular injury, actively participate in vascular neointima formation, and with the exception of TGF-β1 which has not yet been studied, their expression has been shown to be subject to control by the ARE and cytoplasmic factors. Thus, it would be of great interest to know whether upregulation of some of these immediate early response genes is also mediated by LC3 during the development of vascular neointima.

LC3 was initially purified from brain extracts, cloned from a brain cDNA library, and was characterized as a light chain of MT-associated protein 1 (MAP1) (Mann and Hammarback, 1994). It is highly expressed in the brain where many mRNA species are transported via MTs to their destination to be translated. RNAs or polyribosomes have also been shown to associate with MTs in various cell types (St Johnston *et al.*, 1989; Singer, 1992; Steward and Banker, 1992; Suprenant, 1993; Wilhelm and Vale, 1993; St Johnston, 1995). Signals that direct intracellular transport and localization of mRNAs are found exclusively within the 3'UTR of mRNAs (Macdonald and Struhl, 1988; Gottlieb, 1992; Gravis and Lehman, 1992; Mowry and Melton, 1992). Several RNA-binding factors that bind to localized mRNA have also been shown to bind to MTs (Elisha, *et al.*, 1995; Han, *et al.*, 1995; Schumacher, *et al.*, 1995). This highlights the possibility that as a bifunctional protein, LC3 might also involve mRNA localization. While there has been a wealth of evidence suggesting that MTs are involved in the translational regulation of localized mRNA, their effect on the translationally activated mRNAs of secreted proteins such as FN is unexplored. However, we have shown that MTs may involve ER membrane sorting of FN mRNA-ribosome complexes, although the mechanism remains to be delineated.

LC3 differs from all other ARE-binding factors cloned and characterized (Malter, 1989; Bohjanen, *et al.*, 1991; Brewer, 1991; Malter and Hong, 1991; Rondon, *et al.*, 1991; Vakalopoulou, *et al.*, 1991; Bickel, *et al.*, 1992; Bohjanen, *et al.*, 1992; Port, *et al.*, 1992; Stephens, *et al.*, 1992; Hamilton, *et al.*, 1993; Levine, *et al.*, 1993; Zhang, *et al.*, 1993; Katz, *et al.*, 1994; Nakagawa, *et al.*, 1995; Chung, *et al.*, 1996; Ma, *et al.*, 1996). Its highly positive charge, arginine-rich contents, and putative phosphorylation sites might contribute to its mRNA binding (Burd and Greyfuss, 1994). Our chemical analysis and purification studies suggested that LC3 might form aggregates or associate with other proteins through disulfide bonds. It also exists within different cellular compartments as two different forms, possibly due to its phosphorylation status (Mason et al, 1997). This may explain its bi-phasic distribution patterns on polysome profile, that is, its co-distribution with 40s ribosome subunits as well as FN mRNA on polysomes. While its physical association with 40S ribosome subunits needs to be clarified, this phenomenon is of great importance, since it fulfills the 5' and 3' crosstalking model regarding regulation of translational initiation for certain genes by the specific interaction of RNA-binding protein and 3'UTR (Jacobson, 1995; Jacobson and Peltz, 1996; Pain, 1996; Sachs, *et al.*, 1997). In other words, LC3 protein could be the 'bridge' across the 5' and 3'UTR of FN mRNA that facilitates recruitment of 40S ribosomes. This interpretation is also compatible with another working model in which the 3'UTR acts in *cis* to increase the local concentration or transient reservoir of ribosomes for re-recruitment (Tanguay and Gallie, 1996) and the operation of this model may also be modulated by a sequence-specific RNA-protein interaction. Moreover, binding of LC3 to AREs may improve translational efficiency by preventing a physical interaction of AREs with poly(A) tail, which has been shown to reduce translational efficiency (Grafi, *et al.*, 1993).

Our observations suggest a novel paradigm. Previous studies have suggested that microtubule associated proteins regulate transport and repress mRNA translation and that ARE-binding proteins also repress translation, although at least one study suggests a function in enhancement of translation by increased ribosome recruitment and translational initiation. Our studies propose that a microtubule-associated protein that is also an ARE-binding protein may

function both in sorting mRNA and in initiation of tranlsation. This is illustrated in the following hypothetical model of translational control of FN expression by LC3 (Figure 46). Three potential sites where LC3 may play a role in FN mRNA translation are indicated by **A**, **B**, and **C**. In **A**, LC3 binds FN mRNA and attaches to MTs. This might facilitate sorting of FN mRNA to RER directed by nascent signal peptide. In **B**, binding of LC3 to ARE prevent association of ARE with poly(A) (Gafli, *et al,* 1993), resulting in release of poly(A) tail which may promote FN mRNA translation via interaction of poly(A) binding protein (Pab1) and two subunits of mRNA-associated initiation factor eIF4F, eIF4E and eIF4G. The cap binding protein eIF4E then dock the 40S ribosome subunit onto 5' cap structure. This is, in fact, a 5' to 3' close model modified from in Figure 8 in page 50 (Sachs, *et al,* 1997). In **C**, using **B** as a prototype model, binding of LC3 to ARE may directly involve 40S ribosome subunit recruitment through its interaction with unknown 40S-associated factor.

Lack of LC3 expression in HT1080 cells is an unexpected finding. HT1080 cells have low levels of FN production compared to normal human fibroblasts. Expression of LC3 in HT1080 produces 4- to 5-fold more FN protein solely due to enhanced FN mRNA translation and increased cell surface FN deposits. This is associated with re-organization of MT structures, a flattened spread cell shape and slower cell growth. The mechanisms by which LC3 mediates FN mRNA translation have been defined and related to increased ribosome recruitment. Our experimental observations are consistent with a recent finding by Jain and colleagues (Jain, *et al.*, 1997) in which expression of Hel-N1, also an ARE-binding protein, in 3T3-L1 preadipocytes increases glucose transporter (GLUT1) expression, and this is associated with accelerated movement of the GLUT1 mRNA toward the high density region of the sucrose gradient (heavy polysomes). Together, these data strongly suggest that a direct sequence-specific interaction of the 3'UTR AREs with its binding proteins not only modulates mRNA stability but also promotes mRNA translation by increasing translational initiation and ribosome recruitment. The studies also suggest that the function of AREs is not exclusively related to labile mRNA of cytokines, growth factors, and proto-oncogenes, they may also regulate translation of stable mRNAs encoding ECM proteins.

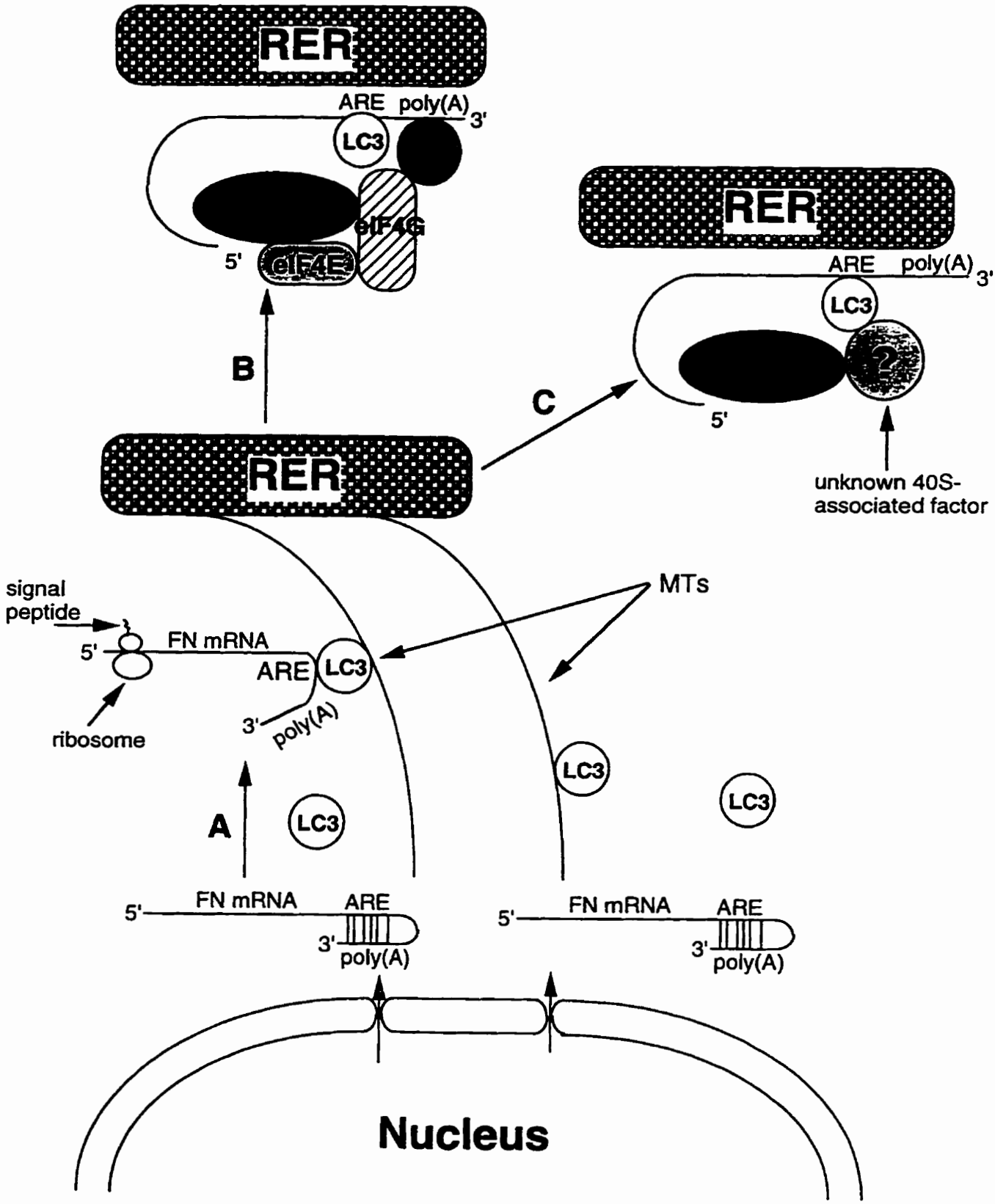
RER
ARE poly(A) 3'
LC3
eIF4G
eIF4E
5'
B
C
RER
ARE poly(A) 3'
LC3
?
5'
unknown 40S-associated factor
RER
signal peptide
5'
FN mRNA
ARE
LC3
3'
poly(A)
ribosome
MTs
A
LC3
LC3
LC3
5'
FN mRNA
ARE
3'
poly(A)
5'
FN mRNA
ARE
3'
poly(A)
Nucleus

Figure 46

Figure 46. Proposed hypothetical model of interaction of LC3 and ARE in translational control of FN mRNA as described in text

FUTURE STUDIES

The findings suggesting that increased TGF-β1 expression in 100-day DA EC is due to increased transcription and translation of a relatively unstable mRNA begs exploration of the possible mechanisms involved. The enhanced transcription of the TGF-β1 gene in DA versus Ao EC can be addressed by further analyzing its promoter activity in those cells. Nested deletion constructs or deletion of the known transcription factor binding domains (Kim, *et al.*, 1989a: Kim, *et al.*, 1989b; Kim, *et al.*, 1989c; Kim, *et al.*, 1990; Scotto, *et al.*, 1990; Kim, *et al.*, 1991) would determine their effect on TGF-β1 gene transcription. DNase I footprinting could be used to define transcriptional regulatory elements. Gel shift assays with nuclear extracts would help to evaluate whether binding complexes were formed with certain *cis* elements in DA versus Ao cells and if the nature of these elements suggest that known transcription factors are involved. Antibody supershift assays could be used to confirm their activity. The potential effect of the ARE-like element in the 3'UTR TGF-β1 mRNA on mRNA stability and translation could also be explored by applying the same strategy used in the study of the FN ARE in this thesis. On the other hand it is entirely possible and consistent with other models that post-transcriptional regulatory elements are present within the 5'UTR or even within the coding region of the TGF-β1 mRNA.

Identifying LC3 as an RNA-binding protein and showing its interaction with the FN ARE has provided new and important information about the translational regulation of FN expression but has also raised additional questions. Above all, what is the relationship of the LC3 protein to the other two RNA-binding activities observed in SMC with molecular weights of approximately 30 kD and 60 kD, or to the 40 to 50 kD protein immunoreactive with LC3 antiserum in human fibroblast cells and HT1080 cells? It is interesting that Mann and Hammarback (Mann and Hammarback, 1994) who initially cloned the LC3 cDNA also found a 50 to 60 kD protein immunoreactive with LC3 antiserum in rat brain tissue, and only a 1.7 kb mRNA species hybridized with a 'full-length' LC3 cDNA of 0.9 kb that has a very short 5'UTR and lacks a consensus sequence consistent with eukaryotic start codons (Kozak, 1986a; Kozak, 1986b). In

addition, in both our study and the one conducted by Mann and Hammarback (Mann and Hammarback, 1994) the amino terminus of LC3 protein is not blocked during N-terminal sequence analysis by Edman degradation. Together, these observations strongly suggest that the cDNA clone of LC3 is not full length, and that LC3 may be derived from a larger polypeptide precursor. To understand its nature, a complete cDNA clone encoding the LC3 peptide is required. This could be done by screening a well established brain cDNA library with the radiolabeled LC3 cDNA.

A combination of biochemical and immunological approaches may also be used to detect other proteins with which LC3 protein associates in cytoplasm, especially as a form of mRNP complex associated with 40S ribosome subunit. For example, cytoplasmic proteins that bind LC3 could be selected using a recombinant GST-LC3 protein column, and then screened by antibodies against translational initiation factors or 40S ribosome subunit-associated factors. In parallel. GST-LC3 protein column could also be used to isolate LC3-targeted mRNAs, and establish a cDNA library selected by LC3 protein. The possible binding of LC3 to RNAs which are known to contain AREs in 3'UTR such as proto-oncogenes, c-*fos* and c-*myc*; cytokines, TNF-α and IL-1; and growth factors, TGF-β1 and VEGF could also be tested by *in vitro* gel shift assays.

Intracellular localization of LC3 protein could be achieved using immunoelectron microscopy with a view to determining whether it co-localizes with membrane-associated ribosomes. Following the distribution of epitope-tagged LC3 protein in living cells with or without intact MT structures may provide insight into how MTs affect FN mRNA translational efficiency and polysomal distribution of both LC3 protein and FN mRNA.

The factors which regulation the dual function of LC3 protein, and its intracellular localization may depend on the LC3 peptide sequence and structural conformation. LC3 is a very basic, positively charged protein, containing several putative phosphorylation sites. It contains no known RNA recognition motif but an arginine-rich sequence similar to that observed in some of RNA-binding proteins (Burd and Greyfuss, 1994). Its MT-binding site has not been identified. Peptide sequence alignment has found no known protein peptide homologous to LC3. These

observations make attempting to crystallize LC3 protein a very attractive task. Successful crystallization of LC3 protein should provide structural information pertinent to its RNA and MT binding functions, which would guide the design of further site-directed mutagenesis studies aimed at specifically defining RNA and MT binding sites. The function of putative phosphorylation sites in LC3 peptide in RNA and MT binding could also be probed by a spectrum of kinase inhibitors or antibodies. It would also be valuable to examine whether LC3 expression and function, could be also regulated by cytokines and growth factors, or alterations in cell-matrix interaction, as has been shown for other ARE-binding proteins [(Sirenko, *et al.*, 1997), and Dr. Wei-Jun Ma, personal communication]. More recent work in our laboratory has shown that LC3 expression in coronary SMC is regulated by TNF-α (Mason, et al 1997).

Another interesting aspect of these studies is the apparent absence of the 16 kD LC3 protein in the malignant HT1080 cells, and the ability to 'reverse' transformed HT1080 cells in tissue cultures by LC3 transfection. The lack of LC3 protein in HT1080 cells may be due to an aberrant post-translational modification resulting in its degradation, if LC3 protein belongs to a polypeptide derived from a larger protein precursor as discussed above. Alternatively a DNA rearrangement in HT 1080 cells may have resulted in loss of LC3. The latter could determined by Southern blot analysis. In addition, inoculation of LC3-transfected HT1080 cells into immunodeficient rats should reveal whether the 'reverse' transformed HT1080 cells really lose or show diminished tumorigenicity *in vivo*.

Animal studies could also be applied to examine whether the same mechanism is responsible for enhanced FN expression in tissue cultures could account for increased FN expression *in vivo*. For example, virus vectors can be used for *in vivo* delivery of decoy AREs into fetal DA before the intimal cushion formation. The idea is that expression of exogenous AREs would sequestrate ARE-binding factors, thereby reducing FN mRNA translation. By comparing FN expression and morphologic changes related to intimal cushion formation in DA transfected with ARE-containing versus ARE-mutated virus-liposome vector complex, one not only could determine whether the ARE functions in modulating FN expression *in vivo*, but also

ascertain whether the FN-enriched matrix is a prerequisite for SMC migration and intimal cushion formation. Indeed, we have recently shown that in fetal lambs delivery of ARE-containing vector into DA prevents intimal cushion formation (Mason et al, 1997).

Our studies therefore reveal important posttranscriptional mechanisms regulating the program which orchestrates intimal cushion formation in the DA. Moreover, a novel relationship is revealed between an RNA/MT binding protein and enhanced efficiency of translation of a secreted matrix protein. Loss of this mechanism in HT1080 human fibrosarcoma cells compared to normal human fibroblasts may be related to their malignant phenotype.

REFERENCES

Aharon T., Schneider R.J. Selective destabilization of short-lived mRNAs with the granulocyte-macrophage colony-stimulating factor AU-rich 3' noncoding region is mediated by a cotranslational mechanism. *Mol. Cell. Biol.* (1993) 13: 1971-1980.

Ahern S.M., Miyata T., Sadler J.E. Regulation of human tissue factor expression by mRNA turnover. *J. Bio. Chem.* (1993) 268: 2154-2159.

Ahuja S.S., Shrivastav S., Danielpour D., Balow J.E., Boumpas D.T. Regulation of Transforming growth factor-β1 and its receptor by cyclosporine in human T lymphocytes. *Transplantation* (1995) 60: 718-723.

Akamatsu H., Ichihara-Tanaka K., Ozono K., Kamiike W., Matsuda H., Sekiguchi K. Suppression of transformed phenotypes of human fibrosarcoma cells by overexpression of recombinant fibronectin. *Cancer Res.* (1996) 56: 4541-4546.

Akashi M., Saito M., Koeffler H.P. Lymphotoxicin: Stimulation and regulation of colony-stimulating factors in fibroblasts. *Blood* (1989) 74: 2383-2390.

Albelda S.M., Buck C.A. Integrins and other cell adhesion molecules. *FASEB J.* (1990) 4: 2868-2880.

Ali I.U., Mautner V., Lanza R., Hynes R.O. Restoration of normal morphology, adhesion and cytoskeleton in transformed cells by addition of a transformation-sensitive surface protein. *Cell* (1977) 11: 115-126.

Amento E.P., Ehsani N., Palmer H., Libby P. Cytokines and growth factors positively and negatively regulate interstitial collagen expression in human vascular smooth muscle cells. *Arterioscler. & Thromb.* (1991) 11: 1223-1330.

Antonelli-Olridge A., Saunders K.B., Smith S.R., D'Amore P.A. An activated form of transforming growth factor beta is produced by cocultures of endothelial cells and pericytes. *Proc. Natl. Acad. Sci. USA* (1989) 86: 4544-4548.

Armstrong P.B., Armstrong M.T. An instructive role for the interstitial matrix in tissue patterning: tissue segregation and intercellular invasion. *J. Cell. Biol.* (1990) 110: 1439-1455.

Assoian R.K., Fleurdelys B.E., Stevenson H.C., Miller P.J., Madtes D.K., Raines E.W., Ross R., Sporn M.B. Expression and secretion of type beta transforming growth factor by activated human macrophages. *Proc. Natl. Acad. Sci. USA* (1987) 84: 6020-6024.

Assoian R.K., Komoriya A., Meyers C.A., Miller D.M., Sporn M.B. Transforming growth factor-beta in human platelets. Identification of a major storage site, purification, and characterization.*J. Biol. Chem.* (1983) 258: 7155-7160.

Bahadori L., Milder J., Gold L., Botney M. Active macrophage-associated TGF-beta co-localizes with type I procollagen gene expression in atherosclerotic human pulmonary arteries. *Am. J. Pathol.* (1995) 146: 1140-1149.

Bassell G.J., Powers C.M., Taneja K.L., Singer R.H. Single mRNAs visualized by ultrastructural in situ hybridization are principally localized at actin filament intersections in

fibroblasts. *J. Cell Biol.* (1994) 126: 863-876.

Bauer J.S., Schreiner C.L., Giancotti F.G., Ruoslahti E., Juliano R.L. Motility of fibronectin receptor-deficient cells on fibronectin and vitronectin: collaborative interactions among integrins. *J. Cell Biol.* (1992) 116: 477-487.

Bauriedel G., Windstetter U., DeMaio S.J.Jr., Kandolf R., Hofling B. Migratory activity of human smooth muscle cells cultivated from coronary and peripheral primary and restenotic lesions removed by percutaneous atherectomy. *Circulation* (1992) 85: 554-564.

Bauters C., Marotte F., Hamon M., Oliviero P., Farhadian F., Robert V., Samuel J.L., Rappaport L. Accumulation of fetal fibronectin mRNAs after balloon denudation of rabbit arteries. *Circulation* (1995) 92: 904-911.

Bickel M., Iwai Y., Pluznik D.H., Cohen R.B. Binding of sequence-specific proteins to the adenosine-plus uridine-rich sequences of the murine granulocyte/macrophage colony-stimulating factor mRNA. *Proc. Natl. Acad. Sci. USA* (1992) 89: 10001-10005.

Birchenall-Roberts M.C., Ruscetti F.W., Kasper J., Lee H.D., Friedman R., Geiser A., Sporn M.B., Roberts A.B., Kim S.J. Transcriptional regulation of the transforming growth factor beta 1 promoter by v-src gene products is mediated through the AP-1 complex. *Mol. Cell. Biol.* (1990) 10: 4978-4983.

Biro S., Fu Y.M., Yu Z.X. , Epstein S.E. Inhibitory effects of antisense oligodeoxynucleotides targeting c-myc mRNA on smooth muscle cell proliferation and migration. *Proc. Natl. Acad. Sci. USA* (1993) 90: 654-658.

Blatti S.P., Foster D.N., Ranganathan G., Moses H.L., Getz M.J. Induction of fibronectin gene transcription and mRNA is a primary response to growth-factor stimulation of AKR-2B cells. *Proc. Natl. Acad. Sci. USA* (1988) 85: 1119-1123.

Bohjanen P.R., Petryniak B., June C.H., Thompson C.B., Lindsten T. An inducible cytoplasmic factor (AU-B) binds selectively to AUUUA multimers in the 3' untranslated region of lymphokine mRNA. *Mol. Cell. Biol.* (1991) 11: 3288-3295.

Bohjanen P.R., Petryniak B., June C.H., Thompson C.B., Lindsten T. AU RNA-binding factors differ in their binding specificities and affinities. *J. Biol. Chem.* (1992) 267: 6302-6309.

Border W.A., Nobel N.A. Transforming growth factor beta in tissue fibrosis. *N. Engl. J. Med.* (1994) 331: 1286-1292.

Botney M.D., Kaiser L.R., Cooper J.D., Mecham R.P., Parghi D., Roby J., Parks W.C. Extracellular matrix protein gene expression in atherosclerotic hypertensive pulmonary arteries. *Am. J. Pathol.* (1992) 140: 357-364.

Boudreau N. Developmentally regulated changes in the extracellular matrix accompany intimal proliferation in the ductus arteriosus. *Thesis* (1990) pp 30-38.

Boudreau N., Clausell N., Boyle J., Rabinovitch M. Transforming growth factor-beta regulates increased ductus arteriosus endothelial glycosaminoglycan synthesis and a post-transcriptional mechanism controls increased smooth muscle fibronectin, features associated with intimal proliferation. *Lab. Invest.* (1992) 67: 350-359.

Boudreau N., Rabinovitch M. Developmentally regulated changes in extracellular matrix in

endothelial and smooth muscle cells in the ductus arteriosus may be related to intimal proliferation. *Lab. Invest.* (1991) 64: 187-199.

Boudreau N., Turley E.A., Rabinovitch M. Fibronectin, hyaluronan and a hyaluronan binding protein contribute to increased ductus arteriosus smooth muscle migration. *Dev. Biol.* (1991) 143: 235-247.

Brewer G. An A + U-rich element RNA-binding factor regulate c-myc mRNA stability in vitro. *Mol. Cell. Biol.* (1991) 11: 2460-2466.

Brewer G., Ross J. Poly(A) shortening and degradation of the 3' AU-rich sequences of human c-myc mRNA in a cell-free system. *Mol. Cell. Biol.* (1988) 8: 1697-1708.

Brewer G., Ross J. Regulation of c-myc mRNA degradation in vitro by a labile destabilizer with an essential nucleic acid component. *Mol. Cell. Biol.* (1989) 9: 1996-2006.

Brown K.E., Kindy M.S., Sonenshein G.E. Expression of the c-myb proto-oncogene in bovine vascular smooth muscle cells. *J. Biol. Chem.* (1992) 267: 4625-4630.

Buck C.A., Glick M.C., Warren L. Glycopeptides from the surface of control and virus-transformed cells. *Science* (1971) 172:169-171.

Buck C.A., Horwitz A.F. Cell surface receptors for extracellular matrix molecules. *Annu. Rev. Cell Biol.* (1987) 3:179-205.

Burd C.G., Greyfuss G. Conserved structures and diversity of function of RNA-binding proteins. *Science* (1994) 265: 615-621.

Busse R., Mulsch A., Fleming I., Hecker M. Mechanisms of nitric oxide release from the vascular endothelium. *Circulation* (1993) 87(Suppl 5): 18-25.

Buzby J.S., Lee S.M., DeMaria G., Brewer G., Cairo M.S. Increased GM-CSF mRNA instability in cord vs adult mononuclear cells is translation dependent and associated with increased levels of A + U-rich element binding factor (AUF1). *Blood* (1996) 88: 2889-2897.

Campbell G.R., Campbell J.H., Manderson J.A., Horrigan S., Rennick R.E. Arterial smooth muscle. A multifunctional mesenchymal cell. *Arch. Patho. Lab. Med.* (1988) 112: 977-986.

Campbell J.H., Campbell G.R. Endothelial cell influences on vascular smooth muscle phenotype. *Ann. Rev. Physiol.* (1986) 48: 295-306.

Caput D., Beutler B., Hartog K., Thayer R, Brown-Shimer S., Cerami A. Identification of a common nucleotide sequence in the 3'-untranslated region of mRNA molecules specifying inflammatory mediator. *Proc. Natl. Acad. Sci. USA* (1986) 83: 1670-1675.

Carrel A., Guthrie C.C. Anastomosis of blood vessels by the patching method and transplantation of the kidney. *JAMA* (1906) 47: 1648-1650.

Cassels D.E. The ductus arteriosus. Published by **Ch. C.** Thomas, Illinois, USA (1973) pp 185-216.

Chambley-Campbell J.H., Cambell G.R., Ross R. Phenotype-dependent response of cultured aortic smooth muscle to serum mitogens. *J. Cell. Biol.* (1981) 89: 379-383.

Chandler L.A., Bourgeois S. Posttranscriptional down-regulation of fibronectin in N-ras-transformed cells. *Cell Growth & Differentiation* (1991) 2: 379-384.

Chandler L.A., Ehretsmann C.P., Bourgeois S. A novel mechanism of Ha-*ras* oncogene action: Regulation of fibronectin mRNA levels by a nuclear posttranscriptional event. *Mol. Cell. Biol.* (1994) 14: 3085-3093.

Chen C.-Y.A., Shyu A.-B. AU-rich elements: characterization and importance in mRNA degradation. *TIBS* (1995) 20: 465-470.

Chen C.-Y.A., Xu N., Shyu A.-B. mRNA-decay mediated by two distinct AU-rich elements from c-fos and granulocyte-macrophage colony stimulating factor transcripts: different deadenylation kinetics and uncoupling from translation. *Mol. Cell. Biol.* (1995) 15: 5777-5788.

Chen L.B., Gallimore P.H., McDougall J.K. Correlation between tumor induction and the large external transformation sensitive protein on the cell surface. *Proc. Natl. Acad. Sci. USA* (1976) 73: 3570-3574.

Chen L.B., Gudor R.C., Sun T.T., Chen A.B., Mosesson M.W. Control of a cell surface major glycoprotein by epidermal growth factor. *Science* (1977) 197: 776-778.

Chen L.B., Summerhayes L., Hsieh P., Gallimore P.H. Possible role of fibronectin in malignancy. *J. Supramol. Struct.* (1979) 12: 139-150.

Chen Q., Adams C.C., Usack L., Yang J., Monde R.-A., Stern D.B. An AU-rich element in the 3' untranslated region of the spinach chloroplast *petD* gene participates in sequence-specific RNA-protein complex formation. *Mol. Cell. Biol.* (1995) 15: 2010-2018.

Chen W.T., Chen J.M., Mueller S.C. Coupled expression and colocalization of 140K cell adhesion molecules, fibronectin, and laminin during morphogenesis and cytodifferentiation of chick lung cells. *J. Cell Biol.* (1986) 103: 1073-1090.

Chen X., Sadlock J., Schon E A. RNA-binding patterns in total human tissue proteins: analysis by northwestern blotting. *Biochem. & Biophy. Res. Comm.* (1993) 191: 18-25.

Chervu A., Moore W.S. An overview of intimal hyperplasia. *Surg Gynecol Obstet* (1990) 171: 433-437.

Chomczynski P., Sacchi N. Single-step method of RNA isolation by acid guanidinium thiocyanate-phenol-chloroform extraction. *Anal. Biochem.* (1987) 162: 156-159.

Chou L., Firth J.D., Uitto V.-J., Brunette D.M. Substratum surface topography alters cell shape and regulates fibronectin mRNA level, mRNA stability, secretion and assembly in human fibroblasts. *J. Cell Sci.* (1995) 108: 1563-1573.

Choy M., Armstrong M.T., Armstrong P.B. Regulation of proliferation of embryonic heart mesenchyme: role of the transforming factor-beta 1 and the interstitial matrix. *Dev. Biol.* (1990) 141: 421-425.

Choy M., Armstrong M.T., Armstrong P.B. Transforming growth-beta 1 localized within the heart of the chick embryo. *Anat. & Embryol.* (1991) 183: 345-352.

Chung S., Jiang L., Cheng S., Furneaux H. Purification and properties of HUD, a neuronal RNA-binding protein. *J. Biol. Chem.* (1996) 271: 11518-11524.

Clark R.A., Folkvord J., Nielsen, L.D. Either exogenous or endogenous fibronectin can promote adherence of human endothelial cells. *J. Cell Sci.* (1986) 82: 263-280.

Clausell N., deLima V.C., Molossi S., Liu P., Turly E., Gotlieb A.I., Adelman A.G., Rabinovitch M. Expression of tumor necrosis factor alpha and accumulation of fibronectin in coronary artery restenotic lesions retrieved by atherectomy. *British Heart J.* (1995) 73: 534-539.

Clausell N., Molossi S., Rabinovitch M. Increased interleukin-1 beta and fibronectin expression are early features of the development of the postcardiac transplant arteriopathy in piglets. *Am. J. Pathol.* (1993) 142: 1772-1782.

Clausell N., Rabinovitch M. Upregulation of fibronectin synthesis by interleukin-1 beta in coronary artery smooth muscle cells is associated with the development of the post-cardiac transplant arteriopathy in piglets. *J. Clin. Invest.* (1993) 92: 1850-1858.

Clowes A.W. Intimal hyperplasia and graft failure. *Cardiovasc. Pathol.* (1993) 2(Suppl): S179-186.

Clowes A.W., Clowes M.M., Fingerle J., Reidy M.A. Mechanisms of stenosis after arterial injury. *Lab. Invest.* (1983a) 49: 208-215.

Clowes A.W., Reidy M.A., Clowes M.M. Kinetics of cellular proliferation after arterial injury: I. Smooth muscle growth in the absence of endothelium. *Lab. Invest.* (1983b) 49: 327-333.

Clyman R.I. Ductus arteriosus: current theories of prenatal and postnatal regulation. *Semin. Perinatol.* (1987) 11: 64-71.

Clyman R.I., Goetzman B.W., Chen Y.Q., Mauray F., Kramer R.H., Pytela R., Schnapp L.M. Changes in endothelial cell and smooth muscle cell integrin expression during closure of the ductus arteriosus: an immunohistochemical comparison of the fetal, preterm newborn, and full-term newborn rhesus monkey ductus. *Pediatr. Res.* (1996) 40: 198-208.

Clyman R.I., Mauray F., Kramer R.H. Beta 1 and beta 3 integrins have different roles in the adhesion and migration of vascular smooth muscle cells on extracellular matrix. *Exp. Cell Res.* (1992) 200: 272-284.

Coceani F. Control of the ductus arteriosus-a new function for cytochrome P450, endothelin and nitric oxide. *Biochem. Pharmacol.* (1994) 48: 1315-1318.

Coceani F., Breen C.A., Lees J.G., Falck J.R., Olley P.M. Further evidence implicating a cytochrome P-450-mediated reaction in the contractile tension of the lamb ductus arteriosus. *Circ. Res.* (1988) 62: 471-477.

Colbert M.C., Kirby M.L., Robbins J. Endogenous retinoic acid signaling colocalizes with advanced expression of the adult smooth muscle myosin heavy chain isoform during development of the ductus arteriosus. *Circ. Res.* (1996) 78: 790-798.

Colletta A.A., Wakefield L.M., Howell F.V., Danielpour D., Baum M., Sporn M.B. The growth inhibition of human breast cancer cells by a novel synthetic progestin involves the induction of transforming growth factor beta. *J. Clin. Invest.* (1991) 87: 277-283.

Cornelius P., Marlowe M., Call K., Pekala P.H. Regulation of glucose transport as well as glucose transporter and immediate early gene expression in 3T3-L1 preadipocytes by 8-bromo-

cAMP. *J. Cell. Physiol.* (1991) 146: 298-308.

Cornelius P., Marlowe M., Lee M.D., Pekala P.H. The growth factor like effects of tumor necrosis factor-α: stimulation of glucose transport activity and induction of a glucose transporter and immediate early gene expression. *J. Biol. Chem.* (1990) 265: 20506-20516.

Cosgaya J.M., Aranda A. Nerve growth factor regulates transforming growth factor-beta-1 gene expression by both transcriptional and posttranscriptional mechanisms in PC12 cells. *J. Neurochemistry* (1995) 65: 2484-2490.

Couchman J., Hook M., Rees D.A., Timpl R. Adhesion, growth, and matrix production by fibroblasts on laminin substrates. *J. Cell Biol.* (1983) 96: 177-183.

Czaja M.J., Weiner F.R., Eghbali M., Giamborne M.A., Eghbali M., Zern M.A. Differential effects of gamma-interferon on collagen and fibronectin gene expression. *J. Biol. Chem.* (1987) 262: 13348-13351.

Darribere T., Guida K., Larjava H., Johnson K.E., Yamada K.M., Thiery J.P., Boucaut J.C. In vivo analysis of integrin beta 1 subunit function in fibronectin matrix assembly. *J. Cell Biol.* (1990) 110: 1813-1823.

Dartsch P.C., Bauriedel G., Schinko I., Weiss H.-D., Hofling B., Betz E. Cell constitution and characteristics of human atherosclerotic plaques selectively removed by percutaneous atherectomy. *Atherosclerosis* (1989) 80: 149-157.

Davies M.G., Hagen P.O. The vascular endothelium. A new horizon. *Ann. Surg.* (1993) 218: 593-609.

Davies M.G., Hagen P.O. Pathobiology of intimal hyperplasia. *British J. Surg.* (1994) 81: 1254-1269.

Davies P.F., Tripathi S.C. Mechanical stress mechanisms and the cell. An endothelial paradigm. *Circ. Res.* (1993) 72: 239-245.

de Reeder E.G., Girard N., Poelmann R.E., van Munsteren J.C., Patterson D.F., Gittenberger-de Groot A.C. Hyaluronic acid accumulation and endothelial cell detachment in intimal thickening of the vessel wall. The normal and genetically defective ductus arteriosus. *Am. J. Patho.* (1988) 132: 574-585.

de Reeder E.G., Poelmann R.E., van Munsteren J.C., Patterson D.F., Gittenberger-de Groot A.C. Ultrastructural and immunohistochemical changes of the extracellular matrix during intimal cushion formation in the ductus arteriosus of the dog. *Atherosclerosis* (1989) 79: 29-40.

de Reeder E.G., van Munsteren J.C., Poelmann R.E., Patterson D.F., Gittenberger-de Groot A.C. Changes in distribution of elastin and elastin receptor during the intimal cushion formation in the ductus arteriosus. *Anat. Embryol.* (1990) 182: 473-480.

Dean D., Bowlus C., Bourgeois S. Cloning and analysis of the promoter region of the human fibronectin gene. *Proc. Natl. Acad. Sci. USA* (1987) 84: 1876-1880.

Dean D.C., Blakeley M.S., Newby R.F., Ghazal P., Hennighausen L., Bourgeois S. Forskolin inducibility and tissue-specific expression of the fibronectin promoter. *Mol. Cell. Biol.* (1989) 9: 1498-1506.

Dean D.C., McQuillan J.J., Weintraub S. Serum stimulation of fibronectin gene expression appears to result from rapid serum-induced binding of nuclear proteins to a cAMP response element. *J. Biol. Chem.* (1990) 265: 3522-3527.

Dean D.C., Newby R.F., Bourgeois S. Regulation of fibronectin biosynthesis by dexamethasone, transforming growth factor β, and cAMP in human cell lines. *J. Cell. Biol.* (1988) 106: 2159-2170.

Delovs U., Gradjusek C., Sage H., Harker L.A., Schwartz S.M. Interactions of vascular wall cells with collagen gels. *Lab. Invest.* (1982) 46: 61-72.

DeMaria C.T., Brewer G. AUF1 binding affinity to A+U-rich elements correlates with rapid mRNA degradation. *J. Biol. Chem.* (1996) 271: 12179-12184.

Der C.J., Stanbridge E.J. Alterations in the extracellular matrix organization associated with the reexpression of tumorigenicity in human cell hybrids. *Int. J. Cancer* (1980) 26: 451-459.

Der C.J., Stanbridge E.J. A tumor-specific membrane phosphoprotein marker in human cell hybrids. *Cell* (1981) 26: 429-438.

Derynck R., Rhee L., Chen E.Y., Van Tilburg A. Intro-extro structure of human transforming growth factor-beta precursor gene. *Nucleic. Acids Res.* (1987) 15: 3188-3189.

Dhawan J., Lichtler A.C., Rowe D.W., Farmer S.R. Cell adhesion regulates pro-a1(I) collagen mRNA stability and transcription in mouse fibroblasts. *J. Biol. Chem.* (1991) 266: 8470-8475.

Diaz A., Jimenez S.A. Interferon-gamma regulates collagen and fibronectin gene expression by transcriptional and post-transcriptional mechanisms. *Inter. J. Biochem. and Cell Biol.* (1997) 29: 251-260.

Dickson M.C., Martin J.S., Cousins F.M., Kulkarni A.B., Karlsson S., Akhurst R.J. Defective haematopoiesis and vasculogenesis in transforming growth factor-beta 1 knock out mice. *Development* (1995) 121: 1845-1854.

DiMilla P.A., Stone J.A., Quinn J.A., Albelda S.M., Lauffenburger D.A. Maximal migration of human smooth muscle cells on fibronectin and type collagen occurs at an intermediate attachment strength. *J. Cell Biol.* (1993) 122: 729-737.

Dubin D., Peters J.H., Brown L.F., Logan B., Kent K.C., Berse B., Berven S., Cercek B., Sharifi B.G., Pratt R.E. Balloon catheterization induced arterial expression of embryonic fibronectin. *Arterioscler. Thromb. Vasc. Biol.* (1995) 15: 1958-1967.

Eckes B., Mauch C., Huppe G., Krieg T. Differential regulation of transcription and transcript stability of pro-alpha 1(I) collagen and fibronectin in activated fibroblasts derived from patients with systemic scleroderma. *Biochem. J.* (1996) 315: 549-554.

Edsall J., Gilbsert G., Scheraga H. The non-clotting component of the human plasma fraction I-1 (cold-insoluble globulin). *J. Am. Chem. Soc.* (1955) 77: 157-161.

Eisenberg P.R. Endothelial cell mediators of thrombosis and fibrinolysis. *Coronary Artery Diseases* (1991) 2: 129-166.

Elisha Z., Havin L., Ringel I., Yisraeli J.K. Vg1 RNA binding protein mediates the association of Vg1 mRNA with microtubules in Xenopus oocytes. *EMBO J.* (1995) 14: 5109-14.

Ellis L., Clauser E., Morgan D.O., Edery M., Roth R.A., Rutter W.J. Replacement of insulin receptor tyrosine residues 1162 and 1163 compromises insulin-stimulated kinase activity and uptake of 2-deoxyglucose. *Cell* (1986) 45: 721-732.

Engvall E., Ruoslahti E. Binding of soluble form of fibroblast surface protein, fibronectin, to collagen. *Int. J. Cancer* (1977) 20: 1-5.

Fagan J.B., Sobel M.E., Yamada K.M., de Crombrugghe B., Pastan I. Effects of transformation on fibronectin gene expression using cloned fibronectin cDNA. *J. Biol. Chem.* (1981) 256: 520-525.

Fagan J.B., Yamada K.M., de Crombrugghe B., Pastan I. Partial purification and characterization of the messenger RNA for cell fibronectin. *Nucleic Acids Res.* (1979) 6: 3471-3480.

Farb A., Virmani R., Atkinson J.B., Kolodgie F.D. Plaque morphology and pathologic changes in arteries from patients dying after coronary balloon angioplasty. *J. Am. Coll. Cardiol.* (1990) 16: 1421-1429.

Farhadian F., Contard F., Sabri A., Samuel J.L., Rappaort L. Fibronectin and basement membrane in cardiovascular organgenesis. *Cardiovasc. Res.* (1996) 32: 433-442.

Ferrandon D., Elphick L., Nüsslein-Volhard C., St Johnston D. Staufen protein associates with the 3'UTR of bicoid mRNA to form particles that move in a microtubule-dependent manner. *Cell* (1994) 79: 1221-1232.

ffrench-Constant C., Hynes R.O. Patterns of fibronectin gene expression and splicing during cell migration in chicken embryos. *Development* (1988) 104: 369-382.

ffrench-Constant C., Van De Water L., Dvorak H.F., Hynes R.O. Reappearance of an embryonic pattern of fibronectin splicing during wound healing in the adult rat. *J. Cell Biol.* (1989) 109: 903-914.

Fine A., Goldstein R.H. Regulation of type I collagen mRNA translation by TGF-beta. *Regional Immunol.* (1993) 5: 218-224.

Folkman J., D'Amore P.A. Blood vessel formation: what is its molecular basis. *Cell* (1996) 87: 1153-1155.

Frazer P.D., Brady F.O. Superoxide dismutase in bovine fetal ductus arteriosus, thoracic aorta, and pulmonary and umbilical arteries. *Proc. Soc. Exp. Biol. Med.* (1978) 159: 30-33.

Frolik C.A., Dart L.L., Meyers C.A., Smith D.M., Sporn M.B. Purification and initial characterization of a type beta transforming growth factor from human placenta. *Proc. Natl. Acad. Sci. USA* (1983) 80: 3676-3680.

Fujii D., Brissenden J.E., Derynck R., Francke U. Transforming growth factor beta gene maps to human chromosome 19 long arm and to mouse chromosome 7. *Somat. Cell. Mol. Genet.* (1986) 12: 281-288.

Furcht L.T., Moshre D.F., Wendelschafer-Crebb G., Foidart J.-M. Reversal by glycorticoid hormones of the loss a fibronectin and procollagen matrix in transformed human cells. *Cancer*

Res. (1979a) 39: 2077-2083.

Furcht L.T., Moshre D.F., Wendelschafer-Crebb G., Woodbridge P.A., Foidart J.-M. Dexamethasone-induced accumulation of a fibronectin and collagen extracellular matrix in transformed human cells. *Nature* (1979b) 277: 393-395.

Gallimore P.H., McDougall J.K., Chen L.B. In vitro traits of adenovirus-transformed cell lines and their relevance to tumorigenicity. *Cell* (1977) 10: 669-678.

Gao F.-B., Carson C.C., Levine T., Keene J.D. Selection of a subset of mRNAs from a combinatorial 3' untranslated region libraries using neuronal RNA-binding protein Hel-N1. *Proc. Natl. Acad. Sci. USA* (1994) 91: 11207-11211.

Gao F.-B., Keene J.D. Hel-N1/Hel-N2 proteins are bound to poly(A)+ mRNA in granular RNP structures and implicated in neuronal differentiation. *J. Cell Sci.* (1996) 109: 579-589.

Garcia-Pardo A., Pearlstein E., Frangione B. Primary structure of human plasma fibronectin. Characterization of a 31,000-dalton fragment from the COOH-terminal region containing a free sulfhydryl group and a fibrin-binding site. *J. Biol. Chem.* (1985) 260: 10320-1-325.

Geiser A.G., Kim S.J., Roberts A.B., Sporn M. Characterization of the mouse transforming growth factor-beta 1 promoter and activation by the Ha-ras oncogene. *Mol. Cell. Biol.* (1991) 11: 84-92.

Gentry L.E., Lioubin M.N., Purchio A.F., Marquardt H. Molecular events in the processing of recombinant type 1 pre-pro-transforming growth factor beta to the mature polypeptide. *Mol. Cell. Biol.* (1988) 8: 4162-4168.

Gentry L.E., Webb N.R., Lim G.J., Brunner A.M., Ranchalis J.E., Twardzik D.R., Lioubin M.N., Marquardt H., Purchio A.F. Type 1 transforming growth factor beta: amplified expression and secretion of mature and precursor polypeptide. *Mol. Cell. Biol.* (1987) 7: 3418-3427.

George E.L., Georges-Labouesse E.N., Patel-king R.S., Rayburn H., Hynes R.O. Defects in mesoderm, neural tube and vascular development in mouse embryos lacking fibronectin. *Development* (1993) 119: 1079-1091.

Gillis P., Malter J.S. The adenosine-uridine binding factor recognizes the AU-rich elements of cytokine, lymphokine, and oncogene mRNAs. *J. Biol. Chem.* (1991) 266: 3172-3177.

Gittenberger-de Groot A.C., Moulaert A.J.M., Hitchcock J.F. Histology of the persistent arteriosus in cases of congenital rubella. *Circulation* (1980) 62: 183-186.

Gittenberger-de Groot A.C., Strengers J.L.M., Mentink M., Poelmann R.E., Patterson D.F. Histologic studies on normal and persistent ductus arteriosus in the dog. *J. Am. Coll. Cardiol.* (1985) 6: 394-404.

Gittenberger-de Groot A.C., van Ertbruggen L., Moulert A.J.M., Harinck E. The ductus arteriosus in the preterm infant: Histological and clinical observations. *J. Pediatr.* (1980) 96: 88-93.

Glukhova M.A., Frid M.G., Shekhonin B.V., Balabanov Y.V., Koteliansky V.E. Expression of fibronectin variants in vascular and visceral smooth muscle cells in development. *Dev. Biol.* (1990) 141: 193-202.

Glukhova M.A., Frid M.G., Shekhonin B.V., Vasilevskaya T.D., Grunwald J., Saginati M., Koteliansky V.E. Expression of extra domain A fibronectin sequence in vascular smooth muscle cells is phenotype dependent. *J. Cell Biol.* (1989) 109: 357-366.

Gottlieb E. The 3' untranslated region of localized maternal messengers contains a conserved motif involved mRNA localization. *Proc. Natl. Acad. Sci. USA* (1992) 89: 7164-7168.

Grafi G., Sela I., Galili G. Translational regulation of human beta interferon mRNA: Association of the 3' AU-rich sequence with the poly(A) tail reduces translation efficiency *in vitro*. *Mol. Cell. Biol.* (1993) 13: 3487-3493.

Grahmberg C.G., Hakomori S.I. Altered growth behavior of malignant cells associated with changes in externally labeled glycoprotein and glycolipid. *Proc. Natl. Acad. Sci. USA* (1973) 70: 3329-3333.

Grande J.P. Role of transforming growth factor-β in tissue injury and repair. *Proc. Soc. Exp. Biol. Med.* (1997) 214: 27-40.

Gravanis M.B., Roubin G.S. Histopathologic phenomena at the site of percutaneous transluminal coronary angioplasty: the problem of the restenosis. *Human Pathol.* (1989) 20: 477-485.

Gravis E.R., Lehman R. Localization of nanos RNA controls embryonic polarity. *Cell* (1992) 71: 301-313.

Grinnell F. Cellular adhesiveness and extracellular substrata. *Int. Rev. Cytology* (1978) 53: 65-144.

Guan J.L., Hynes R.O. Lymphoid cells recognize an alternatively spliced segment of fibronectin via the integrin receptor alpha 4 beta 1. *Cell* (1990) 60: 52-61.

Halloran B.G., Prorok G.D., So B.J., Baxter B.T. Transforming growth factor-beta 1 inhibits human arterial smooth-muscle cell proliferation in a growth-rate-dependent manner. *Am. J. Surg.* (1995) 170: 193-197.

Hamilton B.J., Nagy E., Malter J.S., Arrick B.A., Rigby W.F.C. Association of heterogeneous nuclear ribonucleoprotein A1 and C proteins with reiterated AUUUA sequences. *J. Biol. Chem.* (1993) 268: 8881-8887.

Han J., Brown T., Beutler B. Endotoxin-responsive sequences control cachectin/tumor necrosis factor biosynthesis at the translational level. *J. Exp. Med.* (1990a) 171: 465-475.

Han J., Thompson P., Beutler B. Dexamethasone and pentoxifylline inhibit endotoxin-induced cachectin/tumor necrosis factor synthesis at separate points in the signal pathway. *J. Exp. Med.* (1990b) 172: 391-394.

Han J.R., Yiu G.K., Hecht N.O. Testis/brain RNA-binding protein attaches translationally repressed and transported mRNAs to microtubules. *Proc. Natl. Acad. Sci. USA* (1995) 92: 9550-9554.

Hanke H., Strohschneider T., Oberhoff M., Betz E., Karsch K. R. Time course of smooth muscle cell proliferation. *Circ. Res.* (1990) 67: 651-659.

Hardingham T.E., Fosang A.J. Proteoglycans: many forms and many functions. *FASEB J.*

(1992) 6: 861-870.

Hardwick C., Hoare K., Owens R., Hohn H.P., Hook M., Moore D., Cripps V., Austen L., Nance D.M., Turley E.A. Molecular cloning of a novel hyaluronan receptor that mediates tumor cell motility. *J. Cell Biol.* (1992) 117: 1343-1450.

Harpel J.G., Metz C.N., Kojima S., Rifkin D.B. Control of transforming growth factor-beta activity: Latency vs activation. *Prog. Growth Factor Res.* (1992) 4: 321-335.

Hayman E.G., Engval E., Ruoslahti E. Concomitant loss of cell surface fibronectin and laminin from transformed rat kidney cells. *J. Cell Biol.* (1981) 88: 352-357.

Hayman E.G., Engvall E., Ruoslahti E. Butyrate restores fibronectin at cell surface of transformed cells. *Exp. Cell Res.* (1980) 127: 478-481.

Heath J.P., Holifield B.P. Cell locomotion: new research tests old ideas on membrane and cytoskeletal flow. *Cell Motillity & Cytoskeleton* (1991) 18: 245-257.

Hedin U., Bottger B.A., Forsberg E., Johansson S., Thyberg J. Diverse effects of fibronectin and laminin on phenotypic properties of cultured arterial smooth muscle cells. *J. Cell Biol.* (1988) 107: 307-319.

Hedin U., Bottger B.A., Luthman J., Johansson S., Thyberg J. A substrate of the cell-attachment sequence of fibronectin (Arg-Gly-Asp-Ser) is sufficient to promote transition of arterial smooth muscle cells from a contractile to a synthetic phenotype. *Dev. Biol.* (1989) 133: 489-501.

Hedin U., Thyberg J. Plasma fibronectin promotes modulation of arterial smooth-muscle cells from contractile to synthetic phenotype. *Differentiation* (1987) 33: 239-246.

Heine U.I., Munoz E.F., Flanders K.C., Ellingsworth L.R., Lam H.-Y., Thompson N.Y., Roberts A.B., Sporn M.B. Role of transforming growth factor-beta in the development of the embryo. *J. Cell. Biol.* (1987) 105: 2861-2876.

Hentze M.W., Rouault R.A., Harford J.B., Klausner R.D. Oxidation-reduction and the molecular mechanism of a regulatory RNA-protein interaction. *Science* (1989) 244: 540-546.

Hershey J.W., Mathews M.B., Sonenberg N. Origins and targets of translational control. In Translational Control (ed: Hershey, JW; Mathews, MB, Sonerberg, N.). Cold Spring Harbor Laboratory Press (1996) 1-29.

Hesketh J.E., Pryme I.F. Interaction between mRNA, ribosomes and the cytoskeleton. *Bio chem. J.* (1991) 277: 1-10.

Hinek A., Boyle J., Rabinovitch M. Vascular smooth muscle cell detachment from elastin and migration through elastin laminae is promoted by chondroitin sulfate-induced "shedding" of the 67 kD elastin binding protein. *Exp. Cell Res.* (1992) 203: 344-353.

Hinek A., Mecham R.P., Keeley F., Rabinovitch M. Impaired elastin fiber assembly related to reduced 67 kD elastin-binding protein in fetal lamb ductus arteriosus and cultured aortic smooth muscle cells treated with chondroitin sulfate. *J. Clin. Invest.* (1991) 88: 2083-2094.

Hinek A., Rabinovitch M. 67 kD elastin-binding protein is a protective "companion" of extracellular insoluble elastin and intracellular tropoelastin. *J. Cell Biol.* (1994) 126: 563-574.

Hinek A., Rabinovitch M. The ductus arteriosus migratory smooth muscle cell phenotype processes tropoelastin to a 52 kDa product associated with impaired assembly of elastic laminae. *J. Biol. Chem.* (1993) 268: 1405-1413.

Hoch J.R., Stark V.K., Turnipseed W.D. The temporal relationship between the development of vein graft intimal hyperplasia and growth factor gene expression. *J. Vasc. Sug.* (1995) 22: 51-58.

Hynes R.O. Alteration of cell-surface proteins by viral transformation and by proteolysis. *Proc. Natl. Acad. Sci. USA* (1973a) 70: 3170-3174.

Hynes R.O. Alteration of cell-surface proteins by viral transformation and proteolysis. *Porch. Natl. Acad. Sci. USA* (1973b) 70: 3170-3174.

Hynes R.O. Fibronectins. (1990) Springer-Verlag, New York.

Hynes R.O., Destree A. Extensive disufide bonding at the mammalian cell surface. *Proc. Natl. Acad. Sci. USA* (1977) 74: 2855-2859.

Hynes R.O., Lander A.D. Contact and adhesive specificities in the associations, migration, and targeting of cells and axons. *Cell* (1992) 68: 303-322.

Hynes R.O., Yamada K.M. Fibronectins: multifunctional modular glycoproteins. *J. Cell Biol.* (1982) 92: 369-377.

Icardo J., Manasek F. Fibronectin distribution during early chick embryo heart development. *Dev. Biol.* (1983) 95: 19-30.

Icardo J., Manasek F. An indirect immunofluorescence study of the distribution of fibronectin during the formation of the cushion tissue mesenchyme in the embryonic heart. *Dev. Biol.* (1984) 101: 336-345.

Ip J.H., Fuster V., Badimon L., Badimon J.J., Taubman M.B., Chesebro J.H. Syndromes of accelerated atherosclerosis: role of vascular injury and smooth muscle proliferation. *J. Am. Coll. Cardiol.* (1990) 15: 1667-1687.

Ishiwata T., Aida T., Yokoyama M., Asano G. Fibronectin biosynthesis in endothelial regeneration after intima injury. *Exp. Mol. Pathol.* (1994) 60: 1-11.

Jacobson A. in Translational Controls (Hershey, J. W. B., Mathews, M. B. & Sonenberg, M. B., eds) Cold Spring Harbor Laboratory Press, Cold Spring Harbor NY. (1995) pp. 451-480.

Jacobson A., Peltz S.W. Interrelationships of the pathways of mRNA decay and translation in eukaryotic cells. *Annu. Rev. Biochem.* (1996) 65: 693-739.

Jain R.G., Andrews L.G., McGowan K.M., Pekala P.H., Keene J.D. Ectopic expression of Hel-N1, an RNA-binding protein, increases glucose transporter (Glut1) expression in 3T3-L1 adipocytes. *Mole. Cell. Biol.* (1997) 17: 954-962.

Johnson D.J., Robson P., Hew Y., Keeley F.W. Decreased elastin synthesis in normal development and in long-term aortic organ and cell cultures is related to rapid and selective destabilization of mRNA for elastin. *Circ. Res.* (1995) 77:1107-1113.

Jones P.L., Cowan K.N., Rabinovitch M. Tenascin-C, proliferation and subendothelial

fibronectin in progressive pulmonary vascular disease. *Am. J. Pathol.* (1997) 150: 1349-1360.

Jones T.R., Cole M.D. Rapid cytoplasmic turnover of c-myc mRNA: requirement of 3' untranslated sequences. *Mol. Cell. Biol.* (1987) 7: 4513-4519.

Kahari V.-M., Olsen D.R., Rhudy R.W., Carrillo P., Chen Y.Q., Uitto J. Transforming growth factor-β up-regulates elastin gene expression in human skin fibroblasts. Evidence for post-transcriptional modulation. *Lab. Invest.* (1992) 66: 580-588.

Kahari V.-M., Peltonen J., Chen Y.Q., Uitto J. Differential modulation of basement membrane gene expression in human fibrosarcoma HT-1080 cells by transforming growth factor-β1. *Lab. Invest.* (1991) 64: 807-818.

Kanzaki T., Olofsson A., Moren A., Wernstedt C., Hellman U., Miyazono K., Claesson-Welsh L., Heldin C.H. TGF-beta1 binding protein: A component of the large latent complex of TGF-beta 1 with multiple repeat sequences. *Cell* (1990) 61: 1051-1061.

Kanzaki T., Tamura K., Takahashi K., Saito Y., Akikusa B., Oohashi H., Kasayuki N., Ueda M., Morisaki N. In vivo effect of TGF-beta 1. Enhanced intimal thickening by administration of TGF-beta1 in rabbit arteries injured with a balloon catheter. *Arterioscler. Thromb.* (1995) 15: 1951-1957.

Kasturi R., Joshi V.C., Wakil S.J. Colchicine inhibition of insulin induction of stearoyl-CoA desaturase and fatty acid synthetase in cultured avian liver explants. *Arch. Biochem. Biophys.* (1984) 233: 530-539.

Katz D.A., Theodrakis N.G., Cleveland D.W., Lindsten T., Thompson C.B. AU-A, an RNA-binding activity distinct from hnRNP A1, is selective for AUUUA repeats and shuttles between the nucleus and the cytoplasm. *Nucleic Acids Res.* (1994) 22: 238-246.

Keski-Oja J., Mosher D.F., Vaheri A. Cross-linking of a major fibroblast surface-associated glycoprotein (fibronectin) catalyzed by blood coagulation factor XIII. *Cell* (1976) 9: 29-35.

Kim S., Kawamura M., Wanibuchi H., Ohta K., Hamaguchi A., Omura T., Yukimura T., Mirua K., Iwao H. Angiotensin II type I receptor blockade inhibits the expression of immediate-early genes and fibronectin in rat injury artery. *Circulation* (1995) 92: 88-95.

Kim S.-J., Jeang K.-T., Glick A.B., Sporn M.B., Roberts A.B. Promoter sequences of the human transforming growth factor-beta1 gene responsive to transforming growth factor-beta1 autoinduction. *J. Biol. Chem.* (1989c) 264: 7041-7045.

Kim S.J., Denhez F., Kim K.Y., Holt J.T., Sporn M.B., Robert A.B. Activation of the second promoter of the transforming growth factor-β1 and phorbol ester occurs through the same target sequence. *J. Biol. Chem.* (1989b) 264: 19373-19378.

Kim S.J., Glick A., Sporn M.B., Robert A.B. Characterization of the promoter region of the human transforming growth factor-β1 gene. *J. Biol. Chem.* (1989a) 264: 402-408.

Kim S.J., Lafyatis K., Hattori P.A.R., Kim K.Y., Sporn M.B., Karin M., Roberts A.B. Autoinduction of transforming growth factor beta 1 is mediated by the AP-1 complex. *Mol. Cell. Biol.* (1990) 10: 1492-1497.

Kim S.J., Lee H.D., Robbins P.D., Busam K., Sporn M.B., Roberts A.B. Regulation of transforming growth factor-β1 gene expression by the product of the retinoblastoma-susceptibility gene. *Proc. Natl. Acad. Sci.* (1991) 88: 3052-3056.

Kim S.J., Park K., Koeller D., Kim K.Y., Wakefield L.M., Sporn M.B., Robert A.B. Post-transcriptional regulation of the human transforming growth factor-β1 gene. *J. Biol. Chem.* (1992) 267: 13702-13707.

Klausner R.D., Harford J.B. Cis-trans models for posttranscriptional gene regulation. *Science* (1989) 246: 870-873.

Klausner R.D., Rouault T.A., Harford J.B. Regulation the fate of mRNA: The control of cellular iron metabolism. *Cell* (1993) 72: 19-28.

Kocher O., Gabbiani F., Gabbiani G., Reidy M.A., Cokay M.S., Peters H., Huttner I. Phenotypic features of smooth muscle cells during the evolution of experimental carotid artery intimal thickening: biochemical and morphologic studies. *Lab. Invest.* (1991) 65: 459-470.

Koeller D.M., Horowitz J.A., Casey J.L., Klausner R.D., Harford J.B. Translation and the stability of mRNAs encoding the transferring receptor and c-fos. *Proc. Natl. Acad. Sci. USA* (1991) 88: 7778-7782.

Kohout T.A., O'Brian J.J., Gaa S.T., Lederer W., Rogers T.B. Novel adenovirus component system that transfects cultured cardiac cells with high efficiency. *Circ. Res.* (1996) 78: 971-977.

Komoriya A., Green L.J., Mervic M., Yamada S.S., Yamada K.M., Humphries M.J. The minimal essential sequence for a major cell type-specific adhesion site (CS1) within the alternatively spliced type III connecting segment domain of fibronectin is leucine-aspartic acid-valine. *J. Biol. Chem.* (1991) 266: 15075-15079.

Kondo M., Watanabe M., Amanuma K., Oka S., Ishida N. Overexpression of MP41 gene in a transformed endothelial cell line correlates with the increased fibronectin expression and a decreased incidence of tumorigenicity. *Biochem. Biophys. Res. Comm.* (1996) 219: 398-404.

Kornblihtt A.R., Vibe-Pedersen K., Baralle F.E. Isolation and characterization of cDNA clones for human and bovine fibronectins. *Proc. Natl. Acad. Sci. USA* (1983) 80: 3218-3222.

Kornblihtt A.R., Vibe-Pedersen K., Baralle F.E. Human fibronectin: cell specific alternative mRNA splicing generates polypeptide chains differing in the number of internal repeats. *Nucleic Acids Res.* (1984a) 12: 5853-5868.

Kornblihtt A.R., Vibe-Pedersen K., Baralle F.E. Human fibronectin: molecular cloning evidence for two mRNA species differing by an internal segment coding for a structural domain. *EMBO J.* (1984b) 3: 221-226.

Kozak M. Influences of mRNA secondary structure on initiation by eukaryotic ribosomes. *Proc. Natl. Acad. Sci. USA* (1986a) 83: 2850-2854.

Kozak M. Point mutations define a sequence flanking the AUG initiator codon that modulates translation by eukaryonic ribosome. *Cell* (1986b) 44: 283-292.

Kozak M. An analysis of 5'-noncoding sequence from 699 vertebrate messenger RNAs. *Nucleic Acis Res.* (1987a) 15: 8125-8148.

Kozak M. At least six nucleotides proceeding the AUG initiator codon enhance translation in mammalian cells. *J. Mol. Biol.* (1987b) 196: 947-950.

Kozak M. The scanning model for translation: an update. *J. Cell Biol.* (1989) 108: 229-241.

Kozak M. An analysis of vertebrate mRNA sequences: Intimations of translational control. *J. Cell Biol.* (1991) 115: 887-903.

Kruys V., Beutler B., Huez G. Translational control mediated by UA-rich sequences. *Enzyme* (1990) 44: 193-202.

Kruys V., Marinx O., Shaw G., Deschamps J., Huez G. Translational blockade imposed by cytokine-derived UA-rich sequence. *Science* (1989) 245: 85-88.

Kruys V., Thompson P., Beutler B. Extinction of the tumor necrosis factor locus, and genes encoding the lipopolysaccharide signaling pathway. *J. Exp. Med.* (1993) 177: 1383-1390.

Kruys V., Wathelet M., Poupart P., Contreras R., Fiers W., Content J., Huez G. The 3' untranslated region of the human interferon-β mRNA has an inhibitory effect on translation. *Proc. Natl. Acad. Sci. USA* (1987) 84: 6030-6034.

Kruys V.I., Wathelet M.G., Huez G.A. Identification of a translation inhibitory element (TIE) in the 3' untranslated region of the human interferon-β mRNA. *Gene* (1988) 71: 191-200.

Kubomura S., Obara M., Karasaki Y., Taniguchi H., Gotoh S., Tsuda T., Higashi K., Ohsato K., Hirano H. Genetic analysis of the cell binding domain region of the chicken fibronectin gene. *Biochem et Biophys Acta* (1987) 910: 171-181.

Kuusela P., Ruoslahti E., Engvall E., Vaheri A. Immunological interspecies cross-reactions of fibroblast surface antigen (fibronectin). *Immunochemistry* (1976) 13: 639-642.

Kwon Y.K., Hecht N.B. Binding of a phosphoprotein to the 3' untranslated region of the mouse protamine 2 mRNA temporally represses its translation. *Mol. Cell. Biol.* (1993) 13: 6547-6557.

Laemmli U.K. Cleavage of structural proteins during the assembly of the head of bacteriophage T4. *Nature (Lond.)* (1970) 277: 680-685.

Lagnado C.A., Brown C.Y., Goodall G.J. AUUUA is not sufficient to promote poly(A) shortening and degradation of an mRNA: the functional sequence within AU-rich elements may be UUAUUUA(U/A)(U/A). *Mol. Cell Biol.* (1994) 14: 7984-7995.

Lawrence J.B., Singer R.H. Intracellular localization of messenger RNAs for cytoskeletal proteins. *Cell* (1986) 45: 407-415.

Lee G., Hynes R., Kirschner M. Temporal and spatial regulation of fibronectin in early Xenopus development. *Cell* (1984) 36: 729-740.

Lehnert S.A., Akhurst R.J. Embryonic expression pattern of TGF-beta-1 RNA suggests both paracrine and autocrine mechanisms of action. *development* (1988) 104: 263-273.

Letterio J.J., Geiser A.G., Kulkarni A.B., Roche N.S., Sporn M.B., Roberts A.B. Maternal

rescue of transforming growth factor-β1 null mice. *Science* (1994) 264: 1936-1938.

Levine R.A., Seshadri T., Hann S.R., Campisi J. Post-transcriptional changes in growth factor inducible gene regulation caused by antiproliferative interferons. *Cell Reg.* (1990) 1: 215-226.

Levine T.D., Gao F., King P.H., Andreaws L.G., Keene J.D. Hel-N1: an autoimmune RNA-binding protein with specificity for 3' uridylate-rich untranslated regions of growth factor mRNAs. *Mol. Cell. Biol.* (1993) 13: 3494-3504.

Libby P., Schwartz D., Brogi E., Tanaka H., Clinton S.K. A cascade model for restenosis. A special case of atherosclerosis progression. *Circulation* (1992) 86: 11147-11152.

Linask K., Lash J. Precardiac cell migration: fibronectin localization at mesoderm-endoderm interface during directional movement. *Dev. Biol.* (1986) 114: 87-101.

Linask K., Lash J.W. A role of fibronectin in the migration of avian precardiac cells. II. Rotation of the heart-forming region during different stages and its effects. *Dev. Biol.* (1988) 129: 324-329.

Liu C., Wallace K., Shi C., Heyner S., Komm B., Haddad J.B. Post-transcriptional stimulation of transforming growth factor beta 1 mRNA by TGF-beta 1 treatment of transformed human osteoblasts. *J. Bone & Mineral Res.* (1996) 11: 211-217.

Liu M.W., Roubin G.S., King S.B. Restenosis after coronary angioplasty: potential biologic determinants and role of intimal hyperplasia. *Circulation* (1989) 79: 1374-1387.

Lopez-Candales A., Scott M.J., Wickline S.A. Cholesterol feeding modulates spatial expression of TGF-beta 1 and beta 2 in aortas of Watanabe rabbits. *Cytokine* (1995) 7: 554-561.

Luckow B., Schütz G. CAT constructions with multiple unique restriction sites for the functional analysis of eukaryotic promoters and regulatory elements. *Nucleic Acids Res.* (1987) 15: 5490.

Lyons R.M., Gentry L.E., Purchio A.F., Moses H.L. Mechanism of activation of latent recombinant transforming growth factor β1 by plasmin. *J. Cell Biol.* (1990) 110: 1361-1367.

Lyons R.M., Keski-Oja J., Moses H.L. Proteolytic activation of latent transforming growth factor beta from fibroblast-conditioned medium. *J. Cell Biol.* (1988) 106: 1659-1665.

Ma W.-J., Cheng S., Campbell C., Wright A., Furneaux H. Cloning and characterization of HuR, a ubiquitously expressed Elav-like protein. *J. Biol. Chem.* (1996) 271: 8144-8151.

Macdonald P.M., Struhl G. Cis-acting sequences responsible for anterior localization of bicoid mRNA in Drosophila embryos. *Nature* (1988) 336: 595-598.

Madri J.A., Reidy M.A., Kocher O., Bell L. Endothelial cell behavior after denudation injury is modulated by transforming growth factor-beta1 and fibronectin. *Lab. Invest.* (1989) 60: 755-765.

Majesky M.W., Lindner V., Twardzik D.R., Schwartz S.M., Reidy M.A. Production of transforming growth factor β1 during repair of arterial injury. *J. Clin. Invest.* (1991) 88: 904-910.

Malter J.S. Identification of an AUUUA-specific messenger RNA binding protein. *Science* (1989) 246: 664-666.

Malter J.S., Hong Y. A redox switch and phosphorylation are involved in the post-translational up-regulation of the adenosine-uridine binding factor by phorbol ester and ionophore. *J. Biol. Chem.* (1991) 266: 3167-3171.

Mann S.S., Hammarback J.A. Molecular Characterization of light 3: a microtubule binding subunit of MAP1A and MAP1B. *J. Biol. Chem.* (1994) 269(15): 11492-11497.

Mansour M.M., Dunn M.A., Salah L.A. Effect of colchicine on collagen synthesis by liver fibroblasts in murine schistosomiasis. *Clinica. Chimica. Acta.* (1988) 177: 11-20.

Mason C., Bigras J.L., Zhou B., Rabinovitch M. Bioengineering of patent ductus arteriosus in post-natal lambs. *Circulation* (1997) 96(Suppl):8-I484

Mason C. Rabinovitch M. Post-transcriptional regulation of fibronectin (FN) synthesis by nitric oxide (NO) in motile vascular smooth muscel cells (SMC) is mediated by phosphorylation of a microtubule-associated FN mRNA binding protein, LC3. *Mol. Biol. Cell* (1997) 8S:322a

Marigo V., Volpin D., Bressan G.M. Regulation of the human elastin promoter in chick embryo cells. Tissue-specific effect of TGF-beta. *Biochim. et Biophys. Acta* (1993) 1172: 31-36.

Marinx O., Bertrand S., Karsenti E., Huez G., Kruys V. Fertilization of Xenopus eggs imposes a complete arrest of mRNAs containing 3' UUAUUUAU elements. *FEBS Letters* (1994) 345: 107-112.

Marshall C.J., Franks L.M., Carbonell A.W. Markers of neoplastic transformation in epithelial cell lines derived from human carcinomas. *J. Natl. Cancer Inst.* (1977) 58: 1743-1751.

Massague J. The transforming growth factor-beta family. *Annu. Rev. Cell Biol.* (1990) 6: 597-641.

McCarthy J.E., Kollmus H. Cytoplasmic mRNA-protein interactions in eukaryotic gene expression. *Trends Biochem.Sci.* (1995) 20: 191-197.

McKeown-Longo P.J., Etzler C.A. Induction of fibronectin matrix assembly in human fibrosarcoma cells by dexamethasone. *J cell Biol* (1987) 104: 601-610.

Meijlink F., Curran T., Miller A.D., Verma I.M. Removal of a 67-base sequence in the noncoding region of protooncogene fos converts it to a transforming gene. *Proc. Natl. Acad. Sci. USA* (1985) 82: 4987-4991.

Merrilees M.J., Beaumont B. Structural heterogeneity of the diffuse intimal thickening and correlation with distribution of TGF-β1. *J. Vasc. Res.* (1993) 30: 293-302.

Miano J.M., Tota R.R., Vlasic N., Danishefsky K.J., Stemerman M.B. Early proto-oncogene expression in rat aortic smooth muscle cells following endothelial removal. *Am. J. Pathol.* (1990) 137: 761-765.

Miano J.M., Vlasic N., Tota R.R., Stemerman M.B. localization of Fos and Jun proteins in rat aortic smooth muscle cells after vascular injury. *Am. J. Pathol.* (1993a) 142: 715-724.

Miano J.M., Vlasic N., Tota R.R., Stemerman M.B. Smooth muscle cell immediate-early gene and growth factor activation follows vascular injury. A putative in vivo mechanism for autocrine growth. *Arterioscler. & Thromb.* (1993b) 13: 211-219.

Millan F.A., Denhez F., Kondaiah P., Akhurst R.J. Embryonic gene expression of TGF-β1, β2, β3 suggest different developmental functions in vivo. *Development* (1991) 111: 131-144.

Milligan J.F., Groebe D.R., Witherell G.W., Uhlenbeck O.C. Oligoribonucleotide synthesis using T7 RNA polymerase and synthetic DNA templates. *Nucleic Acids Res.* (1987) 15: 8783-8797.

Miyazono K., Hellmanm U., Wernstedt C., Heldin C.H. Latent high molecular weight complex of transforming growth factor beta 1. Purification from human platelets and structure characterization. *J. Biol. Chem.* (1988) 263: 6407-6415.

Miyazono K., Yuki K., Takaku F., Wernstedt C., Kanzaki T., Olofsson A., Hellman U., Heldin C.-H. Latent forms of TGF-beta: structure and biology. In: Piez, K. A. and Sporn, M. B., Eds. Transforming growth factor betas: Chemistry, Biology, and Therapeutics. New York: New York Academic of Sciences (1990) 593: pp51-58.

Molossi S., Clausell N., Rabinovitch M. Coronary artery endothelial interleukin-1β mediates enhanced fibronectin production related to post-cardiac transplant arteriopathy in piglets. *Circulation* (1993) 88: 248-256.

Molossi S., Clausell N., Rabinovitch M. Reciprocal induction of tumor necrosis factor-alpha and interleukin-1 beta activity mediates fibronectin synthesis in coronary artery smooth muscle cells. *J. Cell. Physiol.* (1995) 163: 19-29.

Morrison P., Edsall J., Miller S. Preparation and properties of serum and plasma proteins XVIII. The separation of purified fibrinogen from fraction I of human plasma. *J. Am. Chem. Soc.* (1948) 70: 3103-3108.

Mosesson M., Umfleet R. The cold-insoluble globulin of human plasma. *J. Biol. Chem.* (1970) 245: 5728-5736.

Mosesson M.W., Chen A.B., Huseby R.M. The cold-insoluble globulin of human plasma: studies of its essential structural features. *Biochim et Biophys Acta* (1975) 386: 509-524.

Mosse P.R., Campbell J.H., Campbell G.R. Smooth muscle phenotypic expression in human carotid arteries. II. atherosclerosis-free diffuse intimal thickenings compared with the media. *Arteriosclerosis* (1986) 6: 664-669.

Mould A.P., Wheldon L.A., Komoriya A., Wayner E.A., Yamada K.M., Humphries M.J. Affinity chromatographic isolation of the melanoma adhesion receptor for the IIICS region of fibronectin and its identification as the integrin alpha 4 beta 1. *J. Biol. Chem.* (1990) 265: 4020-4024.

Mowry K.L., Melton D.A. Vegetal messenger RNA localization directed by a 340-nt RNA sequence element in Xenopus oocytes. *Science* (1992) 255: 991-994.

Munroe D., Jacobson A. mRNA poly(A) tail, a 3' enhancer of translation initiation. *Mol. Cell. Biol.* (1990) 10: 3441-3455.

Muro A., Bernath V., Kornblihtt A. Interaction of the -170 cyclic AMP response element with the adjacent CCAAT box in the human fibronectin gene promoter. *J. Biol. Chem.* (1992) 267: 12767-12774.

Murry M.K., DeSouza M.M. Messenger RNA encoding an estrogen-dependent oviduct secretory protein in the sheep is localized in the apical tips and basal compartments of fimbria and ampulla epithelial cells implying translation at unique cytoplasmic foci. *Mol. Reprod. Dev.* (1995) 42: 268-283.

Myer V.E., Lee S.I., Steitz J.A. Viral small nuclear ribonucleoproteins bind a protein implicated in messenger RNA destabilization. *Proc. Natl. Acad. Sci. USA* (1992) 89: 1298-1300.

Nabel E.G., Shum L., Pompili V.J., Yang Z.Y., San H., Shu H.B., Liptay S., Gold L., Gordon D., Derynck R., Nebal G.J. Direct transfer of transforming growth factor beta 1 gene into arteries stimulates fibrocellular hyperplasia. *Proc. Natl. Acad. Sci.* (1993) 90: 10759-10763.

Nagamine M., Takei H., Toda T., Hokama S. Detection of c-myc gene expression in human coronary arteriosclerosis by immunohistochemistry and in situ hybridization method. *Jan. J. Clin. Pathol.* (1989) 37: 311-315.

Nagy E., Rigby W.F. Glyceraldehyde-3-phosphate dehydrogenase selectively binds AU-rich RNA in the NAD(+)-binding region (Rossmann fold). *J. Biol. Chem.* (1995) 270: 2755-2763.

Nakagawa J., Waldner H., Meyer-Monard S., Hofsteenge J., Jeno P., Moroni C. AUH, a gene encoding an AU-specific RNA binding protein with intrinsic enoyl-CoA hydratase activity. *Proc. Natl. Sci. USA* (1995) 92: 2051-2055.

Nakajima T., Nakamura T., Tsunoda S., Oda K. E1A-responsive elements for repression of rat fibronectin gene transcription. *Mol. Cell. Biol.* (1992) 12: 2837-2846.

Nakamaki T., Imamura J., Brewer G., Tsuruoka N., Koeffler H.P. Characterization of adenosine-uridine-rich RNA binding protein. *J. Cell. Physiol.* (1995) 165: 484-492.

Nakamura T., Nakajima T., Tsunoda S., Nakada S., Oda K., Tsurui H., Wada A. Induction of E1A-responsive-negative factors for transcription of the fibronectin gene in adenovirus E1-transformed rat cells. *J. Virol.* (1992) 66: 6436-6450.

Nanbu R., Kubo T., Hasimoto T., Natori S. Purification of an AU-rich RNA binding protein from Sarcophaga peregrina (flesh fly) and its identification as a thiolase. *J. Biochem.* (1993) 114: 432-437.

Nielson S.E., Puck T.T. Deposition of fibronectin in the course of reverse transformation of Chinese hamster ovary cells by cyclic AMP. *Proc. Natl. Acad. Sci. USA* (1980) 77: 985-989.

Nikol S., Isner J.M., Pickering J.G., Kearney M., Leclerc G., Weir L. Expression of transforming growth factor-β1 is increased in human vascular restenosis lesion. *J. Clin. Invest.* (1992) 990:
Nilsson J. Cytokines and smooth muscle cells in atherosclerosis. *Cardiovascular Res.* (1993) 27: 1184-1190.

Nimmer D., Bergtrom G., Hirano H., Amrani D.L. Regulation of plasma fibronectin biosynthesis by glucocorticoids in chick hepatocyte cultures. *J. Biol. Chem.* (1987) 262: 10369-10375.

Noda M., Kitayama H., Matsuzaki T., Sugimoto Y., Okayama H., Bassin R.H., Ikawa Y. Detection of genes with a potential for suppressing the transformed phenotype associated with activated as genes. *Proc. Natl. Acad. Sci. USA* (1989) 77: 985-989.

Norton P.A., Hynes R.O. Alternative splicing of chicken fibronectin in embryos and in normal and transformed cells. *Mol. Cell. Biol.* (1987) 7: 4297-4307.

Olden K., Yamada K.M. Mechanisms of the decrease in the major cell surface protein of chick embryo fibroblasts after transformation. *Cell* (1977) 11: 957-969.

Oliver N., Newby R.F., Bourgeois S. Regulation of fibronectin biosynthesis by glycocorticoids in human fibrosarcoma cells and normal fibroblasts. *Cell* (1983) 33: 287-296.

Olofsson A., Miyazono K., Kanzaki T., Colosetti P., Engstrom U., Heldin C.H. Transforming growth factor-beta 1, -beta 2, and beta 3 secreted by a human glioblastoma cell line. Identification of small and different forms of large latent complexes. *J. Biol. Chem.* (1992) 267: 19482-19488.

Olson E.N., Sternberg E., Hu J.S., Spizz G., Wilcox C. Regulation of myogenic differentiation by type beta transforming growth factor. *J. Cell Biol.* (1986) 1799-1085.

Owens G.K., Geisterfer A.A., Yang Y.W., Komoriya A. Transforming growth factor-beta-induced growth inhibition and cellular hypertrophy in cultured vascular smooth muscle cells. *J. Cell. Biol.* (1988) 107: 771-780.

Owens G.K., Loeb A., Gordon D., Thompson M.M. Expression of smooth muscle-specific alpha-isoactin in cultured vascular smooth muscle cells: relationship between growth and cytodifferentiation. *J. Cell. Biol.* (1986) 102: 343-353.

Pain V.M. Initiation of protein synthesis in eukaryotic cells. *Eur. J. Biochem.* (1996) 236: 747-771.

Pande H., Terramanni T., Tressel T., Churchill M.A., Hawkins G.G., Asia J.A. Altered expression of the fibronectin gene in cells infected with human cytomegalvirus. *J. Virol.* (1990) 64: 1366-1369.

Parkes J.L., Cardell R.R., Hubbard F.C.J., Hubbard D., Meltzer A., Penn A. Cultured human atherosclerotic plaque smooth muscle cells retain transforming potential and display enhanced expression of the myc protooncogene. *Am. J. Pathol.* (1991) 138: 765-775.

Patel R.S., Odermatt E., Schwarzbauer J.E., Hynes R.O. Organization of the rat fibronectin gene provides evidence for "exon shuffling" during evolution. *EMBO J.* (1987) 6: 2565-2572.

Paterson H., Reeves B., Brown R., Hall A., Furth M., Bos J., Jones P., Marshall C. Activated N-ras controls the transformed phenotype of HT1080 human fibrosarcoma cells. *Cell* (1987) 51: 803-12.

Pauletto P., Chiavegato A., Giuriato L., Giutiato L., Scatena M., Faggin E., Grisenti A., Sarzani R., Paci M.V., Fulgeri P.D., Rappelli A. Hyperplastic growth of aortic smooth muscle cells in renovascular hypertensive rabbits is characterized by an expansion of an immature cell phenotype. *Circ. Res.* (1994) 74: 774-788.

Pearlstein E., Hynes R.O., Franks L.M., Hemmings V.J. Surface proteins and fibrinolytic

activity of cultured mammalian cells. *Cancer Res.* (1976) 36: 1475-1480.

Pende A., Mitchusson K.D., DeMaria C.T., Blaxall B.C., Minobe W.A., Sherman J.S., Bristow M.R., Brewer G., Port J. Regulation of the mRNA-binding protein AUF1 by activation of the β-adrenergic receptor signal transduction pathway. *J. Biol. Chem.* (1996) 271: 8493-9501.

Penttinen R., Kobayashi S., Bornstein P. Transforming growth factor β increase mRNA for matrix proteins both in the presence and in the absence of changes in mRNA stability. *Proc. Natl. Acad. Sci. USA* (1988) 85: 1105-1108.

Perkett E.A., Pelton R.W., Meyrick B., Gold L.I., Miller D.A. Expression of transforming growth factor-beta mRNAs and proteins in pulmonary vascular remodeling in the sheep air embolization model of pulmonary hypertension. *Am. J. Res. Cell Mol. Biol.* (1994) 11: 16-24.

Peterson D.A., Archer S.L., Weir E.K. Superoxide reduction of a disulfide: A model of intracellular redox modulation? *Biochem. Biophys. Res. Commun.* (1994) 200: 1586-1591.

Pierschbacher M.D., Ruoslahti E. Cell attachment activity of fibronectin can be duplicated by small synthetic fragments of the molecule. *Nature* (1984) 309: 3-9.

Pircher R., Jullien P., Lawrence D.A. Beta-transforming growth factor is stored in human blood platelets as a latent high molecular weight complex. *Biochem. Biophys. Res. Commun.* (1986) 136: 30-37.

Polly P., Nicholson R.C. Sequence of the mouse fibronectin-encoding gene promoter region. *Gene* (1993) 137: 353-354.

Port J.D., Huang L.-Y., Malbon C.C. β-adrenergic agonists that down-regulate receptor mRNA up-regulate a Mr 35,000 protein(s) that selectively binds to β-adrenergic receptor mRNAs. *J. Biol. Chem.* (1992) 267: 24103-24108.

Potts J.D., Runyan R.B. Epithelial-mesenchymal cell transformation in the embryonic heart can be mediated in part by transforming growth factor-β. *Dev. Biol.* (1989) 134: 392-401.

Query C.C., Bentley R.C., Keene J.D. A common RNA recognition motif identified within a defined U1RNA binding domain of the 70K U1 snRNP protein. *Cell* (1989) 57: 89-101.

Rabinovitch M., Beharry S., Bothwell T., Jackowski G. Qualitative and quantitative differences in protein synthesis comparing fetal lamb ductus arteriosus endothelium and smooth muscle with cells from adjacent vascular sites. *Dev. Biol.* (1988) 130: 250-258.

Rabinovitch M., Boudreau N., Vella G., Coceani F. Oxygen related prostaglandin synthesis in the ductus arteriosus and other vascular cells. *Pediatr. Res.* (1989) 26: 330-335.

Raghow R., Postlethwaite A.E., Keski-Oja J., Moses H.L., Kang A.H. Transforming growth factor-beta increases steady state levels of type I procollagen and fibronectin messenger RNA posttranscriptionally in cultured human dermal fibroblasts. *J. Clin. Invest.* (1987) 79: 1285-1288.

Rasheed S., Nelson-Rees W.A., Toth E.M., Arnstein P., Gardner M.B. Characterization of a

newly derived human sarcoma cell line (HT-1080). *Cancer* (1974) 33: 1027-1033.

Rasmussen L.M., Wolf Y.G., Ruoslahti E. Vascular smooth muscle cells from injured rat aortas display elevated matrix production associated with transforming growth factor-beta activity. *Am. J. Pathol.* (1995) 147: 1041-1048.

Rasoamanantena P., Thweatt R., Labat-Robert J., Goldstein S. Altered regulation of fibronectin gene expression in Werner syndrome fibroblasts. *Exp. Cell Res.* (1994) 213: 121-127.

Rings E.H., Buller H.A., Neele A.M., Dekker J. Protein sorting versus messenger RNA sorting? *European J. Cell Biol.* (1994a) 63: 161-171.

Rings E.H., Krasinski S.D., van Beers E.H., Moorman A.F., Dekker J., Montgomery R.K., Grand R.J., Buller H.A. Restriction of lactase gene expression along the proximal-to- distal axis of rat small intestine occurs during postnatal development. *Gastroenterology* (1994b) 106: 1223-1232.

Rings E.H., Buller H.A., de Boer P.A., Grand R.J., Montgomery R.K., Lambers W.H., Charles R., Moorman A.F.M. Messenger RNA sorting in enterocytes: Co-localization with encoded proteins. *FEBS Lett.* (1992) 300:183-187

Risau W. Differentiation of endothelium. *FASEB J.* (1995) 9: 926-933.

Risau W., Lemmon V. Changes in the vascular extracellular matrix during embryonic vasculogenesis and angiogenesis. *Dev. Biol.* (1988) 125: 441-450.

Roberts A.B., Anzano M.A., Meyers C.A., Wideman J., Blacher R., Pan Y.-C., Stein S., Lehrman R., Smith D.M., Sporn M.B. Purification and properties of a type beta transforming growth factor from bovine kidney. *Biochemistry* (1983) 22: 5692-5698.

Roberts A.B., Sporn M.B. Regulation of endothelial cell growth, architecture, and matrix synthesis by TGF-β. *Am. Rev. Respir. Dis.* (1989) 140: 1126-1128.

Roberts B.E., Miller J.S., Kimelman D., Cepko C.L., Lemischka I.R., Mulligan R.C. Individual adenovirus type 5 early region 1A gene products elicit distinct alterations of cellular morphology and gene expression. *J. Viral.* (1985) 56: 404-413.

Roman J., McDonald J.A. Expression of fibronectin, the integrin alpha 5, and alpha-smooth muscle actin in heart and lung development. *Am. Respir. Cell and Mol. Biol.* (1992) 6: 472-480.

Romeo D.S., Park K., Roberts A.B., Sporn M.B., Kim S.J. An element of the transforming growth factor-β1 5' untranslated region represses translation and specifically binds a cytosolic factor. *Mol. Endocrinol.* (1993) 7: 759-766.

Rondon I.J., MacMillan L.A., Beckman B.S., Goldberg M.A., Schneider T., Bunn H.F., Malter J.S. Hypoxia up-regulated the activity of a novel erythropoietin mRNA binding protein. *J. Biol. Chem.* (1991) 266: 16594-16598.

Roos E. Cellular adhesion, invasion and metastasis. *Biochem. Biophys. Acta.* (1984) 732: 263-284.

Ross R. The smooth muscle cell II: Growth of smooth muscle in culture and formation of elastic fibres. *J. Cell Biol.* (1971) 50: 172-179.

Ross R. The pathogenesis of atherosclerosis-an update. *New Eng. J. Med.* (1986) 314: 488-500.

Ross R. The pathogenesis of atherosclerosis: a perspective for the 1990s. *Nature* (1993) 362: 801-809.

Rouault T.A., Hentze M.W., Caughman S.W., Harford J.B., Klausner R.D. Binding of a cytosolic protein to the iron-responsive element of human ferritin messenger RNA. *Science* (1988) 241: 1207-1210.

Ruoslahti E. Integrins. *J. Clin. Invest.* (1991) 87: 1-5.

Ruoslahti E., Hayman E.G., Pierschbacher M., Engvall E. Fibronectin: purification. immunochemical properties, and biologic activities. *Methods in Enzymology* (1982) 82(Pt A): 803-831.

Ruoslahti E., Pierschbacher M.D. New perspectives in cell adhesion: RGD and integrins. *Science* (1987) 238: 491-497.

Ruoslahti E., Vaheri A. A novel human serum protein from fibroblast plasma membrane. *Nature* (1974) 248: 789-791.

Ryan U.S., Clements E., Habliston D., Ryan J.W. Isolation and culture of pulmonary artery endothelial cells. *Tissue & Cell* (1978) 10: 535-554.

Ryan U.S., Rubanyi G.M. Endothelial regulation of vascular tone. 1st ed. New York: Marcel Dekker (1992).

Ryseck R.P., MacDonald-Bravo H., Zerial M., Bravo R. Coordinate induction of fibronectin. fibronectin receptor, tropomysin and actin genes in serum-stimulated fibroblasts. *Exp. Cell Res.* (1989) 180: 537-545.

Sachs A.B., Davis R.W. The poly(A) binding protein is required for poly(A) shortening and 60S ribosomal subunits-dependent translation initiation. *Cell* (1989) 58: 857-867.

Sachs A.B., Sarnow P., Hentze M.W. Starting at the beginning, middle, and end: Translation initiation in eukaryotes. *Cell* (1997) 89: 831-838.

Saltis J., Agrotis A., Bobik A. Regulation and interactions of transforming growth factor-β with cardiovascular cells: implications for development and disease. *Clin. Exp. Pharm. Physiol.* (1996) 23: 193-200.

Sambrook J., Frisch E.F., Maniatis T. In Molecular Cloning: A Laboratory Manual. Cold Spring Harbor Laboratory, New York. (1989) vol 3: 33-37.

Samuel J.L., Farhadian F., Sabri A., Marotte F., Robert V., Rappaport. L. Expression of fibronectin during rat fetal and postnatal development: an in situ hybridization and immunohistochemical study. *Cardiovasc. Res.* (1994) 28: 1653-1661.

Sarzani R., Brecher P., Chobanian A.V. Growth factor expression in aorta of normotensive and hypertensive rats. *J. Clin. Invest.* (1989) 83: 1404-1408.

Sarzani, R., Arnaldi, G., Takasaki, I. Brecher P., Chobanian A.V. Effects of hypertension and aging on platelet-derived factor and platelet-derived growth factor receptor in rat aorta and heart. *Hypertension* (1991) 18(Suppl. III):93-99.

Savant-Bhonsale S., Cleveland D.W. Evidence for instability of mRNAs containing AUUUA motifs mediated through translation-dependent assembly of a > 20S degradation complex. *Genes Dev.* (1992) 6: 1927-1939.

Schalken J.A., Ebeling S.B., Isaacs J.T., Treiger B., Bussemakers M.J., de Jong M.E., Van de Ven W.J. Down modulation of fibronectin messenger RNA in metastasizing rat prostatic cancer cells revealed by differential hybridization analysis. *Cancer Res.* (1988) 48: 2042-2046.

Schumacher J.M., Lee K., Edelhoff S., Braun R.E. Spnr, a murine RNA-binding protein that is localized to cytopasmic microtubules. *J. Cell Biol.* (1995) 129: 1023-1032.

Schwarbauer J.E., Tamkun J.W., Lemischka I.R., Hynes R.O. Three different fibronectin mRNAs arise by alternative splicing within the coding region. *Cell* (1983) 35: 421-431.

Schwartz S.M., deBlois D., O'Brien E.R.M. The intima: soil for atherosclerosis and restenosis. *Circ. Res.* (1995) 77: 445-465.

Schwartz S.M., Heimark R.L., Majesky M.W. Development mechanisms underlying pathology of arteries. *Physiol. Rev.* (1990) 70: 1177-1209.

Scotto L., Assoian R.K. A GC-rich domain with bifunctional effects on mRNA and protein levels: Implications for control of transforming growth factor β1 expression. *Mol. Cell. Biol.* (1993) 13: 3588-3597.

Scotto L., Vaduva R.E., Assoian R.K. Type-β1 transforming growth factor gene expression: a corrected mRNA structure reveals a downstream phorbol ester responsive element in human cells. *J. Biol. Chem.* (1990) 265: 2203-2208.

Seebacher T., Linson D.J., Peter T.C., Romano P.R. Cellular fibronectin is induced by epidermal growth factor but not by dexamethazone or cyclic AMP in rat liver epithelial cells. *FEBS Lett.* (1988) 239: 113-116.

Setoyama C., Liau G., deCrombrugghe B. Pleiotropic mutants of NIH 3T3 cells with altered regulation in expression of both type I and fibronectin. *Cell* (1985) 41: 201-209.

Shalaby F., Rossant J., Yamaguchi T.P., Gertsenstein M, Wu X.F., Breitman M.L., Schuh AC. Failure of blood-island formation and vasculogenesis in Flk-1-deficient mice. *Nature* (1995) 376: 62-66.

Shaw G., Kamen R. A conserved AU sequence from the 3' untranslated region of GM-CSF mRNA mediates selective mRNA degradation. *Cell* (1986) 46: 659-667.

Shekhonin B.V., Domogatsky S.P., Idelson G.L., Koteliansky V.E., Rukosuev V.S. Relative distribution of fibronectin and type I, III, IV, V collagens in normal and atherosclerotic intima of human arteries. *Atherosclerosis* (1987) 67: 9-16.

Shi Y., Hutchinson H.G., Hall D.J., Zalewski A. Downregulation of c-myc expression by antisense oligonucleotides inhibits proliferation of human smooth muscle cells. *Circulation* (1993)

88: 1190-1195.

Shyu A.-B., Belasco J.G., Greenberg M.E. Two distinct destabilizing elements in the c-fos message trigger deadenylation as a first step in rapid mRNA decay. *Genes Dev.* (1991) 5: 221-231.

Silver M.M., Freedom R.M., Silver M.D., Olley P.M. The morphology of the human newborn ductus arteriosus: a reappraisal of its structure and closure with special reference to prostaglandin E1 therapy. *Hum. Pathol.* (1981) 12: 1123-1136.

Simons M., Edelman E.R., DeKeyser J.-L., Langer R., Rosenberg R.D. Antisense c-*myb* oligonucleotides inhibit intimal arterial smooth muscle cell accumulation *in vivo*. *Nature* (1992) 359: 67-70.

Simons M., Rosenberg R.D. Antisense nonmuscle myosin heavy chain and c-myb oligonucleotides suppress smooth muscle cell proliferation *in vitro*. *Circ. Res.* (1992) 70: 835-843.

Singer R.H. The cytoskeleton and mRNA localization. *Curr. Opin. Cell Biol.* (1992) 3: 719-721.

Sirenko O.I., Lofquist A.K., DeMaria C.T., Morris J.S., Brewer G., Haskill J.S. Adhesion-dependent regulation of an A + U element-binding Activity associated with AUF1. *Mol. Cell. Biol.* (1997) 17: 3898-3906.

Sistonen L., Keski-Oja J., Ulmanen I., Holtta E., Wikgren B.-J., Altitalo K. Dose effects of transfected c-Ha-ras^{Val12} oncogene in transformed cell clones. *Exp. Cell Res.* (1987) 168: 518-530.

Slomp J., van Munsteren J.C., Poelmann R.E., de Reeder E.G., Rogers A.J., Gittenberger-de Groot A.C. Formation of intimal cushions in the ductus arteriosus as a model for vascular intimal thickening. An immunohistochemical study of changes in extracellular matrix components. *Atherosclerosis* (1992) 93: 25-39.

Sonoda H., Nishida K., Yoshioka T., Ohtani M., Sugita K. Oxamflatin: a novel compound which reverses malignant phenotype to normal one via induction of JunD. *Oncogene* (1996) 13: 143-149.

Sporn S.A., Schwarzbauer J.E. Identification of an enhancer invovled in tissue-specific regulation of the rat fibronectin gene. *Nucleic Acids Res.* (1995) 23: 3335-3342.

Springer T.A. Traffic signals on endothelium for lymphocyte recirculation and leukocyte emigration. *Annu Rev. Physiol.* (1995) 57: 827-872.

St Johnston D. The intracellular localization of messenger RNAs. *Cell* (1995) 81: 161-170.

St Johnston D., Driever W., Berleth T., Richstein S., Nüsslein-Volhard C. Multiple steps in the localization of bicoid RNA to the anterior pole of the Drosophila oocyte. *Development(Suppl.)* (1989) 107: 13-19.

Steele J.G., Savolainen T.A., Smith G.J. Expression of fibronectin on clonally related transformed and control sublines from an epithelial cell strain and a tumor line of mouse alveolus. *Cancer Res.* (1988) 48: 4933-4940.

Stephens J.M., Carter B.Z., Pekala P.H., Malter J.S. Tumor necrosis factor α-induced glucose transporter (GLUT-1) mRNA stabilization in 3T3-L1 preadipocytes. *J. Biol. Chem.* (1992) 267: 8336-8341.

Steward O., Banker G.A. Getting the message from the gene to the synapse: sorting and intracellular transport of RNA in neurons. *Trends Neurosci.* (1992) 15: 180-186.

Strengers J.L.M. Closure of the ductus arteriosus in the rabbits: with reference to the closing process in the monkey and lamb. *In Fetal and postnatal behavior of the ductus arteriosus* (1988) 109.

Suprenant K.A. Microtubules, ribosomes, and RNA: evidence for cytoplasmic localization and translational regulation. *Cell Motil. Cytoskeleton* (1993) 25: 1-9.

Suzuki M., Kuroda C., Oda E., Tsunoda S., Nakamura T., Nakajima T., Oda K. G10BP, an E1A-inducible negative regulator of Sp1, represses transcription of the rat fibronectin gene. *Mol. Cell. Biol.* (1995) 15: 5423-5433.

Tada T., Kishimoto H. Ultrastructural and histological studies on closure of the mouse ductus arteriosus. *Acta Anatomica* (1990) 139: 326-334.

Tai T., Eisinger M., Ogata S., Lloyd K.O. Glycoproteins as differentiation markers in human malignant melanoma and melanocytes. *Cancer Res.* (1983) 43: 2773-2779.

Takasaki I., Takizawa T., Sugimoto K., Gotoh E., Shionoiri H., Ishii M. Effects of hypertension and aging on fibronectin expression in aorta of Dahl salt-sensitive rats. *Am. J. Physiol.* (1994) 267: H1523-1529.

Tanaka Y., Bernstein M.L., Mecham R.P., Patterson G.A., Cooper J.D., Botney M.D. Site-specific responses to monocrotaline-induced vascular injury: evidence for two distinct mechanisms of remodeling. *Am. J. Respir. Cell Mol. Biol.* (1996a) 15: 390-397.

Tanaka Y., Schuster D.P., Davis E.C., Patterson G.A., Cooper J.D., Botney M.D. The role of vascular injury and hemodynamics in rat pulmonary remodeling. *J. Clin. Invest.* (1996b) 98: 434-442.

Tanguay R.L., Gallie D.R. Translational efficiency is regulated by the length of the 3' untranslated region. *Mole. Cell. Biol.* (1996) 16: 146-156.

Tannenbaum J.E., Waleh N.S., Mauray F., Gold L., Perkett E.A., Clyman R. I. Transfroming growth factor-β protein and messenger RNA expression is increased in the closing ductus arteriosus. *Pediatr. Res.* (1996) 39: 427-434.

Tarun S.Z., Sachs A.B. A common function for mRNA 5' and 3' ends in translation initiation in yeast. *Genes Dev.* (1995) 9: 2997-3007.

Tarun S.Z., Sachs A.B. Association of the yeast poly(A) tail binding protein with translation initiation factor eIF4G. *EMBO J.* (1996) 15: 7168-7177.

Thom D., Powell A.J., Rees D.A. Mechanisms of cellular adhesion. IV. Role of serum glycoproteins in fibroblast spreading on glass. *J. Cell Sci.* (1979) 35: 281-305.

Thorne H.J., Jose D.G., Zhang H.Y., Dempsey P.J., Whitehead R.H. Epidermal growth factor stimulates the synthesis of cell-attachment proteins in the human breast cancer cell line PMC42. *Int. J. Cancer* (1987) 40: 207-212.

Thyberg J., Hedin U., Sjolund M., Palmberg L., Bottger B.A. Regulation of differentiated properties and proliferation of arterial smooth muscle cells. *Arteriosclerosis* (1990) 10: 966-990.

Toole B.P., Goldberg R.L., Chi-Rosso G., Underhill C.B., Orkin R.W. Hyaluonate cell interactions. In The role of the extracellular matrix in development. (E. B. Hay, Ed.). A. R. Liss. New York. (1984) pp. 43-66.

Treisman R. Transient accumulation of c-fos RNA following serum stimulation requires a conserved 5' element and c-fos 3' sequence. *Cell* (1985) 42: 889-902.

Turley E.A., Torrance J. Localization of hyaluronate and hyaluonate-binding protein on motile and non-motile fibroblasts. *Exp. Cell Res.* (1985) 161: 17-28.

Tyagi J.S., Hirano H., Merlino G.T., Paston I. Transcriptional control of the fibronectin gene in chick embryo fibroblasts transformed by Rous sarcoma virus. *J. Biol. Chem.* (1983) 258: 5787-5793.

Vaheri A., Mosher D. High molecular weight, cell surface-associated glycoprotein (fibronectin) lost in malignant transformation. *Biochim. Biophys. Acta.* (1978) 516: 1-25.

Vaheri A., Ruoslahti E. Disappearance of a major cell type specific surface glycoprotein antigen (SF) after transformation of fibroblasts by Rous sarcoma virus. *Int. J. Cancer.* (1974) 13: 579-586.

Vakalopoulou E., Schaak J., Shenk T. A 32-kilodalton protein binds to AU-rich domains in the 3' untranslated region of rapidly degraded mRNAs. *Mol. Cell. Biol.* (1991) 11: 3355-3360.

Vanhoutte P.M.E. Endothelial cell mediators of vascular reactivity. *Coronary Artery Diseases* (1991) 2: 291-348.

Varani J., Schuger L., Fligiel S.E., Inman D.R., Chakrabarty S. Production of fibronectin by human tumor cells and interaction with exogenous fibronectin: comparison of cell lines obtained from colon asenocarcinoma and squamous carcinoma of the upper aerodigestive tract. *Inter. J. Cancer* (1991) 47: 421-425.

Villarreal F.J., Lee A.A., Dillamann W.H., Giordano F.J. Adenovirus-mediated overexpression of human transforming growth factor-beta 1 in rat cardiac fibroblasts, myocytes and smooth muscle cells. *J. Mol. Cell. Cardiol.* (1996) 28: 735-742.

Wager R.E., Assoian R.K. A phorbol ester-regulated ribonuclease system controlling transforming growth factor-β1 gene expression in hematopoietic cells. *Mol. Cell. Biol.* (1990) 10: 5983-5990.

Wager R.E., Scotto L., Assoian R.K. Analysis of transforming growth factor beta 1 messenger RNA degradation by the transcript-selective, 12-0-tetradecanoylphorbol-13-acetate-regulated ribonuclease system from U937 promonocytes. *Cell Growth Differ.* (1994) 5: 117-24.

Wakefield L.M., Smith D.M., Flanders K.C., Sporn M.B. Latent transforming growth factor-beta from human platelets. A high molecular weight complex containing precursor elements. *J.*

Biol. Chem. (1988) 263: 7646-7654.

Walker P.R., Whitfield J.F. Colchicine prevents the translation of mRNA molecules transcribed immediately after proliferative activation of hepatocytes in regenerating rat liver. *J. Cell. Physiol.* (1984) 118: 179-185.

Walker P.R., Whitfield J.F. Cytoplasmic microtubules are essential for the formation of membrane-bound polysomes. *J. Biol. Chem.* (1985) 260: 765-770.

West D.C., Sattar A., Kumar S. A simplified in situ hybridization procedure for the determination of DNA and cell number in tissue cultured mammalian cells. *Anal. Biochem.* (1985) 147: 289-295.

Whittemmore L.A., Maniatis T. Postinduction turnoff of beta-interferon gene expression. *Mol. Cell. Biol.* (1990) 10: 1329-1337.

Wight T.N. Cell biology of arterial proteoglycan. *Arteriosclerosis* (1989) 9: 1-20.

Wilhelm J., Vale R. RNA on the move: the mRNA localization pathway. *J Cell Biol.* (1993) 123: 269-274.

Wilson T., Treisman R. Removal of poly (A) and consequent degradation of c-fos mRNA facilitated by AU-rich sequences. *Nature (London)* (1988) 336: 396-399.

Winstall E., Gamache M., Raymod V. Rapid mRNA degradation mediated by the c-fos 3' AU-rich element and that mediated by the granulocyte-macrophage colony-stimulating factor 3' AU-rich element occur through similar polysome-associated mechanisms. *Mol. Cell. Biol.* (1995) 12: 2931-2940.

Wodnar-Filipowicz A., Moroni C. Regulation of interleukin 3 mRNA expression in mast cells occurs at the posttranscriptional level and is mediated by calcium ions. *Proc. Natl. Acad. Sci. USA* (1990) 87: 777-781.

Wolf Y.G., Rasmussen L.M., Ruoslahti E. Antibodies against transforming growth factor-beta 1 suppress intimal hyperplasia in a rat model. *J. Clin. Invest.* (1994) 93: 1172-1178.

Wrana J.L., Maeno M., Hawrylyshyn B., Yao K.L., Domenicucci C., Sodek J. Differential effects of transforming growth factor-beta on the synthesis of extracellular matrix proteins by normal fetal rat calvarial bone cell populations. *J. Cell Biol.* (1988) 106: 915-924.

Wrana J.L., Overall C.M., Sodek J. Regulation of the expression of a secreted acidic protein rich in cysteine (SPARC) in human fibroblasts by transforming growth factor β. Comparison of transcriptional and post-transcriptional control with fibronectin and type I collagen. *Eur. J. Biochem.* (1991) 197: 519-528.

Yamada K.M., Schlesinger D.H., Kennedy D.W., Pastan I. Characterization of a major fibroblast cell surface glycoprotein. *Biochemistry* (1977) 16: 5552-5559.

Yamada K.M., Yamada S., Pastan I. Cell surface protein partially restores morphology, adhesiveness, and contact inhibition of movement to transformed fibroblasts. *Proc. Natl. Acad. Sci. USA* (1976) 73: 1217-1221.

Yamada K.M., Yamada S.S., Pastan I. Quantitation of a transformation-sensitive, adhesive cell

surface glycoprotein. *J. Cell Biol.* (1977) 74: 649-654.

Yamato K., Ei-Hajjaoui Z., Kuo J.F., Koeffler H.P. Granulocyte-macrophage colony-stimulating factor: Signal for its mRNA accumulation. *Blood* (1989) 74: 1314-1320.

Yang N.S., Kirkland W., Jorgensen T., Furmanski P. Absence of fibronectin and presence of plasminogen activator in both normal and malignant human mammary epithelial cells in culture. *J. Cell Biol.* (1980) 84: 120-130.

Yoder M.J., Baumann F.G., Grover-Johnson N.M., Brick I., Imparato A.M. A morphological study of early cellular changes in the closure of the rabbit ductus arteriosus. *Anat. Rec.* (1978) 192: 19-39.

Zhang L., Lo C. Regulation of fibronectin expression by PDGF-BB and IGF-I in cultured rat thoracic adventitia fibroblasts. *Cell Biol. Inter.* (1995) 19: 517-525.

Zhang W., Wagner B.J., Ehrenman K., Schaefer A.W., DeMaria C.T., Crater D., DeHaven K., Long L., Brewer G. Purification, characterization, and cDNA cloning of an AU-rich element RNA-binding protein, AUF1. *Mol. Cell. Biol.* (1993) 13: 7652-7665.

Zhu L., Dagher E., Rabinovitch M. Elastin synthesis and assembly is impaired in the fetal ductus arteriosus. *FASEB* (1990) 4: 095A.

Zubiaga A.M., Belasco J.G., Greenberg M.E. The nonamer UUAUUUAUU is the key AU-rich sequence motif that mediates mRNA degradation. *Mol. Cell. Biol.* (1995) 15: 2219-2230.

IMAGE EVALUATION
TEST TARGET (QA–3)

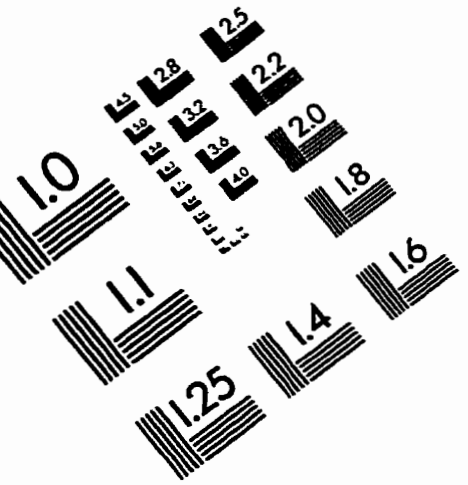

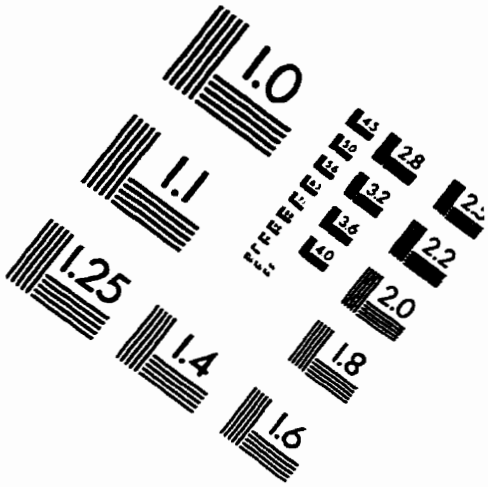

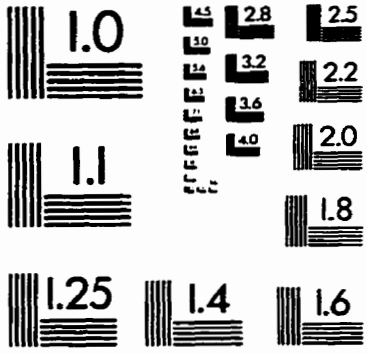

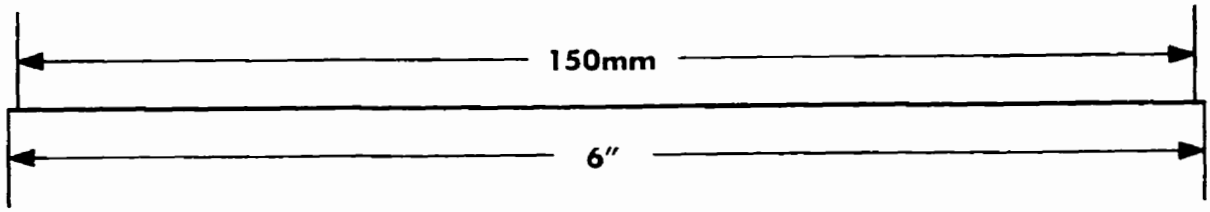

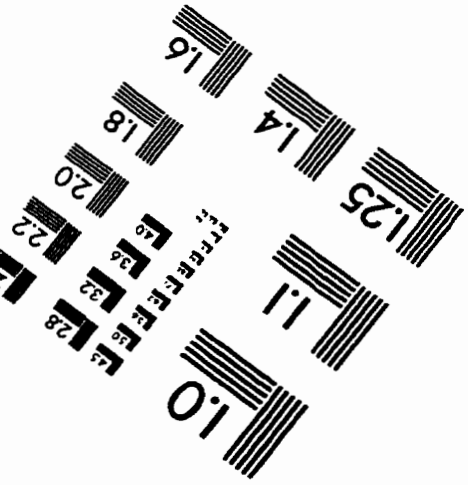

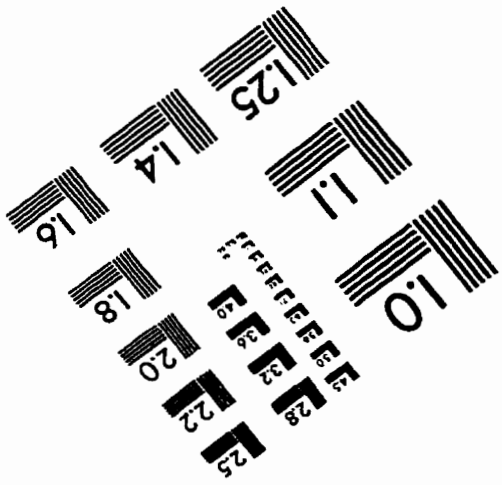

APPLIED IMAGE, Inc
1653 East Main Street
Rochester, NY 14609 USA
Phone: 716/482-0300
Fax: 716/288-5989